Novel biobased epoxy networks derived from renewable resources : Structure-property relationships

Marie Chrysanthos

N° d'ordre 2012ISAL0051 Année 2012

Thèse

Novel biobased epoxy networks derived from renewable resources : Structure-property relationships

Présentée devant
L'institut national des sciences appliquées de Lyon

Pour obtenir
Le grade de docteur

École doctorale : Matériaux de Lyon
Spécialité : Matériaux Polymères et Composites

Par
Marie CHRYSANTHOS
Ingénieur ENSCCF

Soutenue le 21 Juin 2012 devant la Commission d'examen

Jury

	E. BOURGEAT-LAMI	Directrice de recherche CNRS (CPE Lyon)
Rapporteur	B. BOUTEVIN	Professeur (ENSCM)
	J. CHRISTOUD	Responsable service Matériaux (Rossignol)
	J. GALY	Directrice de recherche CNRS (INSA de Lyon)
	P. GOTTIS	Docteur (Huntsman)
Rapporteur	M. LAVORGNA	CNR Researcher (ICBM - Naples, Italy)
	J.P. PASCAULT	Professeur (INSA de Lyon)
	P. SABRE	Renewable Chemistry Management (Roquette Frères)

INSA Direction de la Recherche - Ecoles Doctorales – Quinquennal 2011-2015

SIGLE	ECOLE DOCTORALE	NOM ET COORDONNEES DU RESPONSABLE
CHIMIE	**CHIMIE DE LYON** **http://www.edchimie-lyon.fr** Insa : R. GOURDON	M. Jean Marc LANCELIN Université de Lyon – Collège Doctoral Bât ESCPE 43 bd du 11 novembre 1918 69622 VILLEURBANNE Cedex Tél : 04.72.43 13 95 directeur@edchimie-lyon.fr
E.E.A.	**ELECTRONIQUE, ELECTROTECHNIQUE, AUTOMATIQUE** **http://edeea.ec-lyon.fr** Secrétariat : M.C. HAVGOUDOUKIAN eea@ec-lyon.fr	M. Gérard SCORLETTI Ecole Centrale de Lyon 36 avenue Guy de Collongue 69134 ECULLY Tél : 04.72.18 60 97 Fax : 04 78 43 37 17 Gerard.scorletti@ec-lyon.fr
E2M2	**EVOLUTION, ECOSYSTEME, MICROBIOLOGIE, MODELISATION** **http://e2m2.universite-lyon.fr** Insa : H. CHARLES	Mme Gudrun BORNETTE CNRS UMR 5023 LEHNA Université Claude Bernard Lyon 1 Bât Forel 43 bd du 11 novembre 1918 69622 VILLEURBANNE Cédex Tél : 04.72.43.12.94 e2m2@biomserv.univ-lyon1.fr
EDISS	**INTERDISCIPLINAIRE SCIENCES-SANTE** **http://ww2.ibcp.fr/ediss** Sec : Safia AIT CHALAL Insa : M. LAGARDE	M. Didier REVEL Hôpital Louis Pradel Bâtiment Central 28 Avenue Doyen Lépine 69677 BRON Tél : 04.72.68 49 09 Fax :04 72 35 49 16 Didier.revel@creatis.uni-lyon1.fr
INFOMATHS	**INFORMATIQUE ET MATHEMATIQUES** http://infomaths.univ-lyon1.fr	M. Johannes KELLENDONK Université Claude Bernard Lyon 1 INFOMATHS Bâtiment Braconnier 43 bd du 11 novembre 1918 69622 VILLEURBANNE Cedex Tél : 04.72. 44.82.94 Fax 04 72 43 16 87 infomaths@univ-lyon1.fr
Matériaux	**MATERIAUX DE LYON** Secrétariat : M. LABOUNE PM : 71.70 –Fax : 87.12 Bat. Saint Exupéry Ed.materiaux@insa-lyon.fr	M. Jean-Yves BUFFIERE INSA de Lyon MATEIS Bâtiment Saint Exupéry 7 avenue Jean Capelle 69621 VILLEURBANNE Cédex Tél : 04.72.43 83 18 Fax 04 72 43 85 28 Jean-yves.buffiere@insa-lyon.fr
MEGA	**MECANIQUE, ENERGETIQUE, GENIE CIVIL, ACOUSTIQUE** Secrétariat : M. LABOUNE PM : 71.70 –Fax : 87.12 Bat. Saint Exupéry mega@insa-lyon.fr	M. Philippe BOISSE INSA de Lyon Laboratoire LAMCOS Bâtiment Jacquard 25 bis avenue Jean Capelle 69621 VILLEURBANNE Cedex Tél :04.72.43.71.70 Fax : 04 72 43 72 37 Philippe.boisse@insa-lyon.fr
ScSo	**ScSo*** M. OBADIA Lionel Sec : Viviane POLSINELLI Insa : J.Y. TOUSSAINT	M. OBADIA Lionel Université Lyon 2 86 rue Pasteur 69365 LYON Cedex 07 Tél : 04.78.69.72.76 Fax : 04.37.28.04.48 Lionel.Obadia@univ-lyon2.fr

*ScSo : Histoire, Geographie, Aménagement, Urbanisme, Archéologie, Science politique, Sociologie, Anthropologie

Remerciements

Je tiens dans un premier temps à remercier ma directrice de thèse, Jocelyne GALY, pour m'avoir confié ce travail de recherches, ainsi que pour sa disponibilité, sa gentillesse, et son aide au cours de ces années. Je remercie également Jean-Pierre PASCAULT, de s'être investi dans cette thèse. Merci à lui pour toutes ses idées et remarques qui m'auront aidé à remettre perpétuellement en cause mon travail, à avancer et développer ma curiosité scientifique. Je le remercie également d'avoir accepté de faire partie du jury. Merci enfin à Jean-François GERARD, et Etienne FLEURY, pour m'avoir accepté dans leur laboratoire.

Je tiens également à remercier Marino LAVORGNA, et Monsieur Bernard BOUTEVIN, d'avoir accepté d'être les rapporteurs de ce travail. Merci à Philippe SABRE, de la société Roquette et Frères, Jacky CHRISTOUD de la société Rossignol, et Philippe GOTTIS de la société Huntsman, pour leur aide et leur gentillesse tout au long du projet NAFI et d'avoir accepté de faire partie de mon jury. Je remercie, de même, la présidente du jury Elodie BOURGEAT-LAMI. J'en profite également pour adresser mes remerciements à tous les membres du projet NAFI, dont Françoise MECHIN pour son aide bibliographique.

Pour leur soutien technique mais surtout leur bonne humeur, leur gentillesse et tous ces moments de fous rires, un grand merci aux dames de la RMN : Fernande BOISSON, Annick WATON et surtout Cécile CHAMIGNON, l'inénarrable. Merci à Raphael BRUNEL pour son aide précieuse en rhéologie ainsi qu'à Guilhem QUINTARD qui n'aura jamais perdu patience et aura « presque » su me faire apprécier la machine d'ARES. J'aimerai aussi remercier les secrétaires du laboratoire, Mallou et Isabelle, pour leur gentillesse et leur aide précieuse.

Merci aussi aux nombreux non-permanents du laboratoire, thèsards, post-docs et autres masters, qui auront su égayer ces années de thèse. Un grand merci en particulier à mes compagnons de bureau ; merci à Feliks, à Amélie (ma collègue de voyage !), à Céline, Wenyong, Thomas, Komkriss et *last but not least*, Elie. Merci aux anciens (Morgan, Sandra, Alexia, Arthur) pour leurs conseils précieux à la débutante que j'étais. Merci à Stéphane (Pépito !) et Grégoire qui ont partagé cette expérience en même temps que moi. Merci à ceux qui n'ont pas encore fini (courage) et avec qui j'ai eu plaisir à faire un bout de chemin (Marie-

Laure, Nora, Vincent, Sylvain, Gino, Florent, Thibault, Floriane, Loïc, Cédric, Marie, Hélène, Marianne). Merci également aux post-doc pour leur grande « sagesse » et leur soutien (Nicolas D., Nicolas L., Marco). Merci à Elise, pour m'avoir épaulé et avoir toujours su me redonner confiance. J'ai aussi une pensée affectueuse pour sa famille, pour Jean-Marc et la petite Amandine. Merci à mes amis hors laboratoire : Laure, Saucisse, Yvong, P'ti Nico, Simon, Anais, Aurélien…

Je remercie également Maxime, pour m'avoir soutenu tout le long de mes deux dernières années de thèse avec patience et humour, et les avoir ainsi rendu plus belles et plus heureuses. Merci à sa famille pour m'avoir accueilli en côte Roannaise et m'avoir fait découvrir les vendanges, ainsi qu'à Charlotte, Moun et Flo.

Je remercie enfin chaleureusement ma mère et Serge, mon père, et mes deux frérots pour leur soutien indéfectible au long de ces trois années (et des poussières) de thèse.

MERCI

MISOATRA

Abstract:

In recent years, bio-based polymers derived from renewable resources have become increasingly important as sustainable and eco-efficient products which can replace the products based on petrochemical-derived stocks.

The objective of our work was to develop novel bio-based reactive systems suitable for high performance composite materials especially epoxy systems. The most commonly used starting monomer to formulate epoxy networks is the diglycidyl ether of bisphenol A, DGEBA, derived from bisphenol A and epichlorohydrin. Bio-based epichlorohydrin is commercially available. So the challenge to obtain a fully bio-based epoxy prepolymer is to replace bisphenol A by a bio-based precursor. Another interest for replacing bisphenol A by a bio-based precursor is that bisphenol A has been known to have estrogenic properties.

In this study, we studied different bio-based epoxy systems and compared them to a classical DGEBA based system using, in a first step, isophorone diamine (IPD) as conventional curing agent. Bio-based epoxy prepolymers were derived from natural sugars, sorbitol and isosorbide respectively. Sorbitol polyglycidyl ether is available commercially, while isosorbide diglycidyl ether was synthesized either via conventional epoxidation (i.e. using epichlorohydrin) or via the diallyl isosorbide intermediate. Another bio-based epoxy prepolymer was derived from cardanol and is also a commercial product.

Chemical structure of the bio-based epoxy prepolymers were analyzed by different analytical methods, gelation and crosslinking reactions were studied using rheological measurements and differential scanning calorimetry, respectively. Properties of the cured networks were evaluated using dynamic mechanical analysis and thermo gravimetric analysis. Influence of the bio-based epoxy prepolymer structure on the system properties as well as the influence of the crosslinking agent structure (either derived from renewable resources or bio-based ones) was discussed. Water absorption of the bio-based networks was also studied.

Keywords:
Epoxy networks; bisphenol A; isosorbide; sorbitol; cardanol; structure-properties relationships; reactivity; solid-state properties; water absorption

Résumé:

Récemment, les polymères obtenus à partir de ressources renouvelables ont connus un véritable engouement pour le remplacement de matériaux obtenus à partir de ressources pétrolières. L'objectif de notre étude a été de développer de nouveaux systèmes bio-sourcés réactifs, plus précisément des systèmes époxy, pour des applications dans le domaine des matériaux composites.

Le monomère le plus souvent utilisé pour formuler des réseaux époxy est le diglycidyl éther de bisphenol A, DGEBA, obtenu à partir du bisphenol A et de l'épichlorhydrine. L'intérêt pour le remplacement du bisphénol A par un précurseur bio-sourcé est accentué par la toxicité de ce dernier.

Dans cette étude, nous avons étudié différents systèmes obtenus à partir de prépolymères époxy bio-sourcés et les avons comparés à un système classique à base de DGEBA en utilisant l'isophorone diamine (IPD) comme agent durcisseur.

Parmi les différents prépolymères époxy bio-sourcés étudiés, certains ont été obtenus à partir de dérivés polysaccharides tels que le sorbitol et l'isosorbide. Le sorbitol polyglycidyl éther est disponible commercialement, tandis que le diglycidyl éther d'isosorbide a été synthétisé soit par une voie classique faisant intervenir l'épichlorhydrine soit par l'intermédiaire du diallyle isosorbide. Un autre prépolymère époxy dérivé du cardanol a été étudié et est aussi un produit commercial.

Les structures chimiques de ces prépolymères époxy bio-sourcés ont été analysées. Les phénomènes de gélification et de réticulation des systèmes obtenus à partir de ces prépolymères et de l'IPD ont été étudiés. L'influence de la structure du prépolymère bio-sourcé et de l'agent de réticulation (classique ou dérivé de ressources renouvelables) sur les propriétés des réseaux ainsi que l'absorption d'eau par ces réseaux ont également été discutés.

Mots-clefs:
Réseaux époxy; bisphenol A; isosorbide; sorbitol; cardanol; relation structure propriétés; réactivité; propriétés des réseaux; absorption d'eau

Contents

Chapter I Epoxy thermosetting polymers derived from renewable resources

This chapter presents the recent advances regarding the field of thermosetting polymers from renewable resources, with a particular interest on epoxy networks. With the emergence of the concept of sustainable development, researches have been done on the synthesis of new bio-based polymeric units which can replace the petroleum-based ones.

I. Introduction

In an age of increasing oil prices, global warming, and other environmental problems, the replacement of petroleum-based raw materials, especially polymers, by renewable resources constitutes a major contemporary challenge in terms of both economic and environmental aspects.

Many investigations have been done on the development of bio-based polymers derived from renewable resources such as sugars, polysaccharides, vegetable oils, lignin, pine resin derivatives, furans and other monomers [1-4]. These renewable resources can be turned into viable macromolecular materials and could be good candidates for the replacement of both thermoplastic and thermosetting materials. For instance, vegetable oils, made up of triglycerides molecules (Figure 1), can be interesting renewable raw materials [5], cheap and abundant, for the production of bio-based polymeric units (Figure 2). Besides, emergence of sustainable sugar derived chemicals, such as sorbitol and isosorbide (Figure 3) modified products, offers also attractive prospects [6, 7] in terms of new bio-based polymeric units.

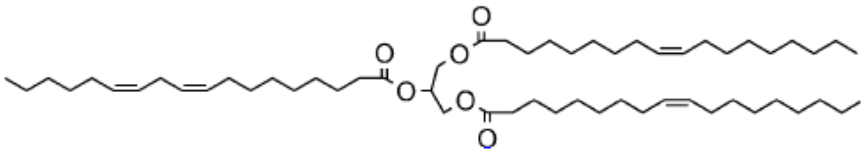

Figure 1. Schematic representation of triglyceride molecule

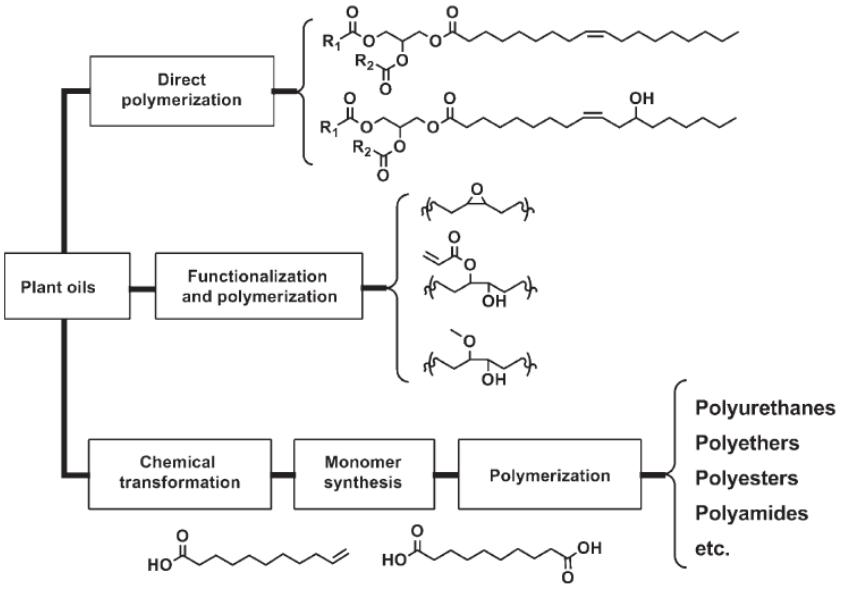

Figure 2. General strategies for the synthesis of plant oil-based polymers. [5]

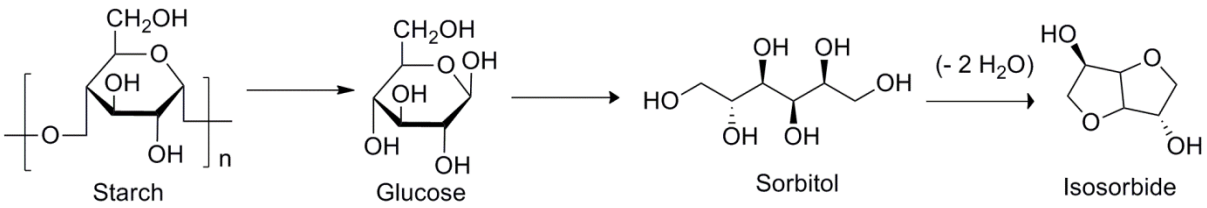

Figure 3. Glucose, sorbitol and isosorbide obtained from starch

Based on their response to temperature, polymers may be classified into two main categories: thermoplastic and thermosetting polymers. A thermoplastic behaves like a liquid above a certain temperature level, but the heating of a thermoset leads to its degradation without going through a fluid state [8].

Actually, among all the polymers produced nowadays, 82 % are thermoplastics [9]. Therefore, research has mainly concerned bio-based thermoplastics. For instance, developments were done on isosorbide-based thermoplastic [7, 10] such as polyester, polyamide [10], polycarbonate [11-13]. Biobased thermoplastic polyurethanes were synthesized using vegetable oils as raw materials. Renewable diols can be developed from oleate derivatives [14, 15] and polymerized using petrochemical-based isocyanate to obtain partially bio-based thermoplastics PU [15]. Linear diols and diisocyanates [16] produced entirely from renewable lipid sources were also used to obtain fully bio-based functional thermoplastics PU [17].

Even if, most of the researches on bio-based polymers were done on the development of bio-based thermoplastic, recent researches focused on the development of bio-based thermosetting polymers [18].

Thermosetting materials [8] are crosslinked polymers that are cured or set using heat, or heat and pressure, and/or light irradiation. This leads to a large range of high performance products for industry due to their high modulus, strength, durability, and resistance towards thermal stress and chemical attacks as provided by their high crosslinking density.

For a given application, replacement of petroleum-based thermosetting materials by renewable resources should not lead to a decrease in network properties. This chapter will therefore focus on the structure-properties relationships in thermosetting polymers derived from renewable resources, with a special interest on epoxy thermosets.

Some standards and methods have been developed to assess the quantity of renewable material. The United State Department of Agriculture defines the bio-based content of a product as the "amount of bio-based carbon in the material or product as a percent of the weight (mass) of the total organic carbon in the product", and radiocarbon analysis in accordance with ASTM D6866-05 standard is a reliable method for experimentally verifying the biobased content [19].

II. Overview on some thermosetting polymers

As previously mentioned, thermosets are characterized by a highly crosslinked structure of the polymer chains. As a consequence, thermosets cannot be remelted as thermoplastics and they are insoluble. As early as 1910, thermoset polymers were manufactured from petrochemical phenol and formaldehyde according to the patents of L.H. Baekeland; this material – phenol formaldehyde polymer (PF) – became widely known under the name Bakelite. In the late 1920s, urea formaldehyde polymer (UF) came on the market followed by melamine formaldehyde polymer (MF) at the end of the 1930s (UF and MF resins together form the category of amino resins). Unsaturated polyesters (UP), especially in the form of fiberglass composites, were first manufactured at large scale in the 1940s (for application in the marine industry). Finally, epoxy polymers are relatively new materials which have been produced since the mid-1950s. Regarding polyurethanes, they represent an

important class of thermoplastics and thermosets depending on the nature of the polyol and isocyanate components used.

Rapid description of some typical classes of thermosets (phenolic polymers, polyurethanes, and epoxy polymers) through their chemistry, properties and resulting applications, is given below.

1. Phenol formaldehyde polymers (phenolic polymers)

Phenolic prepolymers are obtained by step-growth polymerization of a difunctional monomer, CH_2O, with phenol or substituted phenols. The simplified reaction between phenol and formaldehyde is represented in Figure 4.

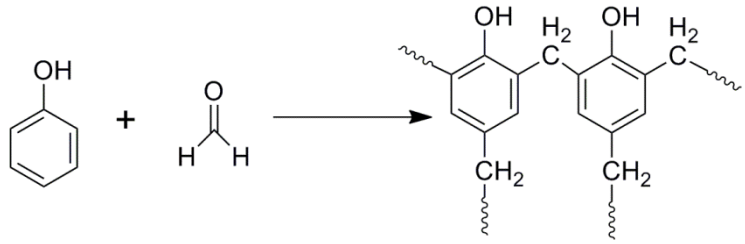

Figure 4. Reactions phenol/formaldehyde

Novolacs are obtained by the reaction of phenol and formaldehyde in acidic conditions. Novolac oligomers are linear or slightly branched addition products linked by methylene bridges. The reaction is usually carried out using a molar ratio CH_2O/PhOH close to 0.8, to avoid gelation. Resols are obtained by phenol-formaldehyde reaction under alkaline conditions and with an excess of formaldehyde, generally from 1.5 – 3.

Despite the emergence of several new classes of thermosets, high-performance polymers and several other new generation materials that are superior in some respects, phenolic polymers retain industrial and commercial interest a century after their introduction. Phenolic polymers are widely used as commodity and engineered materials in the high technology transportation industry. This recognition emerges from the fact that these polymers have several desirable characteristics, such as superior mechanical strength, heat resistance and dimensional stability, as well as high resistance against various solvents, acids and water. They are inherently flame-resistant, and evolve low smoke upon incineration. Although phenolics cannot compete with epoxies for superior engineering areas, their

composites still find markets in thermo-structural applications in the aerospace and railway industries, due to their good heat and flame resistance, excellent ablative properties and low cost. Yet, the main drawback of phenolic polymers remains the toxicity of residual formaldehyde monomer.

2. Polyurethane thermosets

The synthesis of polyurethane (PU) can be carried out by the reaction simplified in Figure 5 of an isocyanate with a diol (or polyol). If the functionality of the hydroxyl-containing compounds or the isocyanate is beyond 2, branched and possibly cross-linked polymers are produced.

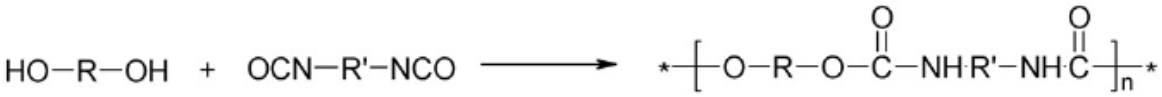

Figure 5. Synthesis of polyurethane where R or R' are of aliphatic or aromatic nature

Polyurethanes are one of the most important and versatile materials with applications ranging from flexible foams in upholstered furniture to rigid foams as insulators in walls, roofs, and appliances of thermoplastics polyurethane used in medical devices and footwear, coatings, adhesives, sealants, and elastomers used on floors and automotive interiors [20]. They represent an important class of thermoplastics and thermosets because their mechanical, thermal, and chemical properties can be tailored by reactions with various polyols (depending on the nature of the polyol: polyether, polyester, polybutadiene… [8]) and isocyanates. PUs exhibit better abrasion resistance, toughness, chemical resistance, and mechanical strength compared to other polymers such as polyesters and polyesteramides.

Usually, both isocyanates and polyols are petroleum based, but in recent years, vegetable oils, fatty acids and their derivatives have attracted significant attention as raw materials for the preparation of polyurethanes [21]. Main developments in PU field have concern replacement of petroleum-based polyols by bio-based ones. However, more and more researches are conducted on the replacement of existing isocyanates, as practically all the isocyanates are declared as carcinogens, mutagens and toxic for reproduction (CMR).

3. Epoxy networks

Epoxy networks are thermosetting materials for which the precursors contain at least one epoxy function. The term “epoxy” is referred generally to molecule’s functional groups consisting of oxirane rings:

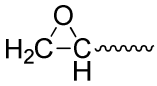

These epoxy functions are highly reactive. The capability of the oxirane group to undergo a large variety of addition and polymerization reactions has been exploited for the production of many different epoxy thermosetting materials.

Epoxy prepolymers are compounds containing a minimum of two functional groups so that they can be converted into infusible products through the formation of networks.
Nowadays, almost 75% of the world production of epoxy prepolymers [9] is based on the reaction between Bisphenol A (BPA) and epichlorohydrin, yielding diglycidyl ether of bisphenol A (DGEBA), as shown in Figure 6.

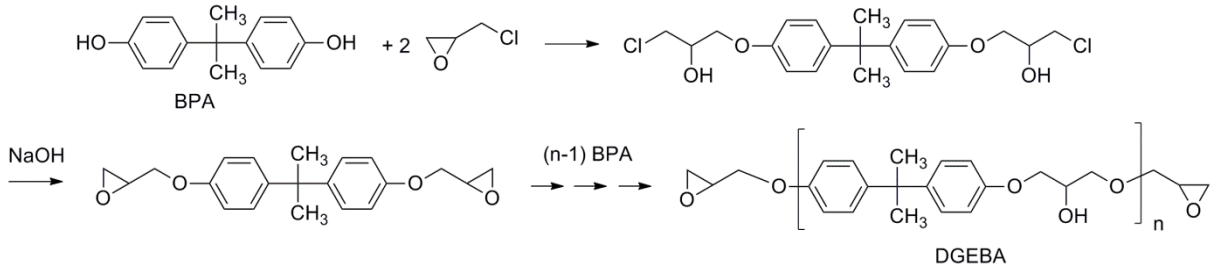

Figure 6. Synthesis of DGEBA

In order to convert epoxy prepolymers into infusible thermoset networks it is necessary to use crosslinking agents, also referred to as hardeners or curing agents. They may either initiate the curing reactions through their catalytic activity (initiators) or may react with the epoxy monomer via a polyaddition/copolymerization reaction. Structure of crosslinking agents has a considerable effect on the properties of the crosslinked products. Among the wide variety of hardeners available nowadays, the main types are amines and anhydrides curing agents.

a) Epoxy – amine reaction mechanism

The main mechanism is step-polymerization / polyaddition:

Addition mechanism:

Between a primary amine and an epoxy group, the addition mechanism is the more important and results, when the epoxy and the amine compounds are multifunctional, to a three dimensional network. It is described by the Equations 1 and 2 represented in the following Scheme:

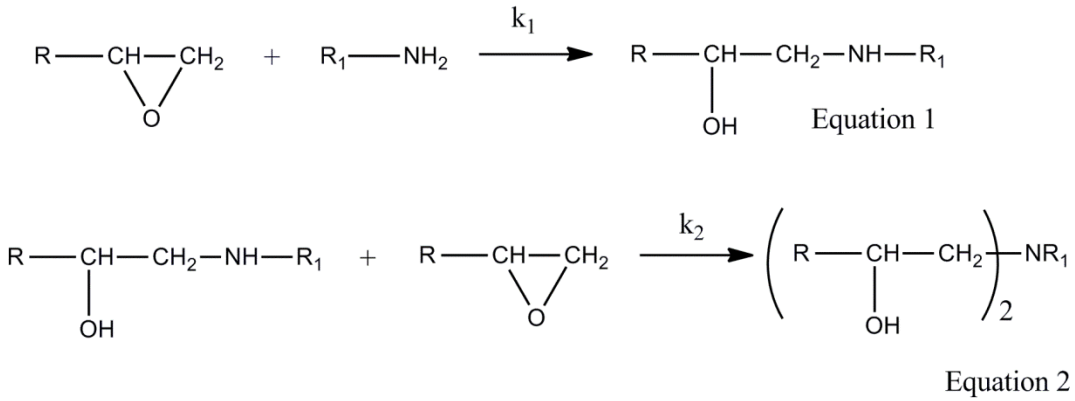

Scheme 1. Addition mechanism

Addition reaction yields secondary (Equation 1) and tertiary (Equation 2) amines. The amines differ by their reactivity; usually primary amines are more reactive than secondary ones with $k_2/k_1 < 1$ [22]. Many factors may influence this ratio, such as hardener nature [23], steric hindrance, temperature [24]… These two addition reactions can also be catalysed by –OH groups, and as the reaction leads to secondary –OH, it is an autocatalytic process.

Etherification mechanism:

Etherification is a side reaction between epoxy and hydroxyl groups and is represented in the Scheme below:

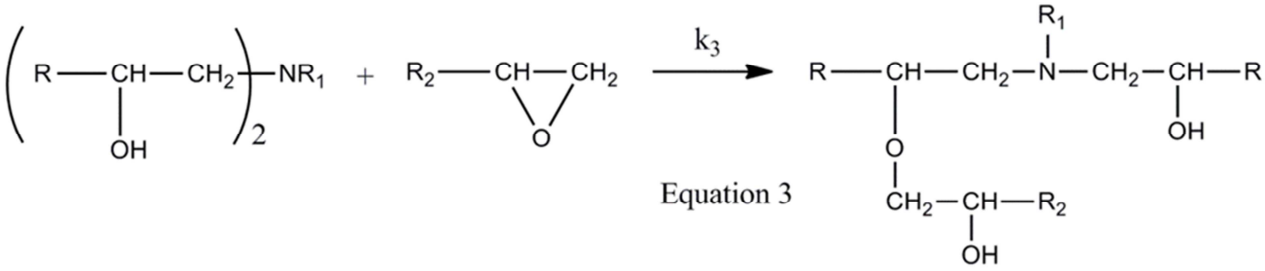

Scheme 2. Etherification mechanism

Without any catalyst, etherification mechanism is unlikely to occur. Indeed, the produced tertiary amine (Equation 2) is not very reactive regarding its steric hindrance. This step is promoted by an excess of epoxy [25] and when all amino hydrogen have been consumed [26].

Various amine curing agents:

Reactivity of amine increases with its nucleophilic character: aliphatic > cycloaliphatic > aromatic. Structures of typical amines hardeners are shown in Figure 7.

Aliphatic and cycloaliphatic amines include among others, ethylene diamine (EDA), diethylene triamine (DETA), triethylenetetramine (TETA), polyetheramines, isophorone diamine (IPD), metaxylilene diamine (MXDA)...

Ethylene diamine is highly reactive and yield tightly crosslinked networks owing to the short distance between the actives sites. For this reason, the networks exhibit excellent solvent resistance and mechanical strength, but limited flexibility.

Aromatic polyamines such as 4,4'-diaminophenylmethane (DDM) and 4,4'-diaminophenylsulfone (DDS) react slowly with the epoxy. All systems cured with these hardeners exhibit excellent resistance to a wide variety of chemicals, coupled with outstanding temperature stability. Yet, some amines like DDM have been identified as CMR and have problems with REACH.

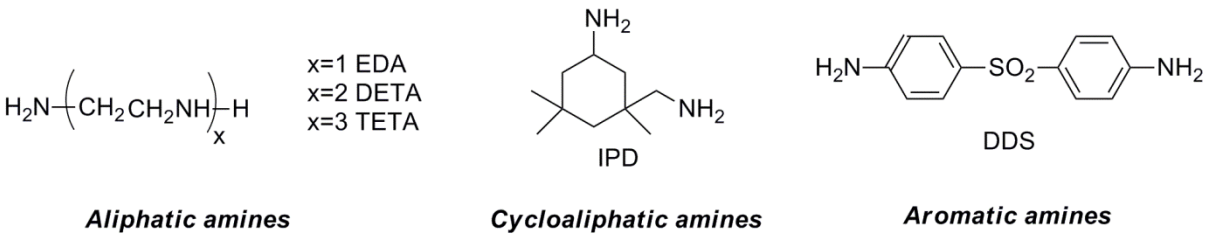

Figure 7. Structure of some amine curing agents

b) Epoxy – anhydride reaction mechanism

Anhydrides curing agents react at high temperatures (higher than 100°C) and require the use of initiators such as tertiary amines or imidazole and prolonged periods to reach completion. Nevertheless, they provide networks with good dimensional stability and insulating and optical properties. The most important dicarboxylic acid anhydrides used as

epoxy hardeners are cycloaliphatic, with the notable exception of phthalic anhydride (PA). Its hydrogenated derivatives hexahydrophthalic anhydride (HHPA) and tetrahydrophthalic anhydride (THPA) are used extensively for electrical applications. Their chemical structures are represented in Figure 8.

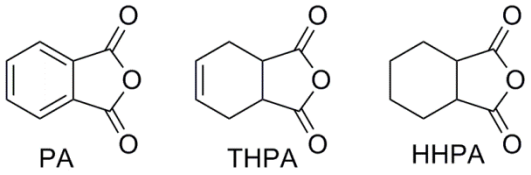

Figure 8. Structures of PA, THPA and HHPA anhydride curing agents

The curing mechanism is more complex than that of the amines and consists on a chainwise anionic copolymerization comprising initiation, propagation, and termination or chain transfer steps [27, 28]. Initiation involves the reaction of the tertiary amine with epoxy group, giving rise to a zwitterion that contains a quaterny nitrogen atom and an alkoxide anion. The alkoxide reacts at a very fast rate with an anhydride group, leading to species containing carboxylate anion as the active center. Propagation occurs through the reaction of the carboxylate anion with an anhydride group, regenerating the carboxylate anion.

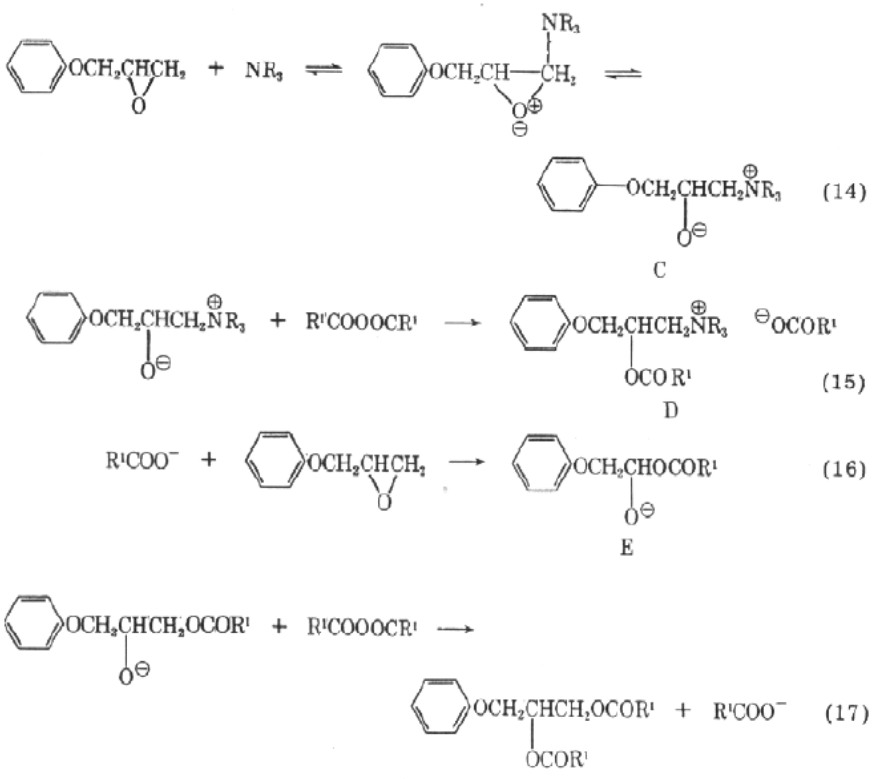

Scheme 3. Mechanism of anhydride –epoxy anionic copolymerization initiated by tertiary amines according to Matejka [28]

c) Ionic homopolymerization of epoxy prepolymers

Anionic polymerization:

The homopolymerization is promoted by the presence of initiators often called "catalytic" curing agents in the literature. In the case of anionic polymerization, homopolymerization is promoted by Lewis acid, tertiary amines, imidazole… [29]. Simplified mechanism is presented below:

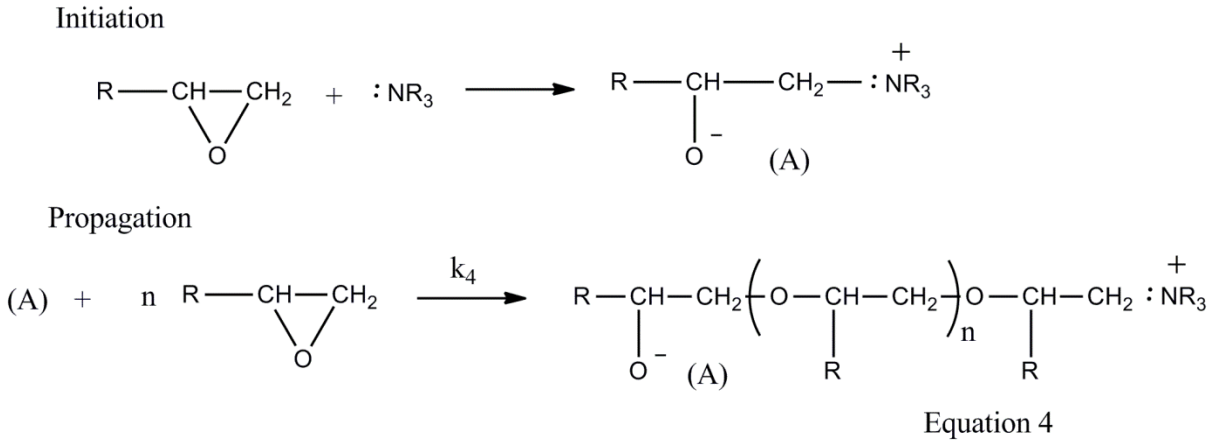

Scheme 4. Anionic polymerization mechanism

Cationic polymerization:

Cationic polymerization has been intensively investigated using various thermal latent cationic catalysts, such as iodonium, ammonium, pyridinium and sulfonium salts (Scheme 5). Latent catalysts are inert under normal conditions, but release active species by external stimulation. Thus, the use of latent catalysts increases the storage stability and handing of thermosetting polymers. It can also be deblocked by UV light.

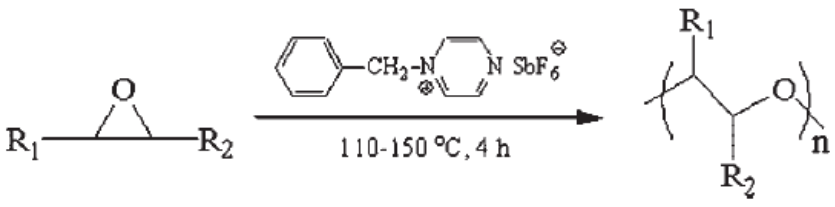

Scheme 5. Thermally induced ring-opening polymerization of internal epoxides initiated by a cationic latent catalyst [30]

III. Bio-based Epoxy networks

An easy way to obtain a partially bio-based DGEBA is to use epichlorohydrin from bio-based glycerol, commercially available. However, molar mass of DGEBA is dominated by Bisphenol A, which is petroleum-based and known to have estrogenic properties [31]. Therefore, the challenge to obtain bio-based epoxy prepolymer is to replace bisphenol A by bio-based polyols.

Besides, epoxy prepolymers are combined with a large variety of co-reactants, as described in the previous section to form tridimensional networks with a broad spectrum of performances depending on both the structure of epoxy prepolymer, nature of curing agent, the extent and density of crosslinking. Using bio-based curing agents fully bio-based epoxy networks can be prepared.

Recent advances in the synthesis of epoxy prepolymers from renewable resources are discussed below, with a focus on solid-state properties of the resulting bio-based networks compared with traditional ones.

1. Biobased epoxy networks derived from vegetable oils

In the formation of sustainable epoxy monomers, epoxidized plants oils and fatty acids have been largely utilized as reported in the literature [1, 3, 18, 32]. Vegetable oils, such as linseed oil, soybean oil, castor oil, appear as excellent renewable raw materials for thermosetting polymers as they are expected to be inexpensive and abundant.

Vegetable oils are already a commercial source of multifunctional monomers and oligomers for polyurethane synthesis, and research on the use of vegetable oils as polymer precursors has mainly concerns the design of novel biobased polyols derived from them for polyurethane applications [20, 33-36]. Nevertheless, they also have been studied as bio-based precursors through their epoxidation for the synthesis of bio-based epoxy prepolymers.

a) Vegetable oils

Natural plant oils such as soybean oil, sunflower oil, palm oil, rapeseed oil, cottonseed oil and linseed oil are predominantly made up of triglyceride molecules. The structure of these natural products can be schematically depicted by the simple generic triglyceride

(Figure 9), where R1, R2 and R3 represent fatty acid chains, which can vary in length (from C12 to C22), in the number of C=C insaturations (from zero to six) and in the possible presence of other moieties, like -OH or epoxy groups. Figure 10 shows the most frequent fatty acid precursors to triglycerides.

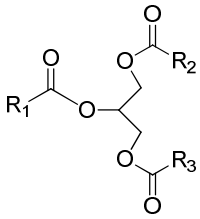

Figure 9. Generic triglyceride formula, with R_1, R_2 and R_3: fatty acids

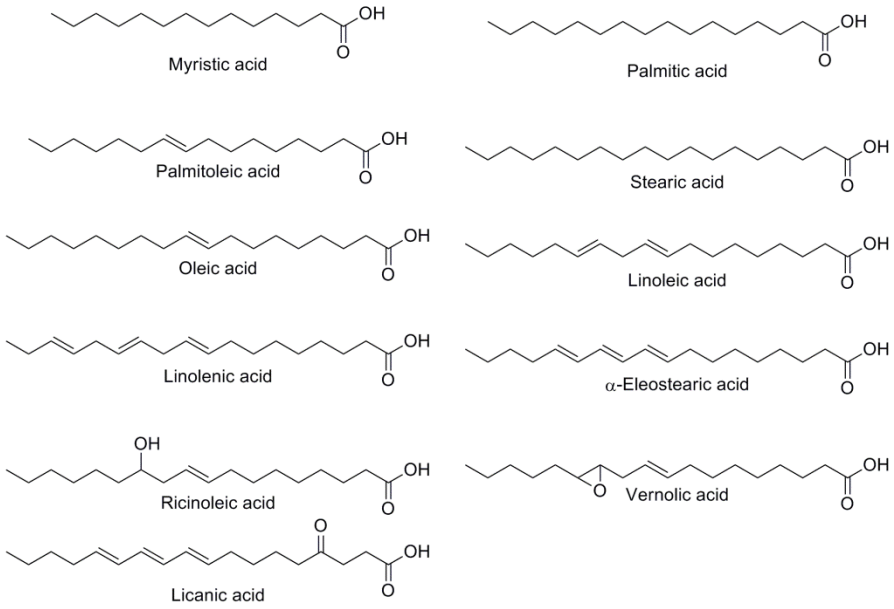

Figure 10. Typical fatty acids borne by vegetable oil triglycerides.

Main structures of some commonly used vegetable oils are presented in Figure 11.

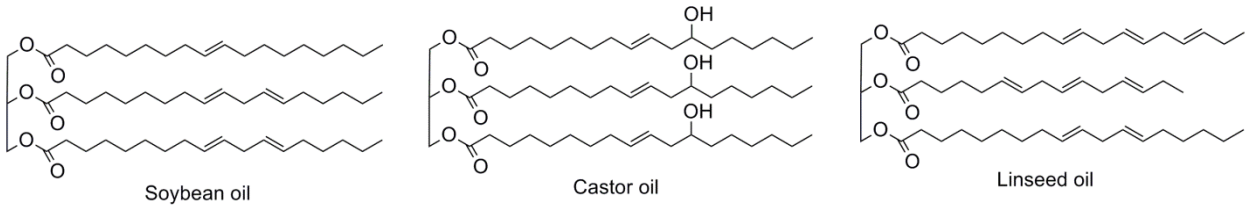

Figure 11. Major structure of some common vegetable oils

Triglycerides contain several reactive positions that are suitable sites to chemical reactions such as C=C double bonds. These can be used for direct polymerization or to modify the triglyceride structure with polymerizable groups to obtain thermosets.

b) Preparation of epoxy prepolymers from vegetable oils

Epoxidation is one of the most important functionalization reaction involving C=C double bonds. The unsaturated fatty compounds can be functionalized by epoxidation with organic peracids or H_2O_2. Park et al performed the epoxidation of soybean oil (Figure 12). Solution of soybean oil, glacial acetic acid, Amberlite and toluene were heated at a constant temperature of 55°C. Then H_2O_2 was added and the solution was heated at 55°C for 7 h. After the reaction was completed the crude product was filtered and washed with distilled water until pH 7.0. The oil phase was dried with anhydrous sodium sulphate and then filtered. Finally, the toluene was removed in a vacuum oven at 80°C. The yield of the reaction was 89 % [37].

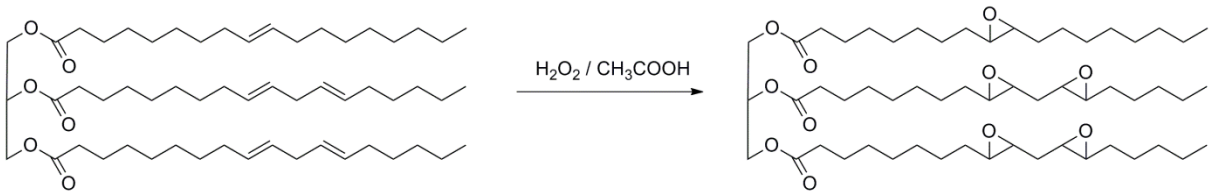

Figure 12. Epoxidation of soybean oil [37]

Vegetable oils differ by the structure of their fatty acids (number of insaturations, presence of –OH groups…) therefore the resulting epoxidized vegetable oils differ by the number of oxirane groups, molar mass and other moieties like –OH groups, and present different reactivities. Some common vegetable oils are presented in Figure 13. Epoxidized vegetable oils with higher level of oxirane groups, such as epoxidized linseed oil, ELO, should give networks with higher crosslinking densities [38-40].

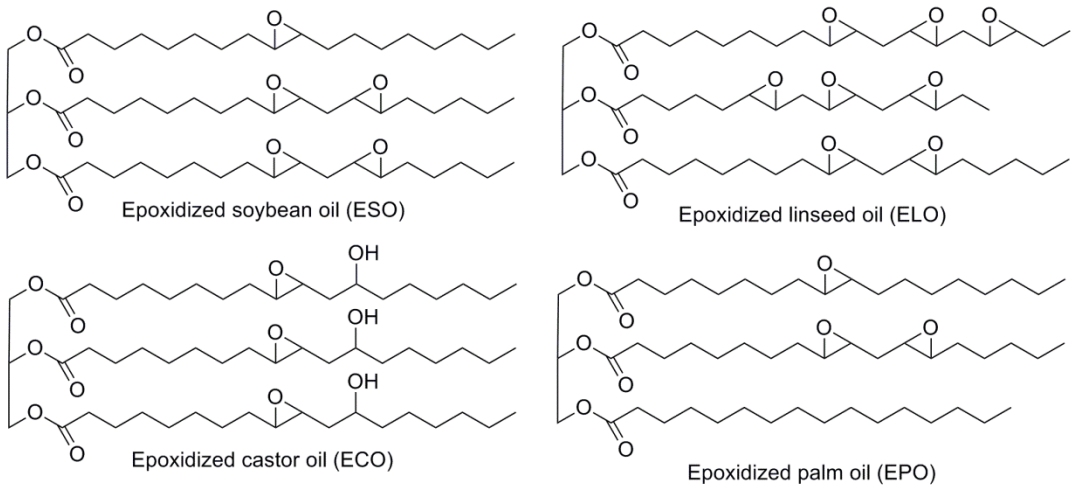

Figure 13. Epoxidized vegetable oils

c) Epoxy networks derived from vegetable oils

Several researchers have investigated the synthesis and mechanical characterization of networks based on epoxidized vegetable oil epoxy monomers using various approaches. Examples are given below of researches on the replacement, either partial or total, of conventional epoxy prepolymers by different epoxidized vegetable oils and the characterization of resulting epoxy networks obtained with various curing agents.

Park et al. [37, 41] synthesized and characterized epoxidized soybean oil (ESO) and epoxidized castor oil (ECO) (Figure 13). The cationic polymerization of epoxidized soybean oil (ESO) and epoxidized castor oil (ECO) with a latent thermal initiator BPH, which structure is shown in Figure 14, was performed at 110°C for 1 h, then at 140°C for 2 h, and finally post-cured at 160°C for 1 h.

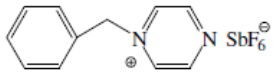

N-benzylpyrazinium hexafluoroantimonate (BPH)

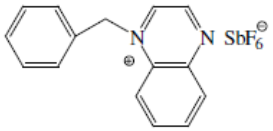

N-benzylquinoxalinium hexafluoroantimonate (BQH)

Figure 14. Chemical structure of thermally latent initiators BPH and BQH [30]

The α-relaxation temperature (T_α) associated to the glass transition temperature (T_g), the storage modulus (G') and the crosslinking density (ρ) calculated using the rubber elasticity theory [42], are summarized in Table 1. ECO/BPH exhibits higher T_α as compared to ESO/BPH, 43°C and 25°C respectively. It is explained by their different structures and the presence of intermolecular interactions such as hydrogen bonding in epoxidized castor oil (ECO) due to the presence of –OH groups. On the contrary the rubbery modulus is higher for the ESO/BPH network, leading to a crosslinking density (ρ) twice the one of ECO/BPH network.

System	T_α	Storage modulus at $T_\alpha + 30$ °C	ρ
	°C	10^9 Pa	10^{-3} mol/cm^3
ESO/BPH	25	0.0147	1.12
ECO/BPH	43	0.0079	0.57

Table 1. Results from a dynamic mechanical analysis of the cured Epoxidized Soybean Oil (ESO)/BPH and Epoxidized Castor Oil (ECO)/BPH systems [37]

The authors also focus on the influence of the initiator, using both BPH and BQH thermally latent initiator (Figure 14) for the cationic polymerization of epoxidized castor oil (ECO) [30]. The results are given in Table 2.

System	T_α (°C)	Storage modulus (GPa)		ρ (10^{-3} mol/cm^3)
		Glassy region[a]	Rubbery region[b]	
ECO/BPH	43	0.36	0.014	1.01
ECO/BQH	39	0.25	0.009	0.84

[a] Storage modulus at 30 °C.
[b] Storage modulus at $T_\alpha + 30$ °C.

Table 2. Results from a dynamic mechanical analysis of cured Epoxidized Castor Oil with either BPH or BQH [30]

The α relaxation is slightly higher for ECO/BPH than for ECO/BQH. It has been attributed to the differences in crosslinking density of cured networks, which were induced by the different activity of the latent initiator.

Yet glass transition temperature values obtained for these bio-based epoxy systems are very low as compared to a DBEGA-based epoxy system, and pure epoxidized vegetable oils-based epoxy systems could not lead to high T_g-materials. Therefore many authors studied blends of classical epoxy prepolymer such as DGEBA, with various amount of epoxidized vegetable oils.

Indeed, Park et al. [41, 43] prepared biobased materials from DGEBA and epoxidized vegetable oils, such as epoxidized soybean oil (ESO) and epoxidized castor oil (ECO), initiated by the thermally latent initiator BPH. Again, the results of α-relaxation temperature (T_α) and storage modulus (G') and crosslinking density (ρ) for these systems are listed in Table 3.

EVO	EVO content (wt%)	T_g (°C)	Storage modulus (10^9 Pa) 35 °C	Storage modulus (10^9 Pa) $T_g + 30$ °C	ρ (10^{-3} mol cm^{-3})
Neat	0	204	1.50	0.098	7.71
ESO	20	159	1.60	0.077	6.17
ESO	40	127	1.49	0.061	5.70
ESO	60	95	0.95	0.049	4.91
ESO	80	55	0.26	0.034	3.82
ECO	20	150	1.45	0.060	5.32
ECO	40	119	1.52	0.041	3.91
ECO	60	94	1.26	0.032	3.25
ECO	80	62	0.56	0.018	1.99

Table 3. Results from a dynamic mechanical analysis for DGEBA/Epoxidized Vegetable Oils systems [41]

The T_α (associated to T_g) and crosslinking density (ρ) of the DGEBA/epoxidized vegetable oils-based networks are systematically decreased with increasing epoxidized vegetable oils content. This can be attributed to the addition of long soft segments of epoxidized vegetable oils into the epoxy networks, which decreases its rigidity, resulting in increased motion of the macromolecular segments in the DGEBA/epoxidized vegetable oils systems.

Miyagawa et al. [39] reported the thermophysical and impact properties of networks based on Diglycidyl Ether of Bisphenol-F (DGEBF) and different amount of epoxidized linseed oil (ELO) presenting high amount of oxirane groups.

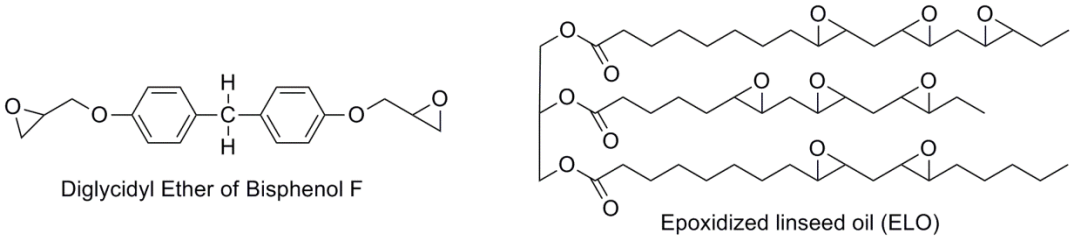

Figure 15. Chemical structure of DGEBF and Epoxidized Linseed Oil (ELO)

Other crosslinking reactions, as compared with Park et al. studies, are involved here, as Miyagawa used on one hand an anhydride (Methyltetrahydrophthalic Anhydride, MTHPA) as curing agent and an imidazole as initiator [44], and on the other hand a triamine curing agent [45].

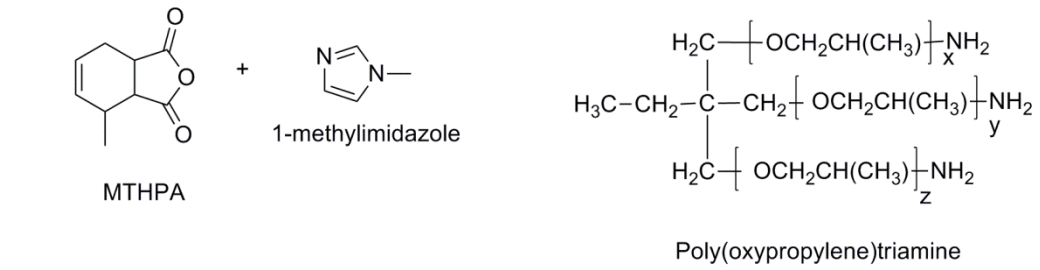

Figure 16. Chemical structure of anhydride curing agent, with methylimidazole initiator, and amine curing agent used by Miyagawa [44, 45]

All the partially bio-based networks were characterized and compared with DGEBF-based network obtained in the same conditions (curing agent, crosslinking cycle). It appears that the storage modulus in the glassy state and glass transition temperature (α-relaxation) decreased with increasing the amount of epoxidized linseed oil. Besides, α-relaxation (associated to T_g) became very broad.

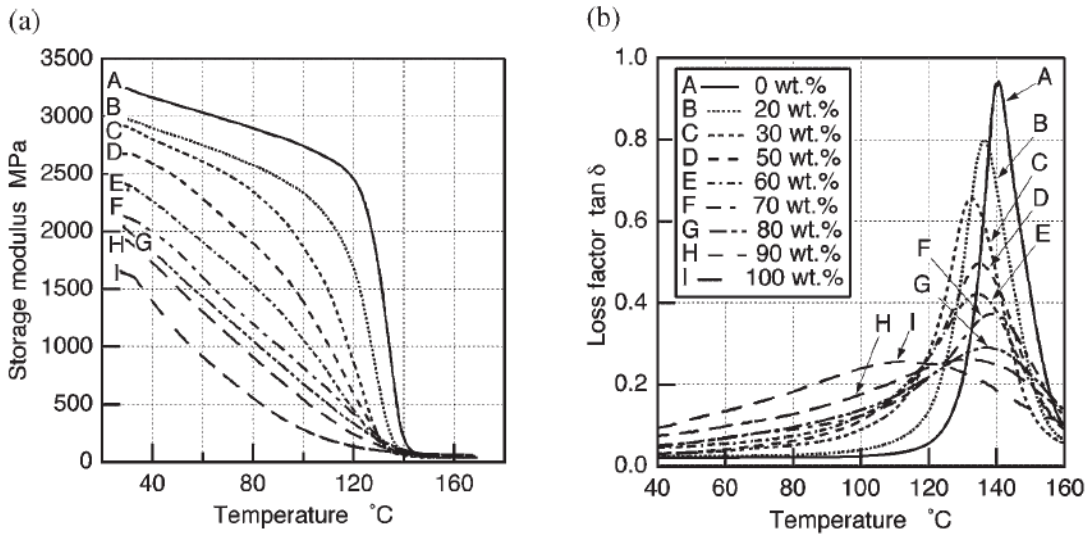

Figure 17. Evolution of a. storage modulus and b. loss factor with the mount of Epoxidized Linseed Oil (wt%) in DGEBF-anhydride cured system

Another point is the influence of the hardener, anhydride or amine, in Miyagawa studies [44, 45]. It appears that a larger decrease of T_α was observed using amine curing agent, as shown in Figure 18. This can be attributed to the structure of the aliphatic amine, poly(oxypropylene) triamine, used in the study.

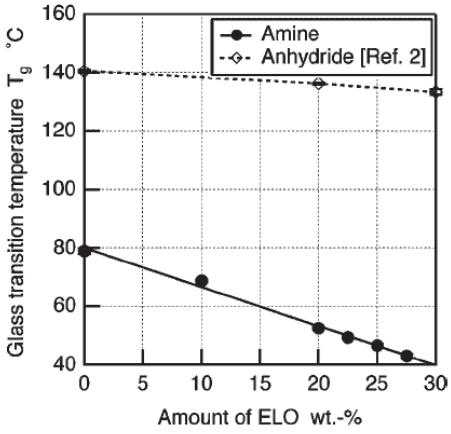

Figure 18. Change in glass transition temperature of amine-cured epoxy with Epoxidized Linseed Oil (ELO) replacing DGEBF (solid line) – compared with anhydride cured epoxy (dashed line) [45]

Same anhydride curing agent, MTHPA, was used in the study of partial replacement of DGEBA by epoxidized soybean oil (ESO) [46]. The DSC thermograms for different weight epoxidized soybean oil contents are shown in Figure 19. The addition of epoxidized soybean oil to the DGEBA – MTHPA mixture changed the shape of the exothermic peaks. Two partially overlapped peaks were clearly distinguished, particularly for epoxidized soybean oil contents higher than 40 %. The addition of increasing amounts of epoxidized soybean oil also shifted the maximum temperature of the first exothermic event to higher values. This result was attributed to the less reactive oxirane rings centrally placed in long aliphatic chains of epoxidized soybean oil.

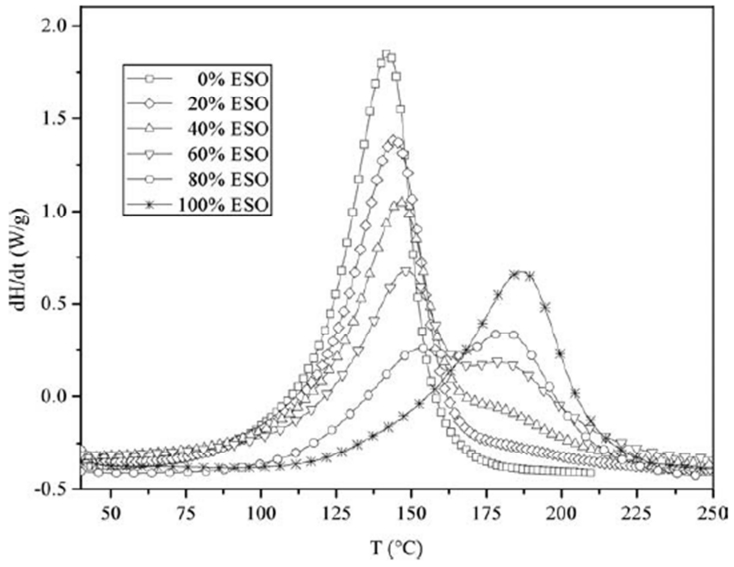

Figure 19. DSC thermograms of the DGEBA- Epoxidized Soybean Oil (ESO) - MTHPA systems [46]

Even if the comparison is difficult as the synthetic epoxy prepolymer replaced is not the same (DGEBA versus DGEBF), it appears that including epoxidized soybean oil leads to a more important decrease in T_α (130°C to 75°C), as shown in Figure 20, as compared to other results with epoxidized linseed oil (see Figure 17). Nevertheless, the networks obtained with epoxidized soybean oil are more homogenous than epoxidized linseed oil-networks with an α-transition less broad than pure epoxidized linseed oil epoxy networks. Besides, introduction of various amount of epoxidized soybean oil seems to have little effect on rubbery moduli.

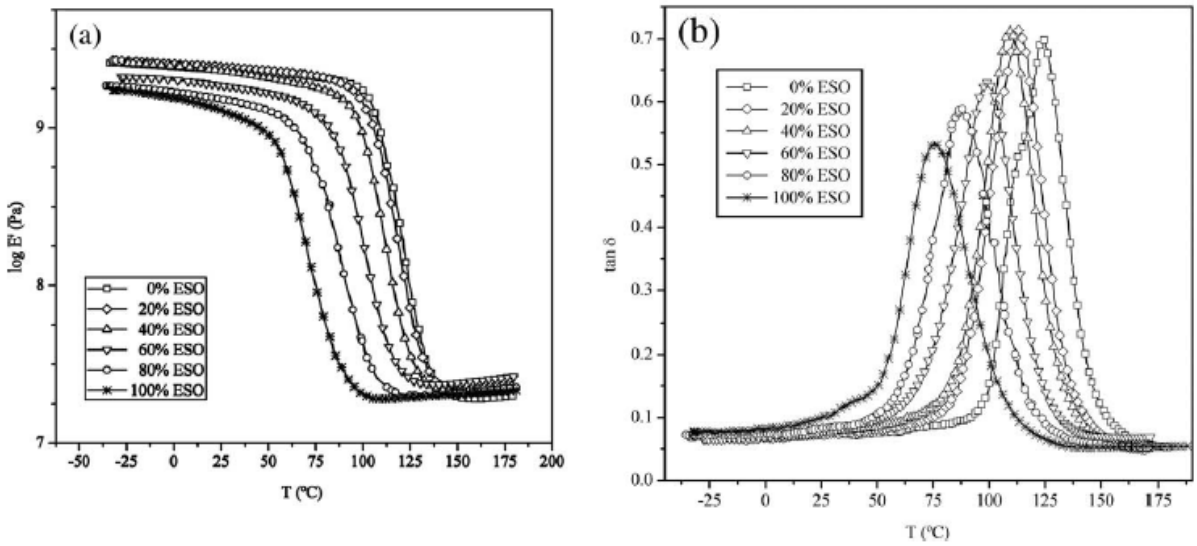

Figure 20. Evolution of a. storage modulus and b. loss factor with the amount of Epoxidized Soybean Oil (ESO) (wt%) in DGEBA-anhydride cured system [46]

Epoxidized linseed oil with a higher amount of oxirane groups leads to epoxy networks with higher T_α than epoxidized soybean oil (pure Epoxidized Soybean Oil (ESO) networks: T_α = 75°C). This was confirmed by Boquillon [40] study on pure epoxidized linseed oil with different anhydride curing agents. Indeed, epoxidized linseed oil – MTHPA network exhibits T_α of 109°C.

Another study was done on the replacement of epoxy prepolymer blends (composed of DGEBA and other petrochemical-based epoxy prepolymers) by different amount of epoxidized palm oil (EPO, Figure 13) in anhydride (Methylhexahydrophthalic anhydride, MHHPA) cured epoxy systems [47]. It appears that the thermo-mechanical behaviours were greatly influenced by the addition of epoxidized palm oil. As an example, the replacement of only 12 wt % of epoxy prepolymer blend by epoxidized palm oil brings a decrease on T_α from 155°C, for neat epoxy system, to 130°C. This can be attributed to the presence of palmitic

fatty acid (see structure Figure 10), in epoxidized palm oil structure, that exhibits no oxirane groups, and remains as a pending flexible chain in the networks structure.

Because of the low reactivity of epoxy groups, its tendency for intramolecular bonding, and the lack of aromatic cycles (as compared to DGEBA for instance), any epoxidized oil leads to poorly cross-linked materials with limited thermal and mechanical properties.

To alleviate this problem, attempts to chemically modify epoxidized oils have been carried out through a two-step procedure [48-50]. This consists to perform transesterification reactions of soybean oil with allyl alcohol, followed by their epoxidation using benzoyl peroxide, yielding epoxidized allyl soyate (EAS) (Figure 21).

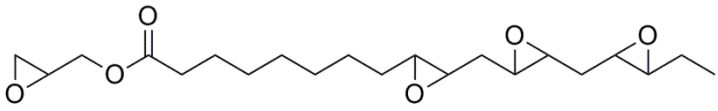

Figure 21. Epoxidized allyl soyate (EAS) [50]

Shabeer et al. [50] have used this soy-based epoxy prepolymer as a replacement of bisphenol A epoxy prepolymer in anhydride-cured systems. The DSC thermograms (Figure 22) showed that the onset temperature for curing and the temperatures of maximum exotherm heat shifted to higher temperatures for soy epoxy systems when compared with pure bisphenol A epoxy systems. This is due to the presence of less reactive internal epoxy groups present in soy epoxy prepolymer. Nevertheless, this decrease in reactivity is weaker than the one observed for the replacement of DGEBA by conventional epoxidized vegetable oils (see Figure 19).

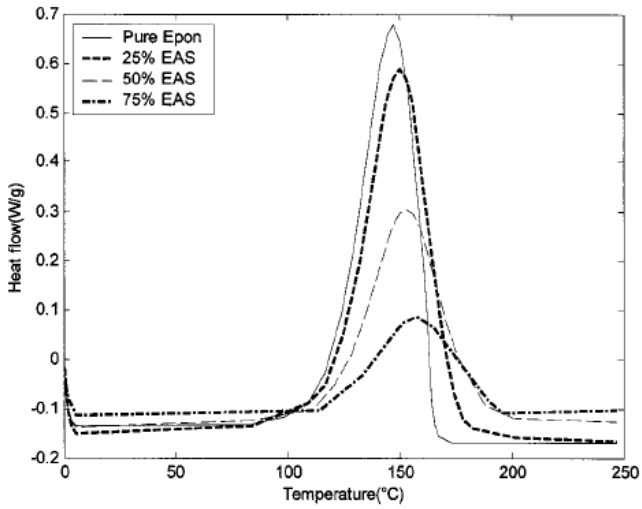

Figure 22. Dynamic thermograms of soy epoxy (EAS) - anhydride systems. (Epon = DGEBA) [50]

Concerning the thermo-mechanical analyses (Table 4), it appears that the crosslinking densities and the α-relaxation of networks decreased with the addition of soy-based prepolymer.

Sample	Crosslinking density, ν_e (mol/m^3)	Molecular weight between crosslinks, M_c (g/mol)	Glass transition temperature, T_g (°C) (from loss tangent curves)
Pure Epon	6426	198	90
25% EAS	5412	224	81
50% EAS	4019	295	66
75% EAS	2805	401	40.5

Table 4. Crosslinking density, Molecular weight between crosslinks, Glass transition temperature of Soy epoxy (EAS) anhydride networks [50] (Epon = DGEBA)

Finally, interesting study have been done by Caillol et al [51] on the synthesis of a novel vegetable oil-based polyamine issued from grapeseed oil (GSO). Synthetic route is summarized in Figure 23 .

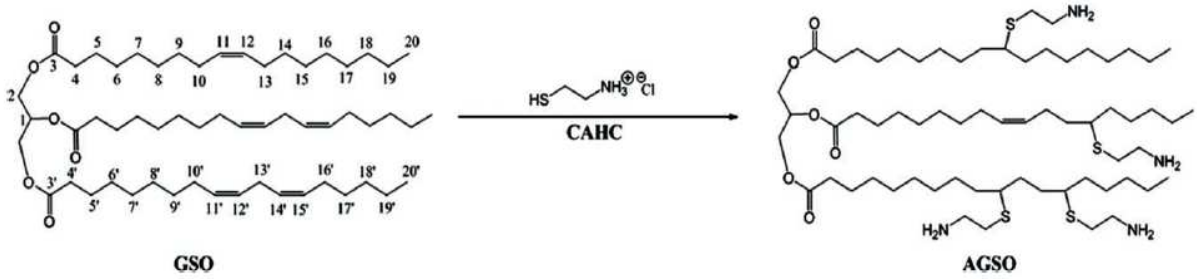

Figure 23. Synthesis of polyamine grapeseed oil (AGSO) : Amination of grapeseed oil (GSO) using cysteamine chloride (CAHC) by UV initiated thiol-ene coupling [51]

Polyamine grapeseed oil (AGSO) was employed as a novel curing agent for epoxidized linseed oil (ELO), yielding a fully bio-based network.

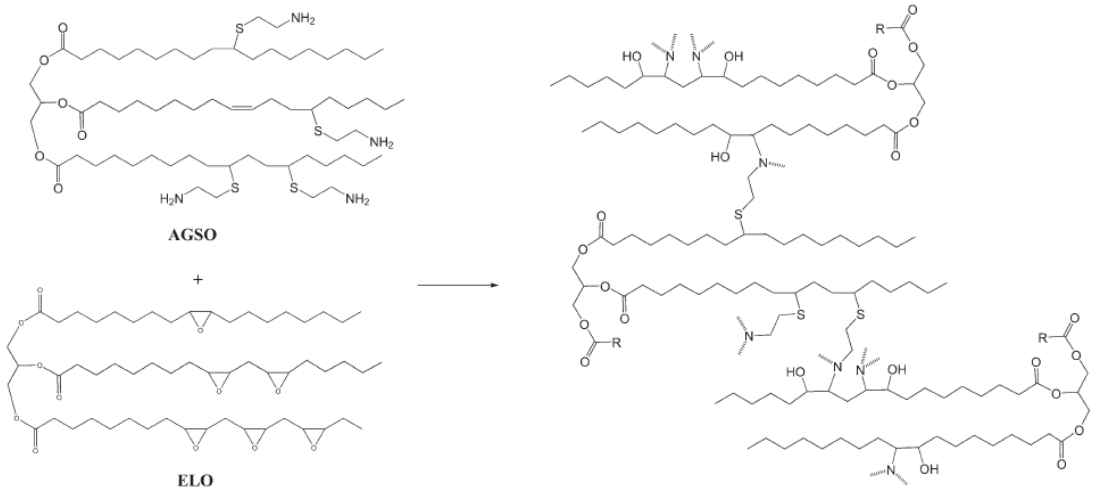

Figure 24. Crosslinking reaction between epoxidized linseed oil (ELO) and polyamine grapeseed oil (AGSO) [51]

The α-relaxation temperature of the bio-based network was very low (T_α = -38°C by DMA). This value is much smaller than the one obtained for epoxidized linseed oil with an anhydride hardener such as MTHPA (T_g = 109°C [40]). This discrepancy was interpreted as a direct consequence of the much higher molecular flexibility of the polyamine grapeseed oil (AGSO) curing agent compared to MTHPA.

d) Conclusion

Bio-based epoxy prepolymers can be successfully developed from vegetable oils, and hold great potential for renewable resource-based and low cost materials.

However, we try to focus on the influence of vegetable oil structures on the solid-state properties of resulting materials. Triglycerides are made up of aliphatic chains and, consequently, the triglyceride-based materials, are incapable of displaying the necessary rigidity and strength required for high-performance applications, for example in composite materials.

First, it appears that epoxidized vegetable oils are miscible with DGEBA as the resulting networks exhibit a single T_g. Nevertheless, formulations with different curing agents such as anhydrides, amines and other polymerization such as cationic polymerization always lead to materials with a decrease in thermo-mechanical properties as compared with traditional epoxy networks, based on DGEBA or DGEBF. It has been shown also that developing epoxy networks with high unsaturated fatty acid triglycerides, such as linseed oil, brings higher results in terms of T_g than epoxy networks developed from palm oil, which exhibits composition with high amount of palmitic fatty acid. Nevertheless, conventional epoxy networks have higher properties.

As a consequence, most industrial applications for the resulting epoxy materials remain limited to non-structural applications like coatings. Still, interesting developments remain to be done the synthesis of fully bio-based epoxy networks, with epoxy prepolymers and curing agents based on vegetable oils [51].

2. Biobased epoxy networks derived from cardanol

a) Extraction of cardanol from cashew nut shell liquid

Among different renewable resources, cashew nut shell liquid, an agricultural by-product abundantly available in tropical countries such as India, Vietnam… is one of the major and economical resources of naturally occurring phenols. Cashew nut shell liquid (CNSL) can be regarded as a versatile and valuable raw material for wide applications in the form of brake linings, surface coatings, paints, and varnishes as well as in polymer production. The cashew nut shell liquid contains four major components with an unsaturated C15-chain, namely cardanol, cardol, anacardic acid and 2-methylcardol (Figure 25).

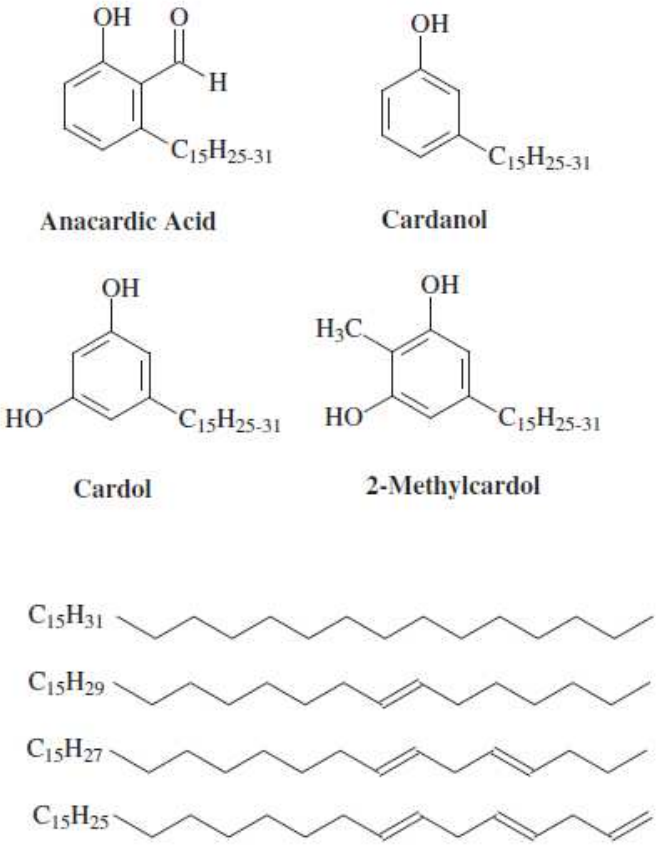

Figure 25. Natural compounds present in the cashew nut shell

Cardanol is obtained by vacuum distillation of cashew nut shell liquid. Cardanol is a phenol with a meta-substituted 15 carbon unsaturated side chain. As shown in Figure 25, the aliphatic side chain may have one, two or three carbon double bonds. It was found that

cardanol and its polymers have attractive structural features for chemical modification and polymerization into specialty polymers.

b) Synthesis of cardanol-based monomers

Cardanol through its interesting structure offers different possibilities for monomers synthesis (phenolic polymers, epoxy…) and have been the subject of many investigations.

Main researches on cardanol focused on its use as an interesting precursor for synthesis of phenolic polymers. In the condensation polymerization process, cardanol can be condensed with active hydrogen-containing compounds such as formaldehyde at the ortho and para positions of the phenolic ring under acidic conditions to yield a series of polymers of "novolac" type [52-55].

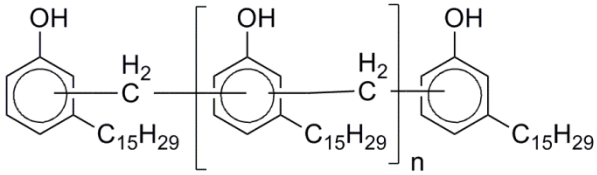

Figure 26. Cardanol-based novolac-type phenolic resin [52, 53, 55]

The cardanol-based novolac-type phenolic polymers may be modified by epoxidation with epichlorohydrin. Epoxydation of cardanol phenolic prepolymers yields epoxy novolac with the aromatic and aliphatic structure shown in Figure 27.

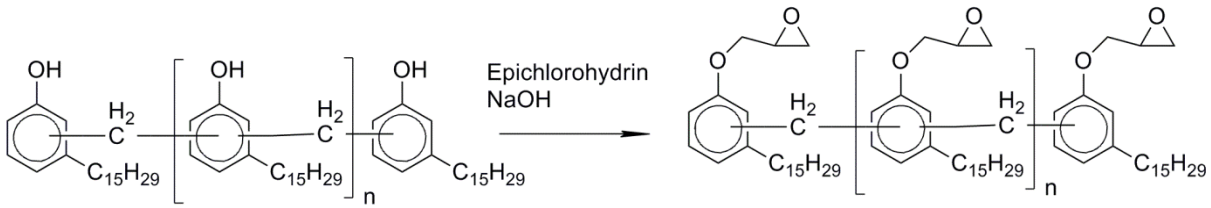

Figure 27. Epoxidation of cardanol novolac-type phenolic resin to obtain cardanol-based epoxidized novolac resin [52, 54, 55]

Fewer researches have concerned the direct use of cardanol as monomer for epoxy prepolymer synthesis.

First, Patel et al. [56] synthesized the diepoxidized cardanol (DEC) with an epoxy equivalent weight of 284.3 g/eq. It exhibits two epoxide groups, one of glycidyl type, introduced by reaction of a hydroxyl group in cardanol with epichlorohydrin, while the other is produced by epoxidation at the olefinic double bond using preformed peroxyacid.

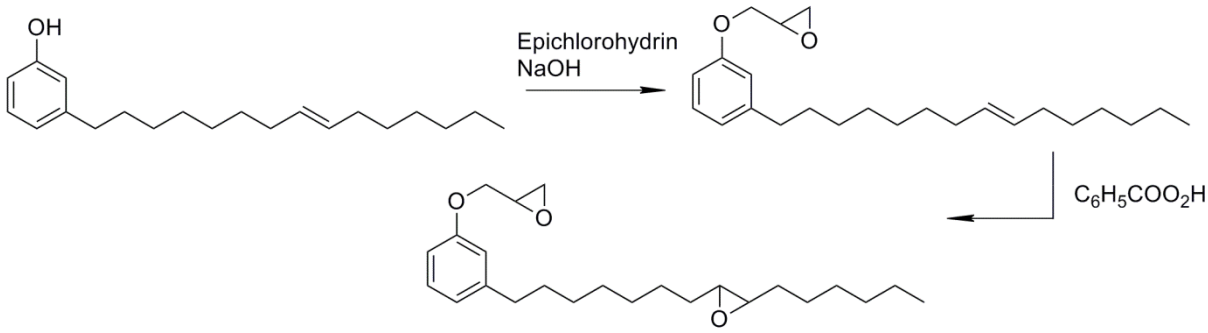

Figure 28. Synthesis of diepoxidized cardanol [56]

Various cardanol based dimers can also be formed by hydrosilation with silanes [57]. Cardanol based dimers may be further reacted to form epoxy prepolymers. Example of epoxy derived from cardanol based dimers is presented below.

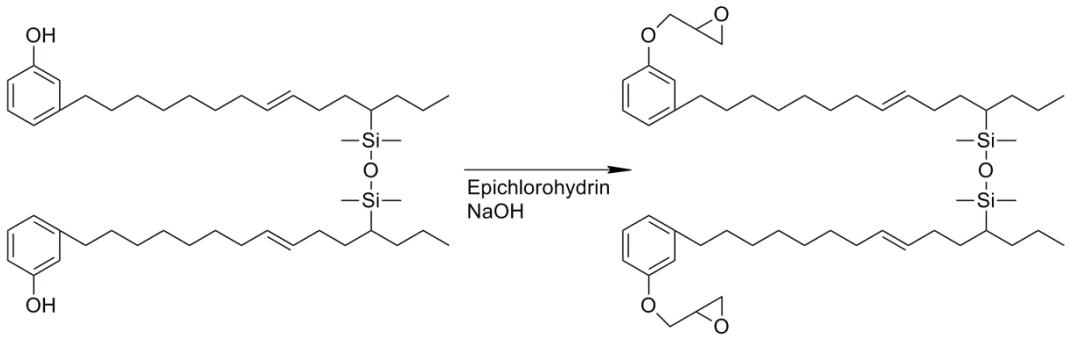

Figure 29. Cardanol-based silane dimers and resulting epoxy prepolymer [57]

Finally another interesting epoxy prepolymer derived from cardanol is commercially available from the company Cardolite (Figure 30) with an epoxy equivalent weight of 490 g/eq. This di-functional reactive epoxy prepolymer with its phenolic structure and aliphatic chain should be used in conjunction with traditional epoxy monomers to increase the flexibility, water resistance, and chemical resistance of coatings without adversely affecting other properties.

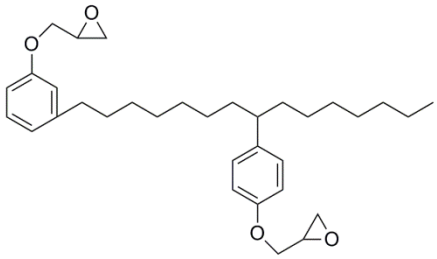

Figure 30. Commercial di-functional epoxy derived from cardanol

c) Epoxy networks derived from cardanol

The investigations done on networks containing cardanol-derived epoxy prepolymers mainly concern the influence of epoxidized cardanol used as reactive diluent on the curing kinetics of the system.

Indeed, the curing behavior of DGEBA with various amount of diepoxidized cardanol (DEC, see Figure 28), with phthalic anhydride (PA) as curing agent and catalyst triethylamine (TEA) was investigated by Patel et al. [56]. Curing characteristics such as the temperatures of onset of curing (T_i), peak exotherm (T_p) and completion of curing (T_f) were obtained by DSC analyses and summarized in Table 5 with the activation energy (E_a) obtained from the Arrhenius plots for these systems. It is observed that the incorporation of diepoxidized cardanol with DGEBA lowers slightly the reactivity of the epoxy system with an increase in the peak exotherm temperatures and activation energies with the amount of diepoxidized cardanol (DEC).

Resin system	Proportions	T_i (°C)	T_p (°C)	T_f (°C)	E_a (kJ/mol)
DGEBA	100 : 0	95	153	190	78.6
DGEBA-DEC	90 : 10	95	155	190	81.8
DGEBA-DEC	80 : 20	98	158	205	84.4
DGEBA-DEC	70 : 30	100	160	200	87.9

Table 5. Curing characteristics of DGEBA with different amounts of diepoxidized cardanol (DEC) epoxy systems with phthalic anhydride (PA) as curing agent and triethylamine (TEA) as catalyst [56]

Apart from having several outstanding characteristics, traditional epoxy networks show low impact resistance. To alleviate this deficiency, one approach is to modify epoxy

systems with the incorporation of reactive liquid rubber without significant loss in other properties. It is well known that in such systems the additive will phase separate from the epoxy matrix and will form spherical particles of a few μm in size. Carboxyl-terminated poly(butadiene-co-acrylonitrile) (CTBN) liquid rubber was used with DGEBA and epoxidized phenolic novolac prepolymers (see Figure 27). Srivastava et al. [52, 54, 55], tried to produce the modified epoxy matrices, based on cardanol, by physical blending with liquid rubber (CTBN) [52, 54] and studied the effect of CTBN addition on mechanical properties changes in the blends cured with stoichiometric amounts of polyamine curing agent. The variation of tensile strength, impact strength and elongation at break is shown in Table 6.

A gradual fall in tensile strength was noted with the increase of liquid rubber content, due to the increase in the relative amount of dissolved rubber in the matrix. The percent elongation-at-break of the blend samples increased continuously with CTBN content. The impact strength showed an abrupt increase up to 15 wt % of CTBN, beyond which it dropped significantly.

Same observation was done with carboxyl-terminated polybutadiene (CTPB) in cardanol-based networks [55] with a maximum impact strength with 15 % CTPB added to the system.

As a remark, no data were available in these studies on the glass transition temperatures of the cardanol novolac networks.

Cardanol-based epoxidized novolac (wt %)	CTBN (wt %)	Tensile Strength (MPa)	Impact Strength (kJ/m^2)	Elongation at break (%)
100	0	283.3	15.6	30.7
95	5	276.7	23.7	38.6
90	10	256.8	30.5	47.4
85	15	191.7	65.6	65
80	20	187.0	33.8	69.5
75	25	178.4	20.5	73.2

Table 6. Mechanical properties of pure cardanol-based epoxidized novolac and its blends with CTBN [52]

d) Conclusions

Because of its interesting structure, cardanol has been mainly studied as a precursor for phenolic polymers synthesis. Nevertheless, various cardanol-based epoxy prepolymers were synthesized, ranging from diepoxidized cardanol to epoxidized cardanol-based novolac phenolic polymers, and have mostly been used in coating applications.

Few mechanical characterizations on cardanol-based epoxy networks have been performed. Blending of reactive-liquid rubber (CTBN) with cardanol-based epoxy novolac systems has shown improvement of properties such as an increase in impact strength and elongation at break (for CTBN content up to 15 %).

Development and thermo-mechanical characterization of pure epoxy system, or blends with DGEBA, based on the diepoxidized cardanol epoxy precursor (Figure 30) should be of interest.

3. Biobased epoxy networks derived from sugar

Sugar is a renewable resource that has the potential to be used as an alternative to petroleum-based polymers. Investigations were done on the synthesis of epoxides based on different carbohydrates based-monomers such as sucrose (Figure 31), sorbitol, maltitol (Figure 34) and isosorbide (Figure 37).

a) Epoxy networks derived from sucrose

Sucrose is a disaccharide composed of glucose and fructose units. The glucose and fructose units are joined by an acetal oxygen bridge in the alpha orientation. The structure is easy to recognize because it contains the six member ring of glucose and the five member ring of fructose. Structure of sucrose is shown in Figure 31.

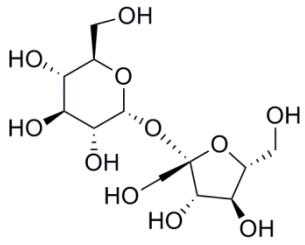

Figure 31. Chemical structure of sucrose

Sucrose–based epoxy monomer, namely, epoxy allyl sucrose (EAS) was prepared by epoxydation of octa-O-allyl sucrose by Sachinvala [58-60]. This involves the methallylation of sucrose using aqueous sodium hydroxide and methallyl chloride, followed by the epoxidation of methallyl intermedium with peracetic acid. The epoxy allyl sucrose was obtained as a mixture of structural isomers and diastereoisomers that contained varying number of epoxy groups per sucrose (Figure 32).

Figure 32. Sucrose base monomers

Sucrose-based epoxy monomer (EAS, 3.7 epoxy groups per sucrose) was cured with diethylenetriamine (DETA) in stoichiometric ratio, and its curing characteristics, glass transition temperatures and temperatures of degradation were determined using DSC and ATG analyses [58]. These characteristics were compared to those obtained on a classical DGEBA/DETA system also in stoichiometric ratio and are summarized in Table 7.

Epoxy	Amine	Curing T_{peak} (°C)	ΔH (kJ/mol)	T_g (°C)	T (°C) Degradation
Epoxy allyl sucrose	DETA	102	98.7	72	327
DGEBA	DETA	97	103.8	134	345

Table 7. Curing, Glass Transition, and thermal degradation characteristic of sucrose-based epoxy and DGEBA with diethylene triamine (DETA) [58]

The peak curing temperature and total heat of cure (ΔH) for DGEBA and epoxy allyl sucrose based systems were approximately the same. Low T_g in epoxy allyl sucrose sample (72°C) can be attributed to flexibility of the chain between crosslinking points. Thermogravimetric analyses (TGA) showed that the DETA-cured polymers containing sucrose-based monomers degraded at lower temperatures than the DETA thermoset

containing DGEBA. This may be attributed to the presence of aromatic structures in DGEBA-based networks.

Recently, novel biobased high functionality epoxy prepolymers were synthesized by the epoxydation of sucrose ester of vegetable oil fatty acids (linseed oil, safflower oil, and two soybean oils with different average degree of substitution) [61]. A general structure of sucrose esters of fatty acids (SEFA) is shown in Figure 33. Sucrose esters of fatty acids were epoxidized by peracetic acid generated in situ from hydrogen peroxide and acetic acid in the presence of ion exchange resin catalyst to produce the epoxidized sucrose esters of fatty acids (ESEFA). The conversion of double bonds to epoxides was greater than 99 %.

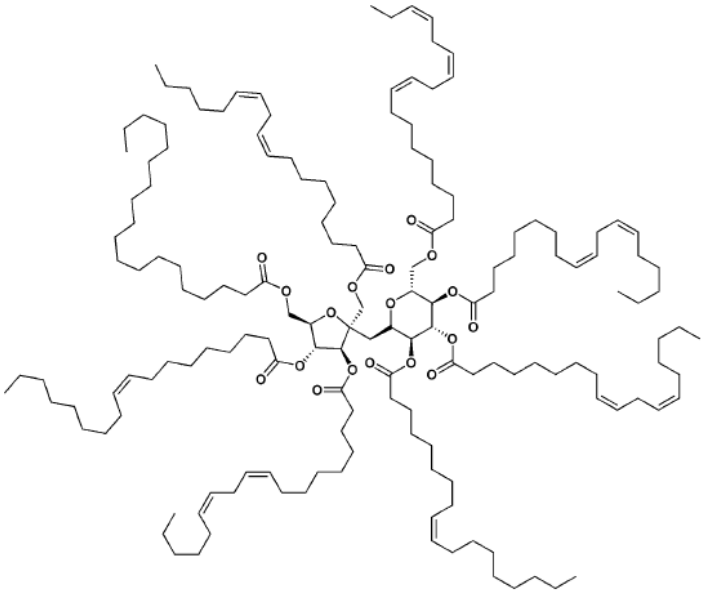

Figure 33. Structure of sucrose esters of fatty acids (SEFA) [61]

Compared with the common fatty epoxy compound-epoxidized vegetable oils, epoxidized sucrose esters of fatty acids (ESEFA) have a rigid sucrose core which can impart hardness to their thermosets, as well as much higher epoxide functionality which can lead to rapid gelation and high crosslink densities.

Indeed, various epoxidized sucrose esters of fatty acids were crosslinked with a liquid cycloaliphatic anhydride (MHHPA) combined with an amine initiator by Pan et al. [62].
We focused on epoxidized sucrose linseedate (ESL), epoxidized sucrose safflower (ESSF) and epoxidized sucrose soyate (ESS). Dynamic mechanical properties and crosslink densities of resulting thermosets compared with network obtained from epoxydized soybean oil (ESO) under the same conditions are summarized in Table 8 (for an epoxide/anhydride ratio 1:0.5).

Epoxy compound	T_α (°C)	E' (MPa) at 20°C	E' (MPa) at T_α + 60°C	ν_e (x 10^3 mol/mm^3)
Epoxidized sucrose linseedate (ESL)	103.7	1500	20.7	1.84
Epoxidized sucrose safflower (ESSF)	71.3	1103	7.7	0.69
Epoxidized sucrose soyate (ESS)	48.4	103	5.6	0.50
Epoxidized soybean oil (ESO)	24.8	36	3.1	0.28

Table 8. Dynamic mechanical properties and crosslink densities of epoxy-anhydride thermosets

The α-relaxation temperatures range from 48°C to almost 104°C with a high T_α value of 104°C for the network obtained from epoxidized sucrose linseedate (ESL).

In all the cases, the epoxidized sucrose esters of fatty acids offer T_α higher than the one obtained for epoxidized soybean oil (ESO)-based network. Besides, higher moduli in the glassy and the rubbery state are obtained for the epoxidized sucrose esters of fatty acids-based networks.

b) Epoxy networks derived from maltitol and sorbitol

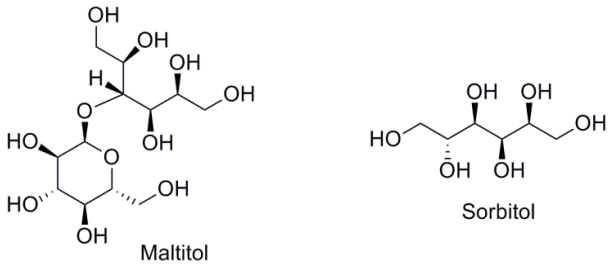

Figure 34. Chemical structure of maltitol and sorbitol

Natural saccharides such as sorbitol and maltitol (Figure 34) were converted by Acierno et al. [63] in multifunctional epoxy monomers to produce epoxy metallyl sorbitol (EMSo) and epoxy metallyl maltitol (EMM). By using an aliphatic trifunctional amine, diethylene-triamine (DETA), as hardener a new generation of epoxy biobased networks were obtained. Epoxy metallyl sorbitol and epoxy metallyl maltitol were prepared using the method of Sachinvala [58] previously described for sucrose epoxidation.

Dynamic-mechanical properties of bio-based epoxy were compared with traditional petroleum-based networks derived from DGEBA prepolymers cured under the same conditions. Storage modulus (E'), α relaxation temperatures (T_α) and experimental

crosslinking densities (ν_e), calculated with the rubber elasticity theory [42], were determined by DMA. Values are reported in Table 9.

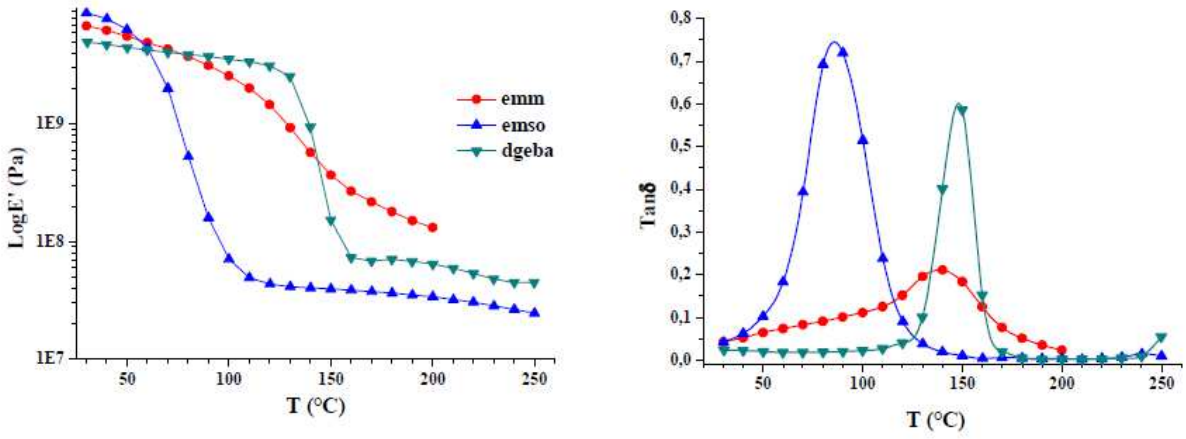

Figure 35. Comparison of E' and tanδ vs temperature at 1 Hz for epoxy networks from epoxy metallyl maltitol (EMM), epoxy metallyl sorbitol (EMSO) and DGEBA epoxy prepolymers.

Epoxy	$E'_{T\alpha + 30°C}$ (MPa)	T_α (°C)	ν_e (mol/dm^3)
EMM	220	140	16.8
EMSo	40	90	3.8
DGEBA	70	150	5.9

Table 9. Dynamic mechanical properties of epoxy metallyl maltitol (EMM), epoxy metallyl sorbitol (EMSo) and DGEBA based epoxy networks [63]

At room temperature, thermosets derived from epoxy saccharides EMSo and EMM exhibit a storage modulus higher than DGEBA. Bio-based networks do not show a clear glassy plateau but their storage modulus quickly decreases as temperature increases becoming lower than that of the DGEBA one for temperatures equal to 80°C and 65°C for epoxy metallyl maltitol (EMM) and epoxy metallyl sorbitol (EMSO) respectively. About the rubbery region, epoxy metallyl sorbitol and DGEBA get to a plateau steady rubber state indicating the stability of networks while epoxy metallyl maltitol based ones show a continuous diminishing modulus probably because an highly heterogeneous crosslinked network was formed containing regions with different crosslinking density where the branched chains have different segmental mobility depending on the amount of crosslinks. The broadness of the α-transition for EMM/DETA network confirms the coexistence of regions with different micro-

structural characteristics. Besides, the conventional DGEBA-based network exhibits the higher α-relaxation temperature.

Other epoxy networks based on sorbitol were studied by Shibata et al. [64]. They have prepared biocomposites composed of bio-based epoxy prepolymer derived from sorbitol (Sorbitol Polyglycidyl ether SPE, commercial reference: Denacol 614B) with a bio-based hardener, tannic acid (TA), and microfibrillated cellulose as filler. The curing reaction of sorbitol polyglycidyl ether with tannic acid was performed by solubilizing the two products in stoichiometric ratio in ion-exchange water; both compounds were soluble in water. The homogenous solution was freeze-dried to remove water and cured at 50°C during 12 h and post cured at 200°C for 2 h.

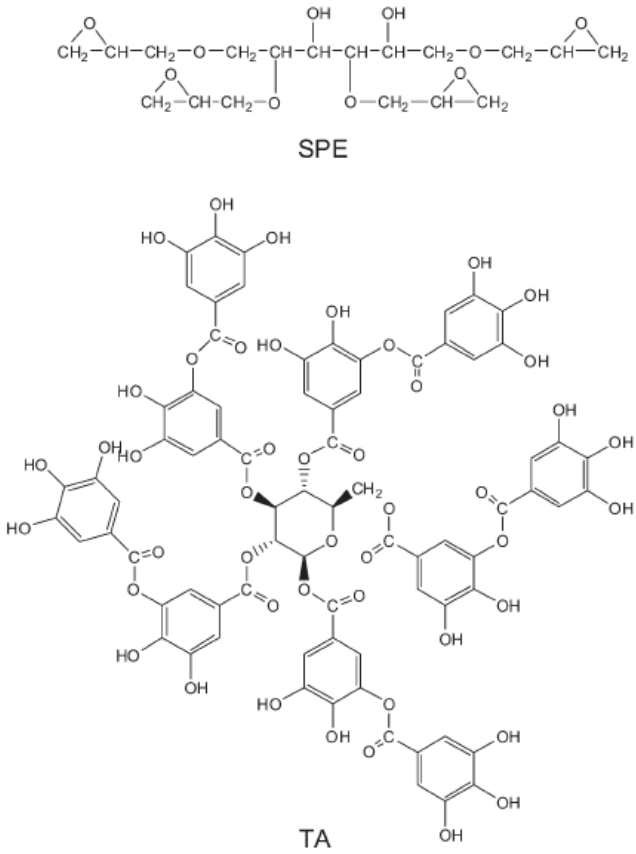

Figure 36. Some of the reagents used in Shibata study : sorbitol polyglycidyl ether (SPE) and tannic acid (TA) [64]

The curing conditions were optimized for the improvement of thermal and mechanical properties; the most balanced properties were obtained for the SPE/TA cured at 160°C for 2-3 h at the epoxy/hydroxyl ratio of 1/1. Under these specific conditions the bio-based epoxy networks SPE/TA had a glass transition temperature of 80°C (measured by DMA analysis).

The sorbitol polyglycidyl ether used in this study is a commercial one obtained by a classical epoxidation involving epichlorohydrin, different from the sorbitol-epoxy prepolymer prepared by Acierno [63]. Nevertheless, as no comparison is done with DGEBA cured under the same conditions for Shibata study, these two sorbitol polyglycidyl ethers cannot be compared.

c) Epoxy networks derived from isosorbide

1,4:3,6-dianhydrohexitols and derivatives

1,4:3,6-dianhydrohexitols are cereal-based chemicals which exhibit rigid structures, chirality and non-toxicity. For these reasons there are expectations that polymers, based on these molecules, with high glass transition can be synthesized [10].

Depending on the chirality, three isomers of the 1,4:3,6-dianhydrohexitols (DAH) exist, namely isosorbide, isomannide and isoidide (Figure 37). The 1,4:3,6-dianhydrohexitols are composed of two cis-fused tetrahydrofuran rings, nearly planar and V-shaped. The hydroxyl groups are positioned on either inside or outside the V-shaped molecule. They are designed, respectively, as endo or exo. Isoidide has two exo hydroxyl groups, whereas for isomannide they are both endo, and for isosorbide there is one endo and one exo hydroxyl group. The three isomers exhibit different reactivities, because of the different reactivities of endo and exo hydroxyl groups, which are more or less accessible, and the existence of intramolecular hydrogen bonds.

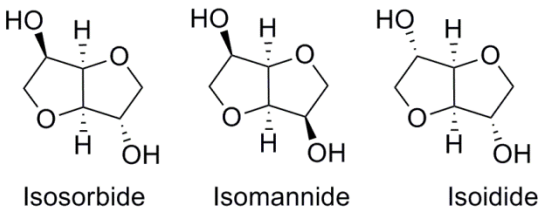

Figure 37. Structures of 1,4:3,6-dianhydrohexitols

Among the three isomers, isosorbide or dianhydrosorbitol (DAS) is the only produced at an industrial scale. Isomannide, is less studied because of its lower reactivity. Finally, the

third isomer isoidide, which is the more reactive, and thus should be the more attractive, remains an expensive monomer because of its difficult extraction from vegetal biomass.

Therefore researches on dianhydrohexitol mainly focused on isosorbide. Isosorbide is a platform chemical of considerable importance for the future replacement of fossil resource-based products [65].

Synthesis of isosorbide-based epoxy monomers

The first polyethers from 1,4:3,6-dianhydrohexitols derivatives were described by Morrison et al. [66]. They synthesized polyglycidyl ethers by reacting isosorbide or isomannide with an excess of epichlorohydrin in the presence of strong alkali, such as sodium hydroxide in a single-stage reactor with continuous removal of water (Figure 38). The epoxy monomers obtained were water soluble, with an epoxy equivalent of 0.467 (isosorbide based) to 0.475 (isomannide based) per 100 g of prepolymer.

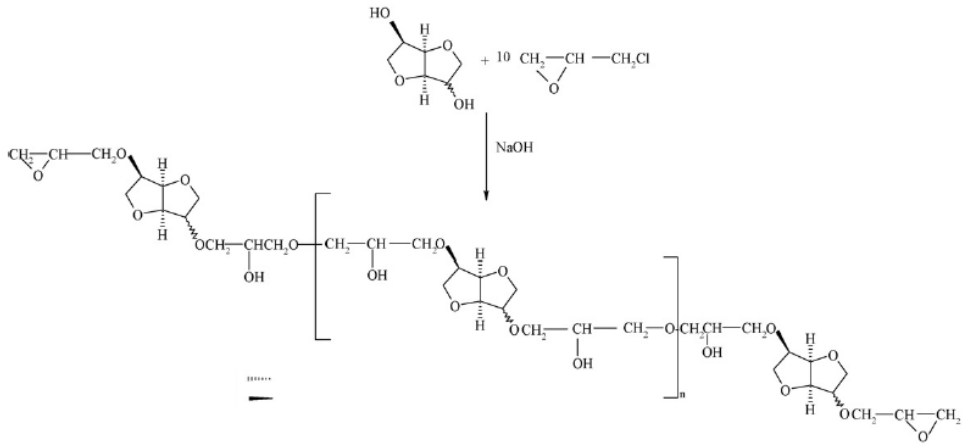

Figure 38. Synthesis of poly(glycidyl ether)s according to Ref. [66]

Pure diglycidyl ethers of isosorbide, isomannide and isoidide were prepared by Zech and Maistre [67]. They used sodium hydride as base in diglyme and a large excess of epichlorohydrin (Figure 39).

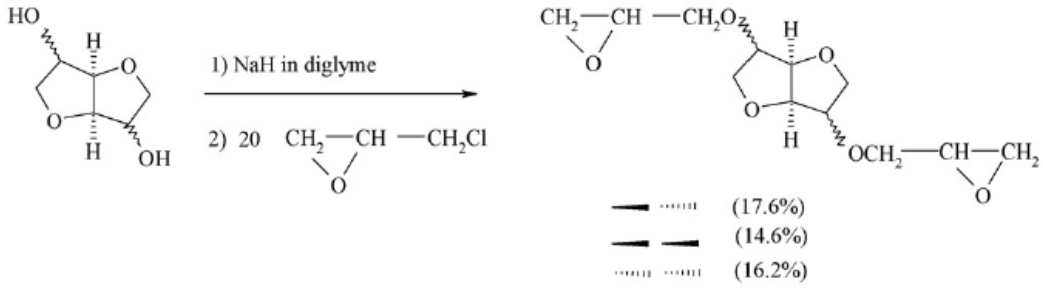

Figure 39. Synthesis of pure diglycidyl ether of isosorbide, isomannide and isoidide according to Ref. [67]

More recently East et al. [6, 68, 69] prepared bis-isosorbide diglycidyl ether by heating isosorbide with 50 % sodium hydroxide solution and a large excess of epichlorohydrin, which was used to azeotrope off the water. Two equivalent isosorbide were linked by three molecules of epichlorohydrin to form the epoxide dimer, as shown in Figure 40.

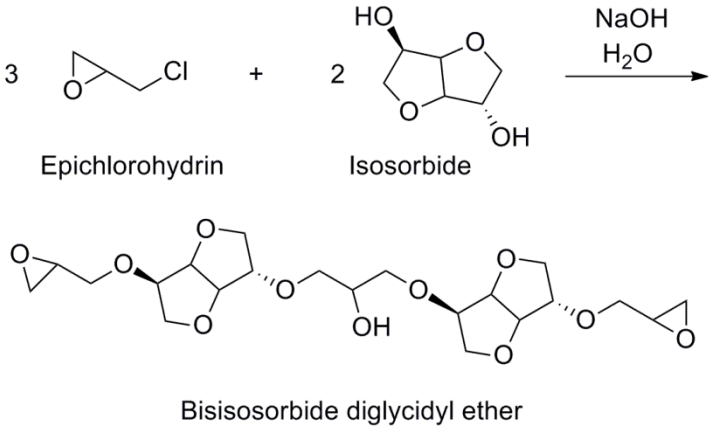

Figure 40. Synthetic route of bisisosorbide diglycidyl ether [6]

East et al. also synthesized the pure diglycidyl ether of isosorbide through its allylic derivative as shown in Figure 41.

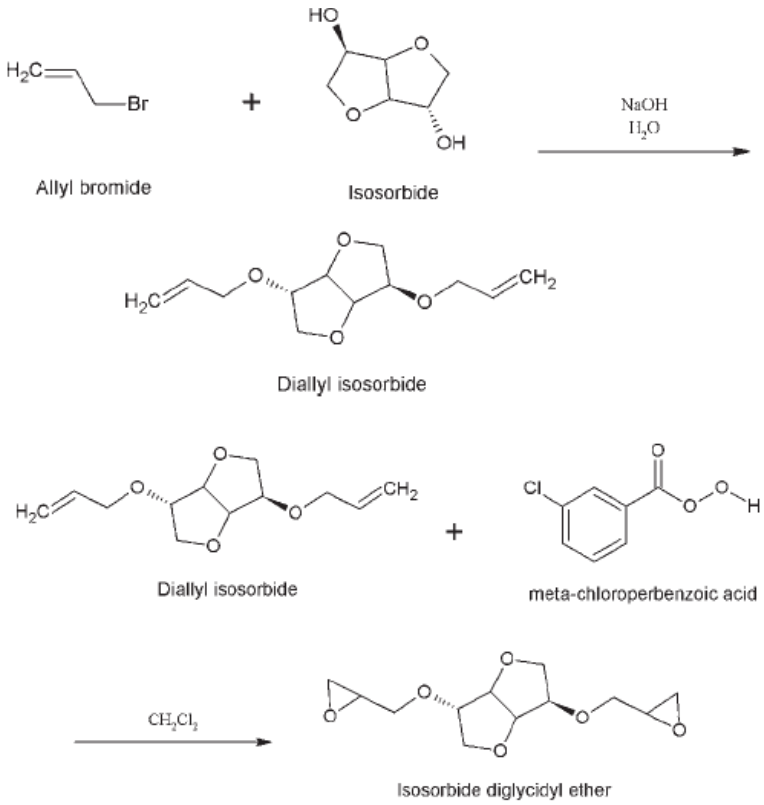

Figure 41. Synthesis of isosorbide diglycidyl ether via allylic derivative [6]

Synthesis using the allylic derivative gives access to the pure isosorbide diglycidyl ether though it is not industrially developed as the epoxidation route involving epichlorohydrin.

Properties of bio-based epoxy networks derived from isosorbide

Isosorbide diglycidyl ether was cured with an aliphatic amine, Jeffamine T403, and compared with DGEBA cured with the same hardener [6].

The tensile modulus and tensile strength of the cured networks were tested. It appears that the tensile strength of the DGEBA-based network is only 96 % of the isosorbide-based network and impact strength of isosorbide is 40 % higher than the DGEBA-based networks.

However, the glass transition of the isosorbide based network as measured by DSC method was shown to be 48°C, which is much lower than DGEBA-based network with a T_g of 90°C. The authors attributed the decrease of T_g to the isosorbide's high affinity for water. They used different cross-linkers, more hydrophobic, to cure isosorbide epoxy prepolymer, such as methyl-5-norbornene-2,3-dicarboxylic anhydride (NMA) with initiator benzyl

dimethyl amine (BDMA). They observed in this case a T_g of 113°C. 4,4'-(hexafluoro-isopropylidene) diphthalic anhydride was also used as a curing agent and it raised the T_g to 200°C but it exhibits an important amount of Fluor which affects the non-toxicity advantage of the use of isosorbide as epoxy precursor.

4. Other renewable resources for the synthesis of bio-based epoxy prepolymers

This part of the chapter presents other renewable resources such as wood derivatives [70] that can also be used as substitutes for BPA allowing reduced waste

a) Fujita et al. have developed wood-based epoxy prepolymers synthesized by a two-step process from wood powder: **liquefied wood** was obtained by reacting wood powder with resorcinol (see Figure 42 for resorcinol structure) and then the glycidyl etherification of liquefied wood was conducted with epichlorohydrin [71]. The flexural strength (150–180 MPa) and the modulus of elasticity (3.2 GPa) of the highly crosslinked wood-based epoxy networks were equivalent to those of the commercially available epoxy monomer, diglycidyl ether of bisphenol A (DGEBA). According to authors, the mechanical and adhesive properties suggested that the wood-based epoxy networks would be well suited for matrix of natural plant-fiber reinforced composites.

Same study was done by Fujita et al. replacing the liquefaction solvent, resorcinol, by other alcohols such as polyethylene glycol (PEG) and glycerin [72]. The T_g, the tensile strength, and the modulus of elasticity of the wood-based epoxy prepolymers cured with polyamide amine were higher than those of corresponding PEG-based epoxy monomer.

The purpose of the latter work was a wood valuation and not a study of the reactivity of hydroxyl groups present in wood compounds toward epichlorohydrin. Indeed, the wood powder was used without any further purification and hydroxyl groups present in liquefied wood can come from various wood components such as cellulose, lignin, and polyphenols.

b) **Polyphenols**, and more specifically condensed tannins, extracted from wastes produced by the wood and wine industries can be an alternative to BPA to produce epoxy prepolymers. Nouailhas et al [73] synthesized bio-based epoxy prepolymers from catechin

one repetitive unit in tannins. The reactivity of catechin toward epichlorohydrin to form glycidyl ether derivatives was studied using two model compounds, resorcinol and 4-methylcatechol, which represent the A and B rings of catechin (Figure 42).

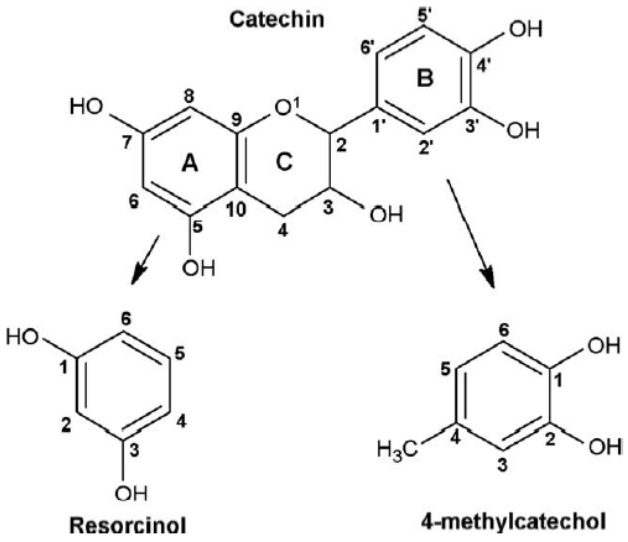

Figure 42. Structure of catechin, resorcinol, and 4-methylcatechol [73]

Furthermore, the functionalized catechin, glycidyl ether of catechin (GEC), was cured, and some properties of the resulting epoxy network were compared to the standard DGEBA-based networks. To evaluate the effect of the glycidyl ether of catechin (GEC) content on α-relaxation temperature and crosslinking density of cured epoxy networks, the storage modulus (G') and loss factor (tanδ) were measured by using DMA. The crosslinking density (ρ) of cured specimens was calculated according to rubber elasticity theory. Results of dynamic mechanical analyses are summarized in the following table:

Samples	T_α (°C)	G'(GPa) at 30°C	G'(GPa) at T_α+30°C	ρ (10^{-3}mol.cm^{-3})
DGEBA	209	2.81	0.019	6.06
75DGEBA/25GEC	221	2.46	0.016	5.12
50DGEBA/50GEC	202	2.40	0.014	4.48

Table 10. Dynamic mechanical analysis of the DGEBA/GEC (glycidyl ether of catechin)-cured epoxy networks [73]

No decrease in the α-relaxation temperature was observed when incorporating glycidyl ether of catechin into the DGEBA epoxy formulation up to 50 %. Indeed, the catechin

derivatives substituted by a benzodioxane-type function on the B ring have also two methyloxirane functions on the A ring and thus participate to the network.

This work shows the feasibility of epoxy formulations based on flavonoid building blocks. These renewable phenolic resources seem to be promising for the replacement of BPA in epoxy formulations. Besides, Nouailhas et al. [74] also studied the development of biocomposites obtained from glycidyl ether of catechin (GEC) and flax fibres.

c) **Lignin** is the second major component of wood and annual plants, and is a highly branched and irregular macromolecule. Its structure varies with the vegetable species, although its basic building blocks can be schematically simplified into "C9" units made up of phenolic moiety bearing three aliphatic carbons, as represented in Figure 43. Small piece of typical structure of lignin polymer is represented in Figure 44.

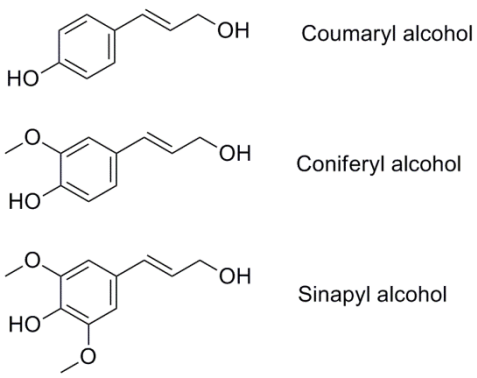

Figure 43. The three fundamental lignin monomer precursors

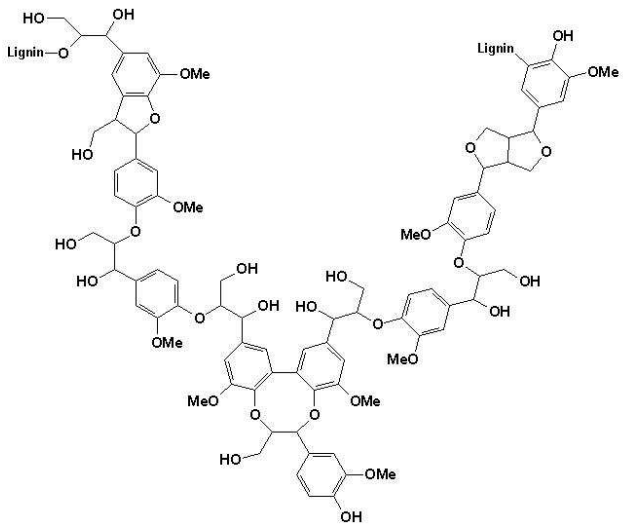

Figure 44. A small piece of lignin polymer

Despite the lignin macromolecular irregularities, it presents the advantage of both aliphatic and phenolic hydroxyl groups, in variable proportions, which can be exploited to synthesized bio-based polymers. Nevertheless, despite the excellent availability of lignin, it has been viewed as a waste material or a low-value by-product of pulping. Lignin was so far mainly used as energy source in combustion applications. Less than 5 % are being processed for other purposes [75].

d) **Diphenolic acid (DPA)** is prepared by the reaction of levulinic acid (obtained from lignocellulosic feedstocks fractionation) with two molecules of phenol as represented in Figure 45.

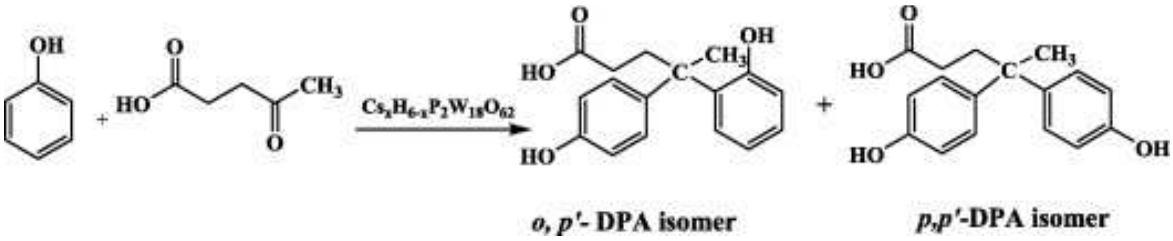

Figure 45. Diphenolic acid (DPA) synthesis from levulinic acid [76]

It may be a direct replacement for bisphenol A (BPA) in polycarbonates, epoxies, polyarylates and other polymers [76]. The acid also has numerous other uses including applications in lubricants, adhesives and paints. It can also copolymerize with BPA or can replace it in various formulations. It contains a carboxyl group, absent from BPA, which confers an additional functionality that could be useful in polymer synthesis.

e) **Terpenes** are naturally occurring substances that can be used as a renewable feedstock. Structures of the most common monoterpenes are represented in Figure 46.

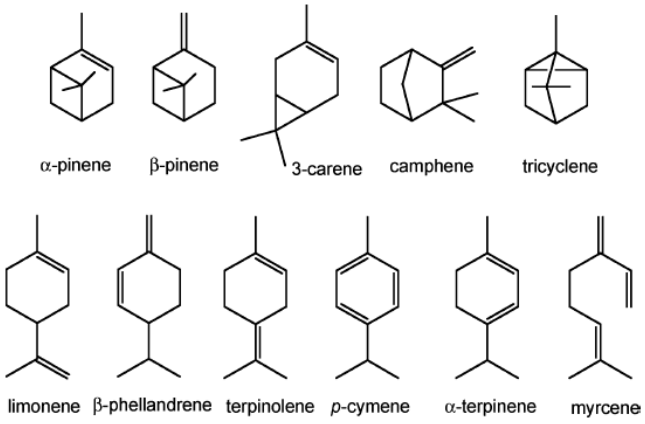

Figure 46. Structure of the most common monoterpenes

Only a few of these molecules have been the subject of extensive studies related to their use as monomers, namely α-pinene, β-pinene, limonene, as they can be readily isolated in viable amounts [3]. Terpene-phenols are low molar mass oligomers, and can be used for the rheological modification of polar polymers. They are used as good tackifiers and heat stability in adhesive, coatings, inks, plastic (PVC), rubber (EVA) and others.

Epoxidation of terpene and more specifically limonene was also studied as described in an US Patent dating from 1968 [77].

f) **Glycerol**, as represented in Figure 47, is also an important bio-based raw material. Recently, glycerol also has gained much attention as a 10 % by-product of bio-diesel production via the transesterification of vegetable oils.

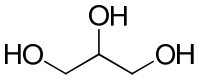

Figure 47. Structure of glycerol

Shibata et al. developed fully bio-based epoxy networks from glycerol polyglycidyl ether (GPE) and polyglycerol polyglycidyl ether (PGPE) combined with ε-Polylysine (PL) as represented in Figure 48.

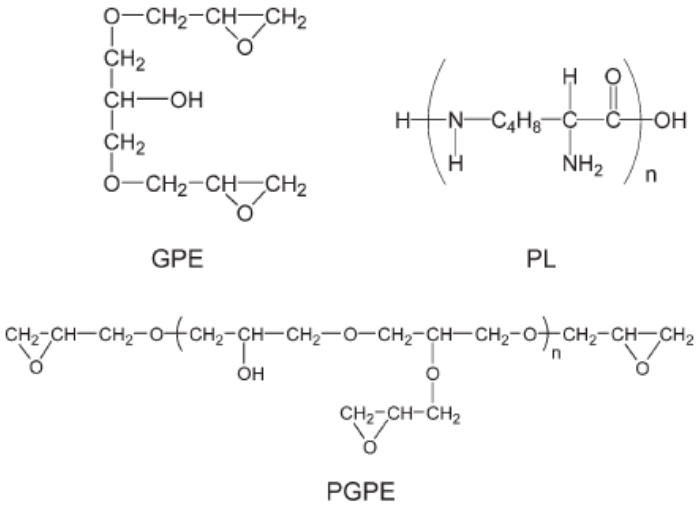

Figure 48. Structures of the reagents used in Shibata study [78]

Table 11 summarizes the T_g measured by DSC for the different networks. PGPE-PL network had greater T_g than the GPE-PL network, which can be attributed to greater epoxy

functionality of PGPE than GPE. In both case, low T_g values were obtained which can be attributed to the long aliphatic structure of ε-Polylysine (degree of polymerization: 25–35).

Epoxy-amine system	Epoxy/amine molar ratio	T_g [DSC] (°C)
GPE – PL	1.0/1.0	37
PGPE – PL	1.0/1.0	47

Table 11. T_g measured by DSC for the cured networks [78]

5. Bio-based epoxy curing agents

As previously mentioned, epoxy networks are obtained by the reaction of an epoxy prepolymers with various co-reactants, hardeners, to form a tridimensional network.

We previously mainly focused on the replacement of conventional epoxy prepolymer, such as DGEBA, by bio-based epoxy prepolymers, to yield partially bio-based epoxy networks using petroleum-derived curing agents such as amines, anhydrides… Replacement of petroleum-based curing agents by bio-based ones, will allow preparing fully bio-based epoxy networks. Still, research on the development of bio-based amine or other curing agents is less abundant than the development of bio-based epoxy prepolymers.

a) Phenalkamines curing agents

Phenalkamines are obtained from cardanol (Figure 25). Their structure is presented in Figure 49.

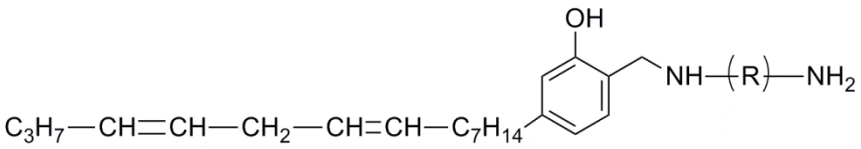

Figure 49. Structure of phenalkamine

Phenalkamines can be synthesized via a Mannich reaction to produce a low molar mass polymer by condensing one mol of cardanol (C_{15} alkylphenol), two moles of formaldehyde and two moles of a polyamine [79, 80]. The polyamine may be aromatic or aliphatic. Commercial phenalkamines are produced using either ethylene diamine

(commercial reference: Cardolite NC541) or diethylenetriamine (commercial reference: Cardolite NC540).

Phenalkamines contain aliphatic polyaminic substituents attached to the aromatic ring. Their unique structure can explain the fact that they have an unusual combination of desirable properties, which can be identified in the resulting cured network. The aromatic backbone is responsible for the high chemical resistance that can be seen in these compounds : the side chain is very hydrophobic; the phenolic -OH group makes phenalkamines very active even at low temperatures, the aminic side is responsible for the high crosslinking density and whenever the molar mass is not too high, these curing agents can have a low viscosity (around 2000 cps at room temperature for Cardolite NC540) [81].

In other works, commercial phenalkamines such as Cardolite NC-540 were blended with a polyamine (DETA, 9 %). Phenalkamines can be used as a curing agent for epoxy systems [79, 82-84] for low temperature curing systems.

The phenalkamines constitute a new class of low temperature curing agents and can improved pot life, and water resistance. They can have applications in many branches of the industrial maintenance and maritime industries.

b) Rosin-based curing agents

Rosin is abundantly available as exudates of pines and conifers or as a byproduct from the pulping process. Rosin is a mixture of acidic (*ca*. 90 %) and neutral (*ca*. 10 %) compounds. The acidic components generally named rosin acids are also a mixture containing namely isomeric abietic-type acids (40-60 %) and pimaric-type (9-27 %) acids (on the basis of total rosin weight). Due to their large hydrogenated phenanthrene ring structure, rosin acids are similar to cyclic aliphatic or aromatic compounds in molecule rigidity. Therefore resulting rosin derivatives may serve as alternatives to petroleum-based cyclic aliphatic and aromatic monomers used in polymer synthesis. Zhang et al. studied the application of rosin derivatives for curing agent applications [85-87].

Two rosin-based acid anhydrides, methyl maleopimarate (MMP) and maleopimaric acid (MPA) were synthesized (Figure 50).

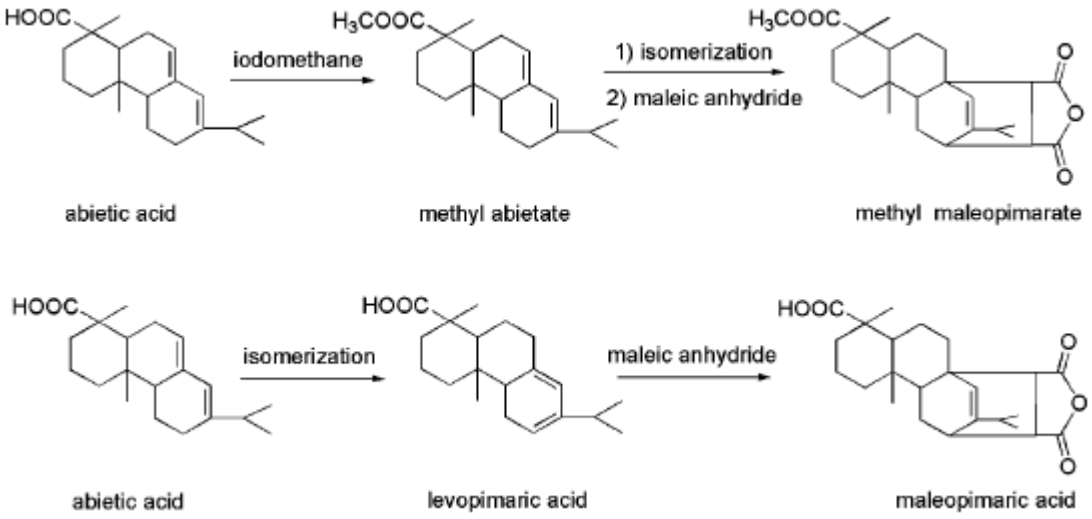

Figure 50. The synthetic route of methyl maleopimarate (MMP) and maleopimaric acid (MPA) [85]

These two rosin-based anhydrides methyl maleopiramate (MMP) and maleopimaric acid (MPA) were used as curing agents for DGEBA epoxy prepolymer and respectively compared with conventional anhydrides hexahydrophtalic anhydride (HHPA) and trimellitic anhydride (TMA) (Figure 51) also used to cure DGEBA.

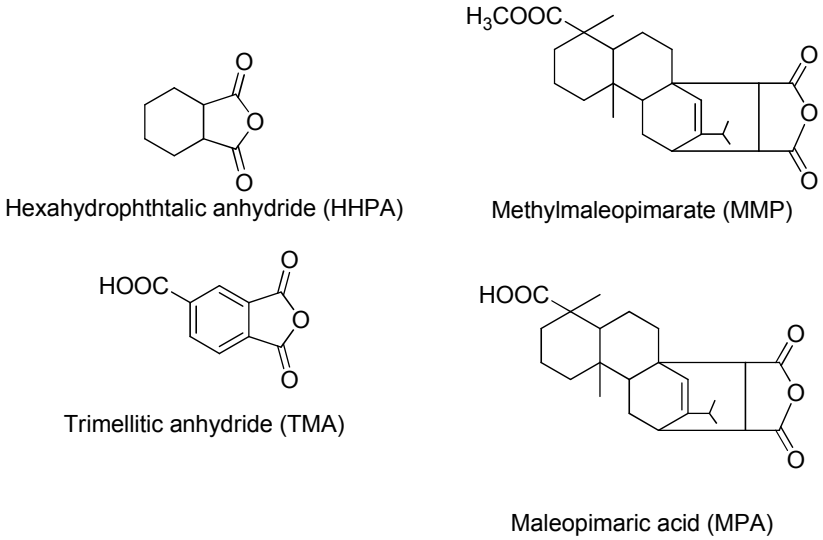

Figure 51. Chemical structure of curing agents used in Zhang et al. study [85]

Dynamic mechanical analyses were performed on the four different networks. Evolution of storage modulus and tanδ with temperature is presented in Figure 52.

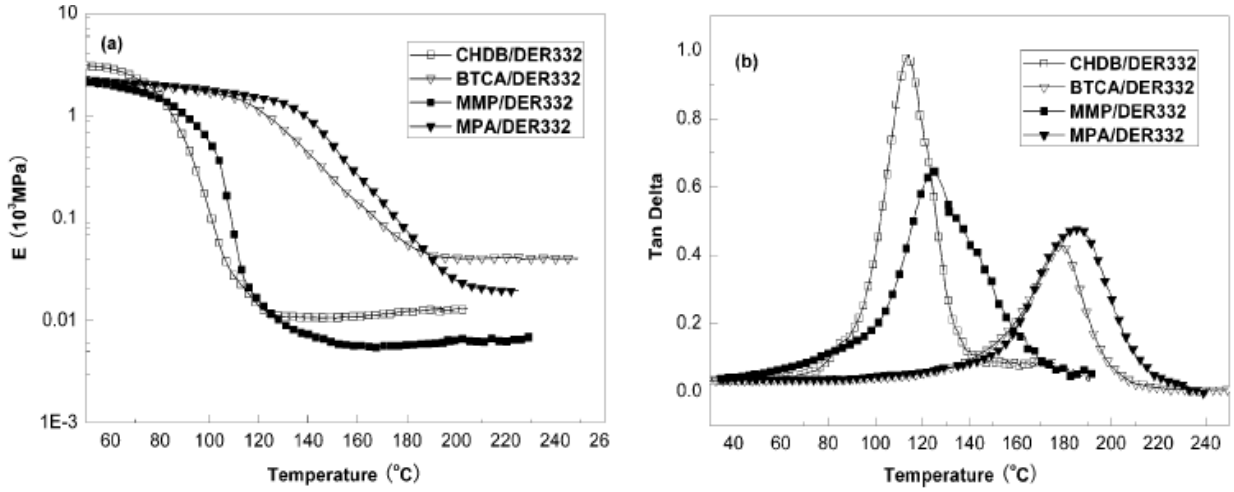

Figure 52. Storage modulus and tanδ versus temperature for DGEBA (DER332) cured with different curing agents [85] – CHDB stands for hexahydrophtalic anhydride (HHPA) and BTCA stands for trimellitic anhydride (TMA)

It appears that the networks cured with rosin-based curing agents exhibited lower moduli in rubbery state than networks obtained with their conventional curing agent analogues. Besides, DGEBA cured with maleopimaric acid (MPA) had higher T_α than DGEBA cured with methylmaleopimarate (MMP). Indeed, the functionality of MPA (f = 3) was higher than that of MMP (f = 2), the epoxy networks cured with maleopimaric acid (MPA) possessed higher crosslink density than the networks obtain with methylmaleopimarate (MMP). It is also noted that the epoxy cured with rosin-based curing agents exhibited higher T_α (*ca*. 10 %) than the epoxy cured with their corresponding commercial counterparts (HHPA and TMA). The bulky fused ring structure of rosin probably imposed considerable restriction on the segmental mobility between crosslink points, hence resulting in higher T_α according to the authors.

Rosin acids have a great potential to replace some of the current aromatic or cycloaliphatic compounds in the synthesis of epoxy curing agents.

More recently, Zhang et al. [88] also used bio-based epoxy curing agent (maleopimaric acid, MPA) in combination with rosin-based epoxy prepolymer in order to obtain a fully bio-based rosin-based epoxy network. A rosin-based epoxy monomer with three functional groups was synthesized as represented in the Figure 53.

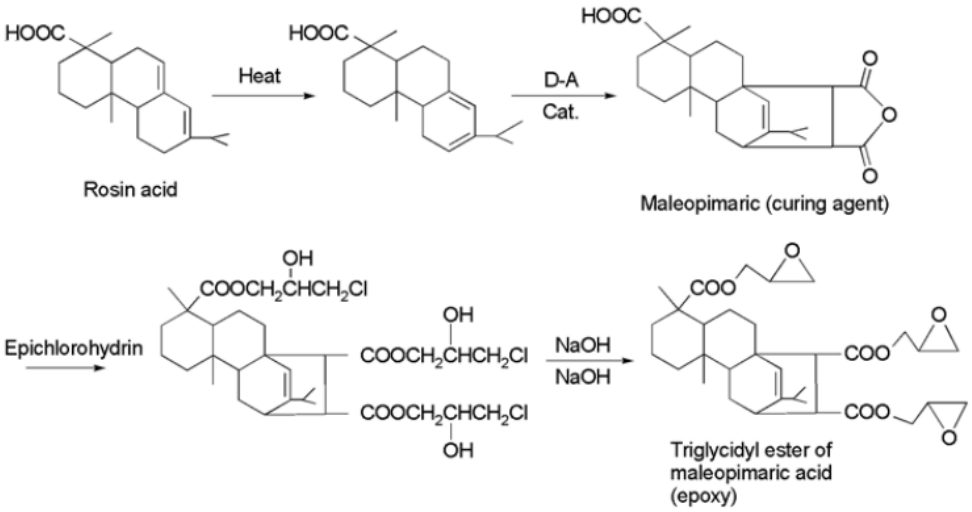

Figure 53. Synthetic route for maleopimaric acid (curing agent) and its triglycidyl ester (epoxy prepolymer) [88]

Triglycidyl ester of maleopimaric acid combined with maleopimaric acid as curing agent and a catalyst (2 ethyl-4-methylimidazole) were crosslinked for 2h at 120°C, 2h at 150°C and 2h at 180°C. The α-relaxation temperature and storage modulus of the resulting network were measured using DMA as represented in Figure 54. This fully bio-based network exhibits high T_α (164°C) and storage modulus (3.2 MPa). Yet, the α-relaxation is broad as compared to conventional epoxy networks which means a regular decrease of its modulus (2.5 MPa at 100°C).

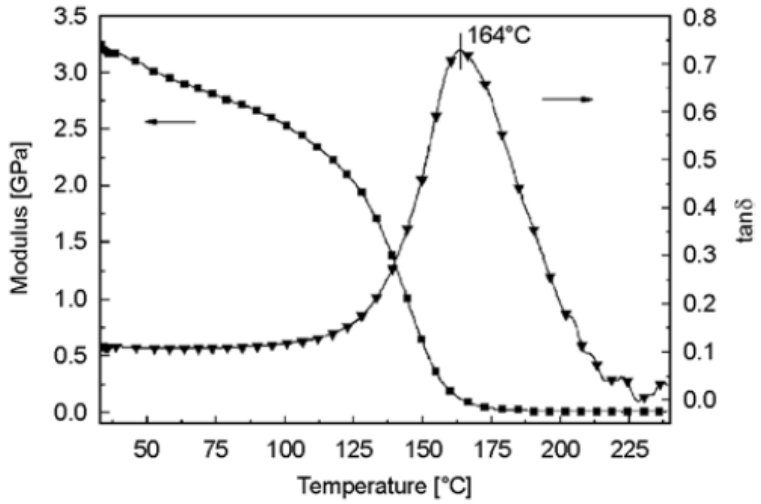

Figure 54. DMA of triglycidyl ester of maleopimaric acid crosslinked with maleopimaric acid (MPA) [88]

c) Other bio-based curing agents

Tannic acid as bio-based curing agent

As introduced before, Shibata et al. [64] prepared fully bio-based epoxy networks using tannic acid (TA). Commercial tannic acid is a powder comprised of mixture of gallotannins from sumac galls, Aleppo oak galls, or sumac leaves. The chemical formula for commercial TA is often given as $C_{76}H_{52}O_{46}$ as shown in Figure 36. But in fact it contains a mixture of related compounds. Its structure is mainly based on glucose ester of gallic acid.

Even if, promising fully bio-based epoxy networks can be obtained using sorbitol polyglycidyl ether and tannic acid, with a glass transition temperature of 80°C (see II.3.b), the main drawback of tannic acid used as a curing agent is the preparation of homogenous systems. Indeed, sorbitol polyglycidyl ether and tannic acid need to be solubilized previously in ion-exchange water to obtain a homogenous solution, as both epoxy prepolymer and curing agent are soluble in water. Solution was then freeze-dried to remove the water for 24 h.

ε-Polylysine as bio-based curing agent

The same authors also developed fully bio-based epoxy networks from glycerol polyglycidyl ether (GPE) and polyglycerol polyglycidyl ether (PGPE) using ε-Polylysine, PL, as represented in Figure 48 as an hardener [78] as described previously.

PL is produced by aerobic bacterial fermentation using *Streptomyces albulus* in a culture medium-containing glucose, citric acid, and ammonium sulfate. PL differs from usual proteins in that the amide linkage is not between the α-amino and carboxylic but between the ε-amino and carboxyl group. The pendant α-amino groups are expected to react with epoxy groups.

Terpene-derived amine as curing agent

Amine curing agent derived from terpene was also used to crosslink DGEBA prepolymer. Indeed, 1,8-diamino-p-menthane, MNDA, (Figure 55) was used by Montarnal et al. [89] in 1989. Nevertheless, at that time, the interest of the amine was more in its structure

rather than its origin and its utility as a bio-based hardener. Indeed, MNDA is a sterically hindered amine and it low reactivity allowed to control the morphology development of DGEBA prepolymer toughened with liquid reactive rubber (CTBN) by changing the cure schedule.

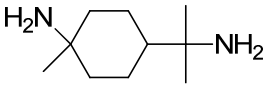

Figure 55. Structure of 1,8-diamine-*p*-menthane

IV. Current industrial bio-based epoxy systems

Despite the recent attention of researchers to bio-based epoxy networks, only a few commercial formulations have been developed. However the market is moving continuously. Different companies claim to sell bio-based epoxies but no detailed information are available to consumers as their origin or exact formulations.

In this paragraph we introduce some commercial bio-based epoxy development such as production of DGEBA using bio-based epichlorohydrin as well as bio-based epoxy formulations commercially available for the replacement of DGEBA prepolymer.

1. Production of DGEBA using bio-based epichlorohydrin

As previously mentioned, diglycidyl ether of bisphenol A (DGEBA) is derived from bisphenol A and epichlorohydrin. The conventional, petrochemical process of producing epichlorohydrin is the chlorohydrination of allyl chloride, which in turn is made by chlorination of propylene. In 2005, Solvay patented the epichlorohydrin production from glycerol via 1,3-dichloropropanol (see Figure 56). Production of partially bio-based DGEBA is therefore possible. Bio-based DGEBA is chemically identical with petrochemical DGEBA and there is hence no difference in product properties.

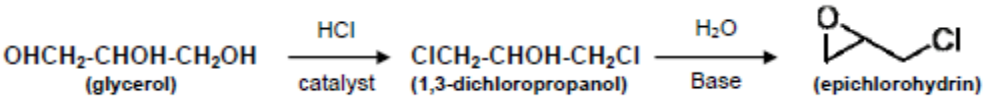

Figure 56. Conversion of glycerol into epichlorohydrin according to the Solvay Epicerol™ process

In March 2007, Dow Epoxy (a business group of Dow) announced that they would build a 150 kt p.a. glycerol-to-epichlorohydrin (GTE) plant and 100 kt p.a. liquid epoxy monomers (LER) in Shanghai, China [9].

In April 2007, Solvay started up its first glycerol-to-epichlorohydrin (GTE) plant in Tavaux in France. The nameplate capacity of the plant is 10 kt p.a. The glycerol is derived from rapeseed oil.

In September 2007, Solvay announced to build a 100 kt p.a. glycerol-epichlorohydrin plant on the Map Ta Phut industrial estate in the eastern province of Rayong in Thailand.

The production capacity scheduled by Solvay and Dow (200 kt p.a.) translates to approximately 600 kt of epoxy monomers, which is a very sizable share of the world-wide production of epoxy monomers (1.15 Mt in 2000).

Nevertheless, the molar mass of DGEBA is dominated by bisphenol A (BPA). Among all the BPA substitutes presented above (vegetable oils, polysaccharides…) some are industrially produced. Recent industrial development of BPA substitutes and their epoxide derivatives production is observed.

2. Industrial bio-based substitutes to DGEBA

a) Derived from vegetable oils

Arkema produces various types of epoxydized vegetable oil under the tradename Vikoflex. For two of these, the type of vegetable oil is reported being soybean oil (Vikoflex 7170) and linseed oil (Vikoflex 7190). The primary application area of Vikoflex is their use as plasticizers for flexible PVC. A further producer of epoxidized soybean oil is Cara Plastics/University of Delaware.

b) Derived from polysaccharides

Sorbitol

Roquette (Lestrem, France) is the first French manufacturer of starch and derivatives and the first worldwide manufacturer of sorbitol, but they do not produce sorbitol polyglycidyl ether.

Sorbitol polyglycidyl ethers are commercially available, produced by JSI Co. (Korea) and Nagase Chemtex (Japan). The latter produces different grades of sorbitol polyglycidyl ether with different epoxy equivalent weigth, viscosity and water solubility. Commercial references of sorbitol polyglycidyl ethers are summarized in the following table:

Reference	Producer	EEW (g/eq)	Viscosity (cps, 25°C)	Solubility in water (%)
EJ 190	JSI Co.	184	4380	N.A.
Denacol 611	Nagase chemtex	163	10820	48
Denacol 612	Nagase chemtex	167	11590	42
Denacol 614	Nagase chemtex	164	17780	78
Denacol 614B	Nagase chemtex	171	4450	94
Denacol 622	Nagase chemtex	191	11440	insoluble

Table 12. Commercial references of sorbitol polyglycidyl ether

Isosorbide

Roquette sells for several years the POLYSORB® P, a high-purity grade isosorbide specially adapted for polymers manufacture. These patented technologies have allowed Roquette to establish several collaborations with major collaborators in the field of polymers. Roquette has announced that its isosorbide production capacity located in Lestrem (France) will reach several thousand tons in early 2011. Roquette thus strengthens its position as world leader for isosorbide, bio-based intermediate for new polymers and plasticizers. Nevertheless, the epoxyde derivatives of isosorbide are not yet commercially available in a large scale.

c) Derived from cashew nut shell liquid

Cardolite Corporation manufactures the world's largest variety of products derived from cashew nutshell liquid (CNSL). With over 20 years of experience, Cardolite is the leader in the production of quality CNSL based materials used in the epoxy coatings industry and offers a line of cardanol derived epoxy monomers and reactive diluent [90].

Cardolite® NC-513 and LITE 2513HP are mono-functional reactive epoxy diluents that can be used to increase the flexibility, impact resistance, chemical resistance, and water

resistance of epoxy coatings. These reactive diluents have very low viscosity and low volatility, which make them ideal for helping formulate high solids and solvent free coatings.

Cardolite® NC-514 and NC-547 are, respectively, di-functional and tri-functional reactive epoxy resins. Structure of these commercial epoxidized cardanol products are shown in Figure 57. They are mainly developed for coating in maritime applications.

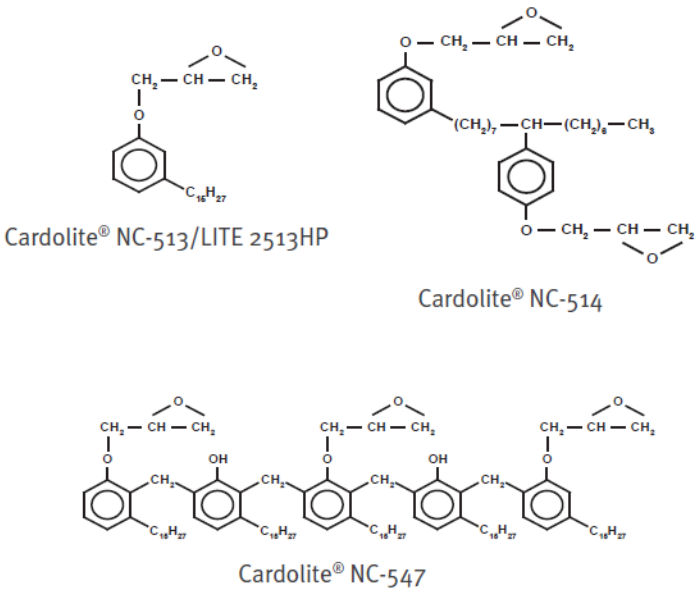

Figure 57. Structure of cardanol epoxy derivatives commercialized by Cardolite

d) Other commercial bio-based epoxy formulations

Among the bio-based epoxy formulations available nowadays, the company Amroy Europe Oy (Finland) commercialized a liquid epoxy system: EPOBIOX™. This system is specially developed for windmill blades and composites industry. It is suitable for infusion, laminating and especially for glue applications. According to the technical data sheet, EPOBIOX™ is made 70 % from industrially grown and harvested natural oils like, for example, epoxidized pine oil waste. This natural prepolymer has a high hydroxyl group content and very long polymer with high molar mass. This results in good elongation at break and adhesion to all kinds of substrates [91].

Conclusion

Renewable resources provide a variety of new structures for thermosetting materials, including epoxy networks. Traditional thermosets are high performance materials for industry, with high modulus strength, durability and resistance towards thermal stress and chemical attacks, provided by their high-cross-linking density and the type of chemical structure between crosslinks.

In the past two decades, developments have been done on bio-based polymers in order to replace petroleum-derived precursors and decrease the toxicity of some polymers... Indeed, in the case of epoxy, bisphenol-A (BPA) is one of the most commonly used precursors. It is used for the synthesis of epoxy prepolymer, DGEBA, and is known to be a toxic compound with estrogenic properties. Therefore, in the field of epoxy networks one driving force is the replacement of BPA by some bio-based non-toxic precursors.

Vegetable oils were the first renewable resources studied, as they are cheap and abundant. Unfortunately, because of the low reactivity of aliphatic epoxy groups, any epoxidized oil leads to poorly cross-linked materials with limited thermal and mechanical properties. Besides, they show a decrease of the network properties because of their long aliphatic structure. If epoxidized vegetable oils should be interesting renewable materials for adhesives and as plasticizers, they could not lead to high performance materials, or through many chemical transformations which will be far from a sustainable approach. Indeed, sustainability means also sustainable synthesis of epoxy monomers and hardener. Green monomers are not always sustainable.

Other bio-based raw materials with interesting structures have been studied such as sugar derivatives. These sugar-derived raw materials such as sorbitol and dianhydrohexitols provide interesting prepolymers especially in the case of isosorbide which has the opportunity to bring a cyclic structure which could lead to high performance materials. Besides, they have been declared as non-toxic precursors. Even if, isosorbide epoxide has been the subject of recent investigations, many prospects should be done on the understanding of all the properties of this monomer and its use as an epoxy prepolymer.

The next chapter will focus on the preparation and the characterization of bio-based epoxy prepolymers derived from isosorbide and resulting epoxy networks.

References

[1] Gandini A. Epoxy Polymers: New materials and innovations: Pascault JP, Williams RJJ, Eds. Wiley-VCH 2010.

[2] Gandini A. Polymers from Renewable Resources: A Challenge for the Future of Macromolecular Materials. *Macromolecules*. 2008;**41**:9491-504.

[3] Gandini A. The irruption of polymers from renewable resources on the scene of macromolecular science and technology. *Green Chemistry*. 2011;**13**:1061-83.

[4] Kaplan DL. Biopolymers from Renewable Ressources. Berlin: Springer-Verlag 1998.

[5] Ronda JC, Lligadas G, Galià M, Cádiz V. Vegetable oils as platform chemicals for polymer synthesis. *European Journal of Lipid Science and Technology*. 2011;**113**:46-58.

[6] Feng X, East AJ, Hammond WB, Zhang Y, Jaffe M. Overview of advances in sugar-based polymers. *Polymers for Advanced Technologies*. 2011;**22**:139-50.

[7] Feng X, East Anthony J, Hammond W, Jaffe M. Sugar-Based Chemicals for Environmentally Sustainable Applications. *Contemporary Science of Polymeric Materials*: American Chemical Society 2010:3-27.

[8] Pascault JP, Sautereau H, Verdu J, Williams RJJ. Thermosetting Polymers: Taylor & Francis Books, Inc. 2002.

[9] Shen L, Haufe J, Patel MK. Product overview and market projection of emerging biobased plastics. *PROBIP 2009*.

[10] Fenouillot F, Rousseau A, Colomines G, Saint-Loup R, Pascault JP. Polymers from renewable 1,4:3,6-dianhydrohexitols (isosorbide, isomannide and isoidide): A review. *Progress in Polymer Science*. 2010;**35**:578-622.

[11] Fuji M, Akita M, Tanaka T. Polycarbonate copolymer and process for production thereof. European Patent EP2033981 A1 2009.

[12] Miyake T, Kinoshita M, Saito M, Hironaka K. Polycarbonate Resin Composition. European Patent EP2149589 A1 2010.

[13] Jansen B, Kamps JP, Looij H, Kung E, Prada L, Steendam W. Isosorbide-based polycarbonates, method of making, and articles formed therefrom. World Patent WO 2009/052463 A1 2009.

[14] Lluch C, Ronda JC, Galià M, Lligadas G, Cádiz V. Rapid Approach to Biobased Telechelics through Two One-Pot Thiol−Ene Click Reactions. *Biomacromolecules*. 2010;**11**:1646-53.

[15] González-Paz RJ, Lluch C, Lligadas G, Ronda JC, Galià M, Cádiz V. A green approach toward oleic- and undecylenic acid-derived polyurethanes. *Journal of Polymer Science Part A: Polymer Chemistry*. 2011;**49**:2407-16.

[16] Hojabri L, Kong X, Narine SS. Fatty Acid-Derived Diisocyanate and Biobased Polyurethane Produced from Vegetable Oil: Synthesis, Polymerization, and Characterization. *Biomacromolecules*. 2009;**10**:884-91.

[17] Hojabri L, Kong X, Narine SS. Functional Thermoplastics from Linear Diols and Diisocyanates Produced Entirely from Renewable Lipid Sources. *Biomacromolecules*. 2010;**11**:911-8.

[18] Raquez JM, Deléglise M, Lacrampe MF, Krawczak P. Thermosetting (bio)materials derived from renewable resources: A critical review. *Progress in Polymer Science*. 2010;**35**:487-509.

[19] Norton GA, Devlin SL. Determining the modern carbon content of biobased products using radiocarbon analysis. *Bioresource Technology*. 2006;**97**:2084-90.

[20] Del Rio E, Lligadas G, Ronda JC, Galià M, Cádiz V. Biobased polyurethanes from polyether polyols obtained by ionic-coordinative polymerization of epoxidized methyl oleate. *Journal of Polymer Science Part A: Polymer Chemistry*. 2010;**48**:5009-17.
[21] Petrović ZS. Polyurethanes from Vegetable Oils. *Polymer Reviews*. 2008;**48**:109-55.
[22] Verchere D, Sautereau H, Pascault JP, Riccardi CC, Moschiar SM, Williams RJJ. Buildup of epoxycycloaliphatic amine networks. Kinetics, vitrification, and gelation. *Macromolecules*. 1990;**23**:725-31.
[23] Grillet AC, Galy J, Pascault JP, Bardin I. Effects of the structure of the aromatic curing agent on the cure kinetics of epoxy networks. *Polymer*. 1989;**30**:2094-103.
[24] Wang X, Gillham JK. Competitive primary amine/epoxy and secondary amine/epoxy reactions: Effect on the isothermal time-to-vitrify. *Journal of Applied Polymer Science*. 1991;**43**:2267-77.
[25] Dušek K, Bleha M, Luňák S. Curing of epoxide resins: Model reactions of curing with amines. *Journal of Polymer Science: Polymer Chemistry Edition*. 1977;**15**:2393-400.
[26] Byrne CA, Hagnauer GL, Schneider NS. Effects of variation in composition and temperature on the amine cure of an epoxy resin model system. *Polymer Composites*. 1983;**4**:206-13.
[27] Matějka L, Pokorný S, Dušek K. Acid curing of epoxy resins. A comparison between the polymerization of diepoxide-diacid and monoepoxide-cyclic anhydride systems. *Die Makromolekulare Chemie*. 1985;**186**:2025-36.
[28] Matějka L, Lövy J, Pokorný S, Bouchal K, Dušek K. Curing epoxy resins with anhydrides. Model reactions and reaction mechanism. *Journal of Polymer Science: Polymer Chemistry Edition*. 1983;**21**:2873-85.
[29] Galante MJ, Vázquez A, Williams RJJ. Macro- and microgelation in the homopolymerization of diepoxides initiated by tertiary amines. *Polymer Bulletin*. 1991;**27**:9-15.
[30] Park SJ, Jin FL, Lee JR, Shin JS. Cationic polymerization and physicochemical properties of a biobased epoxy resin initiated by thermally latent catalysts. *European Polymer Journal*. 2005;**41**:231-7.
[31] Chapin RE, Adams J, Boekelheide K, et al. NTP-CERHR expert panel report on the reproductive and developmental toxicity of bisphenol A. *Birth Defects Research Part B: Developmental and Reproductive Toxicology*. 2008;**83**:157-395.
[32] Galià M, de Espinosa LM, Ronda JC, Lligadas G, Cádiz V. Vegetable oil-based thermosetting polymers. *European Journal of Lipid Science and Technology*. 2010;**112**:87-96.
[33] Lligadas G, Ronda JC, Galià M, Cádiz V. Plant Oils as Platform Chemicals for Polyurethane Synthesis: Current State-of-the-Art. *Biomacromolecules*. 2010;**11**:2825-35.
[34] Del Rio E, Galià M, Cádiz V, Lligadas G, Ronda JC. Polymerization of epoxidized vegetable oil derivatives: Ionic-coordinative polymerization of methylepoxyoleate. *Journal of Polymer Science Part A: Polymer Chemistry*. 2010;**48**:4995-5008.
[35] Rio ED, Lligadas G, Ronda JC, Galià M, Meier MAR, Cádiz V. Polyurethanes from polyols obtained by ADMET polymerization of a castor oil-based diene: Characterization and shape memory properties. *Journal of Polymer Science Part A: Polymer Chemistry*. 2011;**49**:518-25.
[36] Del Rio E, Lligadas G, Ronda JC, Galià M, Cádiz V. Poly-2-oxazoline-derived polyurethanes: A versatile synthetic approach to renewable polyurethane thermosets. *Journal of Polymer Science Part A: Polymer Chemistry*. 2011;**49**:3069-79.

[37] Park SJ, Jin FL, Lee JR. Synthesis and Thermal Properties of Epoxidized Vegetable Oil. *Macromolecular Rapid Communications*. 2004;**25**:724-7.
[38] Peterson L, Golas N. High linolenic linseed oil compositions. US Patent, US2009/0314180 A1 2009.
[39] Miyagawa H, Misra M, Drzal LT, Mohanty AK. Fracture toughness and impact strength of anhydride-cured biobased epoxy. *Polymer Engineering & Science*. 2005;**45**:487-95.
[40] Boquillon N, Fringant C. Polymer networks derived from curing of epoxidised linseed oil: influence of different catalysts and anhydride hardeners. *Polymer*. 2000;**41**:8603-13.
[41] Jin FL, Park SJ. Thermomechanical behavior of epoxy resins modified with epoxidized vegetable oils. *Polymer International*. 2008;**57**:577-83.
[42] Nielsen LE. Cross-Linking–Effect on Physical Properties of Polymers. *Journal of Macromolecular Science, Part C: Polymer Reviews*. 1969;**3**:69-103.
[43] Park SJ, Jin FL, Lee JR. Effect of Biodegradable Epoxidized Castor Oil on Physicochemical and Mechanical Properties of Epoxy Resins. *Macromolecular Chemistry and Physics*. 2004;**205**:2048-54.
[44] Miyagawa H, Mohanty AK, Misra M, Drzal LT. Thermo-Physical and Impact Properties of Epoxy Containing Epoxidized Linseed Oil, 1. *Macromolecular Materials and Engineering*. 2004;**289**:629-35.
[45] Miyagawa H, Mohanty AK, Misra M, Drzal LT. Thermo-Physical and Impact Properties of Epoxy Containing Epoxidized Linseed Oil, 2. *Macromolecular Materials and Engineering*. 2004;**289**:636-41.
[46] Altuna FI, Espósito LH, Ruseckaite RA, Stefani PM. Thermal and mechanical properties of anhydride-cured epoxy resins with different contents of biobased epoxidized soybean oil. *Journal of Applied Polymer Science*. 2011;**120**:789-98.
[47] Tan S, Chow W. Thermal properties of anhydride-cured bio-based epoxy blends. *Journal of Thermal Analysis and Calorimetry*. 2010;**101**:1051-8.
[48] Zhu J, Chandrashekhara K, Flanigan V, Kapila S. Curing and mechanical characterization of a soy-based epoxy resin system. *Journal of Applied Polymer Science*. 2004;**91**:3513-8.
[49] Shabeer A, Garg A, Sundararaman S, Chandrashekhara K, Flanigan V, Kapila S. Dynamic mechanical characterization of a soy based epoxy resin system. *Journal of Applied Polymer Science*. 2005;**98**:1772-80.
[50] Shabeer A, Sundararaman S, Chandrashekhara K, Dharani LR. Physicochemical properties and fracture behavior of soy-based resin. *Journal of Applied Polymer Science*. 2007;**105**:656-63.
[51] Stemmelen M, Pessel F, Lapinte V, Caillol S, Habas JP, Robin JJ. A fully biobased epoxy resin from vegetable oils: From the synthesis of the precursors by thiol-ene reaction to the study of the final material. *Journal of Polymer Science Part A: Polymer Chemistry*. 2011;**49**:2434-44.
[52] Yadav R, Awasthi P, Srivastava D. Studies on synthesis of modified epoxidized novolac resin from renewable resource material for application in surface coating. *Journal of Applied Polymer Science*. 2009;**114**:1471-84.
[53] Devi A, Srivastava D. Cardanol-based novolac-type phenolic resins. I. A kinetic approach. *Journal of Applied Polymer Science*. 2006;**102**:2730-7.
[54] Yadav R, Srivastava D. Studies on cardanol-based epoxidized novolac resin and its blends. *Chemical & Chemical Technology,*. 2008;**2**:173-84.

[55] Devi A, Srivastava D. Studies on the blends of cardanol-based epoxidized novolac resin and CTPB. *European Polymer Journal*. 2007;**43**:2422-32.
[56] Patel MB, Patel RG, Patel VS. Effects of reactive diluent diepoxidized cardanol and epoxy fortifier on curing kinetics of epoxy resin. *Journal of Thermal Analysis and Calorimetry*. 1989;**35**:47-57.
[57] Dai Z, Dalai A, Lawson D, He J. Cardanol based dimers and uses therefor. World Patent WO2008/137706 A1 2008.
[58] Sachinvala ND, Winsor DL, Menescal RK, Ganjian I, Niemczura WP, Litt MH. Sucrose-based epoxy monomers and their reactions with diethylenetriamine. *Journal of Polymer Science Part A: Polymer Chemistry*. 1998;**36**:2397-413.
[59] Sachinvala ND, Litt MH. Epoxy monomers from sucrose. US patent US005571907A 1996.
[60] Sachinvala ND, Ju RF, Litt MH, Niemczura WP. Preparation of poly(methyl methacrylate) and copolymers having enhanced thermal stabilities using sucrose-based comonomers and additives. *Journal of Polymer Science Part A: Polymer Chemistry*. 1995;**33**:15-29.
[61] Pan X, Sengupta P, Webster DC. Novel biobased epoxy compounds: epoxidized sucrose esters of fatty acids. *Green Chemistry*. 2011;**13**:965-75.
[62] Pan X, Sengupta P, Webster DC. High Biobased Content Epoxy–Anhydride Thermosets from Epoxidized Sucrose Esters of Fatty Acids. *Biomacromolecules*. 2011;**12**:2416-28.
[63] Acierno D, Russo P, Savarese R. Mechanical and dynamic-mechanical properties of biodegradable epoxy resins. *Proceedings of the Polymer Processing Society*. Salerno, Italy. 2008.
[64] Shibata M, Nakai K. Preparation and properties of biocomposites composed of bio-based epoxy resin, tannic acid, and microfibrillated cellulose. *Journal of Polymer Science Part B: Polymer Physics*. 2010;**48**:425-33.
[65] Rose M, Palkovits R. Isosorbide as a Renewable Platform chemical for Versatile Applications—Quo Vadis? *ChemSusChem*. 2012;**5**:167-76.
[66] Morrison J. Polyglycidyl ethers of ether anhydrohexitols, method of production, and aqueous solutions thereof. US Patent 3,041,300 1962.
[67] Zech J. Bisglycidyl ethers of isohexides. US Patent 3,272,845 1966.
[68] East A, Jaffe M, Zhang Y, Catalini LH. Thermoset epoxy polymers from renewable resources. US Patent US 2008/0009599 A1 2008.
[69] East A, Jaffe M, Zhang Y, Catalini LH,. Ethers of bisanhydrohexitols. US Patent US 2008/0021209A1 2008.
[70] Hui P. Synthesis of polymers from organic solvent liquefied biomass: A review. *Renewable and Sustainable Energy Reviews*. 2011;**15**:3454-63.
[71] Kishi H, Fujita A, Miyazaki H, Matsuda S, Murakami A. Synthesis of wood-based epoxy resins and their mechanical and adhesive properties. *Journal of Applied Polymer Science*. 2006;**102**:2285-92.
[72] Kishi H, Akamatsu Y, Noguchi M, Fujita A, Matsuda S, Nishida H. Synthesis of epoxy resins from alcohol-liquefied wood and the mechanical properties of the cured resins. *Journal of Applied Polymer Science*. 2011;**120**:745-51.
[73] Nouailhas H, Aouf C, Le Guerneve C, Caillol S, Boutevin B, Fulcrand H. Synthesis and properties of biobased epoxy resins. part 1. Glycidylation of flavonoids by epichlorohydrin. *Journal of Polymer Science Part A: Polymer Chemistry*. 2011;**49**:2261-70.

[74] Nouailhas H, Saint-Macary L, Fulcrand H, Bergeret A, Caillol S. Development of a new biobased epoxy resin/flax fibres pultruded biocomposites for building applications. *Comptes Rendus des JNC 17*. Poitiers, France 2011.
[75] Kleinert M, Barth T. Phenols from Lignin. *Chemical Engineering & Technology*. 2008;**31**:736-45.
[76] Hayes DJ, Ross J, Fitzpatrick S. http://www.carbolea.ul.ie/files/HFHR_Chapter%204_FINAL.pdf.
[77] Sellers RF. Epoxy resins from polyhydric phenol-terpene addition products. US Patent 3,378,525, 1968.
[78] Takada Y, Shinbo K, Someya Y, Shibata M. Preparation and properties of bio-based epoxy montomorillonite nanocomposites derived from polyglycerol polyglycidyl ether and ε-polylysine. *Journal of Applied Polymer Science*. 2009;**113**:479-84.
[79] Sato S, Shah S, Bueno RC, Moon R, Ferreira A. Phenalkamine and salted amine blends as curing agents for epoxy resins. World Patent WO 2009/080209 A1 2009.
[80] Cheng CW, Bedner D, Wang H. Phenalkamine derivatives, their use as curing agents in epoxy resin compositions and curable epoxy resin compositions containing them. World Patent WO 00/01659 2000.
[81] Dai Z, Constantinescu A, Dalal A, Ford C. Phenalkamine Multipurpose Epoxy Resin Curing Agents. *Cardolite Corporation*. 1994.
[82] Sato S, Ferreira A. Curing agents for epoxy resins. US Patent US2010/0012888 A1 2010.
[83] Thieben L. Pigmented epoxy coatings comprising a mixture of polyamide and phenalkamine crosslinking agents for stabilization of the pigment. World Patent WO2004/024792 A1 2004.
[84] Kim YH, An ES, Park SY, Song BK. Enzymatic epoxidation and polymerization of cardanol obtained from a renewable resource and curing of epoxide-containing polycardanol. *Journal of Molecular Catalysis B: Enzymatic*. 2007;**45**:39-44.
[85] Liu X, Xin W, Zhang J. Rosin-based acid anhydrides as alternatives to petrochemical curing agents. *Green Chemistry*. 2009;**11**:1018-25.
[86] Wang H, Liu X, Liu B, Zhang J, Xian M. Synthesis of rosin-based flexible anhydride-type curing agents and properties of the cured epoxy. *Polymer International*. 2009;**58**:1435-41.
[87] Liu X, Xin W, Zhang J. Rosin-derived imide-diacids as epoxy curing agents for enhanced performance. *Bioresource Technology*. 2010;**101**:2520-4.
[88] Liu X, Huang W, Jiang YH, J. Zhu, Zhang CZ. Preparation of a bio-based epoxy with comparable properties to those of petroleum-based counterparts. *eXPRESS Polymer Letters*. 2012;**6**:293-8.
[89] Montarnal S, Pascault JP, Sautereau H. Controlling Factors in the Rubber-Toughening of Unfilled Epoxy Networks. *Rubber-Toughened Plastics*: American Chemical Society 1989:193-223.
[90] Cardolite. Coating Products Brochure. 2009.
[91] Amroy Europe Oy F. Epobiox™ , Technical Data Sheet 2009.

Chapter II Bio-based epoxy networks derived from Isosorbide

This chapter is divided in two parts. The first part presents the preparation and characterization of bio-based epoxy networks obtained from isosorbide derivatives and corresponds to the publication: ***Chrysanthos M, Galy J, Pascault J-P***. *Polymer. 2011;52:3611-20.* The second part of this chapter is dedicated to the use of molecular modelling for the determination of glass transition temperatures.

Part I. Preparation and properties of bio-based epoxy networks derived from isosorbide diglycidyl ether

I.Introduction

In recent years, bio-based polymers derived from renewable resources [1, 2] have become increasingly important as sustainable and eco-efficient products which can replace the products based on petrochemical-derived stocks. Of all polymers produced, the main part is thermoplastics while the minor part is thermosets, 82 and 18 % respectively [3]. This is one important reason why research and development has mainly concerned bio-based thermoplastics such as linear polyesters, polyamides, polyurethanes, etc. Thermosets prepared from renewable resources have been the subject of more limited investigations [2].

Epoxy networks are amongst the most popular thermosetting polymers which are used in various fields: coatings, adhesives, laminates, electrical castings, etc. because they exhibit a broad spectrum of properties, through selection of epoxy prepolymer and curing agent composition [4]. The diglycidyl ether of bisphenol A, DGEBA, is by far the most commonly used starting monomer to formulate epoxy networks: it represents 75 % of all epoxy

precursors [3]. Therefore there is a huge interest in developing a bio-based epoxy oligomer able to replace the classical DGEBA and to lead to high performance materials.

Until now, numerous bio-based epoxy resins deriving from vegetable oils, such as soybean oil, linseed oil and castor oil have been studied [5-10]. These macromonomers have long aliphatic chains; therefore they cannot lead to high performance networks and compete with DGEBA-based networks. They are used in epoxy formulations as a toughening agent, that is, to reduce the inherent brittleness of epoxy networks. Some new bio-based epoxy and / or hardeners are prepared from cardanol which give higher network properties [11, 12].
The objective of our work is to develop novel bio-based reactive systems suitable for high performance composite materials.

DGEBA is derived from bisphenol A and epichlorohydrin. An easy way to obtain a partially bio-based DGEBA is to use epichlorohydrin from bio-based glycerol, an abundant and inexpensive polyol. Such bio-based epichlorohydrin is commercially available. However the molar mass of DGEBA is dominated by bisphenol A, epichlorohydrin accounts only for 20 % of the molar mass of DGEBA. So a challenge to obtain a fully bio-based epoxy prepolymer is to replace bisphenol A by a bio-based polyol. Another interest for replacing bisphenol A is that bisphenol A has been known to have estrogenic properties [13]. The chemical bonds that link bisphenol A in polymer structures are not completely stable and the polymer may release, with time, a small amount of bisphenol A, toxic to living organisms.

Investigations were done on the use of natural polysaccharides in replacement of bisphenol A in the synthesis of bio-based epoxy prepolymers. Sorbitol and maltitol were converted in multifunctional epoxy monomers which were used in combination with DETA (diethylene triamine) to produce bio-based networks [14]. Glycerol is also an important bio-based raw material and epoxy precursors such as glycerol polyglycidyl ether (GPE) and polyglycerol polyglycidyl ether (PGPE) are industrially available and inexpensive. Such products have been used in textile and paper as processing agents and as reactive diluents. However, in a recent study these epoxy monomers were reacted with a bio-based curing agent, ε-poly(L-lysine) to produce fully bio-based epoxy networks, as well as nanocomposites based on montmorillonite [15]. Glucose can be readily hydrogenated and yield sorbitol. Sorbitol polyglycidyl ether (SPE) is also a commercial multifunctional epoxy monomer used for similar applications as GPE and PGPE; SPE and GPE have been associated to tannic acid to obtain bio-based networks and biocomposites with microfibrillated cellulose [16].

Synthesis of polyglycidyl ether derived from 1,4:3,6-dianhydrohexitols are well described in patent literature [17-21]. The double dehydration of sorbitol yields isosorbide (1,4:3,6-dianhydro-D-sorbitol (DAS)), commercially available in industrial quantities. The present study describes bio-based epoxy networks derived from this molecule. It was epoxidized using two different routes. The resulting isosorbide diglycidyl ether (or Diglycidyl Ether of DAS, DGEDAS) was characterized and bio-based epoxy networks containing this isosorbide diglycidyl ether were prepared using one amine curing agent, isophorone diamine (IPD). There structures were evaluated and compared to a conventional epoxy network based on DGEBA cured by IPD.

II. Experimental section

1. Materials

Figure 1 shows the structure of the reagents used in this study. The conventional petroleum-based epoxy monomer used was a diglycidyl ether of bisphenol A (DGEBA) supplied by Huntsman (Araldite 5085), with an epoxide equivalent weight (EEW) of 180 g/eq. The cycloaliphatic diamine curing agent used was isophorone diamine (IPD) supplied by Aldrich; the amine equivalent weight (AEW) is 42 g/eq. Isosorbide with a high purity, commercialized under the trade name Polysorb P has been kindly supplied by Roquette Frères (Lestrem, France). Epichlorohydrin and sodium hydroxide were purchased from Aldrich. All chemicals were used as received.

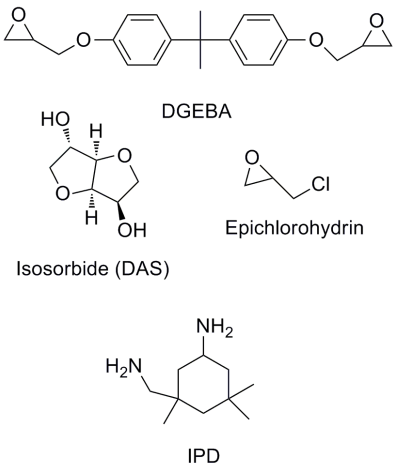

Figure 1. Structure of the reagents used in this study

2. Synthesis of isosorbide diglycidyl ether

In the present work, the synthesis of the diglycidyl ether of isosorbide (DGEDAS) was performed using two different routes. The syntheses were performed in Huntsman laboratory (Basel) in the frame of a collaborative program. The most convenient route is that of the reaction of the isosorbide directly with epichlorohydrin. The synthesis is well described in the literature [19-22] and the synthetic route is presented in Scheme 1. It is based on the traditional and industrial route to produce DGEBA.

A flask fitted with a Dean-Stark water-separator tube was charged with isosorbide (4.0 moles) and epichlorohydrin (40.0 moles). The mixture was stirred under nitrogen flow; the reaction flask temperature was 115°C. When the reaction was steadily refluxing, an aqueous solution of sodium hydroxide (8.0 moles) was added drop by drop to the flask. Gradually water began to appear as an upper layer in the Dean-Stark tube and the reaction was left to proceed steadily. The whole addition step took about 12 hours. Water and epichlorohydrin were drained off under reduced pressure (230 mbar at 70-80°C and 96 mbar at 65°C respectively).

The diglycidyl ether of isosorbide thus obtained, $DGEDAS_n$, was a viscous liquid with an epoxide equivalent weight of 184 g/eq, and a hydroxyl number I_{OH} = 105 mg/gKOH as determined by titrimetry. The yield of the reaction was 96-98 %. We will see that this synthesis of the diglycidyl ether of isosorbide does not give pure diglycidyl ethers since oligomers may be formed by concomitant reaction of the epoxy function with unreacted isosorbide.

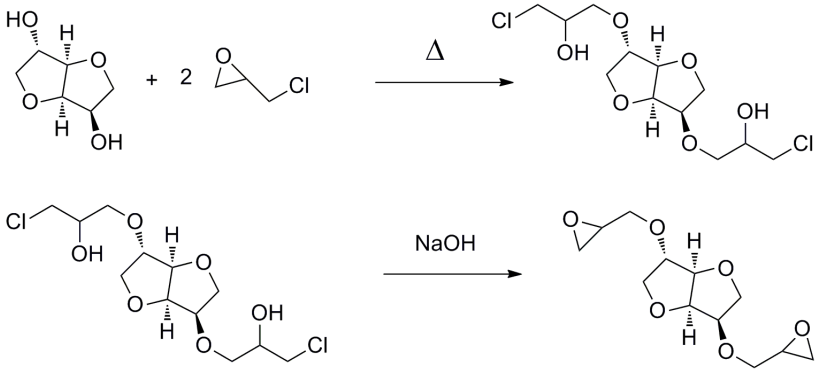

Scheme 1. Synthetic route of isosorbide diglycidyl ether via epichlorohydrin

Another synthetic route, based on the method of sucrose epoxidation developed by Sachinvala et al, [23] was then performed on isosorbide by Feng et al, [22]. As compared to

the first synthetic route discussed above, this one is not industrially exploited. It involved a two-step sequence via allylic derivative (Scheme 2). Diallyl isosorbide ether was prepared by heating the isosorbide (0.4 moles) with allyl bromide (0.88 moles) at 65°C under drop by drop addition of a solution of sodium hydroxide (0.88 moles). The reaction was stopped and cooled at room temperature before washing it with dichloromethane. Freshly prepared diallyl isosorbide was then added slowly to a solution of peracid in dichloromethane. The reaction was stirred at a temperature of 0°C-10°C for 94 hours. The cold solution was filtrated and washed with a solution of 10 % sodium bisulfite followed by saturated sodium bicarbonate and distilled water. The organic layer was then dried over anhydrous magnesium sulphate. Preparative chromatography was used to purify the synthesized product. The monomer of isosorbide diglycidyl ether ($DGEDAS_0$) is thus obtained as a viscous liquid with an epoxide equivalent weight of 143 g/eq; the yield of the reaction was 60 %.

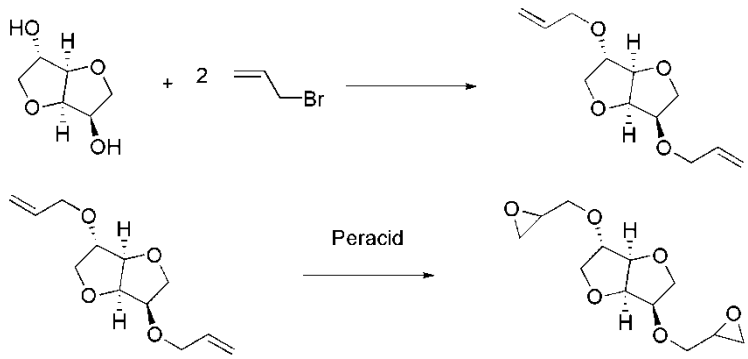

Scheme 2. Synthetic route of isosorbide diglycidyl ether via allylic derivative

3. Preparation of epoxy networks

The formulations used in this study were based on three different epoxy monomers DGEBA, $DGEDAS_0$ and $DGEDAS_n$ cured with the same cycloaliphatic amine, IPD.

To prepare the different networks, the amine curing agent was added to the epoxy prepolymer in different amounts in order to vary the stoichiometric ratio $r = n_{ah}/n_e$ where n_{ah} is the amino hydrogen equivalent and n_e the epoxy equivalent. The epoxy prepolymers and the curing agent, which are all liquid at room temperature, were mixed vigorously and rapidly at room temperature, in order to form a homogenous system. The obtained mixture was poured into a PTFE coated mould and cured at 80°C for 1 h followed by 2 h at 180°C. Networks were stored in dry conditions in order to avoid absorption of atmospheric moisture.

4. Measurements

Size Exclusion chromatography (SEC) was used to measure the molar mass distribution of the epoxy prepolymers. Tetrahydrofuran (THF) was used as the eluent at a flow rate of 1 mL/min. The separation was done on a set of three columns (Waters HR0.5, HR1 and HR2), with a peak detection based on the signal of a refractive index detector (Shimadzu RID-10A).

The positive-ion electrospray ionization time-of-flight (ESI-TOF) mass spectra were acquired by injecting the sample (solubilised in acetone and diluted 100 times in methanol) into the ESI- TOF mass spectrometer (Waters LC-ToF). The spray tip potential was +3200 V and the nozzle potential was +60 V. All the significant peaks present in the mass spectra corresponded to species ionized with sodium ($M+Na^+$).

Fourier Transform Infrared Spectroscopy (FTIR) of the samples was operated on a Nicolet 550 infra-red spectrophotometer, using KBr pellet, in the wavelength range of 500-4000 cm^{-1}. The spectra were acquired using 32 scans at a resolution of four wavenumbers.

^{1}H and ^{13}C NMR were recorded at frequencies of 400 and 100.6 MHz, respectively, using a Bruker AVANCE 400 NMR spectrometer. Deuterated chloroform ($CDCl_3$) was used as a solvent.

Thermogravimetric analysis (TGA) was carried out on a TGA Q500 (TA Instruments, DE, U.S.A.). 10 mg of the sample was loaded in an open platinum pan, and heated from 25°C to 500°C under dry nitrogen at constant heating rates of 10°C/min.

Differential scanning analysis (DSC) measurements were carried out on a DSC Q10 (TA Instruments). The samples were heated at a rate of 10°C/min from -70°C to 200°C under a nitrogen gas atmosphere. A second heating scan with the same conditions was performed after cooling down the samples.

Rheological properties were measured using an ARES Rheometer from TA Instrument equipped with parallel plates with 0.5-1 mm spacing and 50 mm diameter. The reactive mixture was put quickly on the preheated plate (at 80°C) and a multifrequency sweep was started when the temperature equilibrium was reached again. The gel time was determined according to the Winter-Chambon criterion that implies the independence of the loss factor, tan δ (= G''/G'), as a function of frequency [24].

Density of the different epoxy-amine networks was obtained using classical Archimedes method of immersion of the networks in water. Weight measurements were done quickly (<1min) in order to avoid water absorption by the networks.

Dynamic mechanical analysis (DMA) was performed with an ARES Rheometer from TA Instrument using the torsion mode to determine the storage (G'), and loss (G'') moduli as well as tan δ as a function of temperature. Samples (30x10x2 mm^3) were heated from −100°C to 200°C using a heating rate of 3°C/min in a forced convection oven using a nitrogen stream. The sample was deformed sinusoidally with controlled strain amplitude of 0.5 % at a fixed frequency of 1 Hz.

III. Results and discussion

1. Characterization of isosorbide diglycidyl ether

a) SEC characterization

For first information on molar mass distribution, the epoxy prepolymers were analysed by SEC. The SEC chromatograms of the two diglycidyl ether of isosorbide, $DGEDAS_0$ and $DGEDAS_n$, synthesized via two different routes, are presented in Figure 2 as well as the chromatogram of DGEBA for comparison. Whereas the SEC chromatogram of $DGEDAS_n$, obtained via the traditional synthesis route, underlines the presence of oligomers through numerous elution peaks, only one of those peaks is present in the $DGEDAS_0$ chromatogram, at an elution volume of 27.2 ml. This peak corresponds to the pure monomer of diglycidyl ether of isosorbide. The molar mass, calculated from a high molar mass DGEBA (eew = 475 – 550 g/eq) calibration curve, was found equal to 267 g/mol, while the theoretical value is equal to 258 g/mol. By comparing the area of the monomer peak present in $DGEDAS_0$ and $DGEDAS_n$ chromatograms, the proportion of monomer in the $DGEDAS_n$ sample is equal to 30 %. The other part of $DGEDAS_n$ is composed of oligomers of higher molar mass, as it can be observed in more condensed DGEBA.

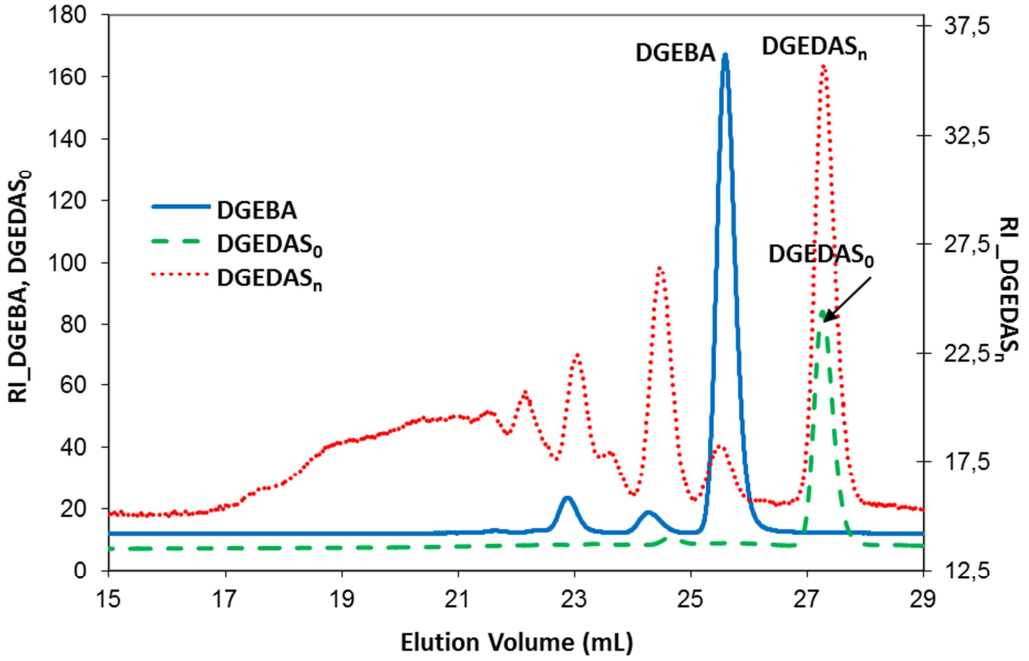

Figure 2. SEC chromatograms of the epoxy prepolymers DGEBA, $DGEDAS_n$ and $DGEDAS_0$ (c = 4 mg/ml).

b) Electro-Spray mass spectroscopy characterization

The epoxy molecule $DGEDAS_n$ was analysed by Electro-Spray mass spectroscopy, to obtain more precise information on molar mass. ESI-TOF mass spectrum is presented in Figure 3; it shows a high number of peaks which indicates the presence of numerous oligomers. The formulae corresponding to some of these species were confirmed by exact molar mass analysis and are given in Table 1 (A represented the isosorbide segment and B the epichlorohydrin segment). Linear oligomers (n = 0, 1, 2) but also branched oligomers (2A + 4B, 3A + 5B, 3A + 6B…) are found, having the chemical structure shown in Figure 4. This result can be explained by a competition during the reaction with epichlorohydrin between the secondary hydroxy groups of isosorbide and the secondary hydroxy groups formed after a first reaction of isosorbide diglycidyl ether with isosorbide. The molar mass of the linear diglycidyl oligomers is given by M = 258 + n x 202. Electro-Spray analysis gives information on the molar mass of the oligomer species of $DGEDAS_n$ but, in the conditions used, the magnitude of the peaks is not quantitative and therefore cannot be linked to the amount of each species.

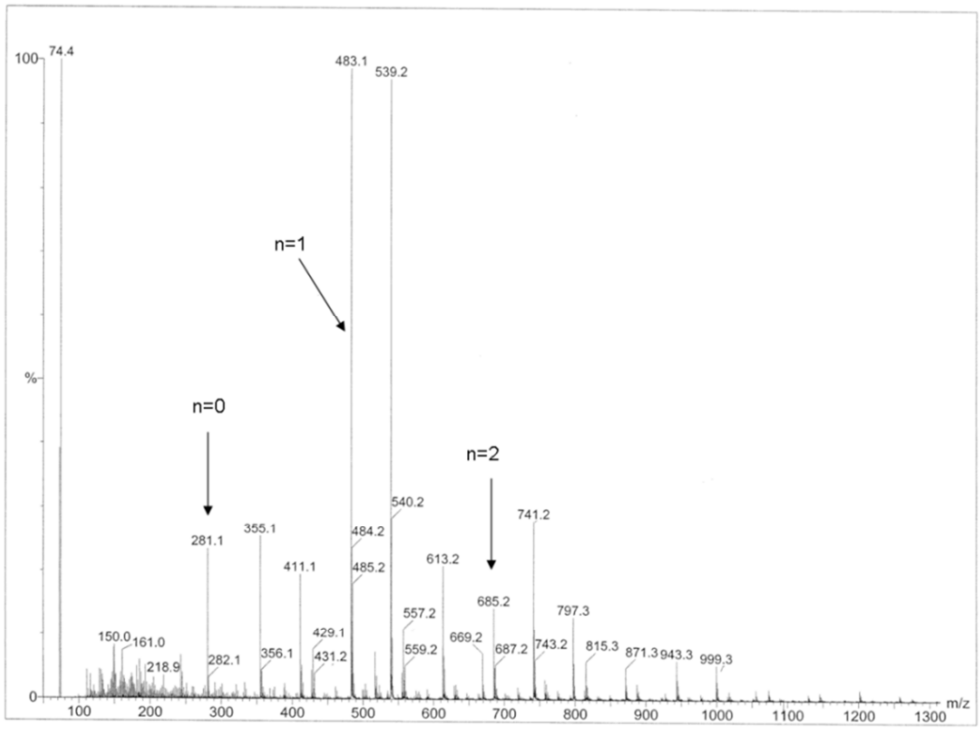

Figure 3. ESI-TOF mass spectrum (positive ion mode) of DGEDAS$_n$

Molar Mass (g/mol)	Formula	Structure
258	$C_{12}H_{18}O_6$	A+2B (n = 0)
404	$C_{18}H_{28}O_{10}$	2A+2B
460	$C_{21}H_{32}O_{11}$	2A+3B (n = 1)
516	$C_{24}H_{36}O_{12}$	2A+4B
662	$C_{30}H_{46}O_{16}$	3A+4B (n = 2)
718	$C_{33}H_{50}O_{17}$	3A+5B
774	$C_{36}H_{54}O_{18}$	3A+6B

Table 1 : Molar mass values of some DGEDAS oligomers revealed by ESI-TOF

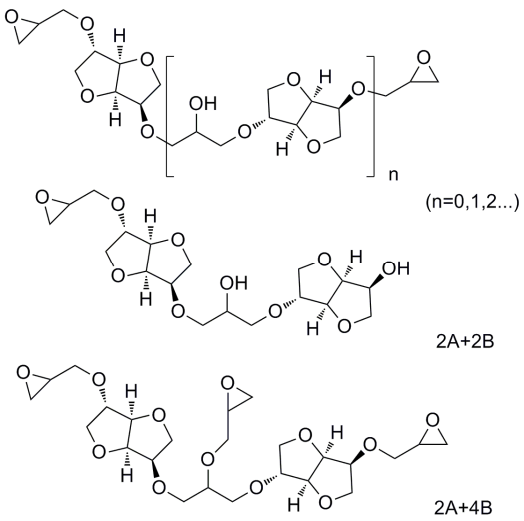

Figure 4. Structures of the oligomers of $DGEDAS_n$ revealed by ESI-Tof

c) FTIR characterization

Fourier transform infrared (FTIR) spectroscopy was used to identify the molecular structure and the chemical bonds of the three different epoxy prepolymers. Referring to the FTIR spectra of $DGEDAS_0$ and $DGEDAS_n$ shown in Figure 5, the different peaks indicate the presence of -OH group (3470 cm^{-1}), -CH bond (2930, 2870 cm^{-1} and 1460, 1370 cm^{-1}), -CO- bond form aliphatic ether (1090 and 1020 cm^{-1}) as well as epoxide group (910 cm^{-1}). The main difference between $DGEDAS_0$ and $DGEDAS_n$ is the very weak intensity of the –OH peak in $DGEDAS_0$ (due to residual moisture) which indicates the absence of –OH group in $DGEDAS_0$. DGEBA (not shown here) mainly differs from DGEDAS by the presence of aromatic structures: -C=C bond (1607, 1579 and 1508 cm^{-1}) and aromatic C-O (1243 cm^{-1}).

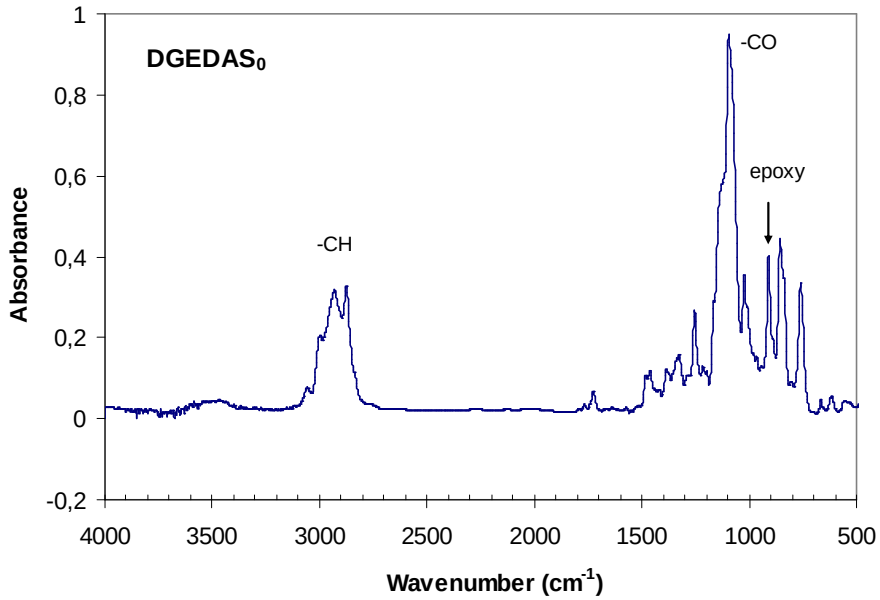

(a)

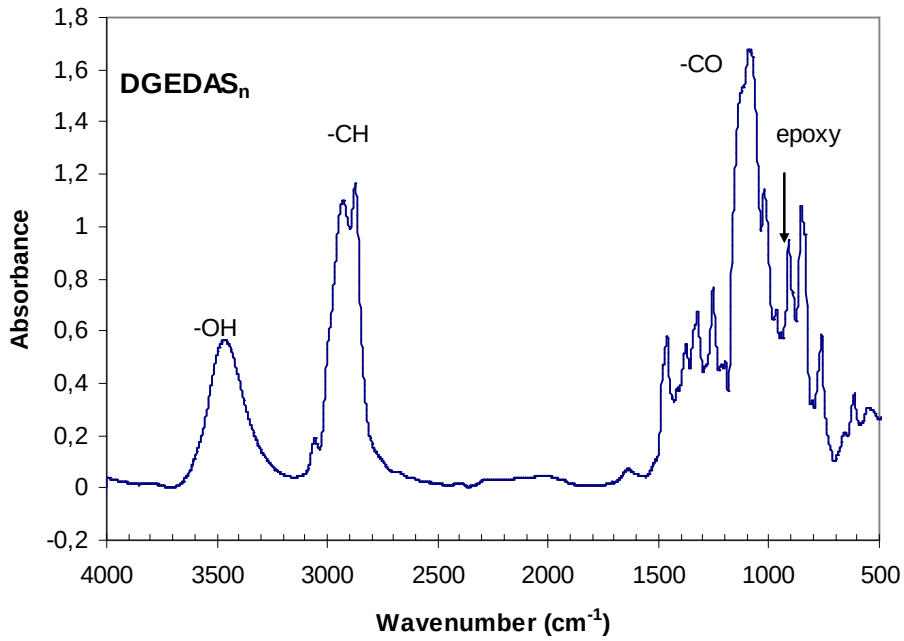

(b)

Figure 5 : FTIR spectra of (a) $DGEDAS_0$, (b) $DGEDAS_n$

d) NMR characterization

Figures 6 and 7 show the ^{1}H NMR and ^{13}C NMR spectra of the diglycidyl ether of isosorbide monomer ($DGEDAS_0$); the proton and carbon assignments are indicated. The epoxy protons H1a, H1b and H2, give the signals between 2.5 and 3.1 ppm. The peaks between 4.4 and 4.6 ppm are assigned to the protons common to the two isosorbide cycles, H*. Because of the conformation of the cycle and thus the non-equivalence of the protons of the isosorbide cycle [25] and the H3 protons, the peaks between 3.3 and 4.1 ppm corresponding to these protons are difficult to assign precisely. The integrated values for the different signals are in good agreement with the structure shown in Scheme 1. The ^{13}C NMR spectrum shows very well-defined peaks: the carbons of the epoxy ring, C1 and C2, show signals at 44 and 50.5 ppm respectively. The carbon, C3, belonging to the glycidyl ether unit has a resonance at 70 ppm. Then the different carbons, from the isosorbide cycle, are observed between 71 and 86 ppm.

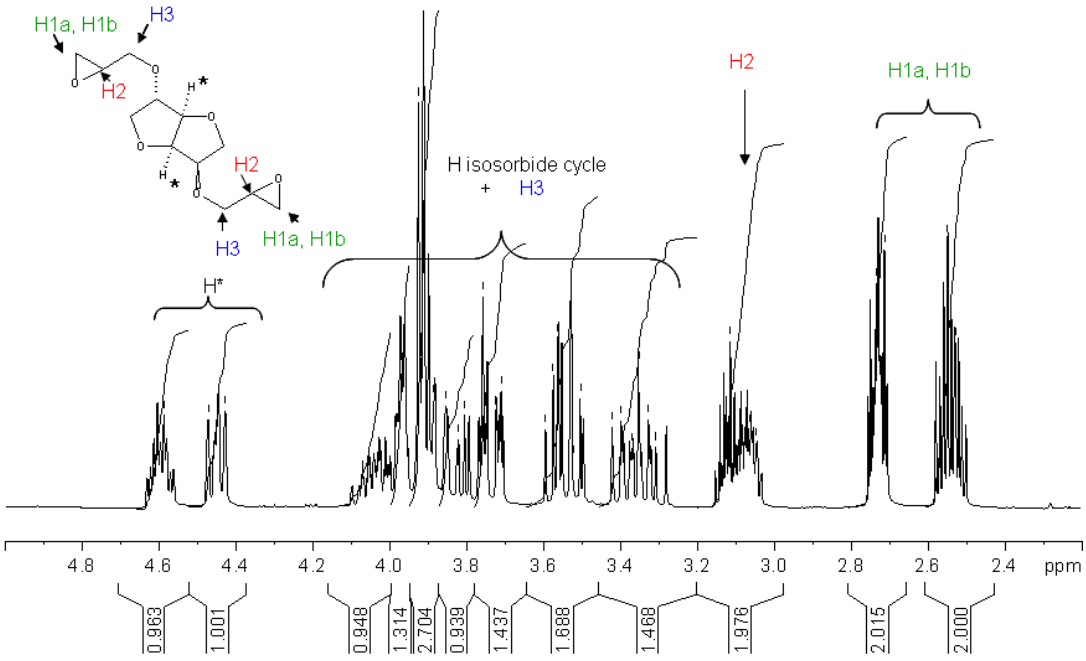

Figure 6. ^{1}H NMR spectra of $DGEDAS_0$

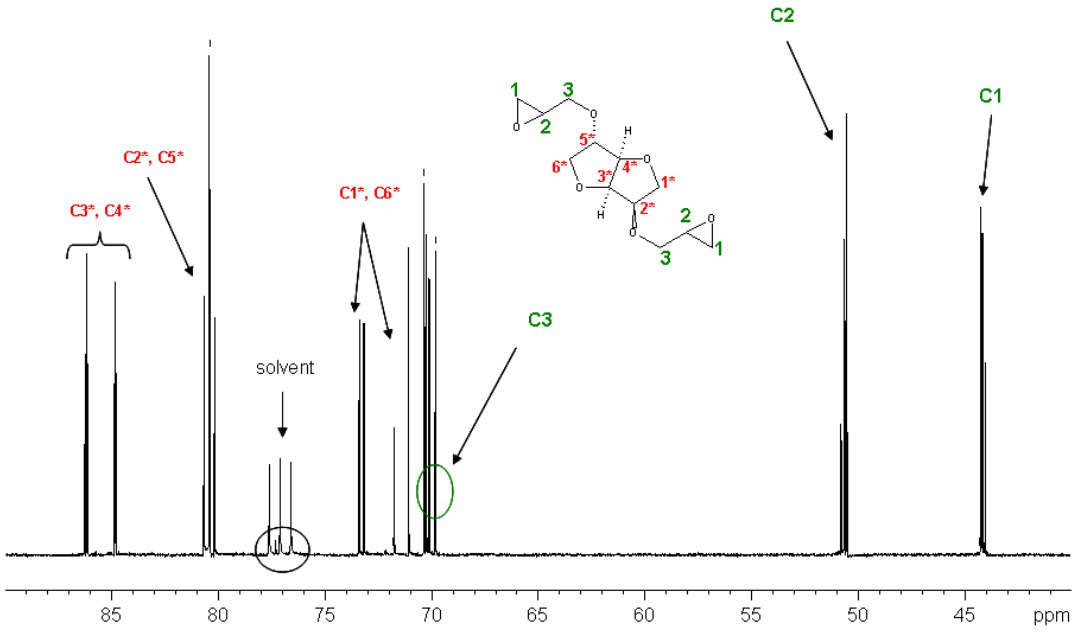

Figure 7. ^{13}C NMR spectra of DGEDAS$_0$

Figures 8 and 9 show the ^{1}H NMR and ^{13}C NMR of the diglycidyl ether of isosorbide oligomer (DGEDAS$_n$). Because of the broad molar mass distribution of the oligomers, the proton NMR interpretation of the DGEDAS$_n$ spectrum becomes complex. Based on the previous assignments of peaks, the integration (I) of signals between 2.6 and 3.2 ppm (protons from epoxy cycle and hydro ether unit) and the peaks at 4.5 and 4.7 ppm (H* from the protons common to the two isosorbide cycle) can be used to calculate R, the ratio of epoxy cycle to isosorbide cycle. However the average degree of polymerization, n, can not be calculated due to the presence of branched oligomers and as a consequence DGEDAS$_n$ has a mean functionality higher than 2.

The ratio R of epoxy cycle to isosorbide cycle is given by the following equation:

$$R=\frac{\text{number of epoxy cycle}}{\text{number of isosorbide cycle}}=\frac{\text{(I protons from epoxy cycle)/3}}{\text{(I protons H* from isosorbide cycle)/2}} \quad \text{(Equation 1)}$$

Protons	I (Integration value)
H1a + H1b	1.063 + 1.000
H2	1.008
H* (common to the isosorbide cycle)	0.842 + 0.806
Ratio R	1.24

Table 2. Determination of R using ^{1}H NMR

Using the proton integration values (Table 2) a value of R = 1.24 is found.

The carbon NMR spectrum of $DGEDAS_n$ is also more complicated. In addition to the resonances assigned previously, new peaks appear at 69 ppm (Ca) and 79 ppm (Cb). These peaks give indication on the structure of some oligomers included in the product: the peak at 69 ppm is assigned to C_a-OH peak from the hydroxy ether segment that links two isosorbide cycles. This peak shifts to 79 ppm with an epichlorohydrin recombination. So the ^{13}C NMR confirms the presence of branched oligomers, previously observed by ESI-TOF mass spectroscopy.

A quantitative carbon NMR was also carried out using an "inverse gate decoupling" sequence in order to calculate R the ratio of epoxy cycle to isosorbide cycle. Using conditions leading to quantitative carbon NMR signals, integration values of the carbons are available (Table 3). The ratio of epoxy cycle to isosorbide cycle R is given by the following equation:

$$R = \frac{\text{number of epoxy cycle}}{\text{number of isosorbide cycle}} = \frac{\text{(I carbons from epoxy cycle)/2}}{\text{(I carbons C* from isosorbide cycle)/2}} \quad \text{(Equation 2)}$$

Carbons	I (Integration value)
C1	2.000
C2	2.020
C* (common to the isosorbide cycle)	1.558+1.590
Ratio R	1.27

Table 3. Determination of R using ^{13}C NMR

The value obtained for R, 1.27, is very close to the one given by ^{1}H NMR. Integration values of the signals corresponding to Ca and Cb are 1.052 and 0.803 respectively; it means that in the oligomers (n > 0) the number of branched units represents 43 % and the number of linear units (hydroxy ether) represents 57 %.

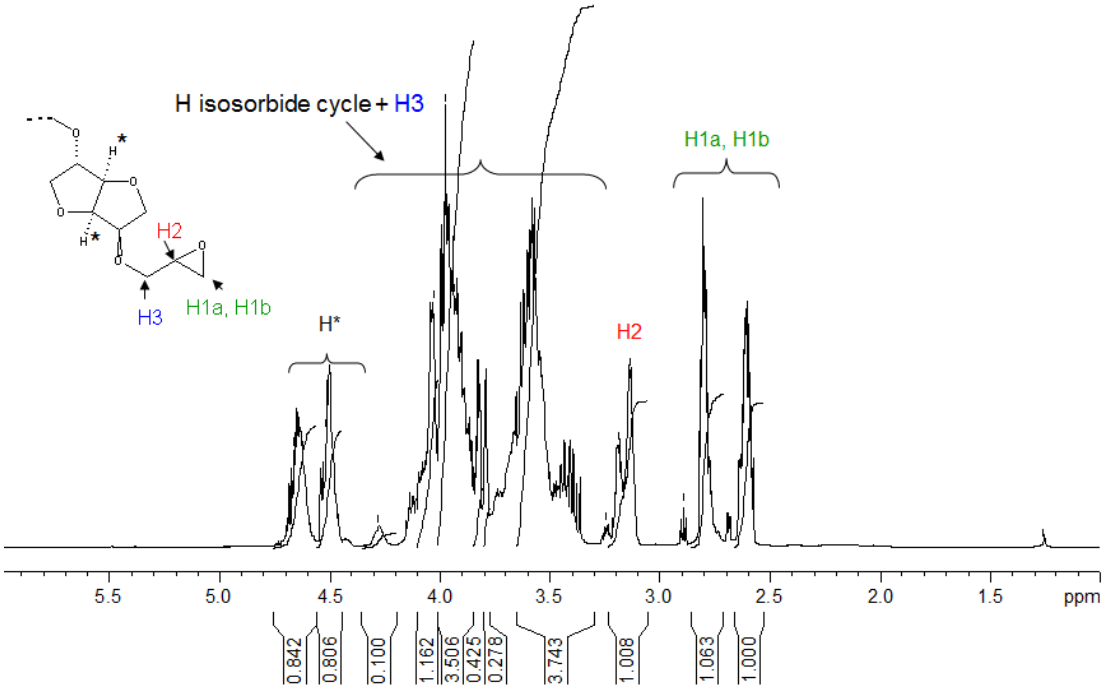

Figure 8. ^{1}H NMR spectra of DGEDAS$_n$

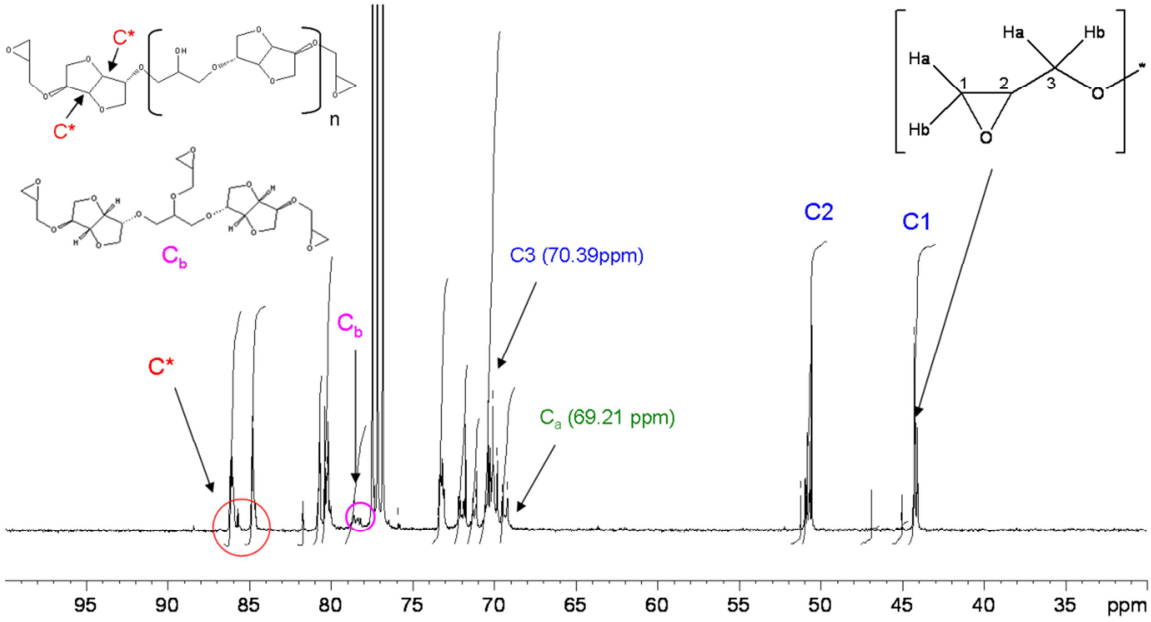

Figure 9. ^{13}C NMR spectra of DGEDAS$_n$

e) TG analysis

The mass loss as a function of temperature for DGEBA, DGEDAS$_n$ and DGEDAS$_0$ prepolymers and their derivatives are shown in Figures 10 (a) and (b). The reference DGEBA thermally degrades mainly through a simple step process with an initial degradation ($T_{5\%}$) close to 250°C and a maximum rate at 320°C. The TGA curve of the monomer of diglycidyl

ether of isosorbide ($DGEDAS_0$) shows a continuous single step degradation process well before DGEBA. It begins after 130°C and with a maximum rate equal to 260°C. In the case of diglycidyl ether of isosorbide oligomer ($DGEDAS_n$), degradation begins like $DGEDAS_0$ around 130°C but with two distinct stages of degradation with maximum rate at 250°C and 410°C. In the first step, the sample lost 30 % of its weight, and in the second step it lost the remaining weight. It revealed that the first step decomposition of the $DGEDAS_n$ is the monomer decomposition. Therefore, $DGEDAS_n$ contains 30 % of monomer $DGEDAS_0$, which confirms the previous results of SEC analysis. Higher molar mass compounds (n=1, 2 and branched oligomers) are more stable or not so volatile.

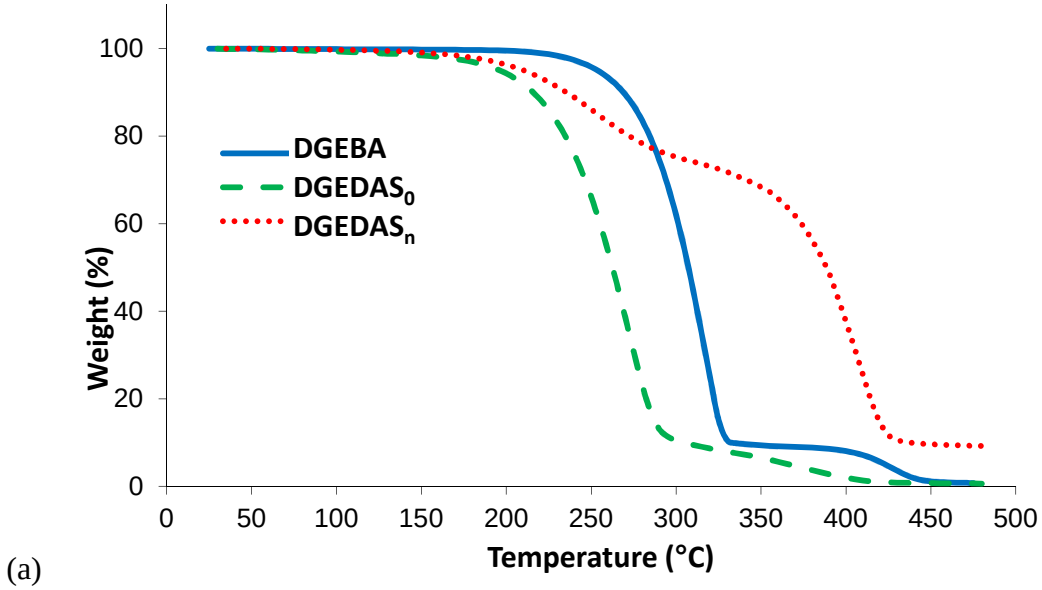

(a)

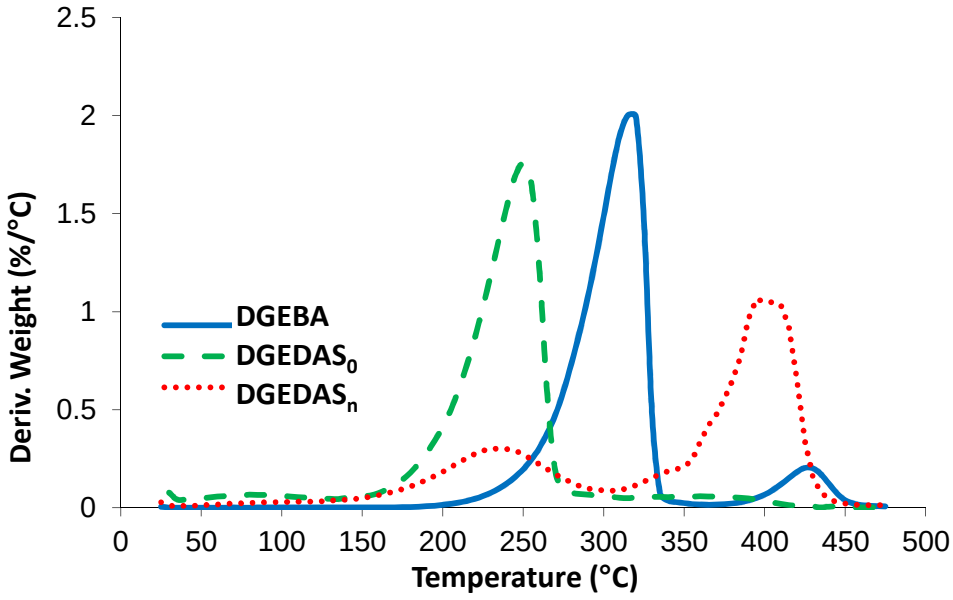

(b)

Figure 10. (a) TGA and (b) DTGA curves of DGEBA, $DGEDAS_0$ and $DGEDAS_n$

2. Curing behaviour

Gel time was determined by rheological measurements, at a temperature equal to 80 °C, for the three reactive systems considered, i.e. epoxy prepolymer with IPD at $n_{ah}/n_e = 1$ calculated from the amino-hydrogen and epoxy equivalent experimental values.

As an example, Figure 11 shows the evolution of the loss factor tanδ as a function of time, in a multifrequency mode (from 1 rad/s to 50 rad/s) for the system $DGEDAS_0$-IPD. The gel time, t_{gel}, is determined by the crossover of the loss factor curves at various frequencies. Table 4 summarizes the gel time for the three different reactive systems. It appears that the new bio-based reactive system $DGEDAS_n$ reacted with IPD has shorter gel time than the traditional one DGEBA-IPD, whereas the system $DGEDAS_0$ - IPD has almost the same gel time as DGEBA – IPD. Different hypotheses can explain the shorter gel time of the system based on the oligomeric bio-based prepolymer: first the epoxy-amine reaction can be catalysed by the hydroxyl groups of this oligomer, secondly the functionality of this compound is probably higher than 2 due to branched molecules which means a conversion at the gel point lower than 0.58-0.60 [26]. At the gelation point, the storage and loss modulus can be described by a power law as a function of the pulsation: $G'(\omega) \propto G''(\omega) \propto \omega^{\Delta}$, where Δ is the relaxation exponent that can be predicted by Rouse's percolation theory. So at gelation tanδ is independent on frequency and its value is: $\delta_{gel} = \pi.\Delta/2$. (Equation 3)
The values obtained for the relaxation component, Δ, are similar for DGEBA-IPD and $DGEDAS_0$-IPD networks (Table 4), these values are in agreement with data reported in the literature on diepoxy-diamine systems [4]. The value obtained for $DGEDAS_n$-IPD system is lower and equal to 0.5; for this system gelation occurs when G' = G''.

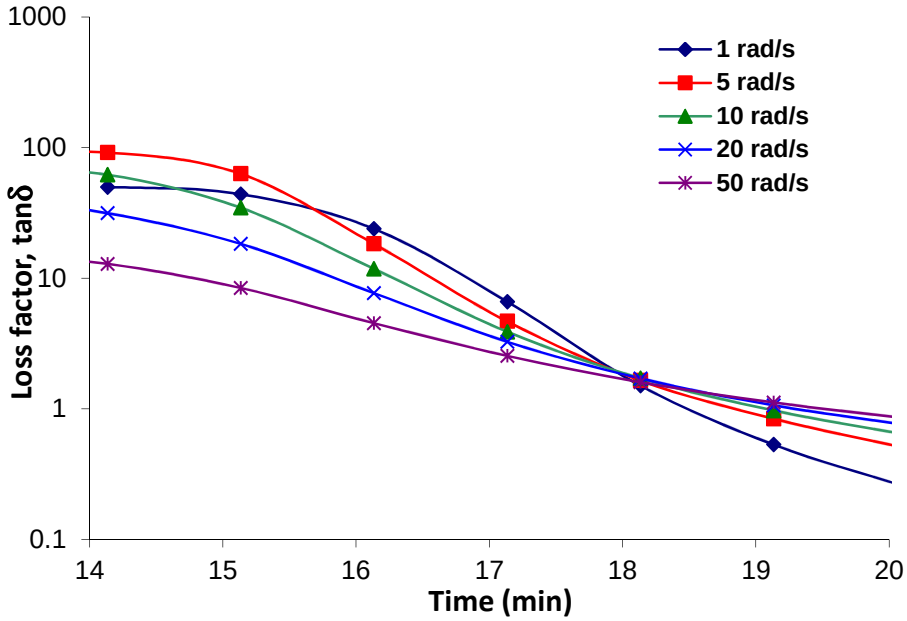

Figure 11. Loss factor tanδ, isotherm at 80°C, example of the reactive system DGEDAS$_0$ – IPD

System	t_{gel} (min)	$tan\delta_{gel}$	Δ
DGEBA – IPD	16	1.5	0.63
DGEDAS$_n$ – IPD	7	1.0	0.50
DGEDAS$_0$ – IPD	18	1.6	0.64

Table 4. Gel time data for the reactive systems DGEBA/IPD, DGEDAS$_n$/IPD and DGEDAS$_0$/IPD

Figure 12 shows the non-isothermal DSC thermograms of the three different epoxy precursors reacted with IPD at n_{ah}/n_e = 1. The glass transition temperature of the systems before reaction, T_{g0}, is the lowest for the system based on DGEDAS$_0$, this monomer has a lower molar mass as compared to the two others. The peak maximum temperature, T_{peak}, and the total heat of reaction (ΔH) obtained from the DSC analysis are summarized in Table 5. There are no large differences between the three systems. DGEBA-IPD and DGEDAS$_0$-IPD thermograms have similar shape, with a main peak at 114 and 108°C respectively, and a shoulder on the high temperature side. This shoulder is explained by the different reactivity of the amino groups of IPD. In the third system, DGEDAS$_n$-IPD, the exothermic peak of reaction is more symmetric, T_{peak} is slightly lower, confirming the highest reactivity of this system as compared to the two others which can be explained also by the fact that due to branching there are two different types of epoxy groups; cycloaliphatic and aliphatic epoxy groups, as shown in Figure 4. The values of the enthalpy of reaction are the same for the three

systems and in the range of the classical value obtained for epoxy-amine reaction at a stoichiometric ratio of 1.

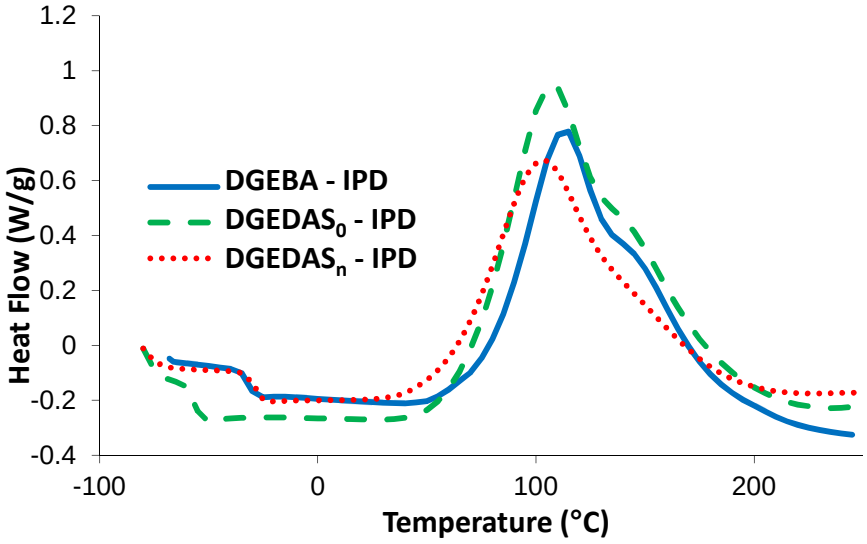

Figure 12. DSC thermograms of dynamic curing of DGEBA, $DGEDAS_n$, and $DGEDAS_0$ with IPD (heating rate 10°C/min), r = 1

System	T_{g0} (°C)	ΔH (J/g)	ΔH (kJ/ee)	T_{peak} (°C)
DGEBA – IPD	-35	415	92	114
$DGEDAS_n$ – IPD	-36	404	91	104
$DGEDAS_0$ – IPD	-60	547	89	108

Table 5. DSC results for DGEBA/IPD, $DGEDAS_n$/IPD and $DGEDAS_0$/IPD

3. Influence of stoichiometry on the value of T_g

The effect of variation of the amino hydrogen-to-epoxy ratio, $r = n_{ah}/n_e$, on T_g is examined in this study as an indicator of possible side reactions. Indeed it has been shown that assuming the only mechanism is epoxy-amine addition without side reaction, the maximum attainable T_g coincides with the stoichiometric composition [27]. For each epoxy prepolymer the variation of the ratio n_{ah}/n_e was studied between 0.5 and 1.5.

For the three systems, the variation of the glass transition temperature, measured during a second DSC run, is plotted versus r in Figure 13. In each case, the curves exhibit a maximum T_g for r equal to 1, which means that the only mechanism occurring during the cross linking

of the reactive systems is the amine-epoxy addition. No side reaction, such as etherification, occurs during the cross linking.

The T_g obtained for both bio-based reactive systems are lower than the T_g observed for the conventional DGEBA – IPD system. This observation can not be attributed to incomplete curing as no residual heat was observed by DSC after the curing cycle and FT-IR showed no peak at 910 cm^{-1}. A similar result was found by Feng et al who noticed a decrease of T_g about 40°C on networks synthesized from diglycidyl ether of isosorbide and Jeffamine T403, an aliphatic curing agent [22]. Because of the short and cyclic structure of the monomer present in the bio-based epoxy resin, higher T_g were expected for those systems. It was shown for aliphatic and aromatic polyesters that isosorbide structure is much more rigid than usual diols like ethane diol or butane diol [28]. In our case we have to compare the effect of bisphenol A and isosorbide, a comparison could be done from linear polycarbonate synthesized from these two diols [29]. It seems that in this case the isosorbide structural unit brings a lower contribution to T_g, with a decrease of 15°C as compared to bisphenol A-based polycarbonate. Besides, for epoxy networks T_g depends on the chain stiffness, through the structure of the epoxy prepolymer and hardener, and also on the crosslink density, ν, given by their respective concentrations [4, 30]. Many methods based on physical or empirical approaches have been developed for the prediction of T_g. The relation established by DiMarzio is well adapted to epoxy-amine networks:

$$T_g = \frac{T_{gL}}{1 - K_{DM} F \upsilon} \qquad \text{(Equation 4)}$$

where K_{DM} is the DiMarzio universal constant, F is a flex parameter and T_{gL} is the glass transition of a hypothetical linear polymer; T_{gL} represents the copolymer effect and can be calculated using an additivity law. The low molar mass of the isosorbide based monomer and thus the increase of the proportion of hardener, IPD, can explain the lower T_g obtained for the $DGEDAS_0$ – IPD networks compared to the one of DGEBA – IPD network. For 100 g of epoxy monomer we need 24 g of IPD in the case of DGEBA (r = 1), and 30 g of IPD in the case of $DGEDAS_0$. The mass fraction of IPD increased from 19.3 % in DGEBA – IPD to 23.1 % in $DGEDAS_0$ – IPD, so the contribution of the hardener to T_g is greater in the case of $DGEDAS_0$ – IPD than DGEBA – IPD.

There is no large variation in T_g for the two bio-based systems: on the one hand the molar mass distribution is very different as well as the epoxy equivalents, but on the other hand the highest functionality of $DGEDAS_n$ may explain why the T_g based on this prepolymer shows

only a slight decrease as compared to $DGEDAS_0$; moreover the variation of T_g versus a/e is less pronounced.

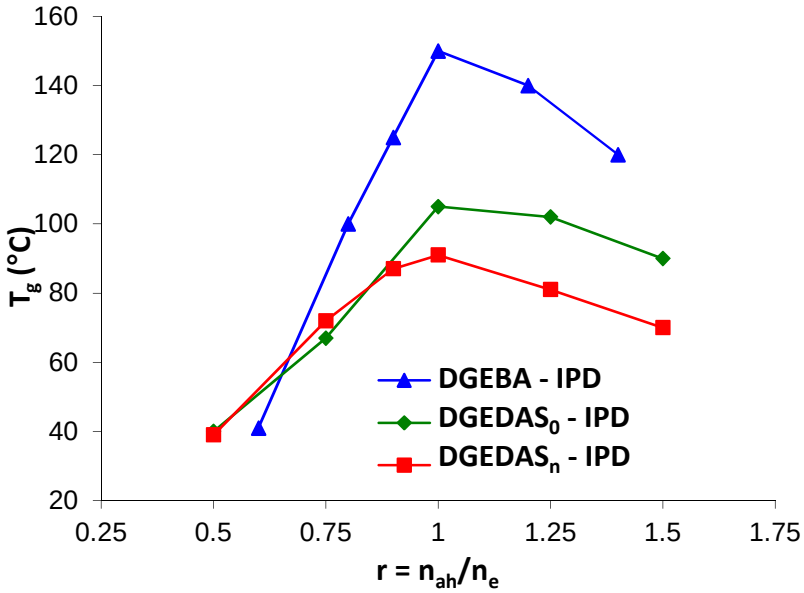

Figure 13. Glass transition temperature versus r for networks based on DGEBA, $DGEDAS_n$ and $DGEDAS_0$ in combination with IPD

4. Thermo-mechanical properties of the networks

The dynamic mechanical properties of the networks were investigated using DMA. In Figures 14 (a), (b) the storage modulus (G') and the loss factor (tanδ) of the two bio-epoxy based networks are compared with the DGEBA based one.

A typical plot of the storage modulus G' and tanδ as a function of temperature exhibits two relaxations. The main transition, α in the high-temperature region, is associated with the glass transition; the secondary relaxation β, below 0°C is assigned to short molecular segment motion, hydroxyl ether groups in the particular case of epoxy-amine networks [31]. The values of T_β, T_α, G'_R are reported in Table 6.

There is no significant difference in the sub-T_g behaviour between the three types of networks: T_β are in the same range of temperatures, around -50°C, but the magnitude of the relaxation is higher for the isosorbide based networks (Table 6). It is linked to the concentration of the relaxing species per unit volume, hydroxy ether units, that is for the same reason explained previously higher in $DGEDAS_0$-IPD networks as compared to DGEBA-IPD

network. For $DGEDAS_n$ – IPD networks, the hydroxy ether groups can come initially from the oligomers and from the epoxy-amine reaction, their concentration in the final network should be more or less the same as in $DGEDAS_0$ – IPD network.

T_α follows the same trend as the T_g measured by DSC: the highest value, 155°C, is obtained for the DGEBA – IPD network, then a decrease of T_α is observed for the bio-based networks which reach 112 and 96°C, for $DGEDAS_0$ – IPD and $DGEDAS_n$ – IPD respectively. The $DGEDAS_n$ – IPD network has the highest rubbery modulus, followed by the $DGEDAS_0$-IPD and the DGEBA – IPD networks with equivalent rubbery moduli. This means that the network in which the molecular motion occurs at the lowest temperature has also the shortest chains between crosslinks. This behaviour is linked to the branched structure of the $DGEDAS_n$ oligomer and to its high functionality as compared to $DGEDAS_0$.

According to the rubber elasticity theory, the following equation is employed to describe the relationship between M_c (average molar mass of the segment between crosslinking points) and storage modulus (G') of a thermoset above the T_g [32] :

$$G' = dRT/M_c \qquad \text{(Equation 5)}$$

where G', d, R, T are the storage modulus at T_g+30K, the density of the polymer, the gas constant (8.314 J/mol.K) and the temperature (K) respectively. The values of molar mass between crosslinking, calculated as cited above, are summarised in Table 6. They are compared to the theoretical value calculated from the molar mass of the epoxy prepolymer and curing agent, M_{cth}.

$$M_{cth} = (M_{amine} + 2M_{epoxy})/3 \qquad \text{(Equation 6)}$$

The molar mass of the epoxy prepolymer was calculated from the value of the epoxy equivalent and assuming a functionality of 2. Theoretical and experimental results concerning M_c are in agreement for the networks based on pure monomers (DGEBA and $DGEDAS_0$) which have a functionality of 2. For the network based on $DGEDAS_n$ oligomer a significant difference is noticed between the experimental value and the theoretical value. This difference is due to the wrong functionality used to calculate the theoretical M_c and thus confirms indirectly the complex chemical structure of $DGEDAS_n$. There are two types of crosslink points in $DGEDAS_n$ based networks (Figure 4):

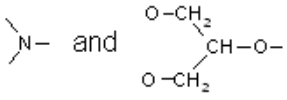

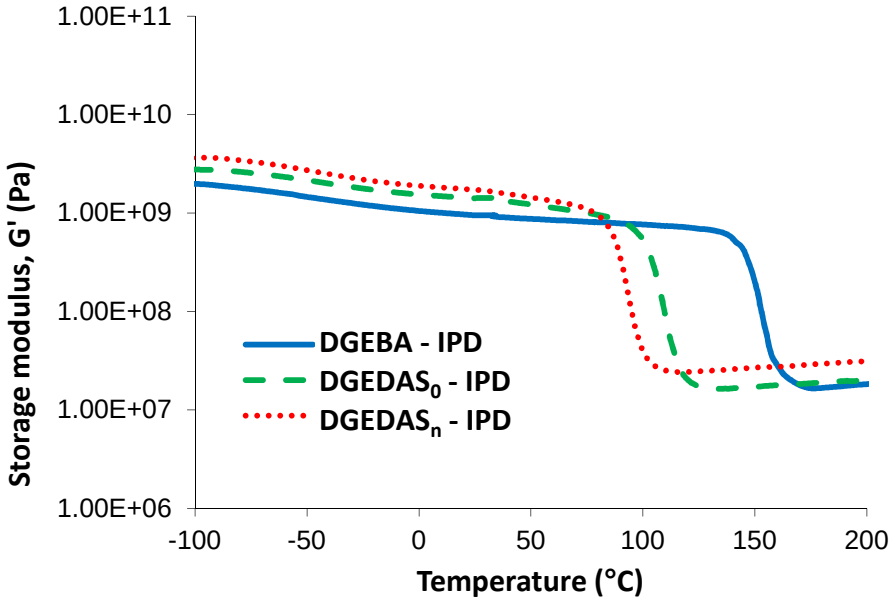

(a)

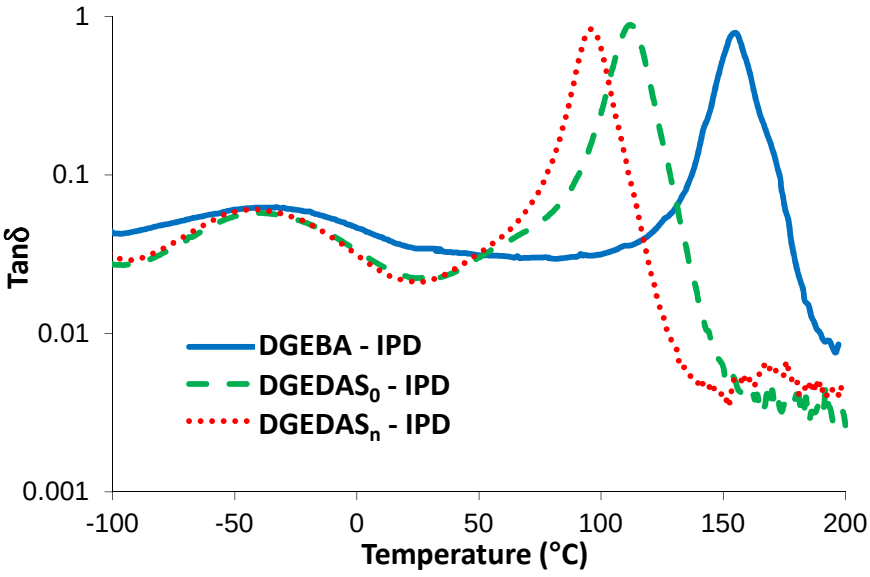

(b)

Figure 14. Storage modulus versus temperature (a) and tan δ versus temperature (b) for DGEBA, $DGEDAS_n$ and $DGEDAS_0$ cured with IPD

System	T_β (°C)	T_α (°C)	G'_R (MPa) (at T_g+30°C)	d (g/cm^3)	M_c (g/mol)	M_{cth} (g/mol)
DGEBA – IPD	-46	155	17.1	1.13	250	300
$DGEDAS_n$ – IPD	-42	96	24.7	1.24	170	302
$DGEDAS_0$ – IPD	-40	112	16.6	1.25	260	247

Table 6. Dynamic mechanical analysis of the networks: DGEBA/IPD, $DGEDAS_n$/IPD and $DGEDAS_0$/IPD for r=1

5. Thermal stability of the networks

The mass loss as a function of temperature for DGEBA, $DGEDAS_0$ and $DGEDAS_n$ cured with IPD are shown in Figure 15. The network DGEBA-IPD thermally degrades through a simple step process with an initial degradation ($T_{5\%}$) close to 330°C and a maximum rate at 370°C. The TGA curve of the network obtained with $DGEDAS_n$ combined with IPD shows also a simple step process with an initial degradation and a maximum rate, respectively at 330°C and 380°C, very close to the values observed for DGEBA-IPD network. The $DGEDAS_0$-IPD network exhibits poorer thermal stability compared to the other networks, with an initial degradation ($T_{5\%}$) at 305°C and a maximum rate at 350°C. It is probably related to the low thermal stability observed on the $DGEDAS_0$ prepolymer (Figure 10).

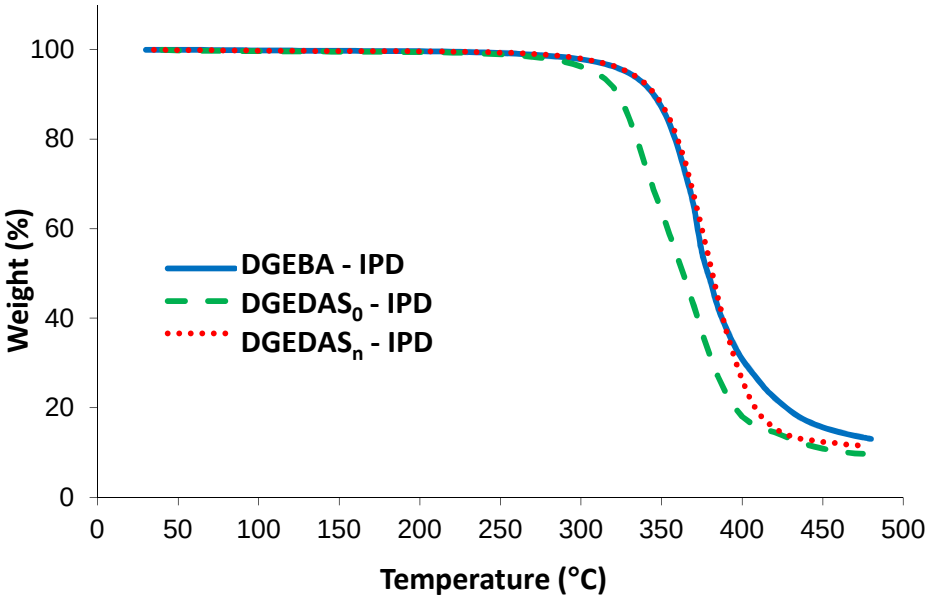

Figure 15. TGA curves of networks based on DGEBA, $DGEDAS_0$ and $DGEDAS_n$ in combination with IPD

IV. Conclusion of Part I

In this work, two novel bio-based epoxy prepolymers were successfully synthesized from renewable resources (isosorbide) via two different routes. The chemical structures were studied in detail using SEC, ESI-TOF MS, ^{1}H and ^{13}C NMR, and FT-IR analysis. Diglycidyl ether of dianhydro-sorbitol (DGEDAS) was obtained either as a pure monomer or as an oligomeric resin of higher functionality. Reactivity and physical properties of these new epoxy prepolymers cured with isophorone diamine (IPD) were compared with a traditional petroleum-derived epoxy prepolymer (DGEBA) cured with the same hardener and under the same conditions. The system based on the oligomeric resin is more reactive than the two others, which behaves similarly. In all cases the maximum glass transition temperature was obtained using a stoichiometric ratio equal to 1 which means that only epoxy-amine reactions occur. Networks synthesized from the bio-based epoxy prepolymers have high glass transition temperature, yet lower than the DGEBA based network. However they have higher rubbery modulus due either to the lower molar mass or to the higher functionality of the prepolymer. These results suggest that isosorbide-based epoxy precursors could be good candidates to replace bisphenol A-based epoxy prepolymers. However storage of these bio-based prepolymers must be done in dry conditions because these compounds are hygroscopic and the presence of water may deteriorate the properties of the networks, depending on the type of hardener used [22].

Part II. Molecular modelling of bio-based polymer derived from isosorbide

I. Introduction

In the first part of this chapter, we presented two different bio-based epoxy prepolymers derived from isosorbide and obtained through two different synthetic routes: $DGEDAS_0$ and $DGEDAS_n$ that differ by the presence of oligomers and –OH groups for $DGEDAS_n$. Glass transition temperatures and thermo-mechanical properties of the resulting networks obtained with IPD were evaluated using differential scanning calorimetry (DSC) and dynamic mechanical analysis (DMA). It appears that $DGEDAS_n$ – IPD and $DGEDAS_0$ – IPD present lower glass transition temperatures than a conventional DGEBA – IPD network (around 40°C less).

We also presented the DiMarzio relation (Equation 4) as a first approach on T_g prediction. Indeed, as previously mentioned, glass transition of epoxy networks mainly depends on two parameters: the crosslinking density and the chain stiffness (which represents the mobility of the chain between two crosslinking points) [4].

We decided to overcome the crosslinking parameter and use molecular modelling to simulate the glass transition, T_{gL}, of a hypothetical linear epoxy chain representing the copolymer effect between the epoxy and hardener monomers. This will allows us to understand the difference between the chain stiffness of the conventional network obtained with DGEBA and the ones obtained with isosorbide epoxy prepolymers. To overcome also the influence of oligomers (higher functionality, presence of –OH groups) molecular simulation will be only performed on $DGEDAS_0$ and DGEBA epoxy monomers in combination with IPD.

Linear epoxy-amine chains were constructed using the structures of the two different epoxy prepolymers studied, the diglycidyl ether of isosorbide ($DGEDAS_0$) and the diglycidyl ether of bisphenol A (DGEBA) with isophorone diamine (IPD) as a chain extender. Semi-empirical modelling, using group contribution, and molecular dynamics (MD) simulations were performed on these two linear chains.

The theoretical values of T_{gL} obtained by molecular modelling of these two linear chains will give an overview on the influence of molecular structure of epoxy prepolymers on T_g (influence of the copolymer effect) and will be compared to the experimental values obtained by DSC analyses and DMA analyses of the two epoxy networks.

II. Molecular modelling

In recent years, the rapidly increasing power of computational hardware and software has encouraged attempts to study the glass transition by fully atomistic simulations. Such simulations can be used to probe the details of the physical processes taking place at length scales which cannot be probed by thermodynamic and kinetic theories which are based on a more global description of the system at larger length scales. Almost any parameter can be modelled using atomistic simulation, provided a suitable force field is used and the atomic structure is known. Concerning the glass transition prediction, an objective of such work is to predict T_g by identifying the temperature at which discontinuities occur in the properties obtained directly from the results of the simulations [33].

1. Group contribution and molecular dynamics simulations

In our study we decide to focus on two different molecular modelling approaches: the group contribution and the molecular dynamics methods.

The **group contribution method** applies the theory developed by Van Krevelen and Fedors [33, 34]. The group contribution method uses the principle that some simple aspects of the structures of chemical components are always the same in many different molecules. So by following this principle, a wide variety of properties of a polymer can be predicted only by knowing its repeating unit. This method is empiric, rapid, and uses data collected on several polymers that have been extensively studied.

On the other hand, **molecular dynamics** (MD) is a more convenient method for simulation of relatively complex molecules such as polymers [35]. An appropriate forcefield is required to describe the interactions between atoms. COMPASS forcefield [36-38] was used in this study as it has been specially developed for dense organic systems, such as polymers. Molecular dynamic simulations allow the construction of a VT (Volume-Temperature) diagram for the epoxy-amine chains and thus the determination of T_g as represented in Figure 16.

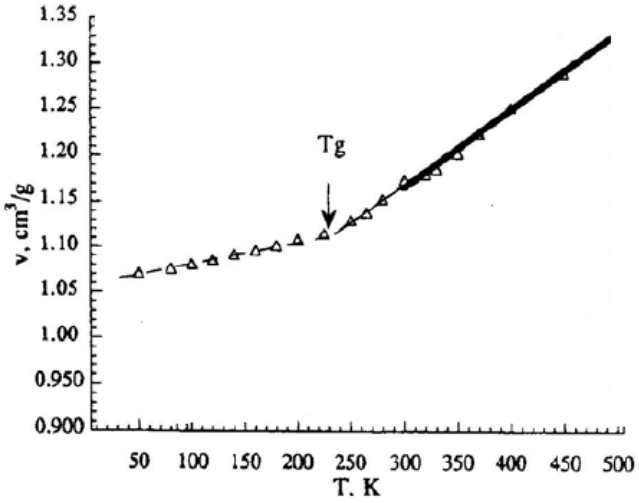

Figure 16. Simulation of diagram volume-temperature (VT) – determination of T_g

Remark: Additional theoretical background on molecular modelling is given in Annex A, with the principle of molecular simulation, forcefields and molecular dynamics.

2. Molecular modelling applied on polymers

In the field of polymers, most of molecular simulation studies have been focused on **thermoplastic materials** such as polyarylethersulfone [39], poly(methylmethacrylate) [40], polystyrene, polycarbonate…

Concerning epoxy, Barton et al [41], illustrated the use of molecular dynamics simulations to calculate T_g from the variation of the specific volume with the simulation temperature for **linear epoxy polymers**. For their simulation, the authors used the conventional Diglycidyl Ether of Bisphenol A (DGEBA) as epoxy prepolymer and 1,2-

dianiloethane (DAE) as curing agent which has only two reactive hydrogens in order to prevent crosslinking. All property calculations were performed by two methods: the group contribution method based on the work of van Krevelen and direct atomistic simulation (Molecular dynamics simulation) using the linear epoxy unit as represented in Figure 17. Good correlation between the simulated and experimental values of T_g were observed.

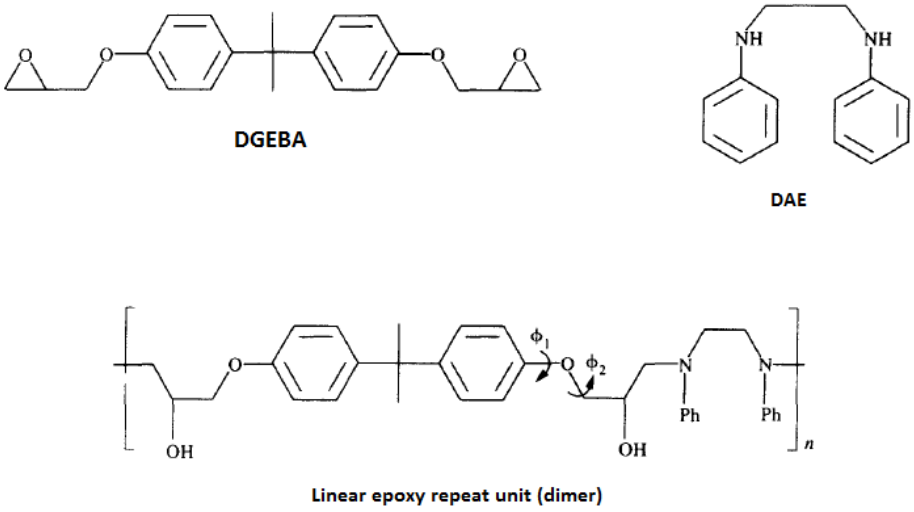

Figure 17. Structure of the reagents used in Barton study [41] and the corresponding linear epoxy unit (dimer) used for molecular modelling study

When **networks** (crosslinked materials) are considered for molecular modelling, there are various constraints and approximations which need to be applied to make the task achievable. The most striking drawback is the complexity of the crosslinking reactions and the sheer sizes of the species involved.

Liu et al. [42] develop a protocol for predicting the glass transition temperatures of epoxy-based thermoset materials as a function of their composition and using group interaction modelling and atomic additivity method. For a linear polymer, it is easy to define the repeat unit if the monomer compositions are known. Thus, the cohesive energy and the number of degrees of freedom can be easily calculated via a range of means. However, for a crosslinked system, it is difficult to define the repeat unit because of the variation in crosslink density at different spots. Thus, Liu et al. arbitrarily broke the crosslinked system into small fragments of epoxy and amine moieties. The individual cohesive energy and degree of freedom can generally be identified for each moiety. Knowing the composition of these moieties, the average cohesive energy and degree of freedom values can be calculated and can

be used to determine T_g by group modelling method. Nevertheless, many approximations need to be done to quantify the different and numerous repeating moieties that need to be taken into account for cohesive energy calculation.

Other methods were used for modelling network polymers and by far the most common one is to create a unit cell which could be considered representative of the polymer bulk:

- Fan et al. [43] "manually" created a unit cell representing a small fragment of DGEBA – TETA network. This fragment of fully cured network consists of 12 molecules of DGEBA and 4 molecules of TETA. Totally 628 atoms were assembled in a cubic cell to represent a piece of the network with a density equal to the experimental value. Molecular dynamics (MD) simulations were performed on this sample to determine T_g. Results were in good agreement with experimental values.

- Wu et al [44] developed a new method for the construction of atomistic polymer network and applied it to epoxy resin system based on DGEBA – IPD. Crosslinked polymer was constructed dynamically using a "home-made" algorithm that performs the reaction of epoxy groups with primary amine hydrogens to form secondary amines hydrogen which can in turn react with epoxy groups. To facilitate the procedure, four aspects were assumed: (1) epoxy prepolymer component is less mobile than curing agent component; (2) primary amine hydrogen has the same reactivity to the secondary amine hydrogen; (3) the etherification reactions can be neglected; and (4) the reactions are diffusion-controlled one.

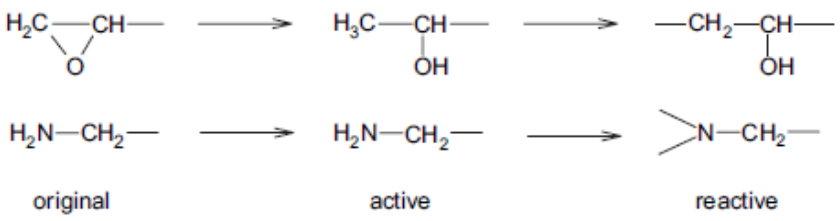

Figure 18. Modelling of functional groups used in the construction procedure [44]

However, there are lots of issues on the identification of the reactive sites and covalent bonds formed between the prepolymer and the curing agent, besides computational

requirements are very important and construction of polymer networks most often implies development of home-made software.

In our case, we decide to model the two linear epoxy polymers obtained from $DGEDAS_0$ and DGEBA epoxy prepolymers combined with IPD. Determination of the T_{gL} of these linear epoxy polymers will give us a comparison of the chain stiffness of the different systems.

III. Experimental section: protocols

All simulations were performed using Materials Studio [45] (Accelrys version 5.0) and the fully atomistic forcefield COMPASS. The repeating units of the different linear chains studied were built knowing the structure of the two epoxy prepolymers, DGEBA and $DGEDAS_0$, and the curing agent IPD (see Figure 1). The two repeating units are shown in Figure 19. It was supposed that only the primary amines from IPD reacted to form the linear polymer.

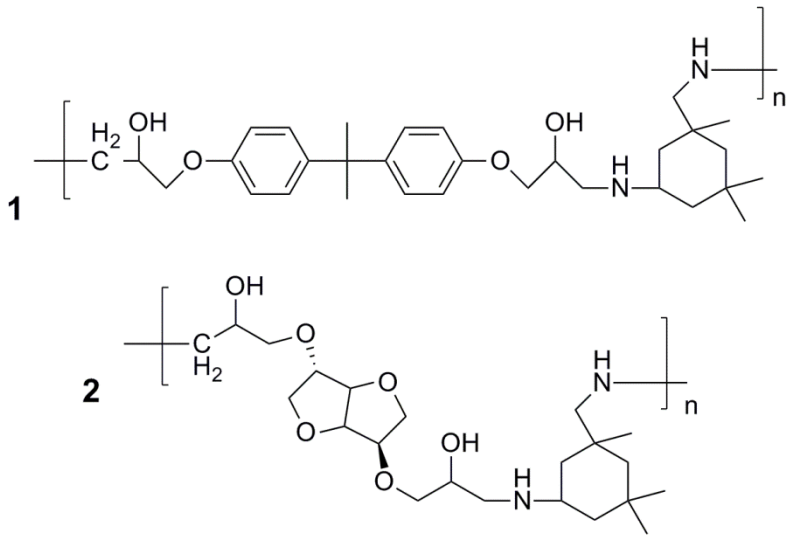

Figure 19. Linear epoxy repeat unit for 1: DGEBA – IPD and 2: $DGEDAS_0$ – IPD

1. Group contribution method

The Synthia [46] module of the Materials Studio software was used to calculate the glass transition temperature and the densities of the polymer modelled. This module uses the group contribution theory from Van Krevelen and Fedors [33]. Group interaction modelling uses the intermolecular energy of interaction between groups of atoms in adjacent polymer

chains as a basis for predicting some properties of bulk polymers as a function of chemical composition and molecular structure.

Group contribution method simulations were directly performed on the two linear epoxy repeating units (see Figure 19). In this study, only density and glass transition temperature were considered while the group contribution method gives access to more than 30 polymer properties.

2. Molecular dynamics method

The general procedure for the construction and equilibration of amorphous cells is the following. First, the repeat units (Figure 19) were built and the polymer chains were constructed at length of 30 repeat units corresponding to a molecular weight of 12800 g/mol (for $DGEDAS_0$ – IPD) to 15300 g/mol (for DGEBA – IPD). This was done using the Build function of the Materials Studio Visualizer. The chains were constructed with a random torsion between successive repeating units. Then a step of geometry optimization was performed with Forcite Plus module with a medium quality and the smart algorithm method from Accelrys. After this optimization, the chains were packed with Amorphous Cell module. This construction was done at the density calculated by Synthia. The result of this packing is presented in Figure 20.

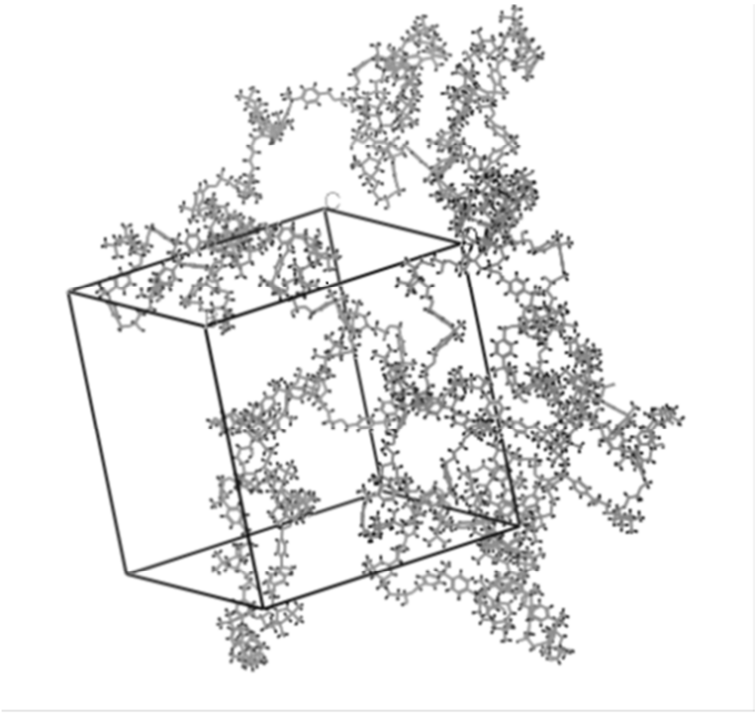

Figure 20. Results of Amorphous Cell Construction (*using DGEBA – IPD linear epoxy repeat unit*)

Next, each cell was equilibrated with a 300 ps Forcite dynamics simulation at 500 K. This molecular dynamic simulation was done in the NPT (constant number of particle, pressure and temperature) thermodynamic ensemble to let the system find its equilibrium density. This step is essential in order to be sure that systems are well equilibrated and that all problems and artifacts that could come during the construction phase are overcome.

After the equilibration of the cells, the main simulation was performed. This simulation consists on a succession of several molecular dynamic steps of 300 ps. During the first 100 ps, the temperature is regulated with a velocity-scale thermostat (temperature difference maximum of 10 K). This thermostat leads to a quick change of the temperature and is efficient to reach the system equilibrium. During the last 200 ps, the temperature is controlled with a Nose-Hoover thermostat. This last step is not good at equilibrating a system but it is a better thermostat during MD calculation step. All along the MD simulation, the pressure is controlled at 1 bar. The starting temperature is 500 K. At the end of each step, the temperature is decreased by 10 K. The final temperature is 300 K and the total time of the simulation is approximately 7 ns, taking into account the equilibrium time.

3. Extracting results from simulation

During the simulation of the specific volume-temperature diagram, the different parameters were calculated at each step of iteration of the simulation (1 fs). Every 1250 steps (1.25 ps), a frame is saved. This frame contains the coordinates, velocities and forces applied on each atom of the system. Then the specific volume and the temperature of the system were calculated at each frame. And at the end of the simulation a study table and a chart plotting volume vs. temperature are displayed. The specific volume is averaged over each tenth of degrees and plotted vs. the temperature.

The glass transition temperature is the intersection of the linear regressions of the two parts of the charts. These two parts correspond to the two state of the polymer material: the glassy state and the molten or rubber-like state. The difference between these two steps leads to a change of the thermal expansion coefficient of the material and then a change in the slope of the volume-temperature chart.

IV. Results and discussion

1. Group contribution results

Using group contribution of the two linear polymers considered, the glass transition of the epoxy-amine linear chain (T_{gL}) and their density were calculated. The values are summarized in the following table:

Repeating unit	T_{gL} (°C), Synthia	d (g/cm^3)
DGEBA – IPD	100	1.09
$DGEDAS_0$ – IPD	73	1.16

Table 7. Synthia simulation results for DGEBA – IPD and $DGEDAS_0$ – IPD linear repeating unit

It appears that the glass transition of the linear chain predicted by group contribution is lower for $DGEDAS_0$ – IPD than for DGEBA – IPD. Besides, as the experimental values for the corresponding networks (Table 6), the density of $DGEDAS_0$ – IPD is higher than the one of DGEBA – IPD which could be explained by the higher proportion of -O- and N in the repeating unit $DGEDAS_0$ – IPD. These theoretical values of density will be used for the construction of a "packing cell" of the linear chain using Amorphous Cell module, on which Molecular Dynamic will be performed.

2. Molecular dynamics (MD) results

Determination of glass transition temperatures using MD simulations

Specific volume of the linear epoxy-amine chains at each temperature were calculated and plotted in Figure 21 (a) and (b). An increase in the volume with temperature and a change in the slope of the specific volume curves were observed. The change in the slope of the volume curves defines the values of the glass transition temperature of the linear epoxy-amine chains. As represented in Table 8, T_{gL} values were 170°C for DGEBA – IPD and 147°C for $DGEDAS_0$ – IPD. Molecular dynamics method gives a higher value of T_{gL} for DGEBA – IPD than for $DGEDAS_0$ – IPD.

Higher values of T_{gL} are obtained by molecular dynamics (MD) than using the group contribution method (Synthia module). Indeed, it was observed that the assigned cooling rate affects the predicted value from MD simulations [47]. The mobility of the polymer chains rapidly decreases when the polymer melt is cooled below T_g, and sufficient long time is needed for the equilibrium structure. Higher cooling rate in the simulation can increase the departure from the equilibrium state, which results in higher value of glass transition from Molecular Dynamics simulations.

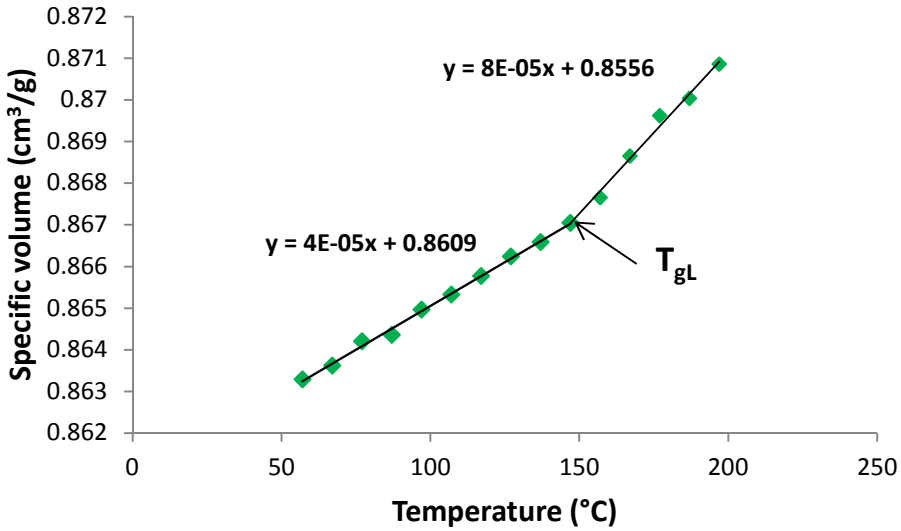

(a)

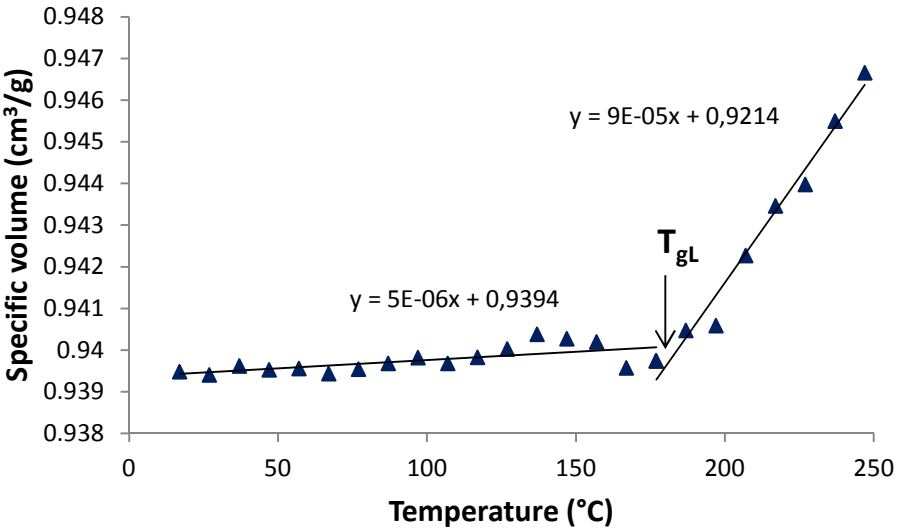

(b)

Figure 21. Specific volume-temperature curve of $DGEDAS_0$ – IPD (a) and DGEBA – IPD (b) linear chains (same scale)

Linear epoxy polymers	T_{gL} (°C) (MD)
DGEBA – IPD	170
$DGEDAS_0$ – IPD	147

Table 8. Simulated values of T_{gL} for DGEBA – IPD and $DGEDAS_0$ – IPD linear epoxy polymers

Using group contribution method and molecular dynamic it is possible to compare the T_{gL} values obtained for the corresponding $DGEDAS_0$ – IPD and DGEBA – IPD epoxy linear polymers. This gives indication on one parameter for the determination of the networks T_g: the chain stiffness.

Influence of crosslink density

The second parameter of interest for the understanding of the variation of T_g of the networks is the crosslink density (ν). This crosslink density is the tertiary amine concentration (assuming fully cure and no free chain ends). Knowing the respective amount of IPD and epoxy prepolymer, for a formulation having a stoichiometric ratio of a/e = 1, the value of ν can be determined theoretically. Indeed, each mole of IPD brings two moles of tertiary amine.

$$\nu_{th} = (2d)/(M_{IPD} + M_{epoxy}) \qquad \text{(Equation 7)}$$

As represented in Table 9, a lower theoretical crosslink density is obtained for DGEBA – IPD network than for $DGEDAS_0$ – IPD network.

Networks	ν_{th} (10^{-3} mol/cm^3)
DGEBA – IPD	2.4
$DGEDAS_0$ – IPD	3.1

Table 9. Theoretical crosslinking densities for DGEBA – IPD and $DGEDAS_0$ – IPD network

Crosslink density influence on the glass transition temperature of DGEBA – IPD and $DGEDAS_0$ – IPD networks is compensated by the influence of chain stiffness, regarding the experimental values of T_g for $DGEDAS_0$ – IPD and DGEBA – IPD.

Determination of linear thermal expansion coefficient using MD simulations

The volumic coefficient of thermal expansion (α) was derived through a similar method as the simulation process for T_g. Using the volume of the unit cells obtained from the cooling-down process, the volumic coefficient of thermal expansion can be approximated simply as follows [48]:

$$\alpha = \frac{1}{V_0}\frac{\partial V}{\partial T} \cong \frac{1}{V_0}\frac{\Delta V}{\Delta T} = \rho_0 \frac{\Delta v}{\Delta T}$$

Where V_0 and ρ_0 are the initial volume and density of a unit cell at the reference temperature, and ν is the specific volume of a unit cell. Δν/ΔT is the slope of the linear regression of the specific volume-temperature relationship. From the two slopes of the specific volume-temperature curves for DGEDAS0 – IPD and DGEBA – IPD, the coefficients of volumic thermal expansion in the glassy and rubbery states were estimated. Assuming the sample is isotropic, the linear coefficient of thermal expansion can be calculated (β = α/3) and are summarized in Table 10.

Linear chains	**β_1 (ppm/K) before T_g**	**β_2 (ppm/K) after T_g**
DGEBA – IPD	1.8	32.8
$DGEDAS_0$ – IPD	15.4	30.9

Table 10. Linear coefficients of thermal expansion determined using MD of DGEBA – IPD and $DGEDAS_0$ – IPD linear chains

Therefore, according to MD, the thermal expansion coefficients of $DGEDAS_0$ – IPD linear chains are higher in the glassy state than the thermal expansion coefficients of DGEBA – IPD, while in the rubbery state they are similar.

The origin of this difference is not clearly understood. This is why the linear coefficient of thermal expansion β of the networks was measured by TMA (thermo mechanical analysis) as reported in Annex B. Similar values were obtained in the glassy state (60 – 65 ppm/K) for the two networks and slightly higher value in the rubbery state for DGEBA – IPD (195 ppm/K) than for $DGEDAS_0$ – IPD (170 ppm/K).

Nevertheless, the thermal expansion coefficients found by Molecular Dynamic simulation of linear-epoxy amine chains are very low as compared to experimental values obtained for the corresponding networks (DGEBA – IPD and $DGEDAS_0$ – IPD).

Comparison can not be done between the values of the coefficients of thermal expansion experimentally measured for the respective networks and the ones modelled for the corresponding linear epoxy polymers.

As a remark, Fan et al. [43] modelled the thermal expansion coefficients of a DGEBA – TETA (aliphatic amine: triethylamine) network and obtained a good accordance with the experimental values. On the opposite, Soni et al. [49] observed that the coefficients of thermal expansion modelled for DGEBA – poly(oxypropylene) diamine networks were at least 30 % lower than their corresponding experimental results.

V. Conclusion of Part II

Many parameters should be taken into account when predicting the glass transition of an epoxy – amine network. The two most important ones are the crosslinking density and the chain stiffness between crosslinking points representing the copolymer effect.

In our study, we decided to overcome the influence of crosslinking density, in order to reduce computational requirements and overcome the difficult modelling of networks, by modelling linear epoxy-amine chains. The glass transition, T_{gL}, of these theoretical linear chains build from the structure of epoxy and amine studied, isosorbide diglycidyl ether ($DGEDAS_0$) and diglycidyl ether of bisphenol A (DGEBA) with isophorone diamine (IPD), should give information on the epoxy-amine chain structure influence on T_g.

It appears that values of T_{gL} are higher for DGEBA – IPD than for $DGEDAS_0$ – IPD linear chains, for the two molecular modelling methods used: molecular dynamics (MD) and group contribution method (Synthia). These results are in good agreement with the experimental observation of T_g higher for DGEBA – IPD networks. Even if direct comparison cannot be done between the experimental glass transition of the two networks studied and the glass transition of linear epoxy-amine chains, first approach on glass transition prediction confirms that the chain stiffness in DGEBA – IPD network is more important than the one of $DGEDAS_0$ – IPD between two crosslinking points. Besides, even if theoretical values of crosslinking densities are higher for DGEBA – IPD and $DGEDAS_0$ – IPD, this does not compensate the influence of chain stiffness.

Conclusion

Within this first Chapter, we focused on the replacement of the conventional DGEBA epoxy prepolymer in a classical epoxy-amine system (with isophorone diamine as a curing agent) by bio-based epoxy prepolymers derived from isosorbide. Two different epoxy prepolymers have been successfully prepared by Huntsman from isosorbide using two different synthetic routes.

We focused in the first part of this Chapter on the characterization of these two DiGlycidyl Ether of Dianhydro-Sorbitol. A complete structural characterization was realized using complementary analytical methods. $DGEDAS_0$ and $DGEDAS_n$ differ, as underlined many times in this chapter, by the presence of numerous oligomers in $DGEDAS_n$ and the resulting higher functionality of this bio-based epoxy prepolymer obtained by the conventional epoxidation with epichlorohydrin. Reactivity of the different formulations and network characterizations, mainly by DSC and DMA, were studied. It appears that the isosorbide based networks exhibit good properties but yet lower T_g are observed. Knowing the short and cyclic structure of isosorbide, higher values for glass transition of networks were expected.

The second part of this chapter therefore consists in a first approach on T_g prediction of $DGEDAS_0$ – IPD and DGEBA – IPD. By modelling linear chains for these two epoxy-amine systems to overcome the crosslinking density parameter, a first trend on the T_g comparison between the two systems was possible. The results of molecular modelling showed that the chain flexibility between crosslinking points was more important for $DGEDAS_0$ – IPD than for DGEBA – IPD; this result could partially explained why the glass transition of DGEDAS – IPD networks were lower than DGEBA – IPD network.

In the next chapter, we will focus on other bio-based epoxy prepolymers, commercially available, that could be interesting also for the replacement of DGEBA and exhibit various structures. These other bio-based epoxy prepolymers will be compared to $DGEDAS_0$ and DGEBA prepolymers.

References

[1] Kaplan DL. Biopolymers from Renewable Ressources. Berlin: Springer-Verlag 1998.

[2] Gandini A. Epoxy Polymers : New materials and innovations: Pascault JP, Williams RJJ, Eds. Wiley-VCH 2010.

[3] Shen L, Haufe J, Patel MK. Product overview and market projection of emerging biobased plastics. *PROBIP 2009*.

[4] Pascault JP, Sautereau H, Verdu J, Williams RJJ. Thermosetting Polymers: Taylor & Francis Books, Inc. 2002.

[5] Miyagawa H, Mohanty AK, Misra M, Drzal LT. Thermo-Physical and Impact Properties of Epoxy Containing Epoxidized Linseed Oil, 1. *Macromolecular Materials and Engineering*. 2004;**289**:629-35.

[6] Miyagawa H, Misra M, Drzal LT, Mohanty AK. Fracture toughness and impact strength of anhydride-cured biobased epoxy. *Polymer Engineering & Science*. 2005;**45**:487-95.

[7] Park SJ, Jin FL, Lee JR. Effect of Biodegradable Epoxidized Castor Oil on Physicochemical and Mechanical Properties of Epoxy Resins. *Macromolecular Chemistry and Physics*. 2004;**205**:2048-54.

[8] Jin FL, Park SJ. Thermomechanical behavior of epoxy resins modified with epoxidized vegetable oils. *Polymer International*. 2008;**57**:577-83.

[9] Park SJ, Jin FL, Lee JR, Shin J-S. Cationic polymerization and physicochemical properties of a biobased epoxy resin initiated by thermally latent catalysts. *European Polymer Journal*. 2005;**41**:231-7.

[10] Shabeer A, Sundararaman S, Chandrashekhara K, Dharani LR. Physicochemical properties and fracture behavior of soy-based resin. *Journal of Applied Polymer Science*. 2007;**105**:656-63.

[11] Patel MB, Patel RG, Patel VS. Effects of reactive diluent diepoxidized cardanol and epoxy fortifier on curing kinetics of epoxy resin. *Journal of Thermal Analysis and Calorimetry*. 1989;**35**:47-57.

[12] Sato S, Shah S, Bueno RC, Moon R, Ferreira A. Phenalkamine and salted amine blends as curing agents for epoxy resins. World Patent WO 2009/080209 A1 2009.

[13] Chapin RE, Adams J, Boekelheide K, et al. NTP-CERHR expert panel report on the reproductive and developmental toxicity of bisphenol A. *Birth Defects Research Part B: Developmental and Reproductive Toxicology*. 2008;**83**:157-395.

[14] Acierno D, Russo P, Savarese R. Mechanical and dynamic-mechanical properties of biodegradable epoxy resins. *Proceedings of the Polymer Processing Society*. Salerno, Italy. 2008.

[15] Takada Y, Shinbo K, Someya Y, Shibata M. Preparation and properties of bio-based epoxy montomorillonite nanocomposites derived from polyglycerol polyglycidyl ether and ε-polylysine. *Journal of Applied Polymer Science*. 2009;**113**:479-84.

[16] Shibata M, Nakai K. Preparation and properties of biocomposites composed of bio-based epoxy resin, tannic acid, and microfibrillated cellulose. *Journal of Polymer Science Part B: Polymer Physics*. 2010;**48**:425-33.

[17] Morrison J. Polyglycidyl ethers of ether anhydrohexitols, method of production, and aqueous solutions thereof. US Patent 3,041,300 1962.

[18] Zech J. Bisglycidyl ethers of isohexides. US Patent 3,272,845 1966.

[19] East A, Jaffe M, Zhang Y, Catalini LH,. Ethers of bisanhydrohexitols. US Patent US 2008/0021209A1 2008.
[20] East A, Jaffe M, Zhang Y, Catalini LH. Thermoset epoxy polymers from renewable resources. US Patent US 2008/0009599 A1 2008.
[21] East A, Jaffe M, Zhang Y, Catalini LH,. Thermoset epoxy polymers from renewable resources. US PAtent US 7,619,056 B2 2009.
[22] Feng X, East AJ, Hammond WB, Zhang Y, Jaffe M. Overview of advances in sugar-based polymers. *Polymers for Advanced Technologies*. 2011;**22**:139-50.
[23] Sachinvala ND, Winsor DL, Menescal RK, Ganjian I, Niemczura WP, Litt MH. Sucrose-based epoxy monomers and their reactions with diethylenetriamine. *Journal of Polymer Science Part A: Polymer Chemistry*. 1998;**36**:2397-413.
[24] Winter HH. Analysis of linear viscoelasticity of a crosslinking polymer at the gel point. *Journal of Rheology*. 1986;**30**:367-82.
[25] Hopton FJ, Thomas GHS. Conformations of some dianhydrohexitols. *Canadian Journal of Chemistry*. 1969;**47**:2395-401.
[26] Miller DR, Macosko CW. A New Derivation of Post Gel Properties of Network Polymers. *Macromolecules*. 1976;**9**:206-11.
[27] Galy J, Sabra A, Pascault J-P. Characterization of epoxy thermosetting systems by differential scanning calorimetry. *Polymer Engineering & Science*. 1986;**26**:1514-23.
[28] Fenouillot F, Rousseau A, Colomines G, Saint-Loup R, Pascault JP. Polymers from renewable 1,4:3,6-dianhydrohexitols (isosorbide, isomannide and isoidide): A review. *Progress in Polymer Science*. 2010;**35**:578-622.
[29] Fuji M, Akita M, Tanaka T. Polycarbonate copolymer and process for production thereof. European Patent EP2033981 A1 2009.
[30] Won YG, Galy J, Pascault JP, Verdu J. Prediction of the glass transition temperature of cycloaliphatic amine–epoxy networks. *Journal of Polymer Science Part B: Polymer Physics*. 1991;**29**:981-7.
[31] Won YG, Galy J, Gérard JF, Pascault JP, Bellenger V, Verdu J. Internal antiplasticization in copolymer and terpolymer networks based on diepoxides, diamines and monoamines. *Polymer*. 1990;**31**:1787-92.
[32] Nielsen LE. Cross-Linking–Effect on Physical Properties of Polymers. *Journal of Macromolecular Science, Part C: Polymer Reviews*. 1969;**3**:69-103.
[33] Bicerano J. Prediction of polymer properties. 3rd ed: Marcel Dekker, 2002.
[34] Van Krevelen D. Properties of polymers: their correlation with chemical strucutre, their numerical estimation and prediction from additive group contribution. Amsterdam, New York: Elsevier 1990.
[35] Frenkel D, Smit B. Understanding Molecular Simulation: From Algorithms to Applications: Academic Press; 2001.
[36] Sun H. COMPASS: An ab Initio Force-Field Optimized for Condensed-Phase ApplicationsOverview with Details on Alkane and Benzene Compounds. *The Journal of Physical Chemistry B*. 1998;**102**:7338-64.
[37] Sun H, Ren P, Fried JR. The COMPASS force field: parameterization and validation for phosphazenes. *Computational and Theoretical Polymer Science*. 1998;**8**:229-46.
[38] Rigby D, Sun H, Eichinger BE. Computer simulations of poly(ethylene oxide): force field, pvt diagram and cyclization behaviour. *Polymer International*. 1997;**44**:311-30.
[39] Ian H, Heald CR, Brendan JH. Molecular modelling of a polyarylethersulfone under bulk conditions. *Modelling and Simulation in Materials Science and Engineering*. 1996;**4**:151.

[40] Tsige M, Taylor PL. Simulation study of the glass transition temperature in poly(methyl methacrylate). *Physical Review E*. 2002;**65**:021805.
[41] Barton JM, Deazle AS, Hamerton I, Howlin BJ, Jones JR. The application of molecular simulation to the rational design of new materials: 2. Prediction of the physico-mechanical properties of linear epoxy systems. *Polymer*. 1997;**38**:4305-10.
[42] Liu H, Uhlherr A, Bannister MK. Quantitative structure–property relationships for composites: prediction of glass transition temperatures for epoxy resins. *Polymer*. 2004;**45**:2051-60.
[43] Fan HB, Yuen MMF. Material properties of the cross-linked epoxy resin compound predicted by molecular dynamics simulation. *Polymer*. 2007;**48**:2174-8.
[44] Wu C, Xu W. Atomistic molecular modelling of crosslinked epoxy resin. *Polymer*. 2006;**47**:6004-9.
[45] Accelrys. Material Studio V5.0, Amorphous Cell, Forcite+. *San Francisco (CA)*. 2009.
[46] Synthia, V5.0. Accelrys. *San Francisco (CA)*. 2009.
[47] Yoshioka S, Aso Y, Kojima S. Prediction of Glass Transition Temperature of Freeze-Dried Formulations by Molecular Dynamics Simulation. *Pharmaceutical Research*. 2003;**20**:873-8.
[48] Choi J, Yu S, Yang S, Cho M. The glass transition and thermoelastic behavior of epoxy-based nanocomposites: A molecular dynamics study. *Polymer*. 2011;**52**:5197-203.
[49] Soni NJ, Lin PH, Khare R. Effect of cross-linker length on the thermal and volumetric properties of cross-linked epoxy networks: A molecular simulation study. *Polymer*. 2012;**53**:1015-9.

Chapter III Influence of the bio-based epoxy prepolymer structure on network properties

I. Introduction

In the previous Chapter, we studied epoxy prepolymers synthesized from isosorbide by different synthetic routes [1-6]. The most convenient synthetic route is that of the reaction of isosorbide with epichlorohydrin, which is industrially exploited for the synthesis of DGEBA but gives access to numerous oligomers. The pure diglycidyl ether of isosorbide ($DGEDAS_0$) has been prepared via a synthetic route involving the allylic derivatives.

In this Chapter, $DGEDAS_0$ was compared with two other bio-based epoxy prepolymers DGECAR (Diglycidyl Ether of Cardanol) and SPGE (Sorbitol PolyGlycidyl Ether). Indeed, bio-based prepolymer derived from cardanol have been studied [7-9] and give interesting network properties. Besides, the use of sorbitol, another natural polysaccharide, has also been studied for the replacement of bisphenol A with the synthesis of bio-based epoxy prepolymer [10, 11]. SPGE and DGECAR have also the advantage to be commercially available. The chemical structures of these three different monomers were analysed by SEC, ESI-TOF MS, FT-IR, ^{1}H RMN and ^{13}C RMN analyses.

Three bio-based epoxy networks containing these epoxy prepolymers were prepared using isophorone diamine (IPD). Gelation and crosslinking reactions of the different systems were studied using rheological measurements and differential scanning calorimetry (DSC). Thermal stability and structure of the epoxy networks were also evaluated using thermogravimetric analyses (TGA) and dynamic mechanical analyses (DMA) respectively.

Influence of the epoxy prepolymer structures on network properties were evaluated and compared to a conventional epoxy network based on DGEBA cured with IPD.

II. Experimental section

1. Materials

Simplified chemical structure of the reagents used in this study is reported in Figure 1. The conventional petroleum-based epoxy monomer used was a diglycidyl ether of bisphenol A (DGEBA) supplied by Hunstman (Araldite 5085), with an epoxide equivalent weight (EEW) of 180 g/eq. Sorbitol polyglycidyl ether (SPGE) with an epoxy equivalent weight of 191 g/eq has been supplied by Nagase Chemtex (reference Denacol 622). The bio-based epoxy prepolymer derived from cardanol (DGECAR) was obtained from Cardolite (reference NC514) with an epoxy equivalent of 490 g/eq. These three epoxy prepolymers are commercially available.

Another bio-based epoxy prepolymer derived from natural sugars, isosorbide diglycidyl ether ($DGEDAS_0$) was synthesized by Huntsman via the diallyl isosorbide intermediate using isosorbide with a high purity commercialized by Roquette Frères [12]. As discussed in the previous chapter (Chapter II. Part I) this synthetic route is different from the one industrially used (*e.g.* synthesis of DGEBA and other commercial epoxy prepolymers using epichlorohydrin). The monomer thus obtained has an equivalent weight of 143 g/eq. The cycloaliphatic diamine curing agent used was isophorone diamine (IPD) supplied by Aldrich, with an amine equivalent weight (AEW) of 42 g/eq.

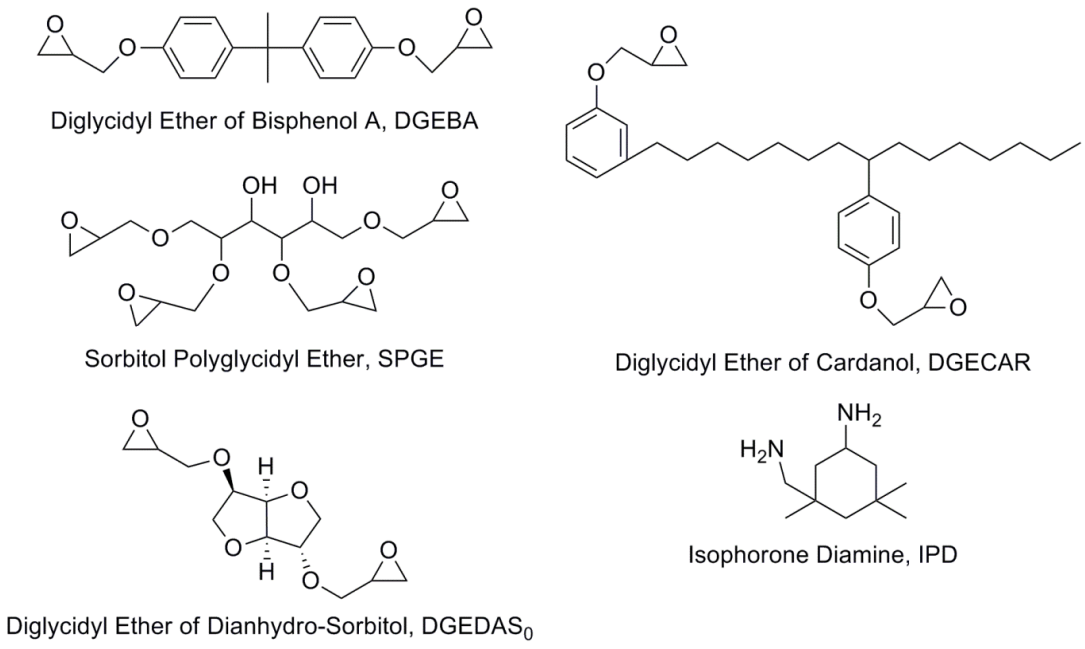

Figure 1. Simplified structure of the reagents used in this study

2. Preparation of epoxy networks

The formulations used in this study were based on the three different bio-based epoxy prepolymers SPGE, $DGEDAS_0$, and DGECAR and the conventional epoxy prepolymer DGEBA cured with the same cycloaliphatic amine, IPD, at different stoichiometric ratios $r = n_{ah}/n_e$ (except for DGEBA – IPD where r was equal to 1). The epoxy prepolymer SPGE and DGECAR are liquid at room temperature and were mixed vigorously with IPD at room temperature and cured in a PTFE coated mould at 80°C for 1h followed by 2 h at 180°C. All the networks were stored in dry conditions in order to avoid absorption of atmospheric moisture.

3. Measurements

The analytical methods used for the characterization of the epoxy prepolymers were the same as the ones described in Chapter II, i.e. *Size Exclusion Chromatography, Fourier Transform Infrared Spectroscopy, Mass Spectroscopy, Thermal Gravimetric Analyses*.

The reactivity of the formulations was evaluated trough *DSC* and *gel time measurements*. The thermo-mechanical properties and thermal stability of the different cured network were measured by *DMA* and *TGA*. These methods were also described in Chapter II.

In addition *elemental analysis* was realized on one of the epoxy prepolymer, SPGE, at the Service Central d'Analyses (SCA) of Solaize, in order to quantify Carbon, Oxygen, Hydrogen, Nitrogen and Chlore contents.

III. Results and discussion

1. Characterization of the different epoxy prepolymers

a) SEC characterization

To obtain information on molar mass distribution, the epoxy prepolymers were analysed by SEC. The SEC chromatograms of the three bio-based epoxy prepolymers are presented in Figure 2 as well as the chromatogram of DGEBA for comparison.

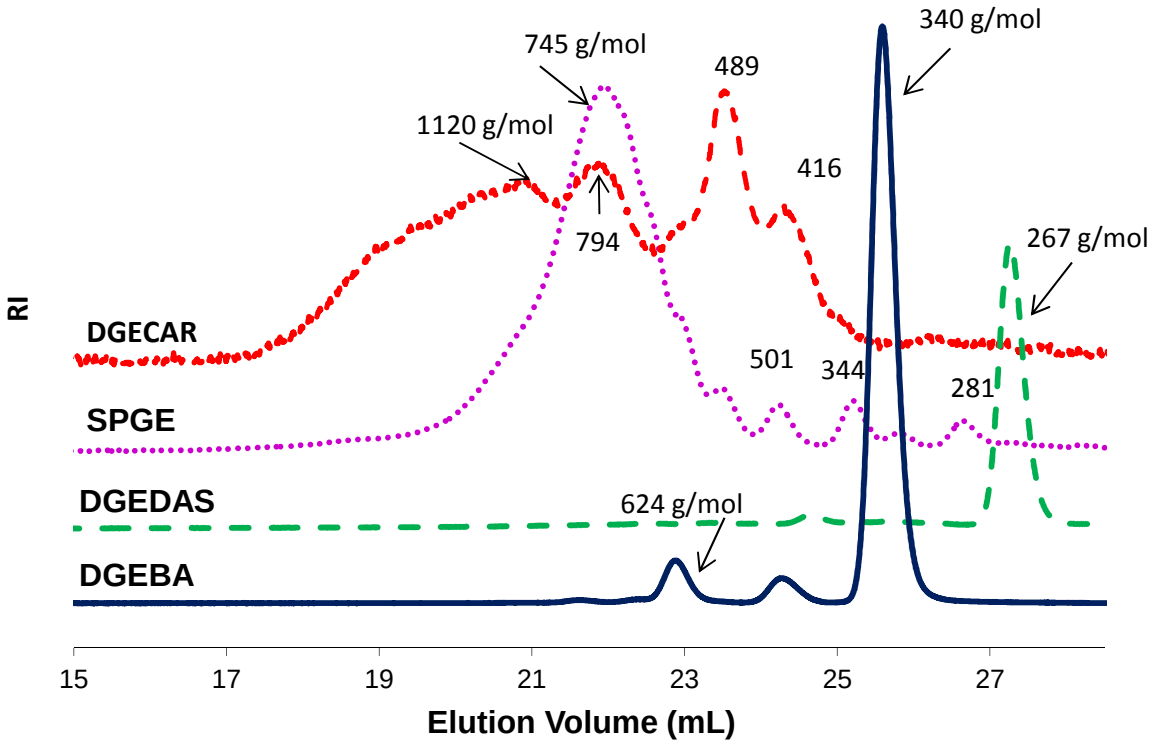

Figure 2 SEC chromatograms of the epoxy prepolymers DGEBA, $DGEDAS_0$, SPGE and DGECAR

SEC chromatograms of the two commercial bio-based epoxy prepolymers, DGECAR and SPGE, underline the presence of oligomers through numerous elution peaks, whereas only one elution peak is present in the $DGEDAS_0$ chromatogram at an elution volume of 27.2 mL, corresponding to the pure monomer of diglycidyl ether of isosorbide. The molar masses of the different epoxy prepolymers were calculated using a calibration curve (details are given in Annexe B) obtained from a high molar mass DGEBA (eew = 475 – 550 g/eq). Using this calibration curve $DGEDAS_0$ molar mass was found equal to 267 g/mol, while the theoretical value is equal to 258 g/mol. Molar masses of different peaks are indicated in Figure 2. The oligomers of highest molar mass were observed in the SEC chromatogram of DGECAR.

b) Electro-Spray mass spectroscopy characterization

The different bio-based epoxy prepolymers were analysed by Electro-Spray mass spectroscopy for more precise information on molar mass than SEC.

ESI-TOF mass spectrum of $DGEDAS_0$ is presented in Figure 3 and confirms the presence of the pure diglycidyl ether of DAS without any oligomers. Indeed, the only peak is

present at M + Na = 281 g/mol, corresponds to the molar mass of the $DGEDAS_0$ (M = 258 g/mol).

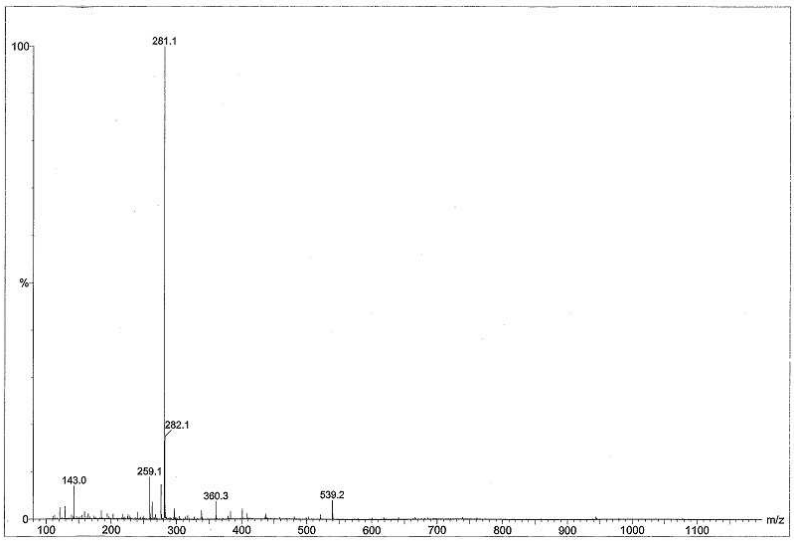

Figure 3. ESI-TOF mass spectrum (positive ion mode) of $DGEDAS_0$

ESI-TOF mass spectra of SPGE and DGECAR are presented in Figure 4 and Figure 5 respectively, and confirm the SEC observation of various oligomers present in both bio-based commercial epoxy prepolymers.

The ESI-TOF mass spectrum of SPGE also reveals that many of the oligomers present in the SPGE contain chlorine groups (see Figure 4). This was confirmed by the technical datasheet of this commercial epoxy prepolymer that indicated a high chlorine content of 19.1 % and by our own elemental analysis which gave a chlorine amount of 19.5 %. This high chlorine content can be explained by the synthesis method with epichlorohydrin (Epi). Traditional epoxidation involves a great excess of Epi on polyol (*i.e.* 30 mol Epi / 1 mol polyol). This is very useful for the epoxidation of BPA for instance, but when the reactivity of the –OH groups strongly decreases, as for sorbitol, where most of the hydroxyl groups are secondary hydroxyl groups, the reaction rate decreases. Formation of chlorohydrines is represented in Scheme 1.

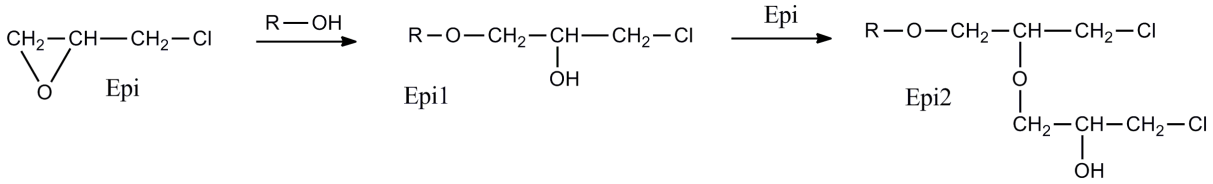

Scheme 1. Formation of chlorohydrines

The new -OH groups originated in the Epi-n are susceptible to be epoxidated and the lateral extension chain is then operative. According to the length and the position of chlorine with respect to the -OH group the epoxy ring can be closed or not (1-4 position) and then residual chlorine is always present [13]. Only under very strict reaction conditions the problem is minimized.

Concerning the last bio-based epoxy prepolymer analysed, the diglycidyl ether of cardanol (M = 508 g/mol) is present, with numerous oligomers, in the ESI-TOF mass spectrum of DGECAR at M + Na = 531 g/mol (Figure 5).

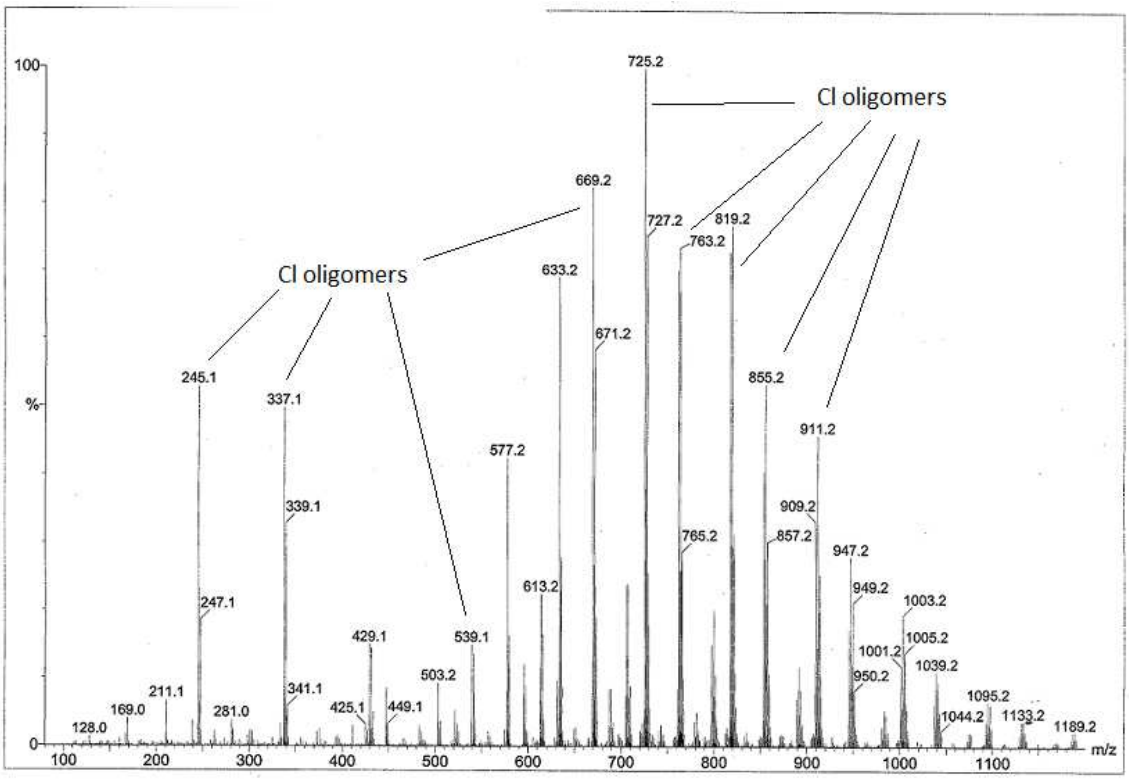

Figure 4. ESI-TOF mass spectrum (positive ion mode) of SPGE

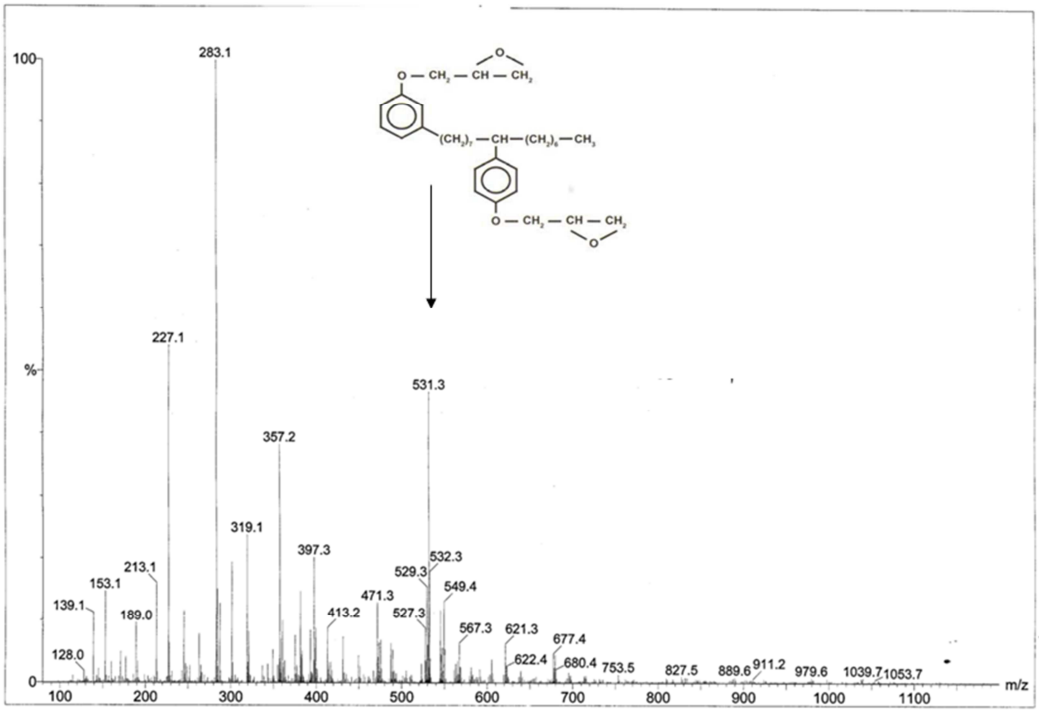

Figure 5. ESI-TOF mass spectrum (positive ion mode) of DGECAR

Finally, Electro-Spray analyses confirm that the $DGEDAS_0$ is composed of the pure monomer of diglycidyl ether of isosorbide and reveal the presence of numerous chlorinated oligomers in SPGE epoxy prepolymer. Nevertheless, in the conditions used, the magnitude of the peaks is not quantitative and therefore cannot be linked to the amount of each species.

c) FTIR characterization

Fourier transform infrared (FTIR) spectroscopy was used to identify the molecular structure and the chemical bonds of the three different bio-based epoxy prepolymers. The FTIR spectra of $DGEDAS_0$, SPGE and DGECAR are shown in Figure 6 (a), (b) and (c) respectively. The different peaks indicate the presence of –OH group (3470 cm-1), -CH bond (2926, 2877 cm^{-1} and 1430, 1340 cm^{-1}), -CO- bond aliphatic ether (1100 and 1040 cm^{-1}) as well as epoxide group (910 cm^{-1}). The main difference between the different IR spectra is the very weak intensity of –OH absorption in $DGEDAS_0$ (mainly due to residual moisture) which indicates the absence of –OH group in $DGEDAS_0$ compared to the high intensity of the –OH peak for SPGE due to the uncomplete epoxidation of sorbitol as explained in the previous paragraphe. In addition, the aromatic structure of DGECAR was confirmed by the -C=C bond (1601 and 1583 cm^{-1}) and aromatic -CO (1244 cm^{-1}). Besides, concerning SPGE

the peak at 703 cm^{-1} can be attributed to C-Cl. Nevertheless, it is difficult to quantify the chlorinated compound by infrared spectroscopy.

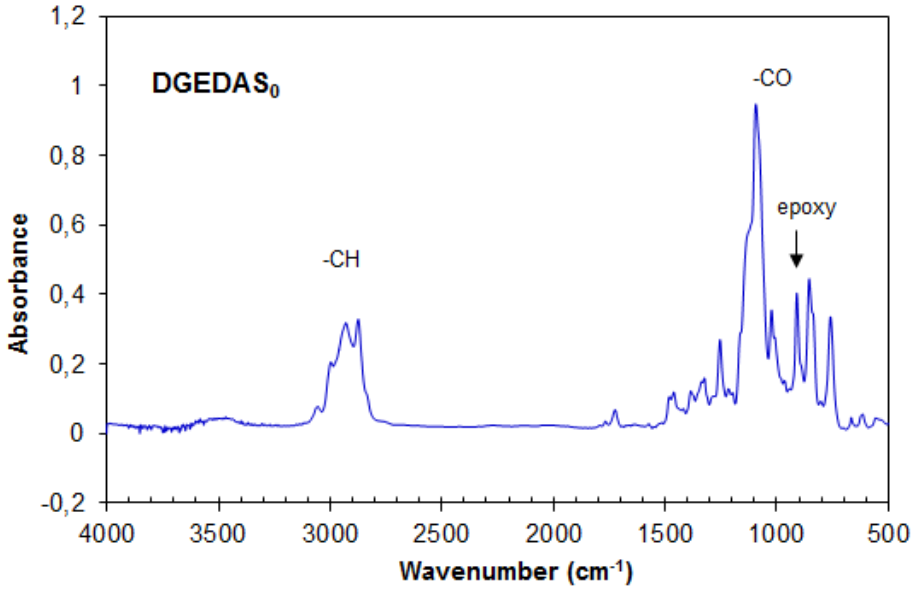

(a)

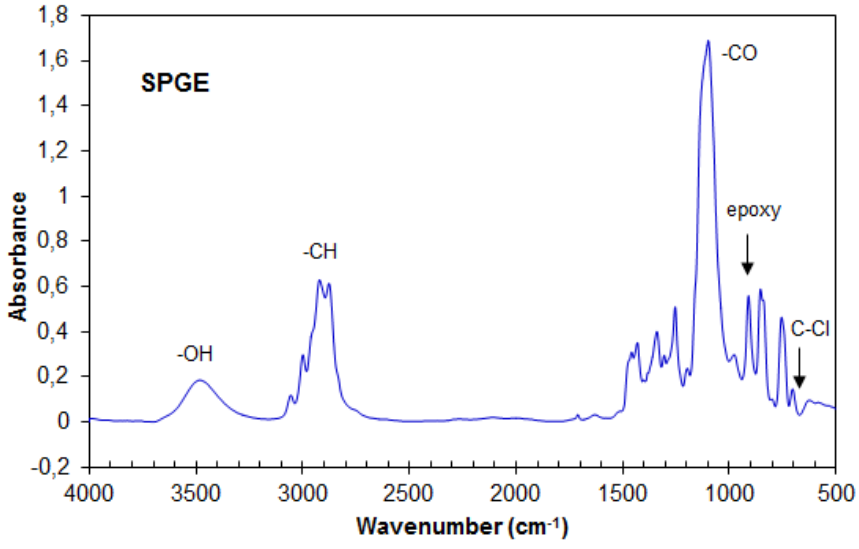

(b)

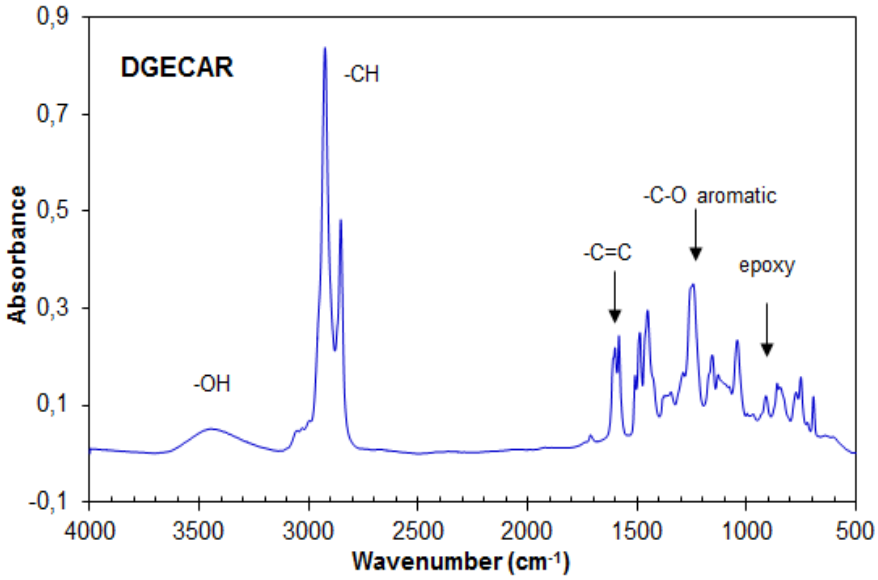

(c)

Figure 6. FTIR spectra of (a) $DGEDAS_0$, (b) SPGE, (c) DGECAR

d) TG analysis

The mass loss (measured under inert atmosphere) as a function of temperature for $DGEDAS_0$, SPGE, DGECAR and DGEBA epoxy prepolymers and their derivatives are shown in Figure 7 (a) and (b). The initial degradation temperature ($T_{5\%}$) and the temperature at a maximum rate of degradation (T_{max}) of the different prepolymers studied are summarized in Table 1. DGEBA, $DGEDAS_0$ and SPGE thermally degrade mainly through a simple step. The monomer of diglycidyl ether of isosorbide degrades before DGEBA, with a maximum rate at 260°C. The more thermally stable epoxy prepolymer is DGECAR, which is mainly composed of high molar mass compounds. Nevertheless it begins to thermally degrade around 210°C. Lower mass species degrades earlier and may be residual moisture (as it begins to degrades at low temperatures) or lower molar mass impurities.

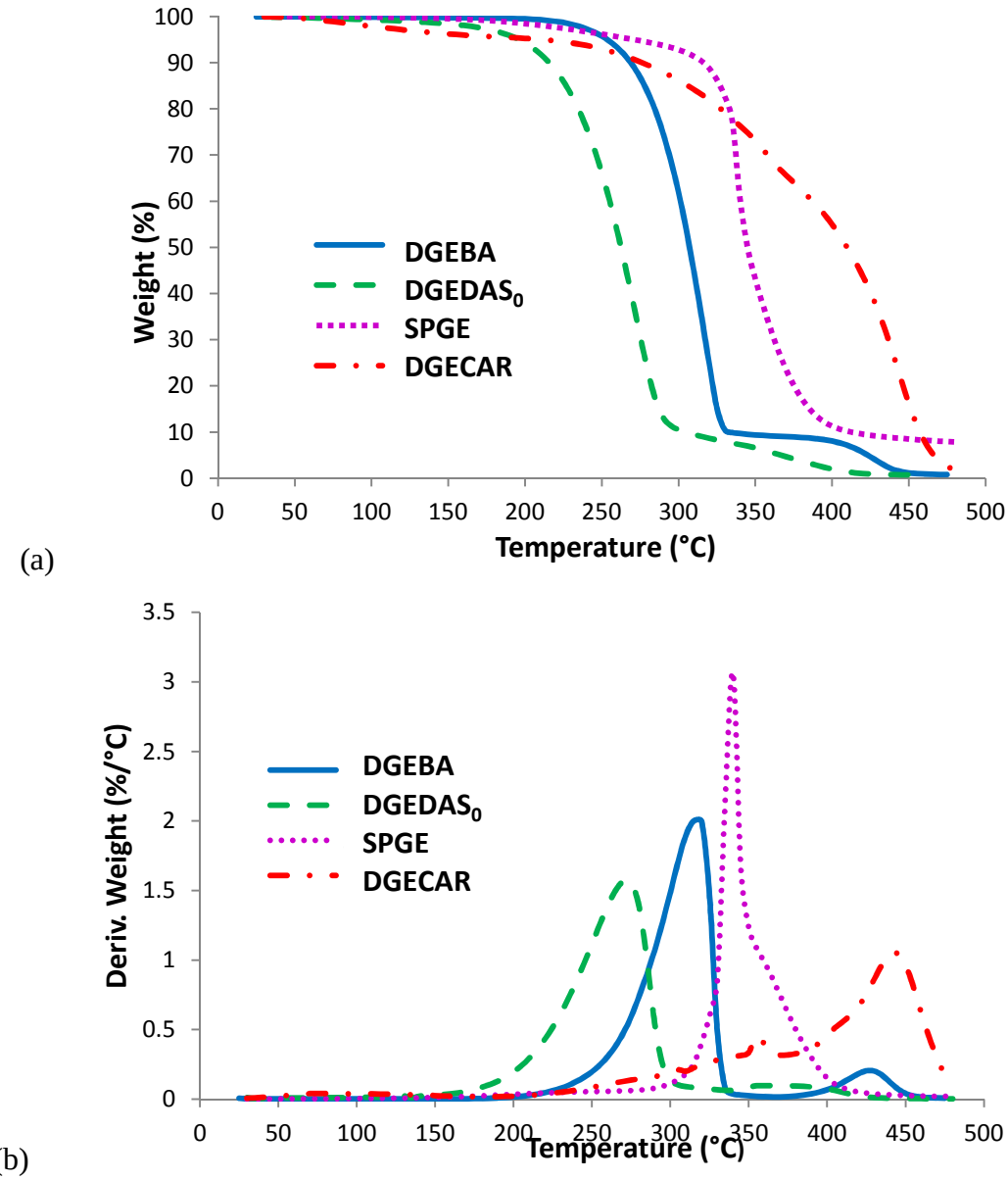

Figure 7. (a) TGA and (b) DTGA curves of DGEBA, DGEDAS, SPGE, DGECAR

Epoxy prepolymers	$T_{(5\%)}$ (°C)	$T_{maximum\ rate}$ (°C)
DGEBA	250	320
$DGEDAS_0$	200	260
SPGE	270	340
DGECAR	212	440

Table 1. Thermal analysis data for the different epoxy prepolymers

2. Curing behaviour

The two main events that occur during the crosslinking polymerization reaction of thermosets are gelation, and vitrification. For epoxy-amine systems there are two specific temperatures T_{ggel} and $T_{g\infty}$, between which the crosslinking process brings successively gelation and vitrification [14]. T_{ggel} is the temperature at which gelation and vitrification simultaneously occur and $T_{g\infty}$ is the maximum T_g attainable. Beyond $T_{g\infty}$, no more vitrification phenomenon is observed. Below T_{ggel} though, the vitrification occurs before the gelation.

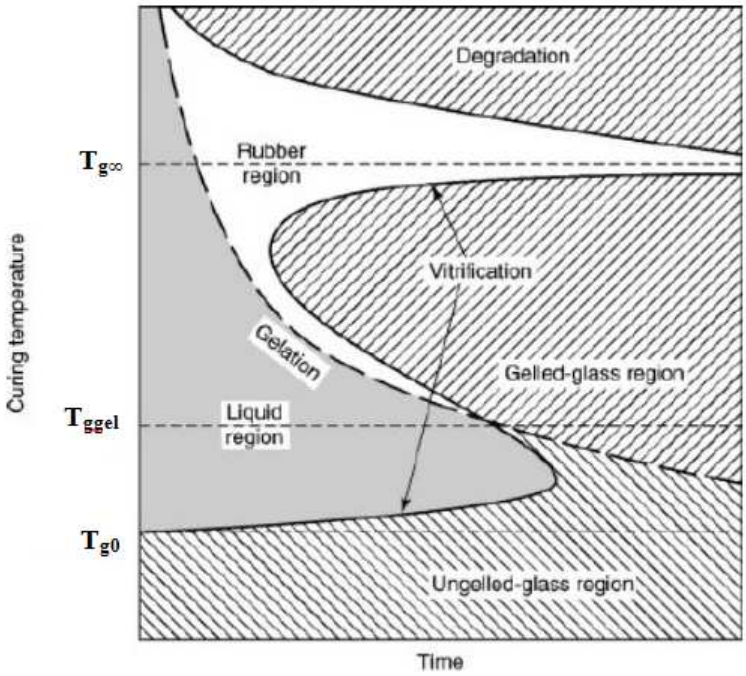

Figure 8. Time – temperature –transformation diagram

Curing behaviour of the four reactive systems, *i.e.* epoxy prepolymer combined with IPD at $n_{ah}/n_e = 1$ were studied by rheological measurements and DSC analyses. Then the influence of the stoichiometric ratio was studied for formulations based on $DGEDAS_0$ and SPGE.

a) Determination of gel time

Gel times (t_{gel}), corresponding to the appearance of a three-dimensional chemical network were determined by rheological measurements, at a temperature equal to 80°C, for the four reactive systems.

As an example, Figure 9 (a) and (b) shows the evolution of the loss factor tanδ as a function of time, in a multifrequency mode (from 1 rad/s to 50 rad/s and from 5 rad/s to 100 rad/s) for the systems DGECAR – IPD and SPGE – IPD. As a remark, the frequency range study for SPGE – IPD was expanded to 100 rad/s to facilitate the determination of gel time; further determination of gel time for the other systems will be performed in this frequency range. The gel time, t_{gel}, was determined by the crossover of the loss factor curves.

The gel times values are summarized in Table 2 and show that the bio-based system SPGE – IPD has the shortest gel time, whereas the other systems $DGEDAS_0$ – IPD, DGECAR – IPD and the conventional epoxy – amine system DGEBA – IPD have almost the same gel time. The short gel time of SPGE – IPD system can be explained by the functionality of the epoxy prepolymer, higher than 2, and the presence of numerous hydroxyl groups which can catalysed the epoxy-amine reaction. The storage and loss moduli can be described at the gelation point by a power law as a function of the pulsation:

$G'(\omega) \propto G''(\omega) \propto \omega^{\Delta}$, where Δ is the relaxation exponent that can be predicted by Rouse's percolation theory. So at gelation tanδ is independent on frequency and its value is:

$\Delta_{gel} = \pi.\Delta/2$ (Equation 1)

The values obtained for the relaxation component Δ are similar for DGEBA – IPD, $DGEDAS_0$ – IPD and DGECAR – IPD systems (Table 2) and in agreement with data reported in the literature on diepoxy-diamine systems [15-17]. The value obtained for SPGE – IPD system is much lower and equal to 0.29. In this case, the relaxation component value is very low. This value is out of the range generally reported in the literature for the value of Δ. This low value can be linked to the difficult determination of Δ due to short gel time (around 5 min) as it can be seen in Figure 9 (b). Yet other parameters may affect the determination of the relaxation parameter such as the high chlorine amount and the isothermal temperature T_i (80°C) lower than the maximum glass transition temperature as it will be discussed in the next sections.

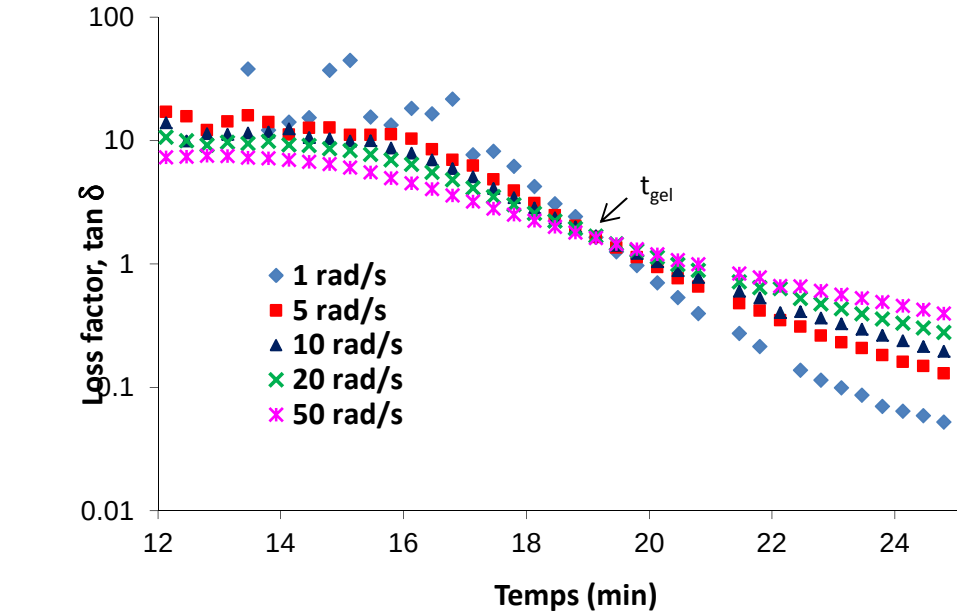

(a)

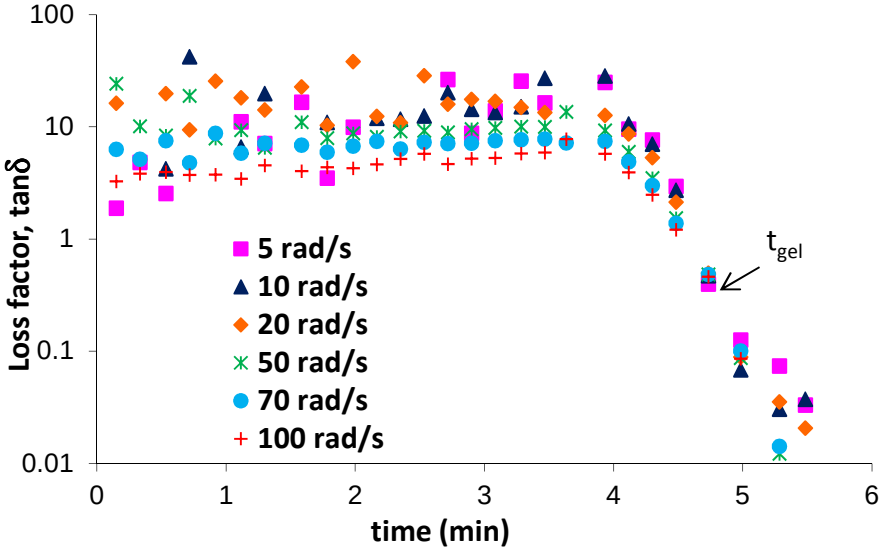

(b)

Figure 9. Loss factor tanδ, isotherm at 80°C for the reactive systems : (a) DGECAR – IPD (b) SPGE - IPD

System	t_{gel} (min)	tanδ	Δ
DGEBA – IPD	16	1.5	0.63
$DGEDAS_0$ – IPD	18	1.6	0.64
SPGE – IPD	4.8	0.5	0.29
DGECAR – IPD	19	1.7	0.66

Table 2 Gel time data for the different reactive systems

Determination of activation energy E_a

Gel times were measured at different temperatures and the activation energy was calculated for $DGEDAS_0$ – IPD and SPGE – IPD formulations. Data from literature were taken for DGEBA – IPD because this system has already been the subject of numerous investigations [18].

The evolution of gel times with temperatures were studied for SPGE – IPD and $DGEDAS_0$ – IPD systems in the temperature range of 40 – 80°C and 60 – 100°C respectively. Gel times and relaxation components obtained at various temperatures are presented in Table 3 and Table 4 for SPGE – IPD and $DGEDAS_0$ – IPD systems respectively.

T_i(°C)	t_{gel} (min)	$tan\delta_{gel}$	Δ
40	72.5	1.7	0.66
60	16.0	1.2	0.55
80	4.7	0.5	0.29

Table 3. Gel time data for SPGE – IPD at various temperatures

T_i(°C)	t_{gel} (min)	$tan\delta_{gel}$	Δ
60	62.1	1.4	0.62
80	18.0	1.6	0.64
90	9.6	1.3	0.58
100	5.6	0.6	0.36

Table 4. Gel time data for $DGEDAS_0$ – IPD at various temperatures

Gel times are lower for SPGE – IPD system than $DGEDAS_0$ – IPD (at 60°C and 80°C). Besides the relaxation component Δ of SPGE – IPD that was very low at 80°C (0.29) is in a classical range at lower temperatures (*e.g.* 0.66 for T_i = 40°C). Same observation is done for $DGEDAS_0$ – IPD. Indeed, the relaxation component Δ is around 0.6 for temperatures between 60°C and 90°C and lower (Δ_{100} = 0.36) for higher temperature (where gel time is shorter: around 5.6 min).

As theory says that the conversion at the gel point is constant for such epoxy-amine systems, the gel times obey an Arrhenius law as a function of temperature (Figure 10). Activation energy (E_a) was determined from the slope (E_a/R) of the $lnt_{gel} = f(1/T)$ curves, and are summarized in Table 5. Values of activation energy are in the same range for SPGE – IDP

and DGEDAS$_0$ – IPD, 63 and 62 kJ/mol, respectively. These values are equivalent to the one found in literature for DGEBA- IPD (63 kJ/mol [18]) and are all in the range of classical values for epoxy-amine system.

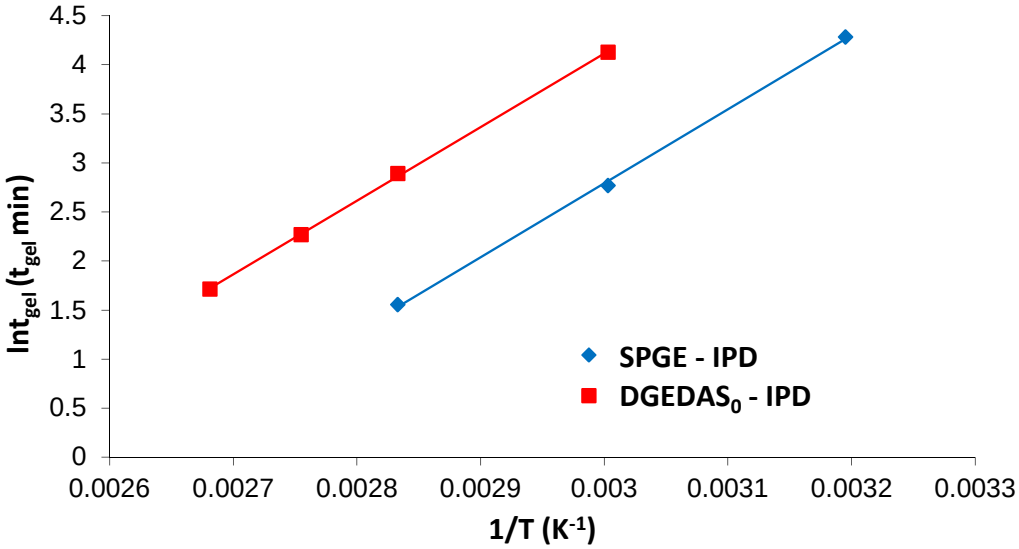

Figure 10. Arrhenius plot of the gelation phenomena for SPGE – IPD and DGEDAS$_0$ – IPD

Systems	E$_a$ (kJ/mol)	Ref.
DGEBA – IPD	63	[18]
DGEDAS$_0$ – IPD	62	-
SPGE – IPD	63	-

Table 5. Values of activation energy

As a conclusion, it appears that gel times determination is correct with classical values of E$_a$ found for the different systems. Yet, the values of relaxation component Δ are in some cases lower than classical values observed in the literature. In the case of SPGE – IPD this could find explanation in the particular nature of the epoxy prepolymer with high chlorine. Besides, sometimes the low gel times may falsify the correct determination of the relaxation component. Yet, another explanation resides in the choice of the isothermal temperature. As it will be outlined below, correct determination of the exponent Δ needs to be made at a temperature T$_i$ higher than the maximum glass transition temperature T$_{g\infty}$ to avoid vitrification [16, 19].

b) DSC calorimetry study

The curing behaviours of the different systems were also studied by DSC. The resulting thermograms of the four systems under stoichiometric ratio are represented in Figure 11. The glass transition temperature of the systems before reaction, T_{g0}, the peak maximum temperature, T_{peak}, and the total heat of reaction (ΔH) obtained from the DSC analyses are summarized in Table 6. T_{g0} is the lowest for the system based on $DGEDAS_0$. This monomer has a lower molar mass as compared to the other prepolymers. T_{go} is almost the same for the other systems. DGEBA – IPD and $DGEDAS_0$ – IPD systems have almost the same enthalpy of reaction, in the range of the classical value obtained for an epoxy –amine reaction at a stoichiometric ratio of 1. The other systems based on reactive precursors SPGE and DGECAR present lower values of enthalpy of reaction, around 80 kJ/ee for SPGE – IPD and 70 kJ/ee for DGECAR – IPD respectively. Besides, the exothermic peak of reaction T_{peak} is lower for SPGE – IPD confirming the highest reactivity of this system.

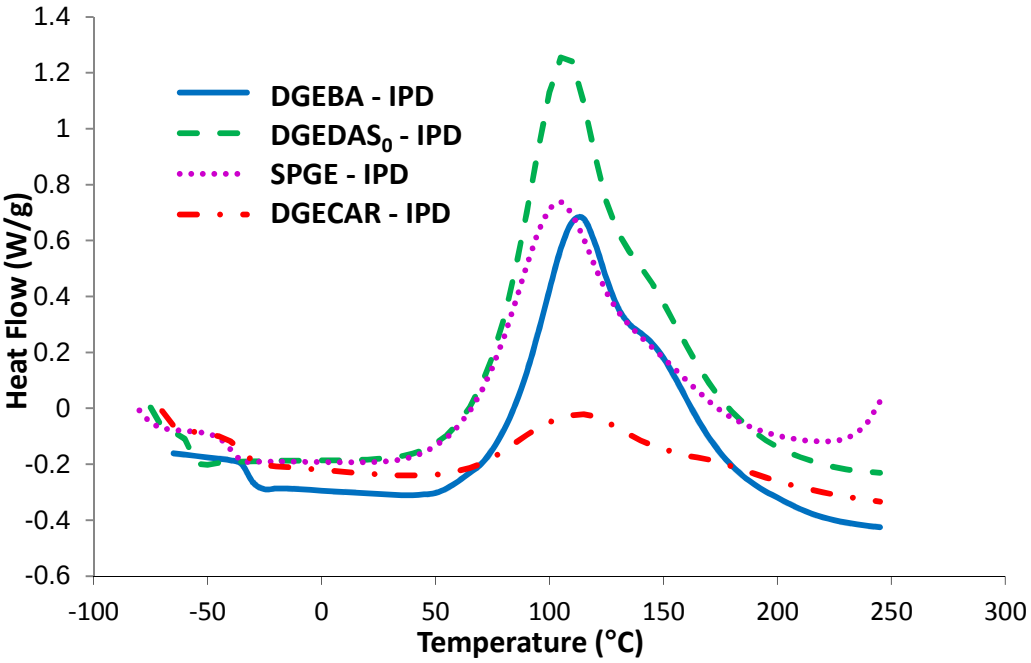

Figure 11. DSC thermograms for the different epoxy-amine systems

System	T_{g0} (°C)	ΔH (J/g)	ΔH (kJ/ee)	T_{peak} (°C)
DGEBA – IPD	-35	415	92	114
$DGEDAS_0$ – IPD	-60	547	89	108
SPGE – IPD	-41	338	79	101
DGECAR – IPD	-41	127	68	116

Table 6. DSC results for the four epoxy-amine systems

3. Determination and evolution of glass transitions with conversion

As mentioned previously, the different networks were obtained after crosslinking of the different reactive systems at 80°C for 1 h followed by 2 h at 180°C. The final glass transition temperature $T_{g\infty}$ was measured during a second DSC run to ensure complete curing of the network. The different values of glass transition obtained for the different systems are represented in Table 7.

The $T_{g\infty}$ obtained for the three bio-based networks, $DGEDAS_0$ – IPD, SPGE – IPD and DGECAR – IPD, are in all cases, lower than the $T_{g\infty}$ of conventional DGEBA – IPD network equal to 145°C. These observations cannot be attributed to incomplete curing as no residual heat was observed by DSC after the curing cycle and no evolution of T_g between the first and second DSC runs was observed. Concerning DGECAR – IPD this low T_g value ($T_{g\infty}$ = 22°C) can be explained by the flexibilizing effect of the long aliphatic chain present in DGECAR structure (see Figure 1) and its high epoxy equivalent (higher molar mass between cross-linking). Regarding the low $T_{g\infty}$ value of DGECAR – IPD it appears that the diglycidyl ether of Cardanol is not an epoxy prepolymer suitable for high performance applications.

In the case of SPGE, its aliphatic structure can explained the lower value of the glass transition of SPGE – IPD network ($T_{g\infty}$ = 100 °C) compensated by the high functionality of SPGE epoxy prepolymer, which brings higher crosslinking density and therefore increased T_g value.

The glass transition of $DGEDAS_0$ – IPD network is also lower than the $T_{g\infty}$ of DGEBA – IPD network. As it was described in the previous chapter, epoxy networks based on isosorbide epoxy prepolymer exhibit lower $T_{g\infty}$ values than expected which can be attributed to the higher flexibility of the linear segment between crosslinking points flexibility

as compared to conventional DGEBA – IPD system. This point was discussed more deeply in the Chapter II, Part II.

Networks	$T_{g\infty}$ (°C)
DGEBA – IPD	145
$DGEDAS_0$ – IPD	102
SPGE – IPD	100
DGECAR - IPD	22

Table 7. Glass transition values determined by DSC

Use of modified DiBenedetto equation for the determination of $T_g = f(x)$

Variation of glass transition T_g with the conversion rate *x* can be modelled by the Di Benedetto equation modified by Pascault and Williams [20] and represented below :

$$\frac{T_g - T_{g0}}{T_{g\infty} - T_{g0}} = \frac{\lambda x}{1-(1-\lambda)x} \qquad \text{(Equation 4)}$$

With $\lambda = \frac{\Delta C_{p\infty}}{\Delta C_{p0}}$

T_{g0} and $T_{g\infty}$ are the glass transition of the initial blend (before any reaction) and the totally crosslinked network, respectively.

ΔC_{p0} and $\Delta C_{p\infty}$ are the change in heat capacity of glass transition of the initial blend and the crosslinked network, respectively.

All these values were taken from DSC runs and are reported in Table 8.

Systems	T_{g0} (°C)	ΔC_{p0}	$T_{g\infty}$ (°C)	$\Delta C_{p\infty}$	λ
DGEBA – IPD	-30	0.12	145	0.10	0.36
$DGEDAS_0$ – IPD	-60	0.13	102	0.07	0.58
SPGE – IPD	-41	0.14	100	0.09	0.62
DGECAR – IPD	-41	0.13	22	0.10	0.79

Table 8. Experimental values for Di Benedetto equation

Evolution of glass transition with conversion modelled by the Di Benedetto equation for the four epoxy-amine systems studied is represented in Figure 12.

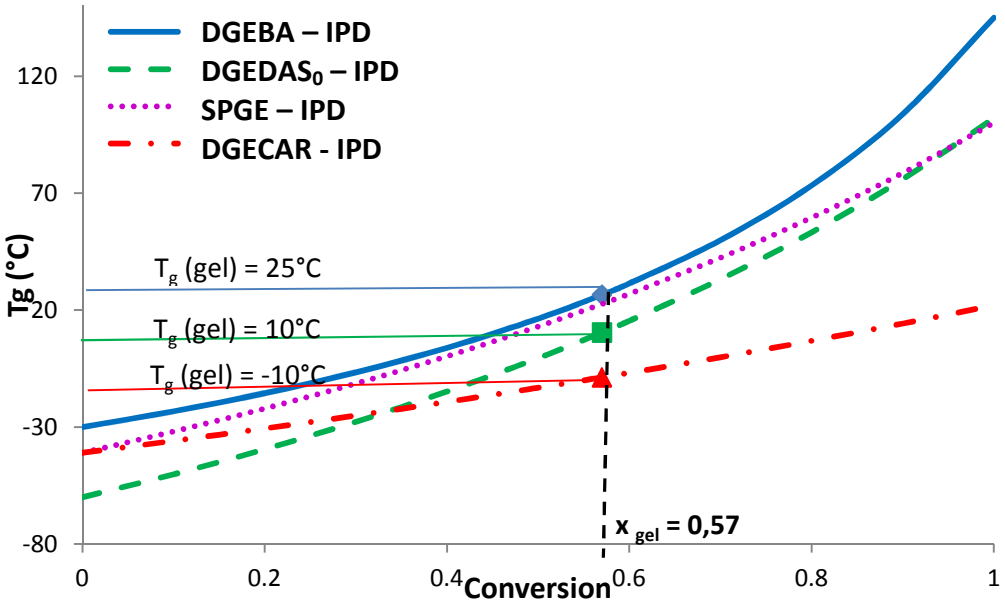

Figure 12. Evolution of glass transition with conversion. Modified Dibenedetto equation

These curves are useful to determine T_{ggel} at a conversion $x = x_{gel}$. Theoretical values of x_{gel} are obtained using the Flory-Stockmayer theory:

$$x_{gel}^2 = \frac{1}{(f_A - 1)(f_B - 1)} \qquad \text{(Equation 5)}$$

Where f_A and f_B are the functionalities of the two components.

In our case, $f_A = 4$ (IPD tetra-functional amino-hydrogen) and $f_B = 2$ (di-functional epoxy for DGEBA, $DGEDAS_0$ and DGECAR). It gives a conversion at gelation equal to 0.577. As the functionality of SPGE epoxy prepolymer is unknown (higher than 2), determination of theoretical value T_{ggel} (at $x = 0.577$) using Di Benedetto curve was not performed for SPGE – IPD system.

The values of T_{ggel} using this approach are around 10°C for $DGEDAS_0$ – IPD system, around -10°C for DGECAR – IPD system and 25°C for DGEBA – IPD system.

➢ These results can explain the difficult determination of the relaxation component Δ. Indeed, this confirms that the isothermal temperatures T_i for gel time's determination were lower than $T_{g\infty}$. In this case, mobilities of macromolecular chains with long relaxation times occur and these chains behave as in a vitreous state. Besides, in some cases, the $\Delta T = T_i$ –

T_{ggel} is low and impact also the correct determination of Δ [16], as T_{ggel} is the temperature at which gelation and vitrification simultaneously occur. Nevertheless, it is not always possible to obtain gel times at $T_i > T_{g\infty}$, where only gelation occurs, especially for such systems that exhibit short gel times at high temperatures.

➢

4. Influence of stoichiometry on the value of $T_{g\infty}$

It has been shown that assuming the only mechanism is epoxy-amine addition without side reaction, the maximum attainable $T_{g\infty}$ coincides with the stoichiometric composition [18]. Therefore, the effect of variation of the amino hydrogen-to-epoxy ratio, $r = n_{ah}/n_e$ on $T_{g\infty}$ is examined in this study as an indicator of possible side reactions.

The variation of the ratio n_{ah}/n_e was studied between 0.5 and 1.5 for DGEBA – IPD, $DGEDAS_0$ – IPD and SPGE – IPD. This study hasn't been performed on DGECAR – IPD regarding the low $T_{g\infty}$ value of the corresponding network. Glass transitions were measured during a second DSC run and the variations of $T_{g\infty}$ with the stoichiometric ratio are plotted in Figure 13.

For the systems based on DGEBA and $DGEDAS_0$ combined with IPD, the curves exhibit a maximum $T_{g\infty}$ for r equal to 1, which means that the only mechanism occurring during the cross-linking of the reactive systems is the amine-epoxy addition. No side reactions such as etherification occur during the cross-linking. Nevertheless, the $DGEDAS_0$ – IPD networks still exhibit lower $T_{g\infty}$ value compared with the conventional DGEBA – IPD networks whatever the stoichiometric ratio studied.

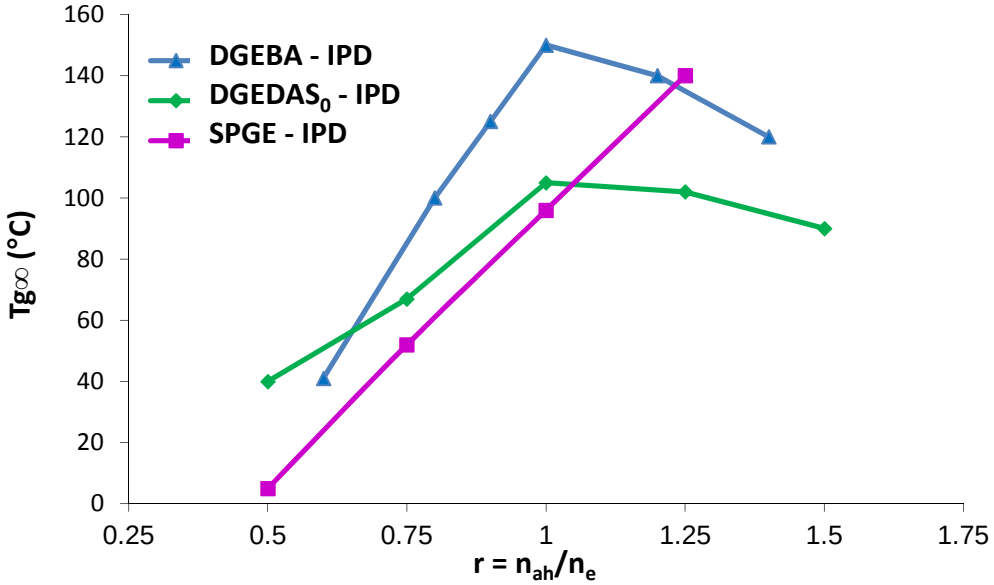

Figure 13. Glass transition temperature versus r for networks based on DGEBA, $DGEDAS_0$ and SPGE combined with IPD

Concerning, the SPGE – IPD epoxy-amine system, an augmentation of $T_{g\infty}$ with r is observed which is an unexpected behaviour and reveals possible side reactions. Besides after r = 1.25, $T_{g\infty}$ became difficult to measure by DSC. To obtain these values, DMA were performed on networks of higher stoichiometric ratio r.

5. Thermo-mechanical properties of the networks

a) Thermo-mechanical properties of the networks at r = 1

First, the dynamic mechanical properties of the different networks in stoichiometric ratio (r equal to 1) were investigated using DMA. In Figure 14 and Figure 15, the storage modulus (G') and the loss factor (tanδ) of the different bio-based epoxy networks are compared with the DGEBA based one. As previously mentioned in Chapter II, the main transition α, in the high-temperature region is associated with the glass transition, whereas the secondary relaxation β, below 0°C, is assigned to short molecular segment motion, and more precisely hydroxyl ether groups' motion in the case of epoxy-amine networks [21]. Values of T_β, T_α and G' are reported in the Table 9.

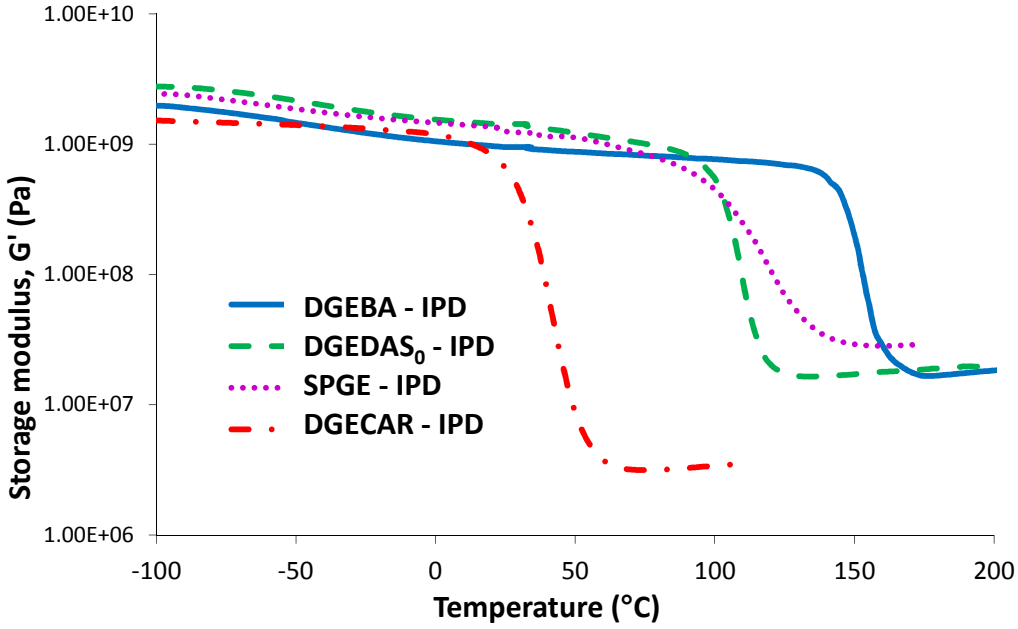

Figure 14: Storage modulus versus temperature for DGEBA, DGEDAS$_0$, SPGE and DGECAR cured with IPD

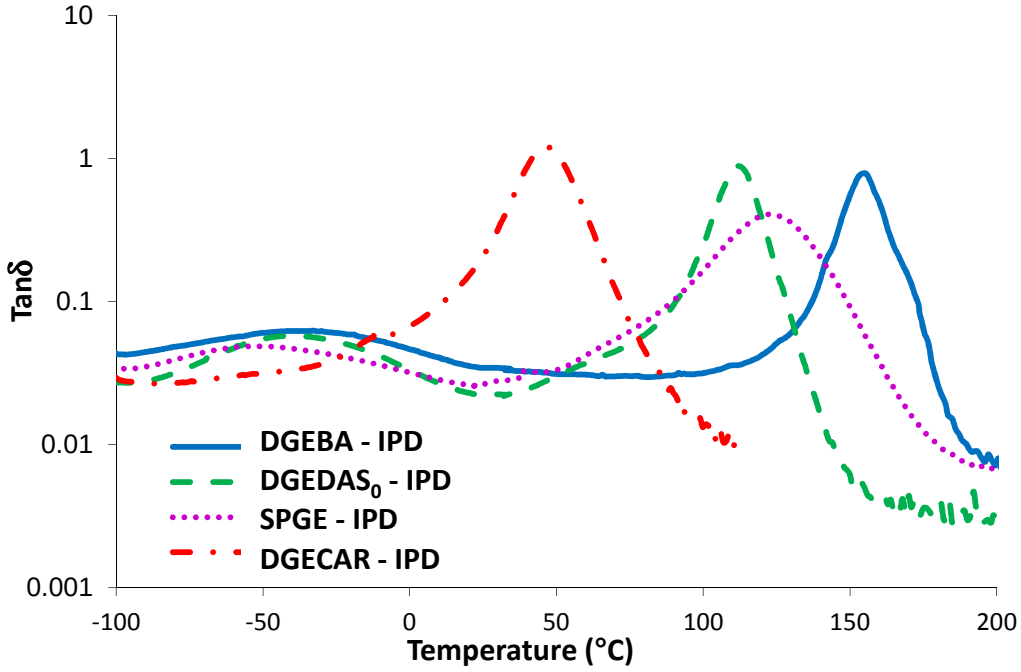

Figure 15: Tanδ versus temperature for DGEBA, DGEDAS$_0$, SPGE and DGECAR cured with IPD

System	T_β (°C)	T_α (°C)	G' (MPa) (at T_α+30°C)	d (g/cm^3)	ν (10^{-3} mol/cm^3)	Mc (g/mol)
DGEBA – IPD	-41	155	17.1	1.13	4.5	250
$DGEDAS_0$ – IPD	-42	112	16.6	1.25	4.8	260
SPGE – IPD	-52	120	29.3	1.24	8.3	150
DGECAR – IPD	-	50	3.2	1.06	1.1	970

Table 9: Dynamic mechanical analyses of the networks

There is no significant difference regarding the secondary relaxation β for DGEBA and $DGEDAS_0$ based networks, with T_β around -40 °C. SPGE-based network exhibits a lower β relaxation temperature at -52°C. Sub-T_g relaxation is not visible in the DGECAR-IPD network analysis, which can be explained by a lower concentration of hydroxyl ether groups due to its high value of epoxy equivalent (eew = 490 g/eq) resulting in a very weak magnitude of the sub-T_g relaxation. Indeed, magnitude of the sub-T_g relaxation is linked to the concentration of the relaxing species per unit volume. Besides, the α-transition begins at a lower temperature for this system (< 0°C) and therefore can mask the sub-T_g transition.

T_α follows the same trend as the T_g measured by DSC. The highest value of T_α is measured for the classical DGEBA-IPD network (T_α = 155 °C). Lower and closed values of T_α are obtained for the bio-based networks $DGEDAS_0$ – IPD and SPGE – IPD, respectively 110°C and 120°C. DGECAR – IPD exhibits the lowest T_α (around 50°C) and the lowest rubbery modulus, due to the flexibility of the long aliphatic chain within the cardanol epoxy prepolymer structure. DGEBA – IPD and $DGEDAS_0$ – IPD have equivalent rubbery moduli, around 17 Mpa. The highest rubbery modulus (29.3 MPa) is obtained for the network based on SPGE, which has a high functionality.

According to the rubber elasticity theory, the following equations are employed to describe the relationship between M_c (average molar mass of the segment between crosslinking points) and ν (crosslinking density) with storage modulus (G') of a thermoset above the T_g [22]:

$$G' = dRT/M_c \qquad \text{(Equation 2)}$$

$$\nu = G'/RT \qquad \text{(Equation 3)}$$

Where G', d, R, T are the storage modulus at T_g + 30K (MPa), the density of the network (g/cm^3), the gas constant (8.314 J/mol.K) and the temperature (K), respectively. The values of

molar mass between crosslinking points (M_c) and crosslinking density (ν) are presented in Table 9. The shortest values of M_c and as a consequence the highest value of crosslinking density are obtained for SPGE – IPD because of SPGE high functionality. Besides, highest value for M_c is obtained for DGECAR – IPD networks.

b) Thermo-mechanical properties of SPGE – IPD networks at different stoichiometry

Previous DSC analyses have underlined an unexpected evolution of glass transition temperature $T_{g\infty}$ with the stoichiometric ratio, $r = n_{ah}/n_e$, for the networks obtained with SPGE combined with IPD. As the determination of T_g was difficult for $r > 1.25$ (glass transition not well defined in DSC runs), and to confirm this unexpected behaviour, dynamic mechanical analyses were performed for the SPGE – IPD networks at various r (from r = 0.75 to r = 2). The storage modulus (G') and the loss factor (tanδ) versus temperature of the different SPGE – IPD networks are plotted in Figure 16 and Figure 17 respectively.

T_β are in the same range, around -50°C, for all the different networks studied. A huge augmentation of T_α with r is observed, and confirms the unexpected behaviour revealed by the previous DSC analyses. Values of T_β and T_α are summarised in Table 10 and the evolution of T_g measured by DMA is represented in Figure 18. T_α varies from 68°C to 208°C. It increases strongly up to r = 1.25, and then more slowly up to r = 2. In addition, the tanδ peak becomes broader and for the highest value of r, two peaks can be distinguished: one near 120°C and the other one occurring between 187°C and 208°C, depending on r. This behaviour with two distinct T_α is typical of heterogeneous networks having phases of different crosslink density.

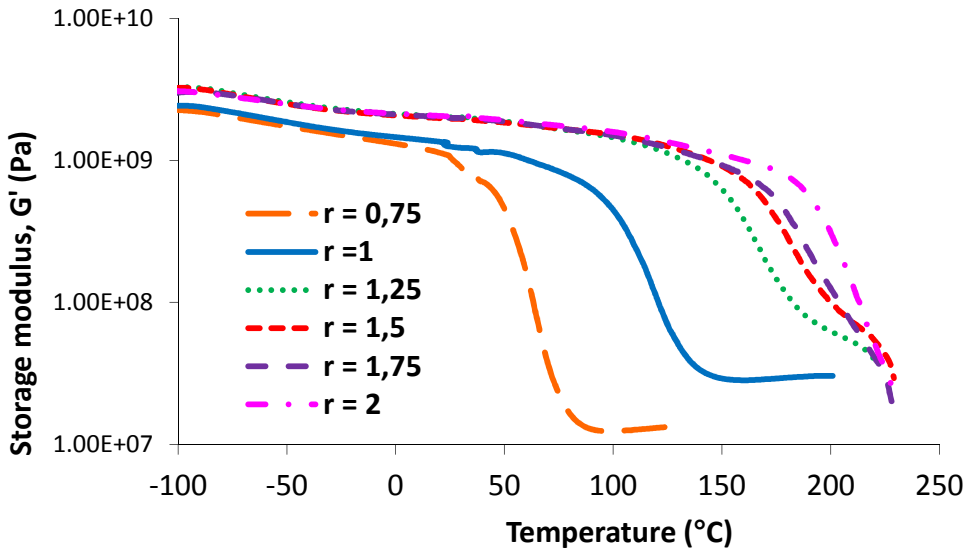

Figure 16. Storage modulus versus temperature for SPGE cured with IPD at different stoichiometry r

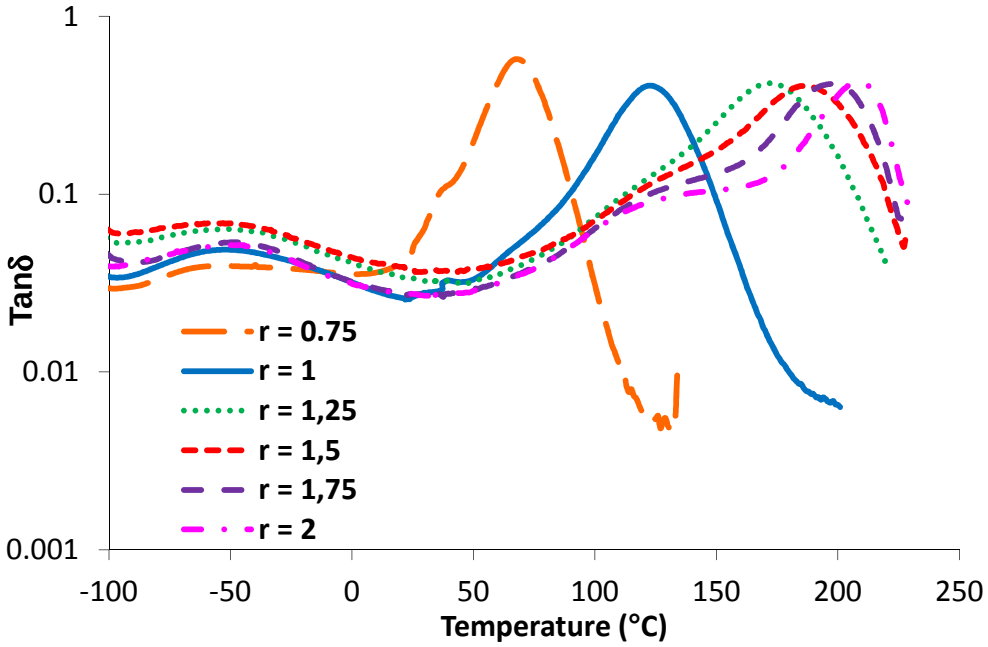

Figure 17. Tanδ versus temperature for SPGE cured with IPD at different stoichiometry r

$R = n_{ah}/n_e$	T_β (°C)	T_α (°C)	tanδ max	ΔT_α (°C)
0.75	-50	68	0.57	27
1	-47	120	0.41	35
1.25	-49	170	0.42	51
1.5	-49	187	0.41	53
1.75	-48	197	0.42	43
2	-49	208	0.43	33

Table 10. T_β and T_α values for SPGE – IPD networks at different stoichiometry

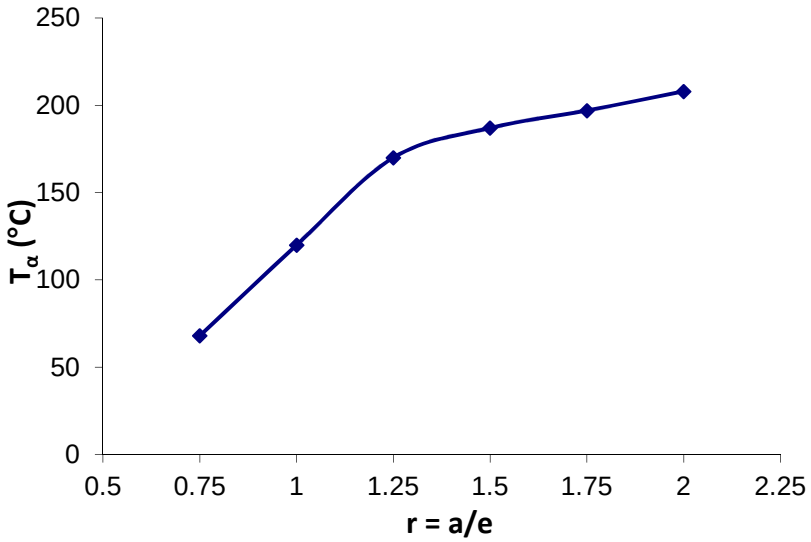

Figure 18. Evolution of T_α (measured by DMA) associated to T_g with r

For the networks with r > 1.25, values of rubbery moduli are not obtained as the rubbery region is not reached. It can be explained by the augmentation of T_α getting closer to the degradation temperature. For SPGE – IPD networks the degradation temperature seems to be very low (around 230°C). This will be confirmed later by thermogravimetric analyses.

Nevertheless for r = 0.75, r = 1 and r = 1.25, storage modulus G' in the rubbery state can be measured, and according to the rubber elasticity theory (Equation 2 and Equation 3), molar mass between crosslinking points (M_c) and crosslinking density (ν) can be calculated. Results are summarized in Table 11. For r = 0.75, a higher molar mass between crosslinking points is observed. M_c decreases with the augmentation of r. Thus, crosslinking density increases with the amine proportion in the system (with r > 1, $n_{ah} > n_e$). This can explain why an augmentation of glass transition is observed with r, as higher crosslinked network leads to higher T_g.

$r = n_{ah}/n_e$	T_β (°C)	T_α (°C)	G' (MPa) (at T_α+30°C)	d (g/cm^3)	ν (10^{-3} mol/cm^3)	M_c (g/mol)
0.75	-50	68	12.4	1.27	4.0	315
1	-52	120	29.3	1.24	8.3	150
1.25	-49	170	38.5	1.22	10.0	122

Table 11. Dynamic mechanical analyses of SPGE – IPD networks at r=1 and r=1.25

To the best of our knowledge such behaviour, *i.e.* increase of T_g and decrease of M_c with an increase of r in epoxy-amine systems, is not reported in literature. In classical systems, the excess of amine hardener results in chain extension and lead to networks with a lower T_g and higher M_c. Different hypotheses can explain this unexpected behaviour:

✓ First, secondary –OH groups in sorbitol structure (Figure 1), which as underlined previously are more difficult to epoxidized and may remain in the sorbitol polyglycidyl ether structure, can be involved in etherification reaction (Scheme 2, Chapter II). As a remark, this etherification reaction does not consume amines.

✓ Secondly, we remind that the particularity of the SPGE is to have a high chlorine content (~19 wt%) with the presence of numerous chlorohydrine segments (Scheme 1). In the presence of an excess of amine and due to its catalytic effect (basic catalyst), Cl can be involved in some side reactions or strong ionic interactions:

$$R\text{-}Cl + R'\text{-}NH_2 \rightarrow R'RNH_2^+ \, Cl^-$$

Evolution of chlorine content in the networks

In order to explain the unexpected evolution of T_g with r, it has been considered previously that the high chlorine content could be at the origin of other side reactions and shift the stoichiometric ratio. Reacting with other organic compound during the cure epoxy-amine reaction Cl may evaporates (HCl, Cl_2 can be formed), which should bring a decrease of Cl content in the resulting epoxy-amine networks.

We wanted to know if some Cl were released by a reaction. Therefore, the evolution of Cl content in different epoxy-amine networks obtained from SPGE – IPD with different stoichiometric ratio were studied by elemental analyses. These measured chlorine contents were compared with the theoretical ones calculated knowing the different amount of epoxy and amine for each composition (epoxy prepolymers were also previously characterized by elementary analyses). The theoretical evolution of Cl with r and the experimental values obtained by elemental analyses are plotted in Figure 19.

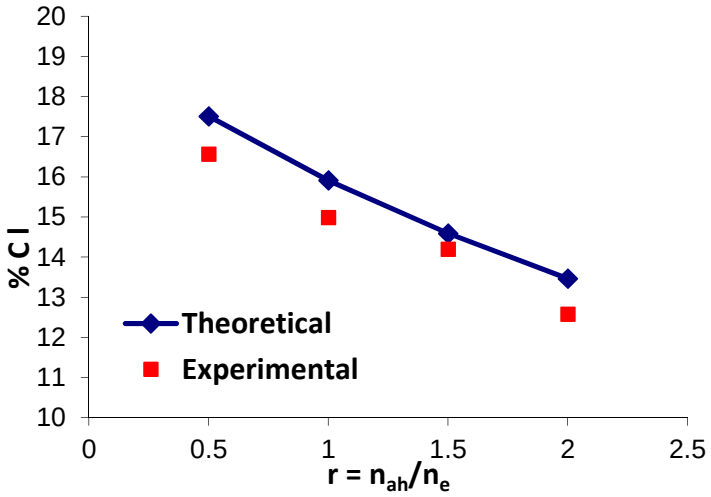

Figure 19. Evolution of chlorine content with r

It appears that measured chlorine contents are in good agreement with the theoretical values calculated for each n_{ah}/n_e ratio considered which means that Cl remains in the network structure and can be linked by strong ionic interactions for instance.

Then, in order to obtain new elements for the interpretation of this behaviour, we realized DSC measurements on the different systems. The thermograms are reported in Figure 20. For the stoichiometric ratio equal to 0.5 and 1, classical thermograms are obtained, with the same shape as DGEBA – IPD thermograms (Figure 11). At higher stoichiometric ratio a second exothermic peak appears at high temperature (194°C). At the same time, the first peak becomes less broad but more intense. Secondary reaction occurs at high temperatures for SPGE – IPD systems with the increase of r.

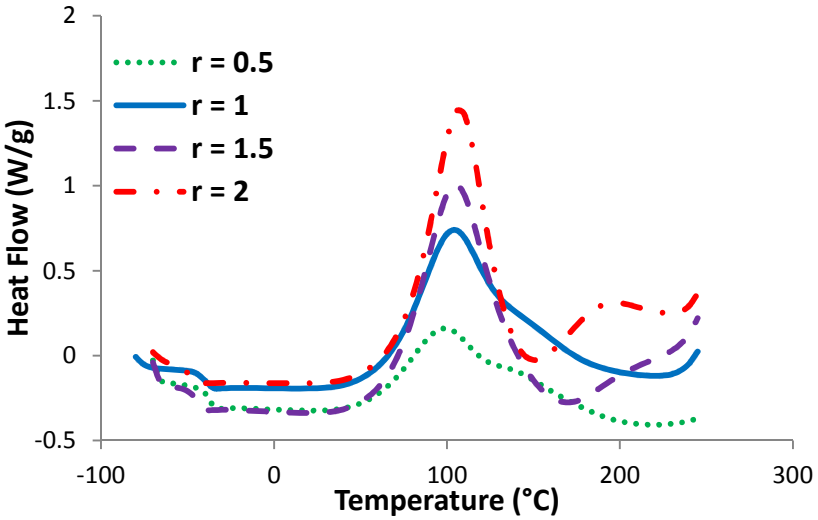

Figure 20. DSC thermograms for SPGE – IPD systems at different stoichiometric ratio r

r = a/e	T_{g0} (°C)	ΔH (J/g)	ΔH (kJ/ee)	T_{peak} (°C)
0.5	-41	229	49	101
1	-41	338	79	101
1.5	-48	384	98	105
2	-53	372	103	107 /194

Table 12. DSC results for SPGE – IPD systems at different stoichiometry

6. Thermal stability of the networks

a) Thermal stability of the networks at r = 1

The mass loss as a function of temperature for DGEBA, $DGEDAS_0$, SPGE and DGECAR cured with IPD and their derivatives are shown in Figure 21 (a) and (b). The network DGEBA – IPD thermally degrades through a single step process with an initial degradation ($T_{5\%}$) close to 330°C and a maximum rate at 370°C. $DGEDAS_0$ – IPD mainly thermally degrades through a simple step process with an initial degradation ($T_{5\%}$) at 305°C and a maximum rate at approximately 350°C. SPGE – IPD network exhibits poorer thermal stability compared with the other networks. Indeed the initial degradation is close to 260°C with a maximum rate at 270°C.

Finally, the DGECAR – IPD networks is the more thermally stable network, but degradation does not undergo a simple step process, with two maximum rates at 350 °C and 440 °C.

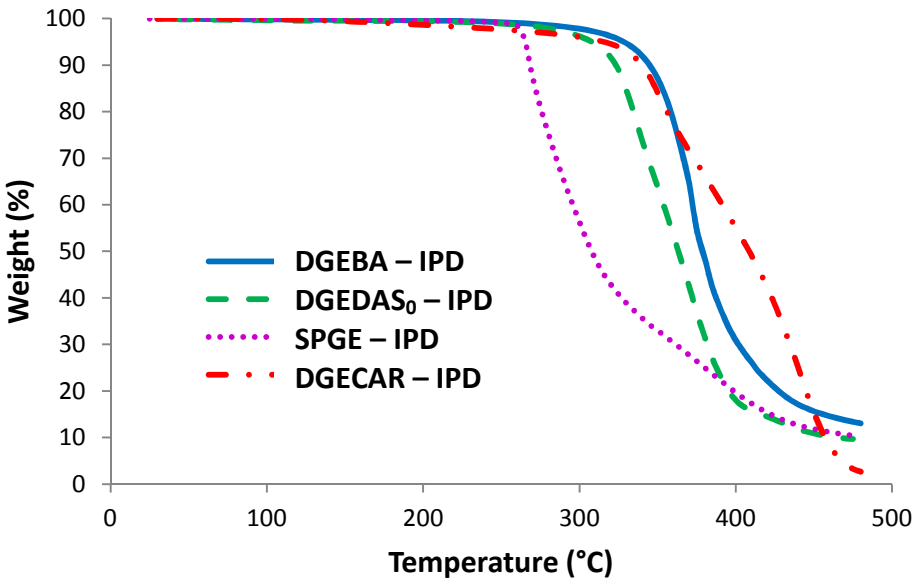

(a)

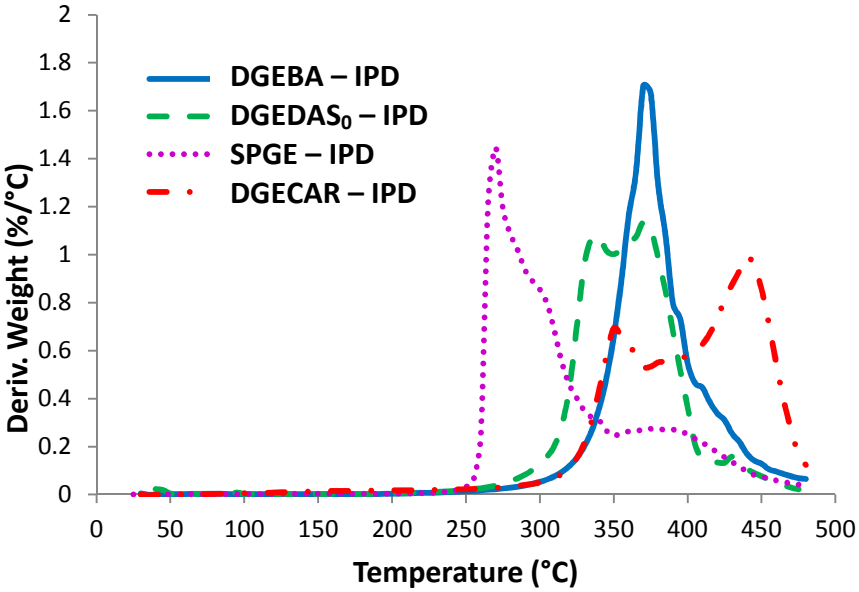

(b)

Figure 21. (a) TGA and (b) DTGA curves of DGEBA, DGEDAS$_0$, SPGE, DGECAR networks with IPD

Networks	$T_{(5\%)}$ (°C)	$T_{maximum\ rate}$ (°C)
DGEBA – IPD	325	370
DGEDAS$_0$ – IPD	305	340/370
SPGE – IPD	265	270
DGECAR – IPD	315	350/440

Table 13. Thermal analysis data for the different epoxy networks

b) Thermal stability of the SPGE – IPD networks at different stoichiometry

The influence of the stoichiometric ratio r on the thermal stability of the SPGE – IPD networks has been studied. The TGA analyses performed on SPGE – IPD at r = 1, r = 1.5 and r = 2 are represented in Figure 22. It appears that the stoichiometric ratio has no influence on the initial degradation temperature (around 260°C). This observation confirms the hypothesis of degradation at 230°C during DMA analyses that prevents the observation of a rubbery plateau. TGA analyses were performed under N_2 atmosphere and therefore the temperature of degradation was higher than the one observed during DMA analyses.

Nevertheless, a shift of the maximum rate temperature to higher temperature is observed for SPGE – IPD network with a stoichiometric ratio r = 2. Two peaks are observed on the derivative curve of the SPGE – IPD network at r = 1.5.

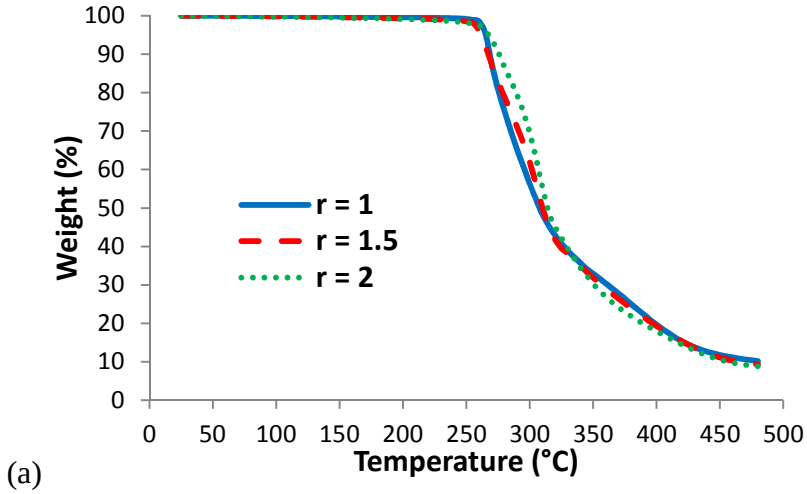

(a)

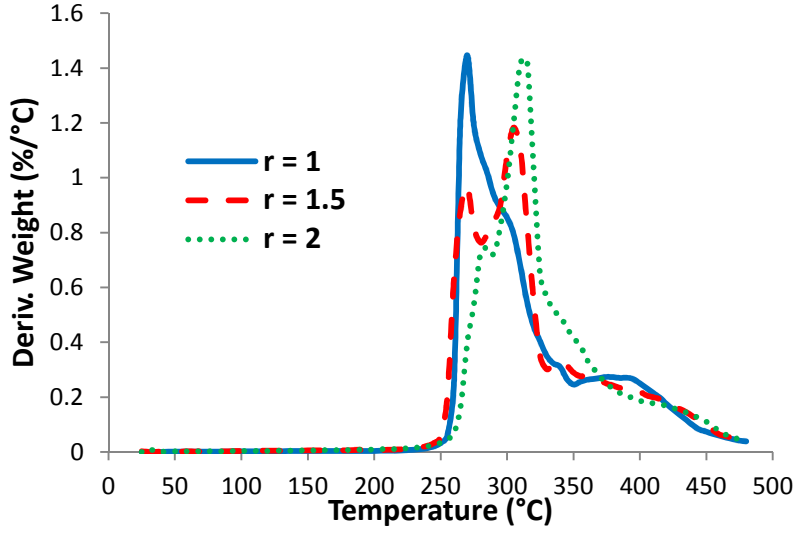

(b)

Figure 22. (a) TGA and (b) DTGA curves of SPGE – IPD networks with different stoichiometric ratio r

Networks	$T_{(5\%)}$ (°C)	$T_{maximum\ rate}$ (°C)
SPGE – IPD r = 1	265	270
SPGE – IPD r = 1.5	260	270/305
SPGE – IPD r = 2	265	310

Table 14. Thermal analysis data for SPGE – IPD networks at various stoichiometry

Conclusion

In this part of the work, three different bio-based epoxy precursors were analysed: two bio-based epoxy commercially available, derived from sorbitol and cardanol, and a novel epoxy monomer successfully synthesized from isosorbide. The chemical structures of these different bio-based epoxy prepolymers were studied by SEC, ESI-TOF MS, FT-IR analyses and compared with conventional DGEBA epoxy prepolymer. Different structure of the epoxy prepolymers have been underlined: phenolic structure with a long aliphatic chain for the epoxy derived from cardanol, multifunctional short aliphatic structure for the sorbitol derivatives, and short and cyclic aliphatic structure for isosorbide diglycidyl ether. Besides, it appears that the commercial epoxy prepolymer derived from sorbitol contains a high chlorinated content which have been explained by the synthetic route (conventional epoxidation through epichlorohydrin).

Reactivity and physical properties of these new bio-based epoxy prepolymers cured with isophorone diamine (IPD) were compared to a traditional petroleum-derived epoxy prepolymer (DGEBA) cured in the same conditions with isophorone diamine (IPD). The system based on sorbitol polyglycidyl ether (SPGE) combined with IPD is more reactive than the other systems. Indeed, SPGE – IPD exhibits the lower gelation time at 80°C, whereas the diglycidyl ether of cardanol (DGECAR) has the longer gel time. Networks obtained from the isosorbide and sorbitol bio-based epoxy prepolymer exhibits interesting glass transition, around 100°C, yet lower than the DGEBA based networks (145°C). Higher rubbery modulus is obtained for the SPGE – IPD network. Sorbitol Polyglycidyl Ether and Diglycidyl Ether of Isosorbide could be good candidate for the replacement of bisphenol A-based prepolymers. However, a particular behaviour of the networks based on SPGE was evidenced, not yet clearly understood: a significant increase in T_g as well as in crosslinking density has been

observed in networks synthesized with an excess of hardener. This is opposite to the general trend observed in epoxy-amine network. We believe this behaviour is linked to the presence of chlorohydrines in the prepolymer. Finally, even if the cardanol based epoxy networks have low glass transition temperatures, cardanol-based epoxy prepolymers can also be interesting for uses as bio-based flexibilizers.

In the next chapter, focus will be put on the influence of crosslinking agent on the network properties of bio-based networks obtained using the epoxy prepolymers described in this chapter.

References

[1] Morrison J. Polyglycidyl ethers of ether anhydrohexitols, method of production, and aqueous solutions thereof. US Patent 3,041,300 1962.

[2] Zech J. Bisglycidyl ethers of isohexides. US Patent 3,272,845 1966.

[3] East A, Jaffe M, Zhang Y, Catalini LH. Thermoset epoxy polymers from renewable resources. US Patent US 2008/0009599 A1 2008.

[4] East A Jaffe M, Zhang Y, Catalini LH,. Ethers of bisanhydrohexitols. US Patent US 2008/0021209A1 2008.

[5] Feng X, East AJ, Hammond WB, Zhang Y, Jaffe M. Overview of advances in sugar-based polymers. *Polymers for Advanced Technologies*. 2011;**22**:139-50.

[6] Fenouillot F, Rousseau A, Colomines G, Saint-Loup R, Pascault JP. Polymers from renewable 1,4:3,6-dianhydrohexitols (isosorbide, isomannide and isoidide): A review. *Progress in Polymer Science*. 2010;**35**:578-622.

[7] Patel MB, Patel RG, Patel VS. Effects of reactive diluent diepoxidized cardanol and epoxy fortifier on curing kinetics of epoxy resin. *Journal of Thermal Analysis and Calorimetry*. 1989;**35**:47-57.

[8] Yadav R, Awasthi P, Srivastava D. Studies on synthesis of modified epoxidized novolac resin from renewable resource material for application in surface coating. *Journal of Applied Polymer Science*. 2009;**114**:1471-84.

[9] Yadav R, Srivastava D. Studies on cardanol-based epoxidized novolac resin and its blends. *Chemical & Chemical Technology,*. 2008;**2**:173-84.

[10] Acierno D, Russo P, Savarese R. Mechanical and dynamic-mechanical properties of biodegradable epoxy resins. *Proceedings of the Polymer Processing Society*. Salerno, Italy. 2008.

[11] Shibata M, Nakai K. Preparation and properties of biocomposites composed of bio-based epoxy resin, tannic acid, and microfibrillated cellulose. *Journal of Polymer Science Part B: Polymer Physics*. 2010;**48**:425-33.

[12] Chrysanthos M, Galy J, Pascault JP. Preparation and properties of bio-based epoxy networks derived from isosorbide diglycidyl ether. *Polymer*. 2011;**52**:3611-20.

[13] Pellin MP, Regueira LN, Gandara JS, Losada PP, Lamela CP, Abuin SP. Epoxy Resins Based on Trimethylolpropane. I. Determination of Chemical Structures. *Journal of Applied Polymer Science*. 1995;**55**:225-32.
[14] Enns JB, Gillham JK. Time–temperature–transformation (TTT) cure diagram: Modeling the cure behavior of thermosets. *Journal of Applied Polymer Science*. 1983;**28**:2567-91.
[15] Pascault JP, Sautereau H, Verdu J, Williams RJJ. Thermosetting Polymers: Taylor & Francis Books, Inc. 2002.
[16] Eloundou J. *Thèse INSA-Lyon:* Gélification de systèmes époxy-amine: études cinétique, rhéologiques et diélectrique; 1996.
[17] Huang ML, Williams JG. Mechanisms of Solidification of Epoxy-Amine Resins During Cure. *Macromolecules*. 1994;**27**:7423-8.
[18] Galy J, Sabra A, Pascault JP. Characterization of epoxy thermosetting systems by differential scanning calorimetry. *Polymer Engineering & Science*. 1986;**26**:1514-23.
[19] Eloundou JP, Feve M, Gerard JF, Harran D, Pascault JP. Temperature Dependence of the Behavior of an Epoxy−Amine System near the Gel Point through Viscoelastic Study. 1. Low-Tg Epoxy−Amine System. *Macromolecules*. 1996;**29**:6907-16.
[20] Pascault JP, Williams RJJ. Glass transition temperature versus conversion relationships for thermosetting polymers. *Journal of Polymer Science Part B: Polymer Physics*. 1990;**28**:85-95.
[21] Won YG, Galy J, Gérard JF, Pascault JP, Bellenger V, Verdu J. Internal antiplasticization in copolymer and terpolymer networks based on diepoxides, diamines and monoamines. *Polymer*. 1990;**31**:1787-92.
[22] Nielsen LE. Cross-Linking–Effect on Physical Properties of Polymers. *Journal of Macromolecular Science, Part C: Polymer Reviews*. 1969;**3**:69-103.

Chapter IV Influence of the curing agent structure on network properties

This chapter is dedicated to the study of the influence of the curing agent structure on the network properties and it is divided in two parts. The first part deals with various formulations with other curing agents, either aromatic or aliphatic amines, and their influence on the reactivity of the system and the resulting network properties. The second part of this chapter focuses on the use of a specific amine curing agent developed for rapid cure during processing of composite materials.

Part I. Influence of the structure of amine curing agents

I. Introduction

Focus has been put in the previous chapters on the characterization of partially bio-based epoxy networks obtained by replacing the petroleum epoxy-based prepolymer DGEBA by bio-based ones. Epoxy prepolymers derived from isosorbide and synthesized through two different routes have been studied and combined with isophorone diamine (IPD) curing agent (Chapter II.). Other bio-based epoxy prepolymers derived from sorbitol and cardanol have also been tested with IPD (Chapter III.). In this Chapter we focus on the influence of crosslinking agent structure. Therefore, other formulations comprising the bio-based epoxy prepolymers previously characterized and different curing agents were characterized.

The curing agents used differ by their structure, as they are either **aliphatic** such as polyetheramine (*Jeffamine D230*), m-Xylylene diamine (*MXDA*), or **cycloaliphatic** such as isophorone diamine (*IPD*), or **aromatic** such as 4,4'-methylene bis (3-chloro-2,6-diethylaniline) (*MCDEA*), diethyl toluene diamine (*DETDA*). Bio-based curing agents were also tested such as phenalkamine (*NC540*) or tannic acid (*TA*). Phenalkamines are derived from Cashew Nut Shell Liquid and have already been used as curing agent for conventional

epoxy prepolymer such as DGEBA [1, 2]. Tannic acid obtained from wood derivative is of interest as it presents another reaction mechanism (epoxy – phenoxy reaction). Tannic acid has already been tested by Shibata [3] in combination with sorbitol diglycidyl ether prepolymer. The use of these bio-based curing epoxy curing agents is of interest as it can lead to 100 % bio-based epoxy networks. The aim of this first part of the chapter is to present the various formulations. Reactivity study of the different systems and glass transition temperatures of their respective networks were analysed and are presented below.

II. Experimental section

1. Structure of curing agents

The epoxy prepolymers used in this study are the ones previously characterized: the isosorbide-based epoxy prepolymers ($DGEDAS_0$ and $DGEDAS_n$) the sorbitol polyglycidyl ether (SPGE) and the cardanol-based epoxy prepolymer (DGECAR).

The different curing agents used are presented in Table 1. The IPD, MXDA, DETDA and TA curing agents were obtained from Aldrich. The Jeffamine D230 was provided by Huntsman, and the phenalkamine NC-540 was kindly supplied by Cardolite Corporation. All the curing agents were used as received.

Name	Structure	Molar Mass (g/mol)	Functionality
IPD, isophorone diamine	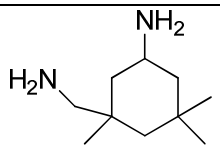	170	4
Jeffamine D230, polyetheramine	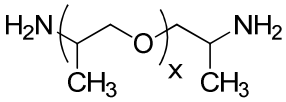	230	4
MXDA, m-xylylene diamine	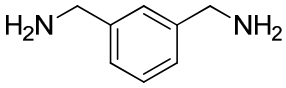	136	4
MCDEA, 4,4'-methylene bis (3-chloro-2,6-diethylaniline)	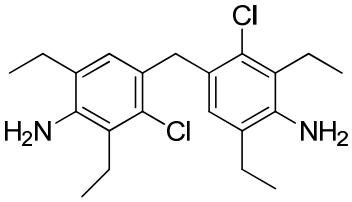	379	4
DETDA, diethyl toluene diamine	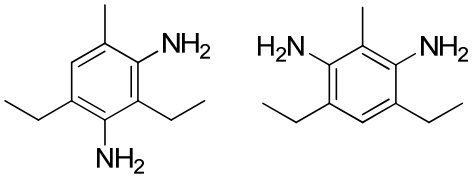 75 - 81 % 18 - 20 %	178	4
NC-540, phenalkamine	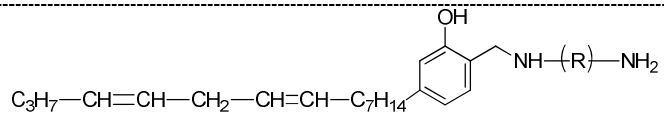	Active Hydrogen equivalent (AHEW) = 81	
TA, tannic acid	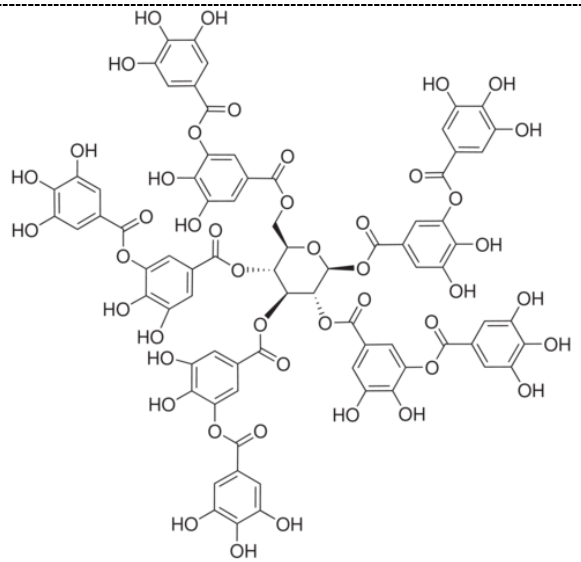	Hydroxyl value I_{OH} = 68,05 g/eOH	

Table 1. Structure of the different curing agent studied

2. Preparation of epoxy networks

To prepare the different networks, the curing agents were added to the epoxy prepolymers at stoichiometric ratio $r = n_{ah}/n_e = 1$.

Liquid amine curing agents (IPD, D230, MXDA, DETDA and NC540) and epoxy prepolymers were mixed vigorously and rapidly at room temperature, in order to form a homogenous system. MCDEA amine curing agent, solid at room temperature, was added to the epoxy prepolymer at room temperature. MCDEA was soluble in $DGEDAS_n$ epoxy prepolymer at room temperature (contrary to DGEBA).

Tannic Acid (TA) is a wood derivative that presents a lots of phenoxy groups. The reaction of epoxy prepolymer with TA is described by the epoxy-phenoxy mechanism represented in Scheme 1.

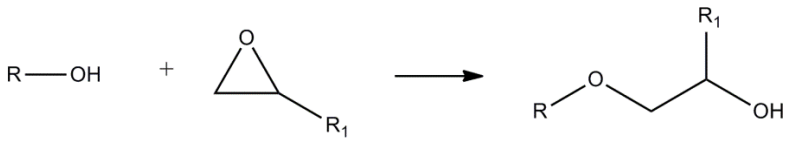

Scheme 1. Epoxy-phenoxy mechanism (with R-OH: phenoxy groups)

TA was tested as a curing agent for SPGE epoxy prepolymer. TA is solid at room temperature and was not soluble in SPGE at room temperature and even after a heating of the reactive mixture at 80°C. We decided to solubilize the TA in a low viscosity reactive bio-based diol in order to obtain reactive liquid mixture. Therefore, TA curing agent was previously solubilized in 1,3-Propane-diol (PDO, Figure 1) (1:1 by weight). The TA/PDO blend was then used as curing agent in combination with SPGE epoxy prepolymer in a stoichiometric ratio $n_{OH}/n_e = 1$ (taking hydroxyl value of PDO into account for n_{OH} calculation). As a remark, the reactive mixture was homogenous (no phase separation or precipitation is observed).

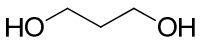

Figure 1. Structure of 1,3-Propane-diol PDO

III. Characterization of bio-based epoxy systems with various curing agents

1. Reactivity of the different systems

a) Bio-based systems with conventional curing agents

DSC calorimetry study was performed on the systems obtained with bio-based epoxy prepolymers and conventional curing agents. Figure 2 and 3 show the DSC thermograms of the formulations realized with petroleum-based curing agents. Results of the DSC analyses are summarized in Table 2. As a reminder, DSC data results for DGEBA – IPD, $DGEDAS_0$ – IPD and $DGEDAS_n$ – IPD are also summarized in this table for comparison.

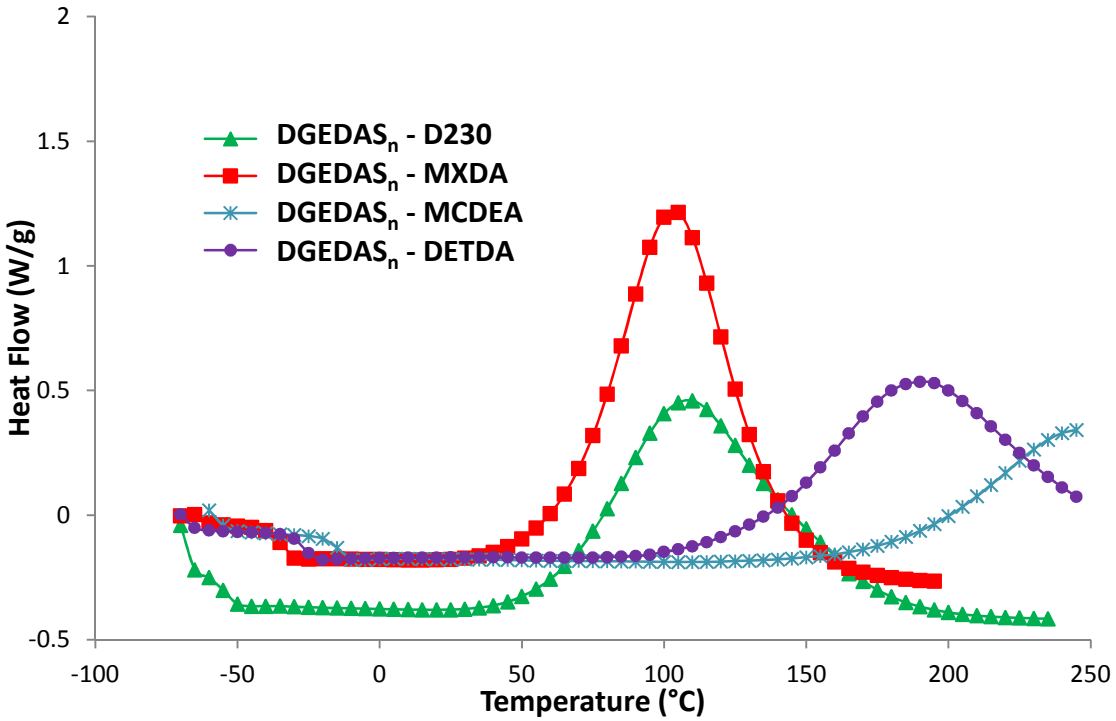

Figure 2. DSC thermograms of dynamic curing of epoxy-amine systems formulated with $DGEDAS_n$ and different curing agents

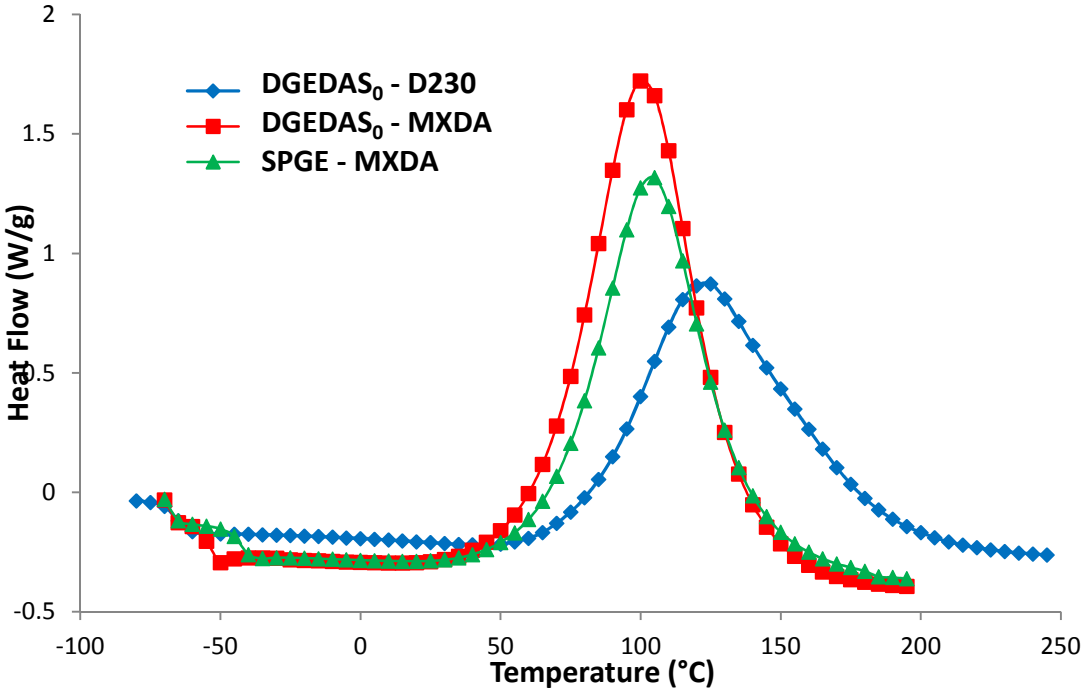

Figure 3. DSC thermograms of dynamic curing of epoxy-amine systems formulated with $DGEDAS_0$ and SPGE with different curing agents

Systems	T_{g0} (°C)	ΔH (J/g)	ΔH (kJ/ee)	T_{peak} (°C)
DGEBA – IPD	-35	415	92	114
$DGEDAS_n$ – IPD	-36	404	91	104
$DGEDAS_n$ – D230	-48	347	86	120
$DGEDAS_n$ - MXDA	-38	438	96	104
$DGEDAS_n$ – MCDEA	-19	NA	NA	>250
$DGEDAS_n$ – DETDA	-30	NA	NA	190
$DGEDAS_0$ – IPD	-60	547	89	108
$DGEDAS_0$ – D230	-70	443	100	124
$DGEDAS_0$ – MXDA	-56	600	102	102
SPGE - IPD	-41	338	79	101
SPGE - MXDA	-47	477	108	104

Table 2. DSC results for the different epoxy-amine systems

Concerning T_{g0}, first observation is that the systems containing $DGEDAS_0$ exhibit the lower T_{g0}, up to -70°C for $DGEDAS_0$ – D230. Indeed, epoxy-amine systems with D230 as curing agent have the lowest T_{g0} because of its flexible chemical structure. On the opposite, the systems obtained with the aromatic curing agents MCDEA and DETDA have the higher values of T_{g0}. More precisely, $DGEDAS_n$ – MCDEA has a T_{g0} of -19°C higher than

$DGEDAS_n$ – DETDA T_{g0} at -30°C, this difference is due to the higher molar mass of MCDEA as compared with DETDA.

Concerning the total heat of reaction ΔH it appears that the values are all comprised between 90 and 100 kJ/ee, which are classical values for epoxy-amine systems in stoichiometric ratio; except for SPGE-based systems. Indeed, SPGE combined with IPD has a low exothermy of 79 kJ/ee whereas SPGE – MXDA has the highest ΔH value (108 kJ/ee). It appears also that the epoxy-amine systems with IPD always present the lowest values (around 90 kJ/ee) whereas systems using MXDA as curing agent are the most exothermic systems (around 100 kJ/ee).

It is known that the reactivity of amino curing agent depends on the chemical structure as follows: aliphatic > cycloaliphatic > aromatic. In addition steric hindrance reduces the reactivity of amino groups.

In our series of epoxy systems, we retrieve this trend. IPD and MXDA give the more reactive systems, followed by D230, then DETDA and MCDEA give the less reactive systems. Indeed, the peak maximum temperature T_{peak} of $DGEDAS_n$ – DETDA is 190°C and is even higher than 250°C for $DGEDAS_n$ – MCDEA. In particular MCDEA has a very low reactivity due to chlorine groups and steric hindrance. As a remark, this high value of T_{peak} explains why determination of ΔH was not done for these two systems. These systems will require high temperature curing cycle to complete crosslinking reaction.

b) Fully bio-based systems

Fully bio-based systems were studied using the commercial epoxy prepolymers DGECAR and SPGE. DGECAR was combined with the phenalkamine curing agent NC540 and SPGE was combined with NC540 and also the reactive mixture TA/PDO. Their curing behaviours were followed by DSC analyses (Figure 4); DSC results are summarized in Table 3. For comparison results of DGECAR – IPD and SPGE – IPD systems studied by DSC are also listed in this table.

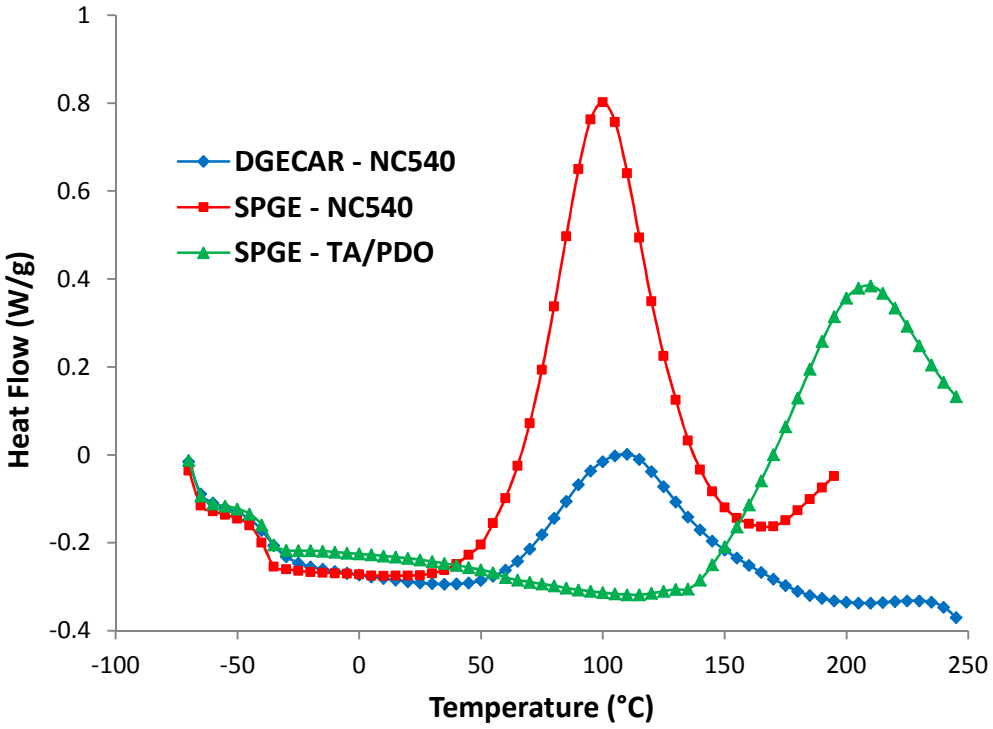

Figure 4. DSC thermograms of dynamic curing of epoxy-amine systems with bio-based curing agents

Systems	T_{g0} (°C)	ΔH (J/g)	ΔH (kJ/ee)	T_{peak} (°C)
DGECAR – IPD	-41	127	68	116
DGECAR – NC540	-44	122	71	110
SPGE – IPD	-41	127	79	101
SPGE – NC540	-43	294	81	99
SPGE – TA/PDO	-42	NA	NA	208

Table 3. DSC results for fully bio-based systems

First, not much difference is observed in the T_{g0} values (around -40°C). For instance, SPGE epoxy prepolymer combined with IPD, NC540 or the reactive mixture TA/PDO always presents a T_{g0} value around -42°C.

Besides not much difference is also observed in the total heat of reaction of SPGE-based system using either IPD or NC540 as curing agent (around 80 kJ/ee) and in the maximum peak temperature (around 100°C). The lowest exothermy of reaction is observed with DGECAR epoxy prepolymer (around 70 kJ/ee), which could perhaps indicate that the system is out of stoichiometry.

Using the reactive mixture TA/PDO as a curing agent for SPGE epoxy prepolymer, we obtained a system with a very low reactivity as compared to the others, with T_{peak} at 208°C.

This system needs a high curing temperature but has the advantage of a high stability and long pot-life at room temperature.

2. Determination of gel time

Determination of gelation times were performed on SPGE and DGECAR based systems using rheological measurements at 80°C. Results are summarized in Table 4 with values of relaxation component Δ.

As a remark, SPGE – MXDA gel time at 80°C was around 3 min and is too short for a correct determination of Δ exponent. Same observation was done for SPGE – NC540 with a gel time at 80°C around 1.5 min. The use of NC540 as curing agent leads to a decrease in gel time which could be explained by the different functionality (f_a) of this amine as compared with the other curing agents. Indeed, gel time at 80°C is 4.5 min for DGECAR – NC540 while it was 19 min for DGECAR – IPD.

Systems	f_a	t_{gel} (min)	$tan\delta_{gel}$	Δ
SPGE – IPD	4	5	0.5	0.29
SPGE – MXDA	4	3	NA	NA
SPGE – NC540	3 + 1 OH	1.5	NA	NA
DGECAR – IPD	4	19	1.7	0.66
DGECAR – NC540	3 + 1 OH	4.5	1.8	0.68

Table 4. Gel time data for the different reactive systems at 80°C with f_a: functionality of the amine

3. Determination of glass transition temperatures

The curing behaviour study was helpful for the choice of a correct curing cycle temperature for the fully bio-based systems that contains uncommon curing agents such as NC540, TA/PDO. Systems using NC540 as curing agent were crosslinked in an oven for 1h at 80°C and 2 h at 180°C. SPGE – TA/PDO system was cured 2 h at a high temperature (180°C) as the system exhibits a high T_{peak} (208°C). The other curing agents are conventional ones and we chose the curing cycle suitable as summarized in Table 5. All the reactive systems were crosslinked and their glass transitions temperature were determined in the second run of DSC analyses to check if complete crosslinking was reached. Curing cycle and T_g values for all the networks studied are summarized in Table 5.

Results show that the DGEBA – IPD network has the highest glass transition temperature at 150°C. Interesting result was also found for the $DGEDAS_n$ – MCDEA network with a T_g at 120°C. Yet this system requires a long curing cycle: 10 h at 170°C. Higher glass transition temperature was observed in the literature for DGEBA - MCDEA network (T_g = 177°C [4]). $DGEDAS_n$ – DETDA network exhibit a lower T_g (T_g = 112°C) than DGEBA – DETDA (T_g = 175°C found in literature [5]). Among all the classical curing agents used, the D230 curing agent leads to networks with the lowest T_g, 48°C for $DGEDAS_n$ – D230 and 52°C for $DGEDAS_0$ – D230. These low values of T_g can be attributed to the aliphatic structure of D230 that brings flexibility to the network. Yet, DGEBA crosslinked with D230 exhibit higher value (T_g = 80°C according to literature [6]) than the DGEDAS-based networks with the same curing agent. Again, lower T_g values were obtained for $DGEDAS_n$ and $DGEDAS_0$ crosslinked with MXDA (T_g = 74 and 79°C respectively) than for conventional network DGEBA – MXDA (T_g = 120°C according to Williams et al. [7]).

Systems	Curing cycles	T_g (°C)
DGEBA – IPD	1 h at 80°C + 2 h at 180°C	150
$DGEDAS_n$ – IPD	1 h at 80°C + 2 h at 180°C	91
$DGEDAS_n$ – D230	2 h at 80°C + 2 h at 180°C	48
$DGEDAS_n$ – MXDA	1 h at 80°C + 2 h at 160°C	74
$DGEDAS_n$ – MCDEA	10 h at 170°C	120
$DGEDAS_n$ – DETDA	2 h at 180°C	112
$DGEDAS_0$ – IPD	1 h at 80°C + 2 h at 180°C	102
$DGEDAS_0$ – D230	2 h at 80°C + 2 h at 180°C	52
$DGEDAS_0$ – MXDA	1 h at 80°C + 2 h at 160°C	79
SPGE – IPD	1h at 80°C + 2 h at 180°C	100
SPGE – MXDA	1h at 80°C + 2 h at 160°C	67
SPGE – NC540	1h at 80°C + 2 h at 180°C	76
SPGE – TA/PDO	2 h at 180°C	41
DGECAR – IPD	1 h at 80°C + 2 h at 180°C	22
DGECAR – NC540	1h at 80°C + 2h at 180°C	33

Table 5. Glass transition temperature values determined by DSC analyses

Glass transition temperatures for the different networks studied can be classified for each epoxy prepolymer as followed:

- $DGEDAS_n$ – D230 < $DGEDAS_n$ – MXDA < $DGEDAS_n$ – IPD < $DGEDAS_n$ – DETDA < $DGEDAS_n$ – MCDEA
- $DGEDAS_0$ – D230 < $DGEDAS_0$ – MXDA < $DGEDAS_0$ – IPD
- SPGE – MXDA < SPGE – IPD

IPD curing agent leads to networks with higher T_g than the one obtained using MXDA and then D230.

Another observation is that regardless of the crosslinking agent used, the $DGEDAS_n$ – based networks always present T_g lower than the ones of $DGEDAS_0$ – based networks.

Concerning the fully bio-based networks, very low T_g were obtained for DGECAR – based networks. DGECAR – NC540 presents a T_g of 33°C; which is a higher value than DGECAR – IPD glass transition temperatures of 22°C. On the contrary, SPGE – IPD's T_g is higher than the one of SPGE – NC540 network, respectively 100°C and 76°C.

As a remark, Shibata et al [3] prepared a network based on another epoxy prepolymer derived from sorbitol (Denacol 614B) with TA. TA and sorbitol-based epoxy prepolymer were solubilized in water, freeze-dried and cured for 2 h at 180°C; resulting network presents a T_g of 84°C. The lower value obtained in our case can be attributed to the use of PDO to solubilize the TA as PDO is a short and aliphatic diol and brings flexibility to the network.

4. Thermo-mechanical properties of the networks

Thermo-mechanical properties of SPGE – MXDA, SPGE – NC540 and DGECAR – NC540 networks synthesized in stoichiometric ratio were determined by DMA. The tanδ and storage modulus evolution with temperature are represented in Figure 5 and Figure 6 respectively.

Values of T_β, T_α and G' are reported in Table 6 with calculated values of M_c and ν.

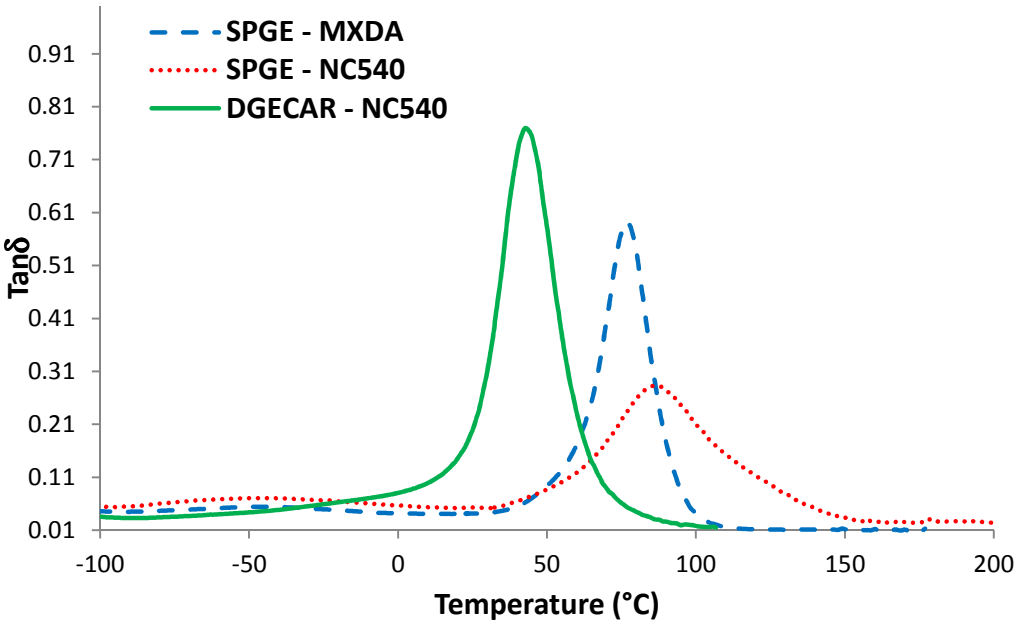

Figure 5. Tanδ versus temperature for SPGE – MXDA, SPGE – NC540 and DGECAR – NC540 networks

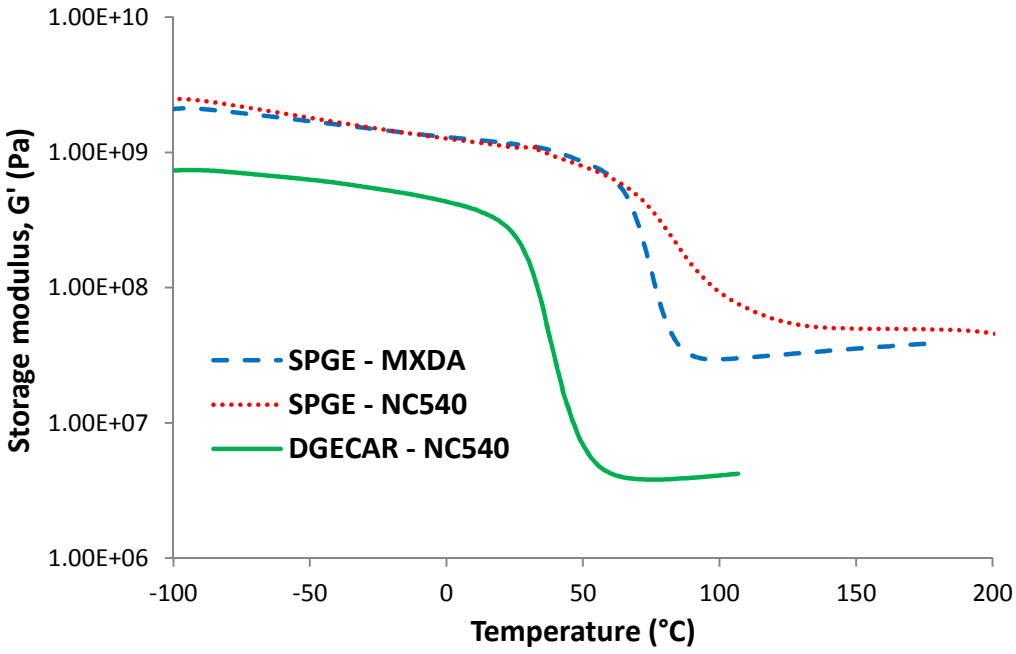

Figure 6. Storage modulus versus temperature for SPGE – MXDA, SPGE – NC540 and DGECAR – NC540 networks

It appears that the different values of T_α measured by DMA follow logically the same trend as the values measured by DSC. Indeed, the DGECAR – NC540 network exhibits the lowest glass transition temperature value (T_α = 43°C), even lower than the T_α measured for DGECAR – IPD system (T_α = 50°C). The highest T_α is obtained for SPGE – NC540 network (T_α = 85°C) closed to the T_α of SPGE – MXDA network (T_α = 77°C).

Besides, an important observation is that the α-transition of SPGE – NC540 is the largest, which implies that a less homogenous network is obtained for SPGE – NC540.

Indeed, ΔT for SPGE – NC540 transition is 48°C whereas it was 35°C for SPGE – IPD one and 20°C for SPGE – MXDA.

Concerning the rubbery modulus, the lowest value is obtained for DGECAR – NC540 network (3.8 MPa); this rubbery modulus is closed to the one obtained for DGECAR – IPD network (3.2 MPa, Chapter II). These low rubbery moduli are due to the DGECAR long chain flexibility.

Another point is the low value of modulus in the glassy state (0.7 GPa at -100°C) as compared with classical epoxy-amine network (around 2 GPa).

The higher value of crosslinking density is obtained for SPGE – NC540; more than twice the value obtained for SPGE – IPD. Crosslinking point of different nature may be at the origin of the low value of molar mass between crosslinking and the heterogeneity of the network. This could also be explained by the influence of the high chlorine content of SPGE epoxy prepolymer as underlined in Chapter III. The higher molar mass between crosslinking is obtained for DGECAR – based network using either IPD or NC540 as curing agent.

Networks	T_β (°C)	T_α (°C)	tanδ max	ΔT (°C)	G' (MPa) (at T_α+30°C)	d (g/cm^3)	ν (10^{-3} mol/cm^3)	M_c (g/mol)
SPGE – IPD	-52	120	0.41	35	29.3	1.24	8.3	150
SPGE – MXDA	-44	77	0.59	20	30.1	1.31	9.5	137
SPGE – NC540	-45	85	0.28	48	63.5	1.25	19.7	63
DGECAR – IPD	NA	50	1.21	20	3.2	1.06	1.1	970
DGECAR – NC540	NA	43	0.77	23	3.8	1.07	1.3	810

Table 6. Thermo-mechanical properties of SPGE – MXDA, SPGE – NC540 and DGECAR – NC540 networks

IV.Conclusion of Part I

In this part of our study, various formulations were characterized using the epoxy prepolymers previously studied (SPGE, $DGEDAS_0$, $DGEDAS_n$ and DGECAR) combined with different curing agent either petroleum based ones or bio-based ones such as NC540 and TA/PDO.

Different reactivity and glass transition range were obtained by changing the curing agent. Nevertheless, higher T_g is always obtained using DGEBA as epoxy prepolymer.

Interesting formulations are obtained using SPGE as epoxy prepolymer as it has the advantage of been commercially available contrary to the present position of DGEDAS epoxy prepolymers.

Concerning the choice of a curing agent, TA/PDO brings flexibility to the network because of the use of PDO for solubilisation of TA. Further investigations should be performed either on the direct solubilisation of TA in epoxy prepolymer or the choice of another reactive diol for TA solubilisation. The phenalkamine NC540 is also of interest, as it can be used to enhance the system reactivity even at moderate temperature.

Finally, SPGE – MXDA and SPGE – IPD are interesting systems, still investigations should be performed for complete understanding of SPGE reaction mechanism.

Part II. Synthesis of epoxy networks by dual crosslinking reactions

I. Introduction

In the previous chapters we studied the replacement of DGEBA by bio-based epoxy prepolymers derived from isosorbide, sorbitol and cardanol. IPD was mainly used because it is a conventional curing agent widely used for the preparation of epoxy-amine networks. Therefore, it was very useful for a first investigation on the influence of bio-based epoxy prepolymer structure on network properties.

Nevertheless, the main goal of the NAFI project was to develop a bio-based epoxy composite material for the production of ski boards. A bio-based epoxy prepolymer should replace the classical DGEBA while linen fibres were supposed to replace glass fibres. This last topic was investigated by our colleagues at CERMAV, Chomarat and Rossignol. On our side we focused on the organic matrix. The industrial constraints for a high productivity imposed to have short curing cycle under press (10 min at 110°C), but also long pot-life of the reactive formulation (90 min at 25°C). These two characteristics are a priori antagonist. This is why a very specific curing agent was formulated by Huntsman, and is currently used for the manufacturing of ski boards in association to DGEBA. This epoxy-amine system has the

double function of leading to a high performance structural material and of bonding this laminate material to the other components of the ski boards.

In this part of the chapter, the industrial formulation will be characterized and we will explain the particularity of the curing agent used. Then, the classical DGEBA will be replaced by the isosorbide-based epoxy prepolymers presented in the previous chapters.

II. Experimental section

1. Materials

In this part of our study we focused on the specially formulated epoxy-amine system used by Rossignol, composed of DGEBA epoxy prepolymer (Araldite 5085) and an amine curing agent formulated by Huntsman, Aradur 1019 called HA[1] in this study.

The epoxy prepolymers used in this study, DGEBA, $DGEDAS_0$, and $DGEDAS_n$, have been previously described. The HA curing agent has been supplied by Huntsman Advance Materials (Basel, Switzerland). According to the MSDS datasheet, HA is a liquid curing agent mainly composed by two aliphatic amines; its composition is presented in Table 7. It is important to notice that both HA1 and HA2 have a tertiary amine.

Name	wt %	Structure	Molar mass (g/mol)	functionality
HA1: N(3-dimethylaminopropyl)-1,3-propylenediamine	30	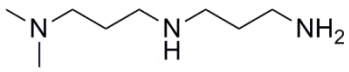	$M_{a1} = 159$	$f_{a1} = 3$
HA2: 3-[[3-(dimethylamino)propyl]-amino]propiononitrile	70	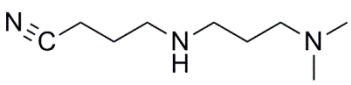	$M_{a2} = 155$	$f_{a2} = 1$

Table 7. Composition of HA curing agent

[1] HA acronym stands for Huntsman Amine

2. Network synthesis

a) Determination of the stoichiometric ratio r = n_{ah}/n_e for the epoxy-amine reference system

The epoxy-amine reference formulation is 100 phr of DGEBA combined with 15 phr of HA. Knowing the proportion of epoxy prepolymer and amine in the reference system, together with HA composition, it is possible to calculate the stoichiometric ratio r = n_{ah}/n_e with the following equation:

$$r = \frac{n_{ah}}{n_e} = \frac{f_{a1}\times\frac{m_{a1}}{M_{a1}} + f_{a2}\times\frac{m_{a2}}{M_{a2}}}{\frac{m_e}{EEW}} = \frac{3\times\frac{4.5}{159}+\frac{10.5}{155}}{\frac{100}{180}} = 0.27 \qquad \text{(Equation 1)}$$

Where: m_{a1}, m_{a2} and m_e: mass of HA for the two amines and mass of DGEBA

f_{a1} and f_{a2}: functionality of the two different amines

M_{a1} and M_{a2}: amines molar masses

EEW: DGEBA equivalent weight

The ratio r is less than 1, which means that this system is formulated with a large epoxy excess.

b) Formulations studied

The formulations used in this study were based on the three different epoxy prepolymers DGEBA, $DGEDAS_0$ and $DGEDAS_n$ cured with HA. To prepare the networks, the amine curing agent was added to the epoxy with the stoichiometric ratio of r = 0.27, in order to have a good comparison between the DGEBA – HA system and the two bio-based ones obtained by replacing DGEBA by $DGEDAS_0$ and $DGEDAS_n$ respectively. The reactive liquid mixture was mixed vigorously at room temperature and cured in PTFE coated moulds for 1 h at 80°C. Table 8 recapitulates the composition of the different systems studied:

Epoxy-amine system	$r = n_{ah}/n_e$	Epoxy proportion	Amine proportion
DGEBA – HA	0.27	100 phr	15 phr
$DGEDAS_0$ – HA	0.27	100 phr	29.7 phr
$DGEDAS_n$ – HA	0.27	100 phr	15 phr

Table 8. Compositions of the different formulations studied

III. Results and discussions

1. Epoxy-amine reaction mechanism; special case of HA curing agent

As described in the first chapter[2], between a primary amine and an epoxy group, the addition mechanism is the more important. Nevertheless under specific conditions other reactions may occur such as etherification or homopolymerization. Etherification mechanism is unlikely to occur for temperatures lower than 150°C and without the use of catalyst. Etherification, which represent the first step of homopolymerization mechanism, is promoted by an excess of epoxy [8] or when all amino hydrogen have been consumed [9]. Homopolymerization is also promoted by the presence of a catalyst such as tertiary amine [10].

Tertiary amines could therefore act as catalyst and can accelerate the polyaddition reactions, promote the reaction between the hydroxyl groups and the epoxy groups and also the epoxy groups homopolymerization reaction [10].

The curing agent, HA, considered in this study presents a specific structure with the presence of tertiary amines that may act as catalyst for reaction such as homopolymerization which will compete with the classical epoxy-amine addition reaction. Besides, the epoxy-amine system, DGEBA – HA, is formulated with an excess of epoxy (r = 0.27). Dual polymerization may be observed with a competition between classical epoxy-amine addition (at low temperature) and homopolymerization of epoxy cycle at higher temperature [11].

First, in order to focus on the influence of homopolymerization, systems obtained using only tertiary amines as catalysts were studied. Then, reactivity of the HA-based systems

[2] See Chapter I, Epoxy-amine reaction mechanism

were studied by DSC and gel time measurements. The evolution of the epoxy conversion were measured by infrared spectroscopy. Finally, the glass transition temperatures were evaluated by dynamic mechanical analyses.

2. Tertiary amines used as curing agent

Galante et al. [10] have studied the influence of homopolymerization by using tertiary amines, benzyldimethylamine (BDMA, 0.06 mol/epoxy equivalent), in the 80°C – 140°C temperature range. They noticed that an increase in the polymerization temperature produced an increase in the macroscopic gel conversion and a decrease in the glass transition temperature of regions of high crosslink density. This was ascribed to the increase in the ratio of intramolecular chain transfer over propagation rates, leading to shorter primary chains. Particular evolution of T_g with the curing temperature was observed: higher T_g obtained for networks crosslinked at lower temperature (Figure 7).

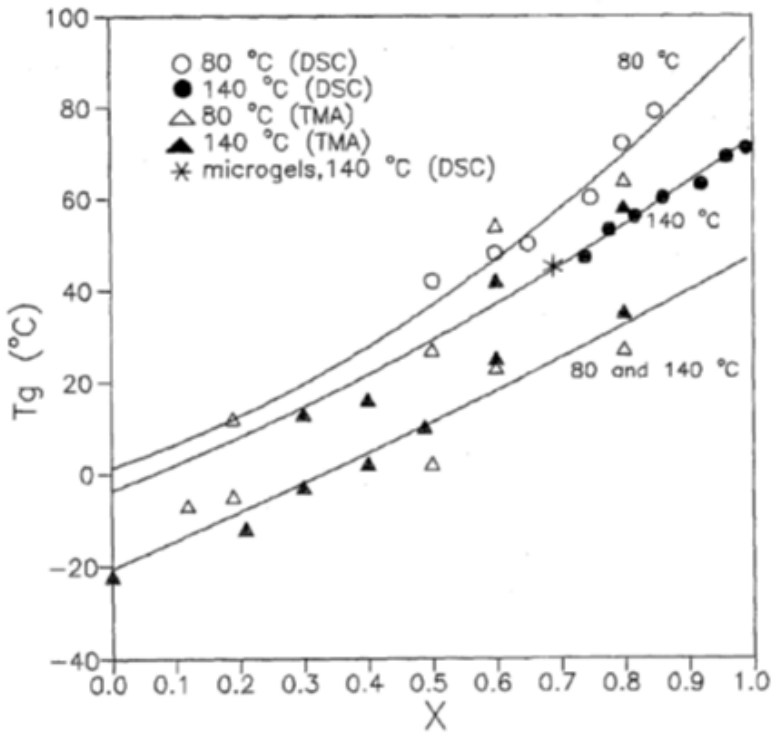

Figure 7. Evolution of both Tg's as a function of conversion for specimens cured at 80°C and 140°C. Results from DSC and TMA techniques are plotted [10]

In order to focus only on the influence of homopolymerization initiated by tertiary amine in HA curing agent, the same study as Galante was performed. Epoxy prepolymers (DGEBA, $DGEDAS_0$ and $DGEDAS_n$) were combined with tertiary amine BDMA (Table 9)

with the same proportion as in Galante's study (BDMA 0.06 mol/epoxy eq.). Another tertiary amine, Dimethylbutylamine (DMBA), was tested as its structure is closed to the HA tertiary amine structure (see Table 7). The crosslinking was carried out at temperatures comprised in the range 80°C to 140°C.

Name	Structure	Molar mass (g/mol)
BDMA : N,N - Dimethylbenzylamine	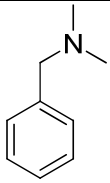	135
DMBA : N,N - Dimethylbutylamine	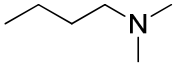	101

Table 9. Description of tertiary amines used

a) Study of reactivity by DSC

Figure 8 shows the non-isothermal DSC thermograms of the different epoxy prepolymers (DGEBA, $DGEDAS_0$, $DGEDAS_n$) reacted using BDMA as catalyst. The glass transition temperatures of the systems before reaction, T_{g0}, the peak maximum temperatures, T_{peak}, and the total heat of reaction (ΔH) obtained from the DSC analyses are summarized in Table 10. It appears that T_{g0} shows the same trend as in IPD-based systems.

An important observation concerning the calorimetry study of these three systems is that DGEBA – BDMA and $DGEDAS_0$ – BDMA exhibit very low total heat of reaction as compared with $DGEDAS_n$ – BDMA. Indeed, the –OH groups present in $DGEDAS_n$ oligomers may catalyze the homopolymerization initiated by BDMA tertiary amines.

Besides, the cure reaction of $DGEDAS_0$ – BDMA system exhibits two very distinct exothermic peaks at 112°C and 194°C with enthalpy of reaction equal to 28 J/g and 20 J/g. The second exothermy observed for $DGEDAS_0$ – BDMA may be attributed to side reaction. The origin of this second exotherm peak has not been studied more deeply in the frame of this work.

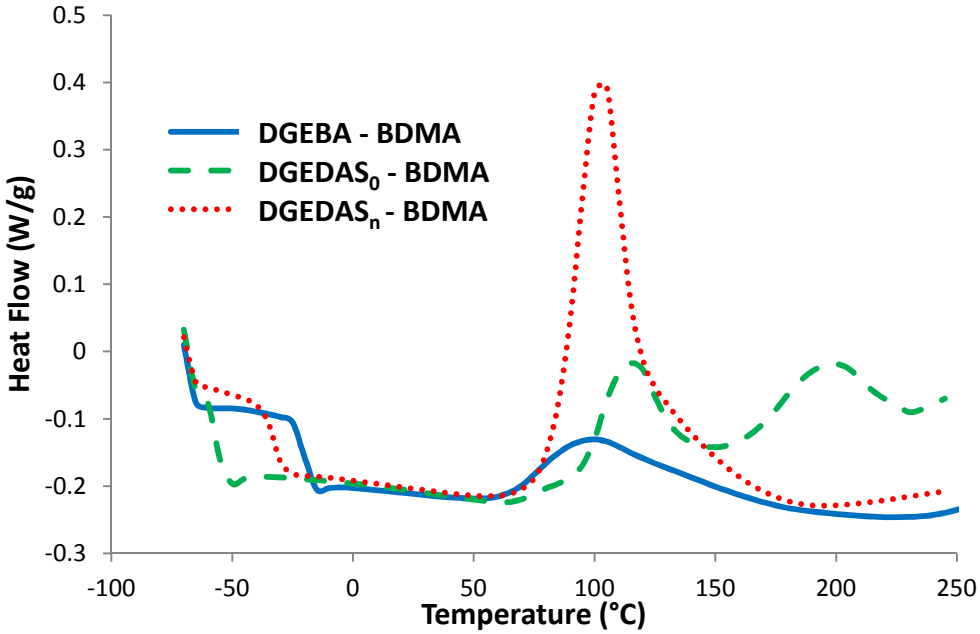

Figure 8. DSC thermograms for the epoxy-BDMA systems

Systems	T_{g0} (°C)	ΔH (J/g)	T_{peak} (°C)
DGEBA – BDMA	-22	40	102
$DGEDAS_0$ – BDMA	-57	28– 20	112 - 194
$DGEDAS_n$ – BDMA	-37	120	104

Table 10. DSC results for DGEBA, $DGEDAS_0$ and $DGEDAS_n$ cured with BDMA tertiary amine curing agent.

Regarding the very low value of ΔH of reaction obtained for DGEBA and $DGEDAS_0$ epoxy prepolymers combined with BDMA, focus was put on $DGEDAS_n$ to study the influence of tertiary amine used as independent curing agent.

Following figure compares the DSC calorimetry study of the two systems $DGEDAS_n$ – BDMA and $DGEDAS_n$ – DMBA. Results of the DSC study are summarized in Table 11.

First, the tertiary amine used does not have an influence on the T_{g0} value of the systems. Indeed, the proportion of curing agent is too low (0.06 mol/eq) to have an influence on T_{g0}. Concerning the total heat of reaction, it appears that $DGEDAS_n$ – DMBA has an higher value: more than twice the value obtained for $DGEDAS_n$ – BDMA system. $DGEDAS_n$ – DMBA is slightly more reactive than $DGEDAS_n$ – BDMA with a lower value of T_{peak}.

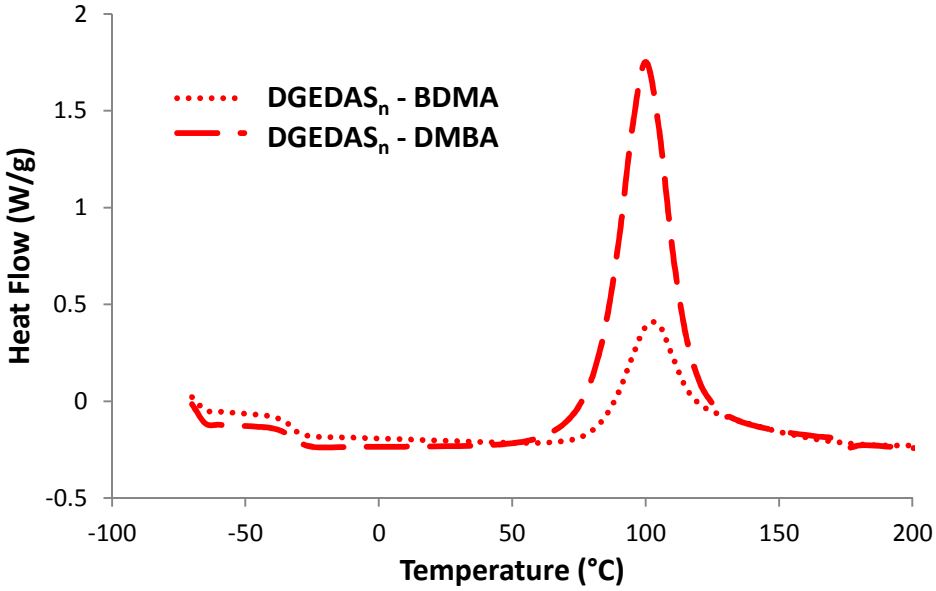

Figure 9. DSC thermograms for the DGEDAS$_n$ – tertiary amines systems

Systems	T_{g0} (°C)	ΔH (J/g)	T_{peak} (°C)
DGEDAS$_n$ – BDMA	-37	120	104
DGEDAS$_n$ – DMBA	-37	280	100

Table 11. DSC results for DGEDAS$_n$ cured with BDMA and DMBA tertiary amine curing agents

b) Glass transition temperatures for epoxy networks obtained using tertiary amines

The DGEDAS$_n$ – BDMA and DGEDAS$_n$ – DMBA systems were crosslinked in an oven at 80°C and 140°C. After 2 h, a network was obtained for the two systems considered. The glass transition temperatures of the two systems cured at different temperatures were determined by DSC. Values of T_g are summarized in Table 12. T_g values were measured at the second run.

Systems	Curing cycles	T_g (°C) (DSC)
DGEDAS$_n$ – BDMA	2 h at 80°C	68
	2 h at 140°C	40
DGEDAS$_n$ – DMBA	2 h at 80°C *	76
	2 h at 140°C	66

Table 12. T_g of DGEDAS$_n$ – BDMA and DGEDAS$_n$ – DMBA networks crosslinked at various temperatures
* residual heat of reaction at 1st scan

For $DGEDAS_n$ – BDMA networks there is few difference between the T_g measured during the first and second DSC run. Nevertheless, for $DGEDAS_n$ – DMBA network obtained after 2 h at 80°C, the first run in DSC (between -70°C to 250°C) exhibit a small exothermic phenomenon. Indeed, T_{peak} of this exotherm corresponds to the peak maximum temperature observed during the DSC calorimetry study of $DGEDAS_n$ – DMBA system (Figure 10). Therefore, this exotherm represents a residual ΔH of reaction.

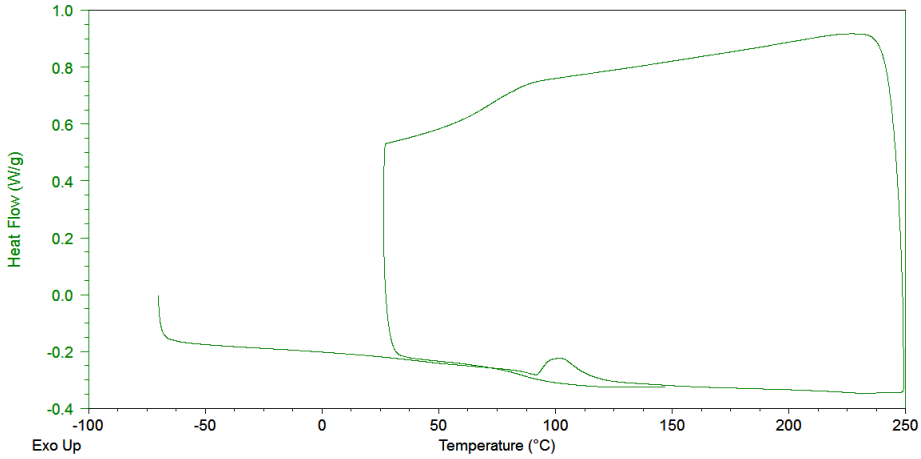

Figure 10. DSC curing study: first and second DSC runs for DGEDASn – DMBA (2h at 80°C)

T_g of networks obtained at lower temperature are higher than the T_g of networks obtained at higher temperature. This phenomenon is more visible for $DGEDAS_n$ – BDMA system than $DGEDAS_n$ – DMBA with an important difference: 28°C for $DGEDAS_n$ – BDMA and 10°C for $DGEDAS_n$ – DMBA.

Yet, as described by Galante study [10], higher T_g are observed for networks obtained at lower temperature for epoxy networks crosslinked using tertiary amine as curing agent.

Contrary to classical epoxy-amine systems, the structure of networks obtained through homopolymerization reactions is dependent upon the temperature of curing.

3. Study of the reactivity of HA – based systems

After a first study of the influence of homopolymerization using only tertiary amines, the dual polymerization induced by HA curing agent was investigated.

a) DSC calorimetry study

Figure 11 shows the DSC thermograms of the three different epoxy prepolymers combined with HA. The glass transition temperatures T_{g0} before reaction, the peak maximum temperatures (T_{peak}) and the total heat of reaction (ΔH) obtained from these analyses are summarized in Table 13.

T_{g0} is the lowest for the system $DGEDAS_0$ – HA, around -60°C, whereas the other systems exhibit T_{g0} at -40°C. This low value of T_{g0}, was also observed for $DGEDAS_0$ – IPD system, and can be explained by the lower molar mass of $DGEDAS_0$ prepolymer as compared to the others.

The two systems DGEBA – HA and $DGEDAS_0$ – HA have almost the same peak maximum temperatures, around 120°C, whereas T_{peak} is lower for $DGEDAS_n$ – HA (T_{peak} = 98°C) and in the same range as $DGEDAS_n$ – DMBA (Table 11). Moreover, the shape of the exothermic peak is different; it is less broad than the two others. This high reactivity is explained by the chemical structure of $DGEDAS_n$ with numerous oligomers bearing –OH groups which are known to catalyse the epoxy-amine reaction.

The exothermic peak of the $DGEDAS_0$ – HA system shows a shoulder on the low temperature side while the one of DGEBA – HA system is broader and shows a “classical shape”.

Concerning the total heat of the reaction, it appears that the DGEBA – HA system presents the highest exothermy (around 430 J/g) whereas the two other systems exhibit lower ΔH (318 J/g and 307 J/g for $DGEDAS_0$ – HA and $DGEDAS_n$ – HA respectively).

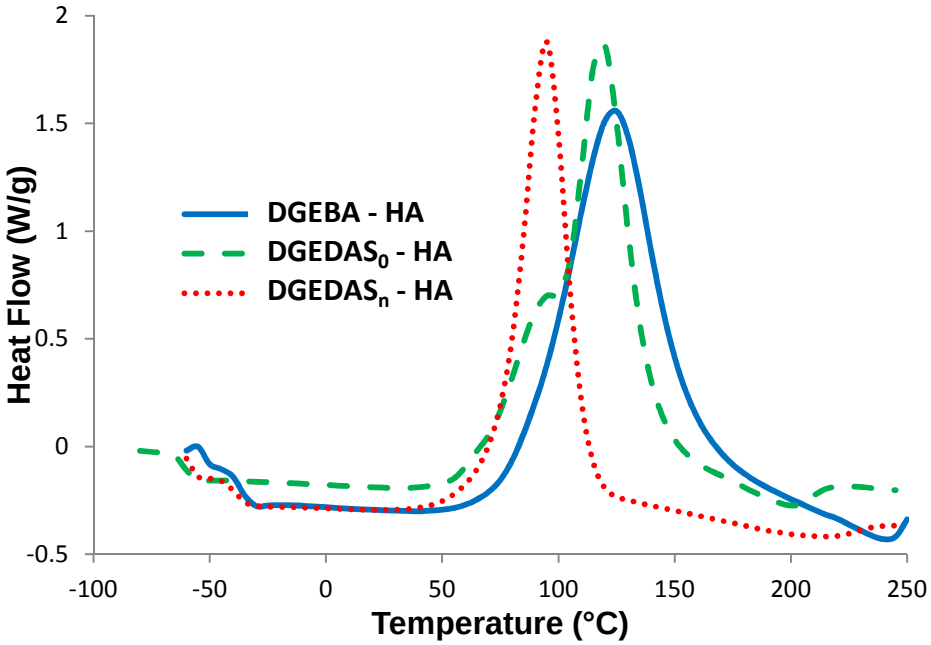

Figure 11. DSC thermograms of dynamic curing of DGEBA, $DGEDAS_0$ and $DGEDAS_n$ with HA (heating rate 10°C/min), r=1

Systems	T_{g0} (°C)	ΔH (J/g)	T_{peak} (°C)
DGEBA – HA	-40°C	430	125
$DGEDAS_0$ – HA	-60°C	318	98 / 120
$DGEDAS_n$ – HA	-40°C	307	98

Table 13. DSC results for DGEBA – HA, $DGEDAS_0$ – HA and $DGEDAS_n$ – HA

b) Study of gelation

Gel times were determined by rheological measurements at different temperatures, for the three reactive systems considered.

The limiting factor in this study was the choice of the temperature range. Indeed, for high crosslinking temperature, the gelation times are too short and the measurements are little reliable because of the time needed to reach a thermal equilibrium. Beside for low cure temperature, vitrification may perturb the gelation time determination. Therefore the study of variation of gelation times with temperatures were performed for DGEBA – HA and $DGEDAS_0$ – HA in the temperature range of 60°C – 80°C.

As an example, Figure 12 shows the evolution of the loss factor tanδ as a function of time, in a multifrequency mode (from 1 rad/s to 100 rad/s) for the system of reference DGEBA – HA, at 60°C.

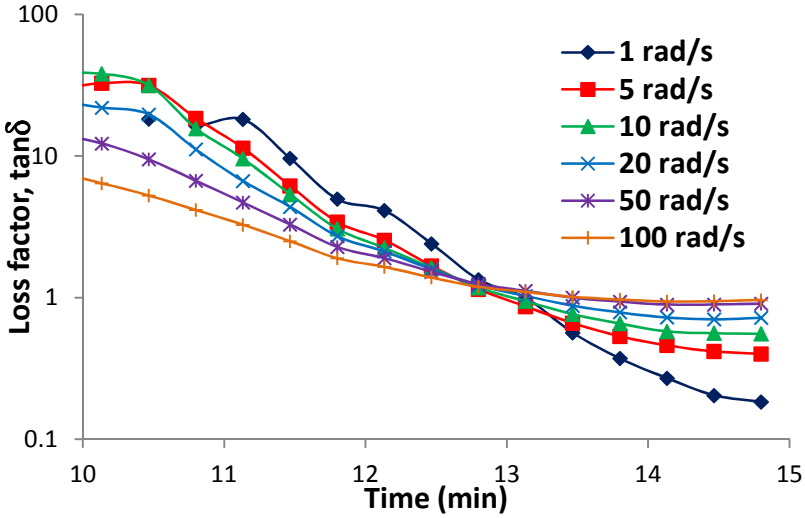

Figure 12. Loss factor tanδ, isotherm at 60°C, example of DGEBA – HA

The gel time, t_{gel}, is determined by the crossover of the loss factor curves at various frequencies. The gel times for the three different systems, the value of tanδ at gel point and the relaxation component Δ are summarized in Table 14 for various temperatures.

In all cases, short gel times were observed. For the $DGEDAS_n$ – HA system the gelation time is too short (around 9 minutes at 60°C) to allow a correct determination of gel time for higher temperatures.

This low value of gel time for $DGEDAS_n$ – HA may be explained by the catalysis effect of –OH groups present in the oligomer structures. The other system based on isosorbide epoxy prepolymer, $DGEDAS_0$ – HA has the higher value of gel time for each temperature of crosslinking considered. This observation is different of the one done on $DGEDAS_0$ – IPD and DGEBA – IPD systems that exhibit almost equivalent gel times at 80°C.

Concerning the relaxation component Δ the values obtained are around 0.6, these values are slightly lower than data on diepoxy-amine systems, where Δ was around 0.7 [12]. Exception should be done for the high temperature measures (at 80°C: Δ equal to 0.53 for DGEBA – HA and 0.40 for $DGEDAS_0$ – HA) where the gel time is short and determination of Δ is less reliable.

Systems	T of measure (°C)	t_{gel} (min)	$tan\delta_{gel}$	Δ
DGEBA – HA	60	12.8	1.2	0.56
	70	7.4	1.4	0.61
	80	4.9	1.1	0.53
$DGEDAS_0$ – HA	60	27.1	1.5	0.63
	70	12.5	1.3	0.58
	80	7.6	0.7	0.40
$DGEDAS_n$ – HA	60	9.5	1.3	0.58

Table 14. Gel time data for the reactive systems DGEBA – HA, $DGEDAS_0$ – HA and $DGEDAS_n$ – HA

c) Determination of activation energy

We check if the gel times obey an Arrhenius law as a function of a temperature by plotting $lnt_{gel} = f(1/T)$ (Figure 13). It appears that activation energy could be determined. It was not straight forward; as we showed previously that homopolymerization depend on curing temperature. Activation energy E_a of 47 kJ/mol was found for DGEBA – HA system and of 62 kJ/mol for $DGEDAS_0$ – HA. The E_a value obtained for $DGEDAS_0$ – HA is closed to the one obtained for classical epoxy-amine systems (around 60 kJ/mol [13, 14]). In contrast the value obtained for DGEBA – HA is low. However, complex and competitive mechanisms occur in the systems based on HA. The amount of homopolymerization versus epoxy-amine addition is dependent on temperature and epoxy monomer structure. For a comparison, an activation energy of 63 kJ/mol was found in the literature for the epoxy-amine system DGEBA – IPD [15].

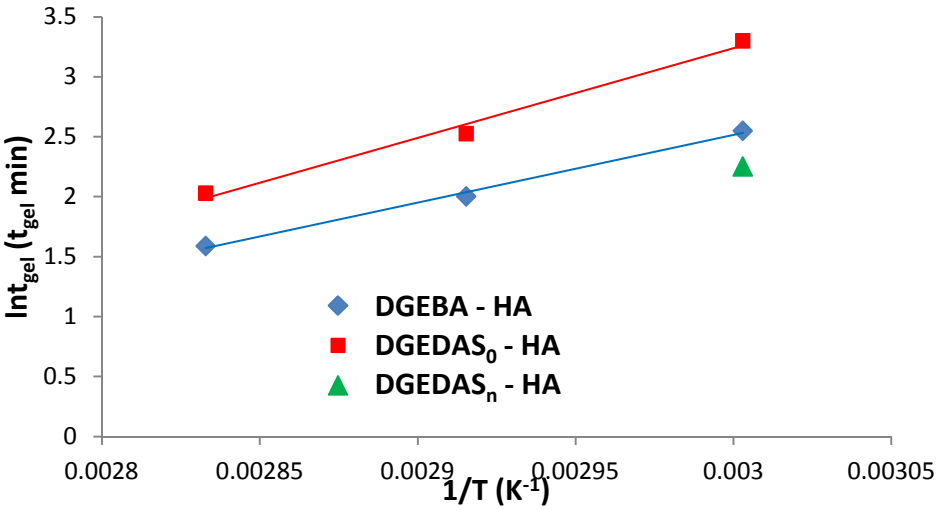

Figure 13. Arrhenius plot of the gelation phenomena for DGEBA – HA and $DGEDAS_0$ – HA

d) Reaction kinetic followed by IR

Infrared spectroscopy was used to follow the epoxy-amine crosslinking reaction. The epoxide groups' reduction has been monitored in real time during the samples heating at different temperatures. In order to estimate the conversion degree, α, of epoxide groups with respect to their initial concentration, the following relationship has been applied:

$$\alpha = \frac{C_0 - C_t}{C_0} = 1 - \frac{C_t}{C_0}$$

Where C represents the concentration of epoxide groups and the subscripts *0* and *t* denote, the initial and the generic reaction time t, respectively. According to the Lambert-Beer law, the relation between the conversion degree and the absorbance A (at 916 cm^{-1} for the epoxide group) can be obtained. Furthermore, because of the reduction of film thickness during the curing cycle, a correction of the absorbance area has to be done. To this end, the area corresponding to the absorbance of epoxide group must be normalized by using the area of an internal reference. To this end, the stretching of aromatic groups at 1509 cm^{-1} was used, so that the epoxide conversion degree could be assessed according to the following relationship:

$$\alpha = \frac{\overline{A}_0^{916} - \overline{A}_t^{916}}{\overline{A}_0^{916}} \qquad \text{where} \qquad \overline{A}^{916} = \frac{A^{916}}{A^{1509}}$$

This FT-IR study of reaction kinetic was only performed on DGEBA – HA because of the difficulty to find for $DGEDAS_0$ – HA and $DGEDAS_n$ – HA systems an internal reference such as aromatic groups present in DGEBA – HA system.

Figure 14 shows some of the FT-IR spectra of DGEBA – HA during the cure at 80°C as an example. The arrow indicates the time evolution of the spectra. Using the previous equations, the evolution of the conversion degree of epoxide groups was obtained at different temperature and the resulting trend is shown in Figure 15.

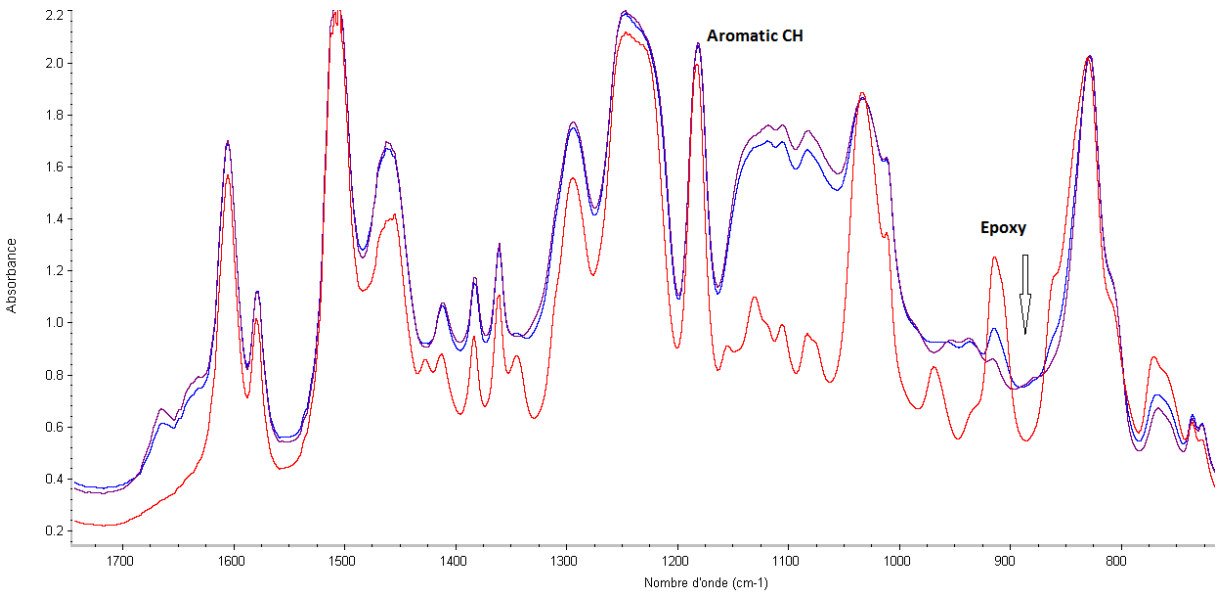

Figure 14. Superposition of FT-IR spectra at various times during DGEBA – HA cure at 80°C (between 500 cm^{-1} and 1700 cm^{-1})

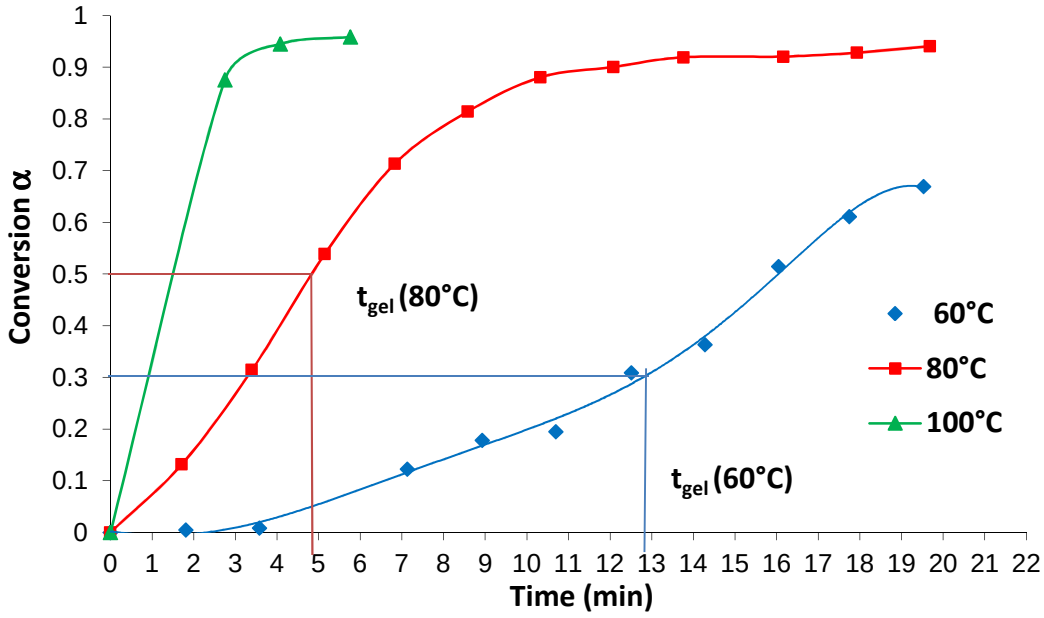

Figure 15. Evolution of conversion at different temperatures for DGEBA – HA system

Knowing the evolution of conversion with time at different temperatures, it is therefore possible to determine the conversion x_{gel} where gelation occurs. An important observation is that x_{gel} at 60°C, around 0.3, is different of x_{gel} at 80°C, around 0.5. This should not occur for classical epoxy-amine systems where conversion at gelation is constant. This is explained by the influence of the reactions such as homopolymerization which extent depends on reaction temperature.

4. Relation between crosslinking cycle and glass transition temperature for HA systems

DGEBA – HA networks, at a ratio r = 0.27, were cured at different temperatures, 1h at 80°C, 1h at 110°C and 1h at 150°C. In order to follow the evolution of glass transition temperatures with the cure temperatures, thermo-mechanical analyses were performed on DGEBA – HA networks. Results of DMA analyses are presented in Figure 16. Values of T_α, G' in the rubbery region, (M_c) and the crosslinking density (ν) [16] are summarized in Table 15.

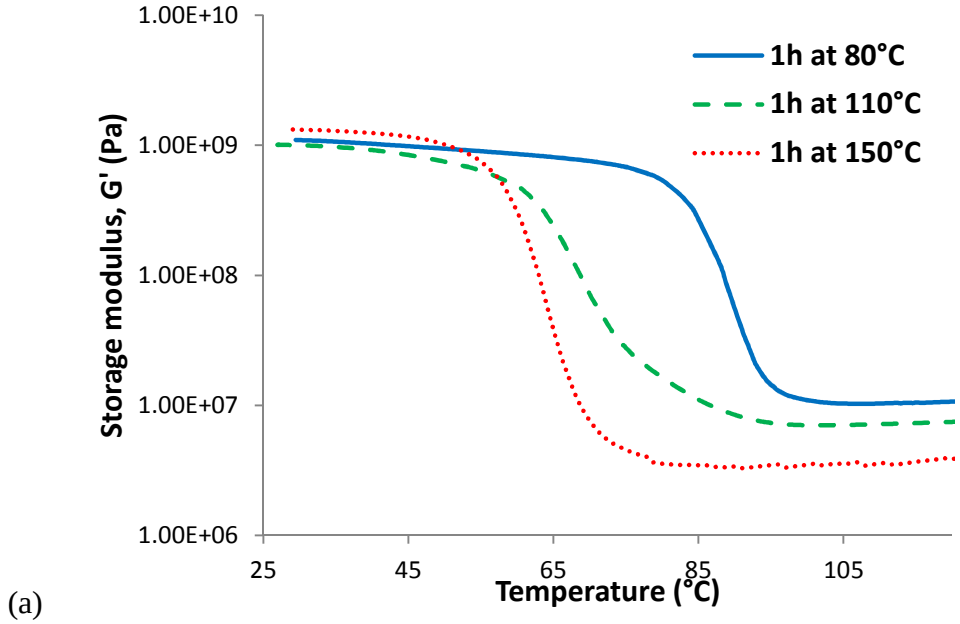

(a)

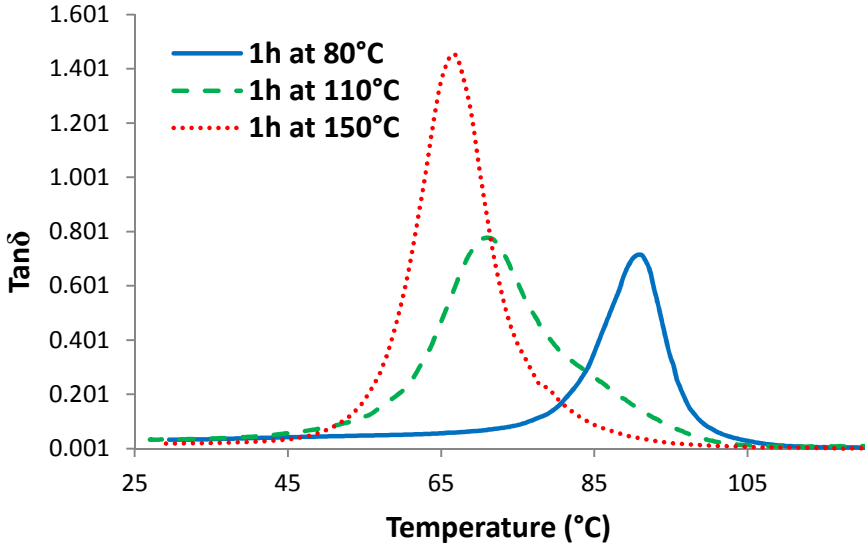

(b)

Figure 16. Storage modulus versus temperature (a) and tanδ versus temperature (b) for DGEBA cured with HA at different temperatures

Curing cycle	T_α (°C)	tanδ max	ΔTα (°C)	G' (MPa) (at T_α +30°C)	d (g/cm^3)	ν (10^{-3} mol/cm^3)	M_c (g/mol)
1 h at 80°C	90	0.70	10	10.7	1.17	3.3	357
1 h at 110°C	70	0.77	16	7.1	1.17	2.3	511
1 h at 150°C	67	1.45	10	3.3	1.16	1.1	1081

Table 15. Dynamic mechanical analyses of DGEBA – HA networks cured at different temperatures

There is a huge influence of the reaction temperature on the network properties. The first observation is that α-relaxation associated to the glass transition temperature T_g decreased with increasing the cure temperature. Indeed, network cured 1 h at 150°C exhibits lower α-relaxation temperature, 67°C, than network cured 1 h at 80°C, 90°C. Besides, networks cured at lower temperature have higher rubbery moduli. These networks are more densely crosslinked, with lower molar mass between crosslinking points, than networks obtained at a higher temperature.

Concerning the homogeneity of the networks, the more heterogeneous network is the one obtained at 110°C as the α-relaxation is larger (ΔT_α = 16°C). As a remark, this temperature is used in the industrial process of manufacturing ski boards.

Same observation was done for the DGEDAS-based networks. For instance, $DGEDAS_0$ – HA network crosslinked for 2 h at 80°C had a higher T_g than the network crosslinked for 2 h at 140°C. Values of T_g measured by DSC for $DGEDAS_0$ – HA networks are represented in Table 16.

Crosslinking cycle	T_g (°C)
2 h at 80°C	68
2 h at 140°C	55

Table 16. T_g values of $DGEDAS_0$ – HA networks (DSC)

As underlined by our previous study using BDMA and DMBA, such evolution of glass transition with curing temperature is attributed to the influence of homopolymerization initiated by tertiary amines that compete with classical polycondensation mechanism in our system.

IV. Conclusion of Part II

In this part of our study, we focused on the characterization of the commercial epoxy-amine system based on diglycidyl ether of Bisphenol A combined with a curing agent formulated for processing of composite material by Huntsman.

This curing agent (called HA in the study) is composed of two aliphatic amines. These aliphatic amines contain primary and secondary amines but also tertiary amines that act as catalysts in the epoxy-amine reaction and also promote homopolymerization reaction. This epoxy-amine system was characterized and the two bio-based epoxy prepolymers $DGEDAS_0$ and $DGEDAS_n$ were also studied in combination with HA under the same conditions. DGEBA – HA system exhibits interesting reactivity (T_{peak} = 125°C, higher than DGEBA – IPD: T_{peak} = 114°C) with a high exothermy. Concerning the gelation times, they are shorter than the values obtained for the curing agent IPD with low energy activation, 47 kJ/mol for DGEBA – HA.

The impact of HA tertiary amines induced reactions are also underlined in the study of dynamic mechanical properties with T_α values higher when the system is cured at low temperatures (*e.g.* 80°C) than at high temperatures (*e.g.* 140 - 150°C), and simultaneously higher crosslink density.

Conclusions

Within this Chapter we focused on the influence of curing agents using different formulations with various curing agents either aliphatic, cycloaliphatic or aromatic ones and studied the influence of their structure on the properties of the resulting systems. These hardener were either conventional ones (from petroleum resources) or bio-based ones.

Besides, we also characterized the Rossignol epoxy – amine system composed of DGEBA and a curing agent HA. This curing agent promotes dual polymerization with polyaddition and homopolymerization. The epoxy – amine system, HA combined with DGEBA, is highly suitable for Rossignol process with adapted pot-life, glass transitions and also interesting properties for composites application (that are not analysed in our study).

The replacement of DGEBA by one of the bio-based epoxy prepolymers is not sufficient to obtain an epoxy-amine network with interesting properties for Rossignol applications. Formulation study with appropriate curing agents is needed to approach the desired properties.

In terms of reactivity, the maximum peak temperatures T_{peak}, the exothermies of reaction ΔH and also the gel times and the activation energies should be compared. In terms of solid-state properties, the glass transition temperatures T_g and the rubbery moduli G'_R, should be taken into account. Below are summarized the main results concerning DGEBA – HA reactivity and solid-state properties.

Main characteristics of DGEBA – HA systems: *the target*

Reactivity: T_{peak} = 125°C
ΔH = 430 J/g
t_{gel} = 13 min at 60°C; 5 min at 80°C
E_a = 47 kJ/mol

Solid-state properties: (for a curing at 110°C, close to industrial conditions)
T_α = 70°C
G'_R = 7.1 MPa
M_c = 511 g/mol

Replacing the current system with a bio-based system should bring similar properties. Therefore, DGECAR is not an appropriate bio-based epoxy prepolymer for the application as it leads to low T_g networks. Concerning the curing agents, aromatic amines can be excluded, as they have low reactivity, as well as the D230 curing agent that has also a low reactivity as

it is a sterically hindered amine. IPD and MXDA are interesting as curing agents as well as NC540. MXDA is slightly more reactive than IPD.

Bio-based competing systems:

SPGE – IPD

Reactivity: T_{peak} = 101°C
ΔH = 338 J/g
t_{gel} = 16 min at 60°C; 5 min at 80°C
E_a = 63 kJ/mol

Solid-state properties: (for a curing of 1 h at 80°C and 2 h at 180°C)
T_α = 120°C
G'_R = 29 MPa
M_c = 150 g/mol

Yet, the network may be too dense, too brittle

SPGE – MXDA

Reactivity: T_{peak} = 104°C
ΔH = 438 J/g
t_{gel} = 3 min at 80°C

Solid-state properties: (for a curing of 2 h at 80°C and 2 h at 180°C)
T_α = 77°C
G'_R = 63.5 MPa
M_c = 137 g/mol

Yet, the network may also be too dense with a low value of molar mass between crosslinking points.

It is difficult to use only a binary system epoxy – amine. The use of epoxy prepolymer blends should be of interest in order to obtain an appropriate reactivity, glass transition temperature and M_c. Therefore, use of DGECAR in combination with SPGE will increase M_c but also increase gel time and decrease the T_g of the network (*e.g.* SPGE+DGECAR / MXDA or SPGE+DGECAR / IPD)

Concerning the isosorbide-based epoxy prepolymers, $DGEDAS_0$ is of interest as it leads to high T_g (T_α = 110°C, G'_R= 16.6 MPa, M_c = 260 g/mol with IPD) but its reactivity is too low (t_{gel} = 18 min with IPD). $DGEDAS_0$ can be combined with NC540 to decrease gel time and increase M_c.

In the next chapter, water resistance of the different systems previously characterized will be discussed.

References

[1] Dai Z, Constantinescu A, Dalal A, Ford C. Phenalkamine Multipurpose Epoxy Resin Curing Agents. *Cardolite Corporation*. 1994.

[2] Sato S, Shah S, Bueno RC, Moon R, Ferreira A. Phenalkamine and salted amine blends as curing agents for epoxy resins. World Patent WO 2009/080209 A1 2009.

[3] Shibata M, Nakai K. Preparation and properties of biocomposites composed of bio-based epoxy resin, tannic acid, and microfibrillated cellulose. *Journal of Polymer Science Part B: Polymer Physics*. 2010;**48**:425-33.

[4] Girard-Reydet E, Riccardi CC, Sautereau H, Pascault JP. Epoxy-Aromatic Diamine Kinetics. Part 1. Modeling and Influence of the Diamine Structure. *Macromolecules*. 1995;**28**:7599-607.

[5] Mounif E. *Thèse ENSAM Paris*. Résines époxy/amine pour le rotomoulage réactif: Etude de la rhéocinétique et simulation numérique de l'écoulement. 2008.

[6] Fernandez-Nograro F, Valea A, Llano-Ponte R, Mondragon I. Dynamic and mechanical properties of DGEBA/poly(propylene oxide) amine based epoxy resins as a function of stoichiometry. *European Polymer Journal*. 1996;**32**:257-66.

[7] Zucchi IA, Galante MJ, Williams RJJ. Comparison of morphologies and mechanical properties of crosslinked epoxies modified by polystyrene and poly(methyl methacrylate)) or by the corresponding block copolymer polystyrene-b-poly(methyl methacrylate). *Polymer*. 2005;**46**:2603-9.

[8] Dušek K, Bleha M, Luňák S. Curing of epoxide resins: Model reactions of curing with amines. *Journal of Polymer Science: Polymer Chemistry Edition*. 1977;**15**:2393-400.

[9] Byrne CA, Hagnauer GL, Schneider NS. Effects of variation in composition and temperature on the amine cure of an epoxy resin model system. *Polymer Composites*. 1983;**4**:206-13.

[10] Galante MJ, Vázquez A, Williams RJJ. Macro- and microgelation in the homopolymerization of diepoxides initiated by tertiary amines. *Polymer Bulletin*. 1991;**27**:9-15.

[11] Rozenberg B. Kinetics, thermodynamics and mechanism of reactions of epoxy oligomers with amines, Epoxy Resins and Composites II. In: Dušek K, ed.: Springer Berlin / Heidelberg 1986:113-65.

[12] Pascault JP, Sautereau H, Verdu J, Williams RJJ. Thermosetting Polymers: Taylor & Francis Books, Inc. 2002.

[13] Eloundou JP. Gélification de systèmes époxy-amine: études cinétique, rhéologiques et diélectrique; 1996.

[14] Eloundou JP, Feve M, Gerard JF, Harran D, Pascault JP. Temperature Dependence of the Behavior of an Epoxy−Amine System near the Gel Point through Viscoelastic Study. 1. Low-Tg Epoxy−Amine System. *Macromolecules*. 1996;**29**:6907-16.

[15] Galy J, Sabra A, Pascault JP. Characterization of epoxy thermosetting systems by differential scanning calorimetry. *Polymer Engineering & Science*. 1986;**26**:1514-23.

[16] Nielsen LE. Cross-Linking–Effect on Physical Properties of Polymers. *Journal of Macromolecular Science, Part C: Polymer Reviews*. 1969;**3**:69-103.

Chapter V. Water absorption of bio-based networks derived from sorbitol, isosorbide and cardanol

I. Introduction

In many applications the epoxy networks may be exposed to moist conditions or a humid environment (boat, pipes, tanks, etc…). To improve the performances of epoxy networks at harsh, humid environment, it is essential to obtain a clear picture of water diffusion in the material. Indeed, the problem of moisture absorption in epoxy networks is one of significant technical importance. The absorbed moisture has deleterious effects on the physical properties of the material. Some of these effects are a decrease of the glass transition temperature, T_g, and of the Young modulus, a change in deformation mechanisms, moisture-induced swelling and swelling stresses, the creation of microcracks and crazes, and sometimes chain scission through hydrolysis reaction. The topic of moisture absorption in epoxies has been studied for several decades.

In this chapter, we first summarized the models which have been proposed to describe water absorption and we will show the influence of the chemical structure. Then, the water uptake will be measured by a gravimetric method for a series of bio-based epoxy networks and the results will be discussed. Isosorbide and sorbitol are sugar-derived diol and polyol, and are highly soluble in water. Such high affinity with water may impact the resistance of the resulting epoxy networks to water. With the phenolic structure of cardanol, cardanol-based epoxy networks should be more resistant to water. To our knowledge, water sorption of bio-based epoxy networks is not yet reported in the literature.

As for the other properties measured in the previous chapters, the networks based on DGEBA and IPD will be considered as a reference network.

II. Water sorption behaviour in epoxy networks

1. Water-epoxy network interactions

Water diffusion in a network and more precisely in epoxy-network may be described by two main approaches [1]:

- (a) The “volumic” approach states that the water equilibrium concentration is mainly governed by the available free volume [2] or that water molecules occupy mainly the microvoids, internodular areas and morphological defects [3-6] which can offer preferential ways for their diffusion.

- (b) The “interaction” approach: Water is a highly polar molecule and specific water epoxy interactions occur. A vast majority of epoxies are crosslinked with amine-based curing agent that results in tertiary and secondary amines. These species are also polar and demonstrate an affinity for water. Water molecules are neither distributed randomly in the network nor concentrated in its morphological defects, but rather linked by strong hydrogen bonds mainly to hydroxyl groups [7] or tertiary amines ones [8] (Figure 1). The contribution of both groups could be interdependent.

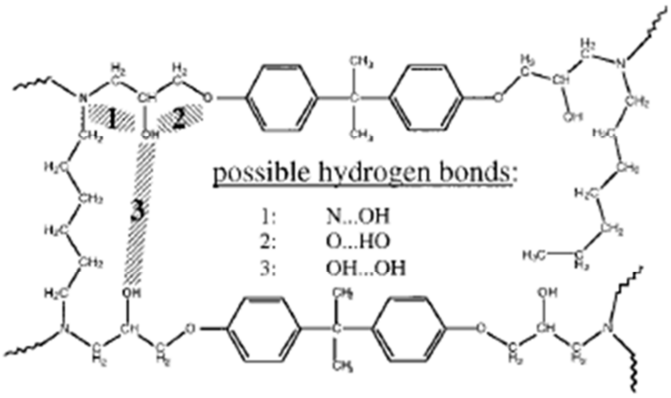

Figure 1. Three possible types of hydrogen bonds involving the hydroxyl of an amine-cured epoxy [9]

In the “volumic” approach the water absorption is controlled by the physical state of the network, whereas in the “interaction” approach it is the chemical structure of the network that matters.

These two approaches may be complementary as “volumic” approach fails to explain why free-volume rich substances such as silicone hydrocarbons are hydrophobic. According to Soles [9, 10] topology (nanopores), polarity and molecular movements should be taken into account to described water diffusion in epoxy networks. Water traverses the epoxy through

the network of nanopores, which are also coincident with the polar hydroxyls and tertiary amines. In this respect, the nanopores provide access to the polar interaction sites (Figure 2).

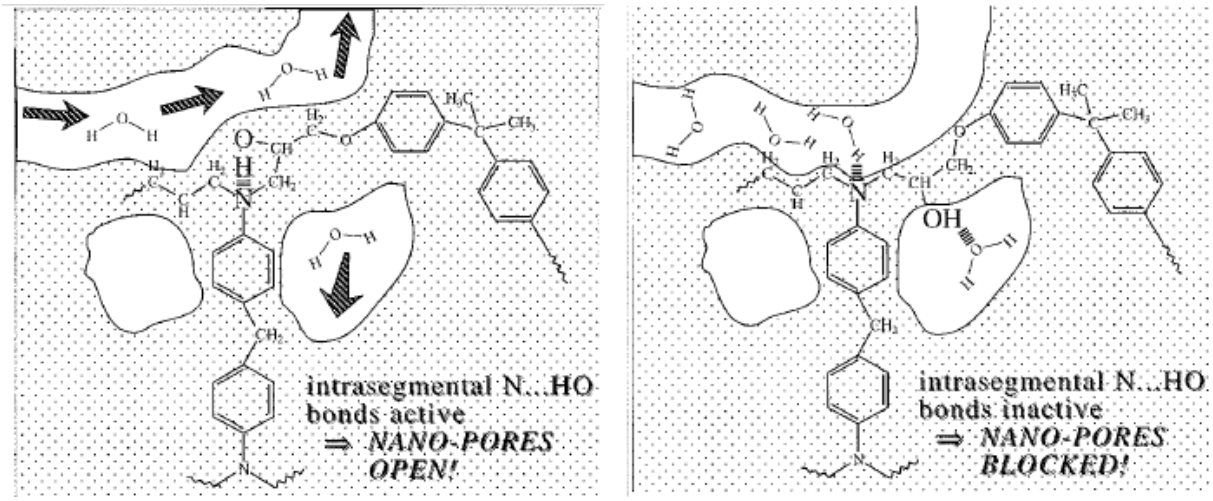

Figure 2. Water diffusion in epoxy-amine networks through the nanopores where specific interactions between the water and polar hydroxyls and amines regulate transport [9]

2. Nature of sorbed water

Based on the results of dielectric studies [11], time-resolved FTIR [12] and NMR water molecules sorbed in epoxy network were classified into free and bound water :

- The term “free water” represents water that has diffused in the free volume of network and could be at the origin of clusters.

- Two types of bound water were found in epoxy networks using NMR. The binding types are classified as Type I or Type II bonding, depending on difference in the bond complex and activation energy [13]. The activation energy of Type I and Type II bound water is ~10 and ~15 kcal/mol, respectively. Type I bonding corresponds to a water molecule which forms a single hydrogen bond with the epoxy network. This water molecule possesses lower activation energy and is easier to remove from the network. Type II bonding is a result of water molecule forming multiple hydrogen bonds with the network. This water molecule, therefore, possesses higher activation energy and is correspondingly harder to remove (Figure 3).

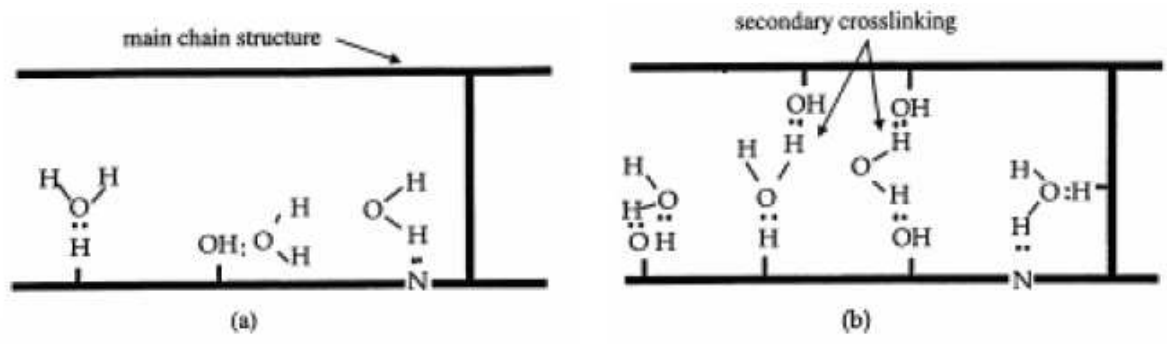

Figure 3. Nature of water sorbed according to Zhou [13] (a) type I, (b) type II

Nevertheless, the exact nature of the interaction between water and epoxy network is still not clearly understand and the theory of free and bound water is controversial. The formation of hydrogen bonding between water and the matrix is supported by many authors [14]. Some suggested that interactions could occur with the hydroxyl groups resulting from the oxirane group opening during epoxy-amine addition [15] and with the tertiary amines [16].

3. Physical consequences of water absorption

a) Swelling

According to Zhou [13], only the bounded water molecule of type I, that are only partially linked to the network can bring swelling of the network, whereas the water molecule of type II reinforced the chains cohesion and should not lead to swelling. The water molecules that occupy the free volume of the network should not also bring swelling.

b) Plasticization

Plasticization is a result of the diffusion of water which consequence is the decrease in glass transition temperature of the networks.

Using the classical hypotheses of the free volume theory, the glass transition temperature for a polymer (p) and solvent (s), with a free fraction of volume v is given by the Kelley and Bueche model [17]:

$$T_g = \frac{(1\text{-}v)_p T_{gp} + v\alpha_s T_{gs}}{(1\text{-}v)\alpha_p + v\alpha_s}$$

Where T_{gp} and T_{gs} are the glass transition temperatures of the dry polymer and the solvent and α_p and α_s are the respective coefficients of free volume expansion. Glass transition temperature of water is not clearly defined; some authors assumed it is comprised between 100 K and 150 K [18].

This relationship can be simplified assuming the validity of the Simha-Boyer rule [19], αT_g = const., which leads to :

$$\frac{1}{T_g} = \frac{1}{T_{gp}} + Av$$

Where : $A = \frac{1}{T_{gs}} - \frac{1}{T_{gp}}$

This equation underlines the fact that the plasticizing effect increases with the equilibrium water content and with the initial glass transition T_{gp} of the network in the dry state.

c) Degradation of the network

Sorbed water may have more severe consequences to the network integrity. Indeed, although relatively short-term exposure can lead to plasticization, more prolonged aging or thougher conditions (higher temperatures) can lead to crack growth and degradation of the network [20].

Such phenomenon may be caused by differential swelling either due to a gradient of water concentration in the network that enhance formation of water clusters [6] and craze initiation [5] or to the presence of hydrophobic loads.

Hydrolysis reactions may also be at the origin of network degradation:

$$\sim X\text{-}Y\sim + H_2O \rightarrow \sim X\text{-}OH + HY\sim$$

This hydrolysis brings chain cuts, diminution of crosslinking density and is complex to quantify.

4. Diffusion kinetics

The most commonly used model for the sorption behaviour in epoxy networks is the Fick diffusion model and more precisely the Fick's second law that represents the diffusion of water in the direction of the concentration gradient, which, in the unidimensional case, may be written as:

$$\frac{\partial C}{\partial t} = D\,\frac{\partial^2 C}{\partial x^2}$$

Where: D is the diffusion coefficient, x the coordinate along the sample's thickness (h) and C the water concentration.

The resolution of this equation, with approximation at short times (when $C \leq 0.5\ C_\infty$), gives :

$$\frac{M_t}{M_\infty} = \frac{4}{h\sqrt{\pi}}\sqrt{D_x t}$$

Where M_∞ is the mass of water absorbed at saturation and M_t is the weight of water at time t.

Using this equation, the diffusion coefficient D may be calculated from the slope of the curve representing the evolution of weigth gain, M_t, as a function of the $\sqrt{t}/h$.

5. Effect of the network structure on the water sorption

The molecule architecture in an epoxy network can be varied via different methods:

-the chemical structure of monomers

-the stoichiometric ratio between curing agent and epoxy prepolymer

-the conversion reached after different curing cycles

Below are given some typical examples of water sorption behaviour for the different cases cited above.

a) Influence of chemical structure

Zinck et al. [21] have investigated the influence of the chemical structure of epoxy network on the sorption behaviour and water-absorption consequences on mechanical properties. They studied two types of epoxy networks obtained with DGEBA combined with an aromatic diamine, 4,4' methylenebis[2,6-diethyleneaniline] (MDEA) and an anhydride 4-methyl 1,2,3,6-tetrahydrophtallic (MTHPA).

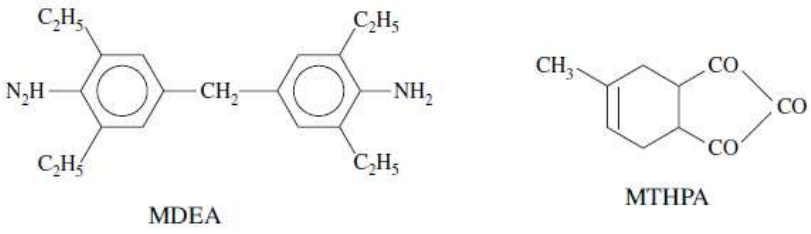

Figure 4. Structure of methylene diethyleneaniline (MDEA) and methyl tetrahydrophtallic (MTHPA)

Sorption experiments were carried out on these samples. Weight gains for immersion in water at 60°C are presented in Figure 5. The initial portion of the curves is linear, followed by equilibrium, highlighting behaviour close to Fickean sorption. Diffusivity values are underlined in Table 1. The lower diffusivity observed for the amine based network was explained on the basis of a more rigid network as compared to the anhydride based system. Amine based networks containing also hydroxyl –OH groups show a more important weight gain at the equilibrium than anhydride based ones that leads to a plasticization of higher magnitude. Besides, the plasticization the degradation is reversible for the anhydride based network but irreversible for the amine based network, as the initial value of the glass transition temperature was not recovered after water desorption (samples stored in oven at 60°C for 4 months).

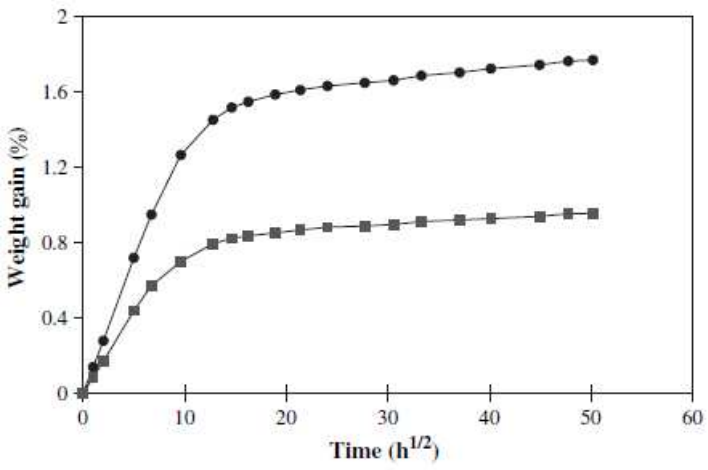

Figure 5. Water sorption kinetics for MTHPA (squares) and MDEA (circles) based DGEBA networks at 60°C as a function of $t^{1/2}$ [21]

Network	Diffusivity (10^9 cm^2 s^{-1})	M^a (%)	Specific volume (cm^3 g^{-1})	T_g dry^c (°C)	T_g eq.^{d} (°C)
DGEBA/MTHPA	36	0.90	0.83	124	102
DGEBA/MDEA	29	1.66	0.88	158	124

Table 1. Diffusivity, weight gain at equilibrium, specific volume and glass transition temperature for MTHPA and MDEA based polyepoxide networks dry and at equilibrium sorption at 60°C. [21]

Influence on the network structure on hydrogen bonding with water has also been presented in Zinck work [21]. In fact, hydroxyl groups in epoxide amine networks are involved in different types of hydrogen bonding interactions:

1- $OH_{polymer} - N$ intra-segmental bonds

2- intramolecular dimeric associations between 2 hydroxyl groups linked to the same nitrogen atom, $OH_{polymer} - OH_{polymer}$.

Such interactions are indeed affected in the presence of water. Therefore the sorbed water modifies/disrupts the $OH_{polymer} - N$ hydrogen bonds to form $OH_{water} - OH_{polymer}$ hydrogen bonds (and probably $OH_{water} - N$ hydrogen bonds).

Water molecules can establish interactions of sufficient intensity to modify substantially the stronger $OH_{polymer} - OH_{polymer}$ and $OH_{polymer} - N$ pre-existing hydrogen bonds. Intensity of water bonds in the case of epoxide aromatic amine networks is less important (as represented in Figure 6). The curing agent structure can therefore impart the interaction of water within the network.

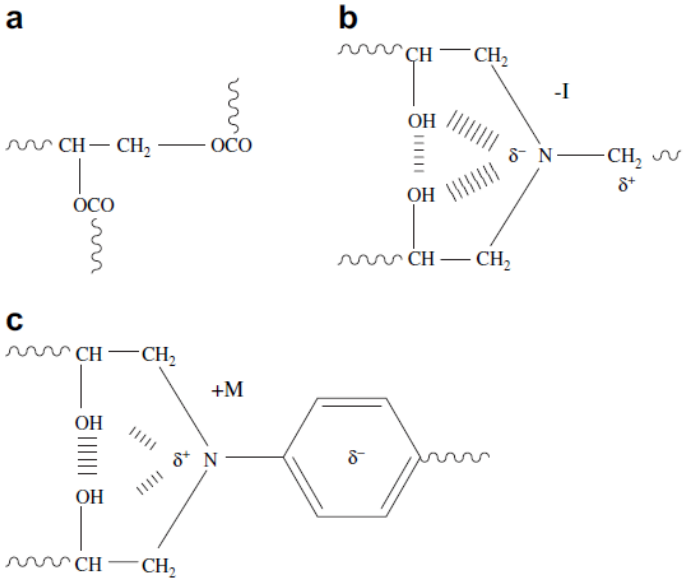

Figure 6. Network crosslinks for (a) anhydride, (b) aliphatic and (c) aromatic amine based polyepoxide networks

Li et al. [22] also studied the influence of the network structure on the water sorption. Indeed, water sorption behaviour of six epoxy systems with different chemical structure of amines and epoxies were monitored at five temperatures ranging from 35 to 75°C. Three different epoxy prepolymers were studied the diglycidyl ether of bisphenol A (DGEBA), the triglycidyl-p-aminophenol epoxy prepolymer (TGAP) and the tetraglycidyl-4,4'-diaminodiphenylmethane epoxy prepolymer (TGDDM) as represented in Figure 7. These epoxy prepolymers were combined with two different curing agents 4,4'-diamino-diphenylsulfone (DDS) and 4,4'-diamino-diphenylmethane (DDM) represented in Figure 8.

Among the different conclusions of their work, it appears that:

- The equilibrium water contents of networks are strongly dependent on the chemical structures of epoxy prepolymers and curing agents. Networks cured with same curing agent (no matter DDS or DDM) followed the equilibrium water content sequence TGAP > TGDDM > DGEBA, while for the same epoxy prepolymer, DDS-cured network always had a higher equilibrium water content than DDM-cured network.

- The polarity of the system is a decisive predictor of equilibrium water contents. Increase the polarity of the epoxy prepolymers and curing agents results in higher equilibrium water sorption.

According to the authors, the free volume fraction is not a decisive factor in governing the equilibrium water content.

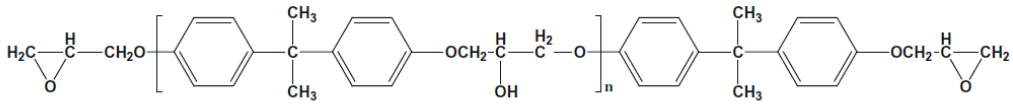

DGEBA

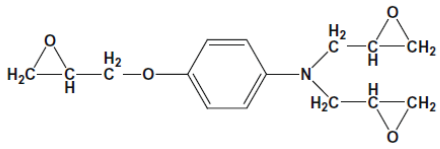

TGAP

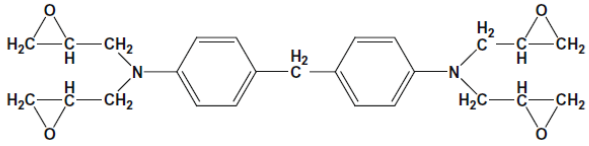

TGDDM

Figure 7. Structure of epoxy prepolymers used in Li study (DGEBA, TGAP, TGDDM)

DDS DDM

Figure 8. Structure of curing agents used in Li study (DDS and DDM)

b) Influence of stoichiometric ratio

Carfagna et al. [8] studied the influence of stoichiometric ratio of an epoxy – amine system on the water sorption of its network. Epoxy networks based on diglycidyl ether of bisphenol-A (DGEBA) epoxy cured with different amounts of triethylenetetramine (TETA) have been characterized. The authors observed an increase of water uptake at 20°C (S^{20}) and 70°C (S^{70}) and a decrease of glass transition temperatures for the samples cured with an increased content of amino hardener as represented in Table 2. It was attributed to the high hydrophilic character of the amine.

Amount of TETA	T_g dry (°C)	T_g wet* (°C)	S^{70} (%)	S^{20} (%)
5 phr	109	105	1.92	1.50
14 phr	142	109	3.30	3.90
25 phr	95	59	8.66	10.80

Table 2. Some physical properties of DGEBA epoxy resin cured with different amounts of TETA [8]
(*: wet glass transition of networks saturated at 70°C)

The system crosslinked with a large excess of diamine (25 phr), when immersed in liquid water, sorbs 10.80 and 8.66 % of water which is much higher than the two other compositions. The strong influence of stoichiometry may be related to the increase of the number of hydrogen sites due to the presence of unreacted amines.

Tcharkhtchi [18] studied the water sorption of diglycidyl ether of butane diol (DGEBD) – DETDA network with different amine/epoxide molar ratio (r). It appears that for the samples free of unreacted epoxides (r > 1), the process of water sorption is Fickian. For the samples having an excess of epoxide groups (r < 1), a two-step process was observed. The second step was attributed to epoxide hydrolysis.

Besides, the main hydrophilic site in epoxy-amine is the amino-alcohol group:

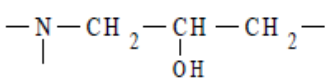

The contribution of this group to water absorption depends on its neighbour, and considering there is no other hydrophilic site (*i.e.* of different nature), the equilibrium water concentration should be proportional to the hydroxyl concentration. Yet, it appears that the dependence is rather parabolic than linear as represented in Figure 9. This could be explained by the fact that water can be double bonded. A pair of close hydroxyl groups could be, then a favourable site for water absorption.

As a remark, Tcharkhtchi observed a very small volume change but without clustering or microvoids.

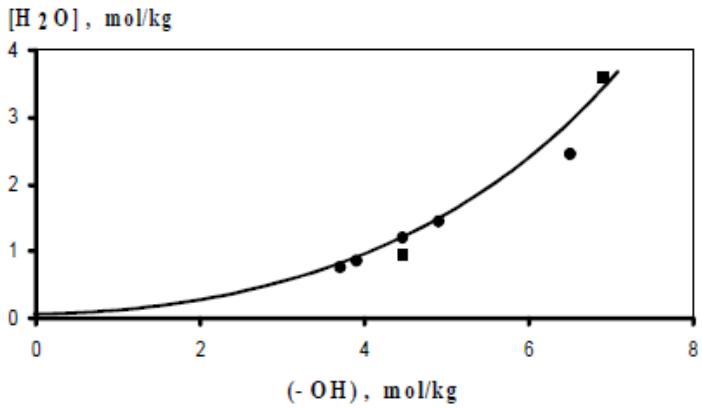

Figure 9. Number of sorbed water moles per kg against hydroxyl concentration [18]

→ Water sorption in epoxy network is strongly linked to the network structure. Many parameters can enhance the inherent affinity of water with the network such as: presence of hydrophilic sites due to available amine sites for non-stoichiometric systems, higher hydroxyl concentration and their proximity in the network structure.

III. Experimental section

1. Materials

The various epoxy prepolymers and curing agents studied in this section have been already described in the previous chapters. First, the influence of curing agent on water absorption will be studied. The water sorption of isosorbide-based networks obtained with either diamines, tertiary amines or HA curing agent (dual polymerization) will be studied. Then the influence of the epoxy prepolymer structure will be discussed using sorbitol and cardanol derived epoxy prepolymer. All the epoxy networks were prepared as described in the previous chapters.

2. Measurements

Water resistance of the different networks was monitored in this Chapter using:

Gravimetric measurements: Samples of approximately 2-3 mm thick were immersed in distilled water at room temperature and weighted periodically. The samples were removed from the water and wiped to remove excess water. As a remark, samples were stored under inert atmosphere before the test in order to avoid initial water absorption. For some systems, the whole sorption kinetic was followed whereas for other systems a comparison was established with the water absorption amount after 5 days of immersion. Besides, gravimetric measurements were also performed on samples stored in controlled atmosphere (T = 20 ± 1°C and 50 ± 5 % RH)

Glass transition temperatures of the aged networks were determined by DSC analyses. Indeed, with the samples regularly weighted to follow the water sorption kinetic, one piece for each system considered was used to follow the evolution of T_g. Regularly, small part of this "test piece" were cut and used to measure T_g by DSC analyses. These measures allow us to follow the evolution of T_g with the water absorption.

Structural characterization: The fracture surfaces of some epoxy – amine networks were observed by scanning electron microscopy (SEM, Philips XL 20). The samples were immersed in liquid nitrogen and fractured; one part of the sample was stored under inert

atmosphere whereas the other one was immersed in water for 10 min (Figure 10). The fracture areas were coated with gold. The 2 areas of fracture were then observed by SEM.

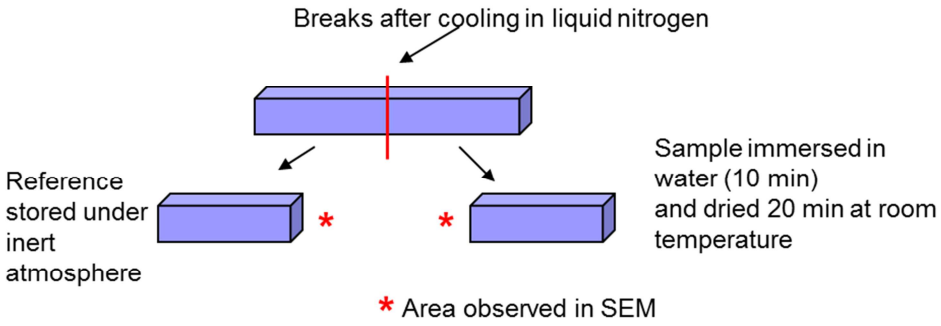

Figure 10. Preparation of samples for SEM analyses

IV. Water Absorption of Isosorbide-based epoxy networks

The first bio-based epoxy prepolymer studied were the isosorbide-based epoxy $DGEDAS_n$ and $DGEDAS_0$ (the purified form of $DGEDAS_n$).

1. Influence of the curing agent structure on the water absorption

For a first estimation of the stability of the bio-based networks towards water absorption, the weight gain of a serie of $DGEDAS_n$ – based networks was measured at room temperature. Various curing agents were used: diamine, tertiary amines as well as dual curing agent (HA).

a) DGEDAS networks obtained with diamine curing agents

Water sorption of DGEDAS-based networks obtained with diamines such as IPD, D230, MXDA, MCDEA and DETDA were characterized. The percent weight gain obtained after 5 days of immersion in distilled water at room temperature are summarized in the

following table. We report also the values of initial glass transition temperatures and the data related to DGEBA based network cured with IPD.

Networks	T_g (°C) initial	wt % water (5 days)	Comments
DGEBA - IPD	150	1	Reference system
$DGEDAS_0$ – IPD	102	26	
$DGEDAS_0$ – D230	52	29	
$DGEDAS_0$ - MXDA	79	ND	Some fragments after 5h of immersion
$DGEDAS_n$ – IPD	91	ND	Light swelling, fragmentation after 1h
$DGEDAS_n$ – D230	48	ND	Medium swelling, fragmentation after 30 min
$DGEDAS_n$ – MCDEA	120	8.4	
$DGEDAS_n$ - DETDA	112	29	

Table 3. Water absorption of different DGEDAS-based networks after 5 days of immersion in distilled water at room temperature

All networks synthesized from DGEDAS show very high water absorption, even some of them show degradation. The lower water absorption is observed for MCDEA (8.4 wt %) that has an aromatic structure and contains Cl atoms. As underlined in Zinck study [21] the use of aromatic curing agent decrease the polarity of the network structure.

An unexpected behaviour is observed with the fragmentation of some $DGEDAS_n$ and $DGEDAS_0$-based networks cured with MXDA, IPD or D230. Fragmentation starts from the edges of the sample and propagates to the core of this one. If the fragmentation is rapid it seems that no further evolution of the fragments is visually observable. This unexpected behaviour underlines the high affinity of these networks with water.

On the opposite, the reference network DGEBA – IPD has a very good resistance to water as it absorbs 1 wt % of water.

Even when fragmentation was not observed, the amount of water absorbed for DGEDAS networks were very important. This very bad water resistance for these bio-based networks was unexpected. It appears that it could be the main drawback of these materials.

Influence of DGEDAS structure

Even if DGEDAS-based networks present high affinity with water as compared with conventional network such as DGEBA – IPD, it appears that $DGEDAS_0$ have better water resistance than $DGEDAS_n$. $DGEDAS_0$ and $DGEDAS_n$ epoxy prepolymers differ by the presence of numerous oligomers in $DGEDAS_n$ composition. These oligomers contain –OH groups. It is well known that the presence of –OH groups enhance the water absorption of the resulting networks. Different –OH groups can be observed in network structures, the one already present within the oligomers structure and the one formed during the epoxy-amine addition mechanism. It appears that the –OH groups already present in $DGEDAS_n$ structure increase its affinity with water.

Remark: Investigations were performed to block these oligomers –OH groups by reaction with *p*-tolyl isocyanate (pTI) in order to obtain a free –OH epoxy prepolymer. Results of this experiment are described in the Annex D. Nevertheless, the resulting epoxy prepolymer exhibit an important viscosity and network was not obtained using this epoxy prepolymer.

Influence of stoichiometry

The influence of stoichiometry for $DGEDAS_n$ – D230 and $DGEDAS_n$ – IPD were evaluated. Results of water immersion in distilled water at room temperature are presented in Table 4. Whatever the stoichiometric ratio, the fragmentation is observed in all cases. The only difference can be observed in the swelling of $DGEDAS_n$ – D230 networks at different stoichiometry.

Networks	r	T_g (°C) initial	Beginning of fragmentation	Swelling	Number of fragments	Size of fragments
$DGEDAS_n$ – IPD	0.5	39	1 h	Light	-	Small
	1	91	1 h	Light	-/+	Small
	1.5	70	1 h	Light	+	Small
$DGEDAS_n$ – D230	0.5	15	30 min	Light	- (4 parts)	Big
	1	48	30 min	Medium	++	Small
	1.5	25	30 min	Important	+++	Small

Table 4. $DGEDAS_n$ – IPD and $DGEDAS_n$ – D230 networks at different stoichiometry immersed in water.

b) DGEDAS based networks obtained with tertiary amine (BDMA) or HA curing agent

In order to focus on the special case of homopolymerization and its consequence on water absorption of the network, $DGEDAS_n$ combined with BDMA (to focus on homopolymerization only) and HA (special curing agent: dual polymerization) were studied. DGEBA – HA is presented here as a reference.

DGEBA – HA and $DGEDAS_n$ – HA systems were prepared at the specific stoichiometric ratio r = 0.27 and crosslinked at two different temperatures. Their behaviours in water are summarized in Table 5.

Networks	Curing cycles	T_g (°C) initial	wt % water (5 days)	Comments
DGEBA – HA	1 h at 80°C	90	0.9	Reference system
$DGEDAS_n$ – BDMA	1 h at 80°C	68	ND	Fragmentation
$DGEDAS_n$ – BDMA	1 h at 140°C	40	ND	
$DGEDAS_n$ – HA	1 h at 80°C	61*	ND	Fragmentation after 15 min
$DGEDAS_n$ – HA	1 h at 140°C		ND	

Table 5. Behaviour of $DGEDAS_n$ – BDMA and $DGEDAS_n$ – HA networks immersed in water

Whatever the curing temperature, $DGEDAS_n$ – BDMA and $DGEDAS_n$ – HA have poor water resistance. The main difference for $DGEDAS_n$ – HA cured 1 h at 80°C and 1h at 150°C remains in the size of the fragments. Indeed, the fragments are smaller for the network crosslinked for 1h at 80°C than for 1 h at 140°C.

As a comparison, DGEBA – HA sample retains its original form and no swelling is visually observed.

Besides, HA curing agent induced **dual polymerization** with both addition and homopolymerization mechanisms. Depending on the cure temperature either addition or homopolymerization is enhanced which could impart the number of –OH groups formed during polymerization. According to Rozenberg, homopolymerization reduced -OH groups formation as compared with classical epoxy-amine formation [23]. Yet, whatever the cure

temperature of the networks, HA curing agent contains **tertiary amines** that enhance water affinity of the network.

As a remark, no swellings of the networks were visually observed before their rapid fragmentations.

2. Water sorption of $DGEDAS_n$ – HA and $DGEDAS_n$ – IPD networks

a) Water sorption kinetics

Even if $DGEDAS_n$ – IPD exhibited higher resistance to water than $DGEDAS_n$ – HA, these networks still have high affinity to water and fragmentation was observed in both cases when networks were immersed in water. In order to follow the water sorption kinetics, networks were aged under more gentle conditions in a controlled atmosphere (T = 20 ± 1°C and 50 ± 5 % RH) to follow the water absorption kinetics of the networks.

For each system, 3 samples of 30 x 20 x 2 mm^3 were aged during 60 days in these conditions and regularly weighted.

The water sorption kinetics for $DGEDAS_n$ – HA and $DGEDAS_n$ – IPD are represented in Figure 11.

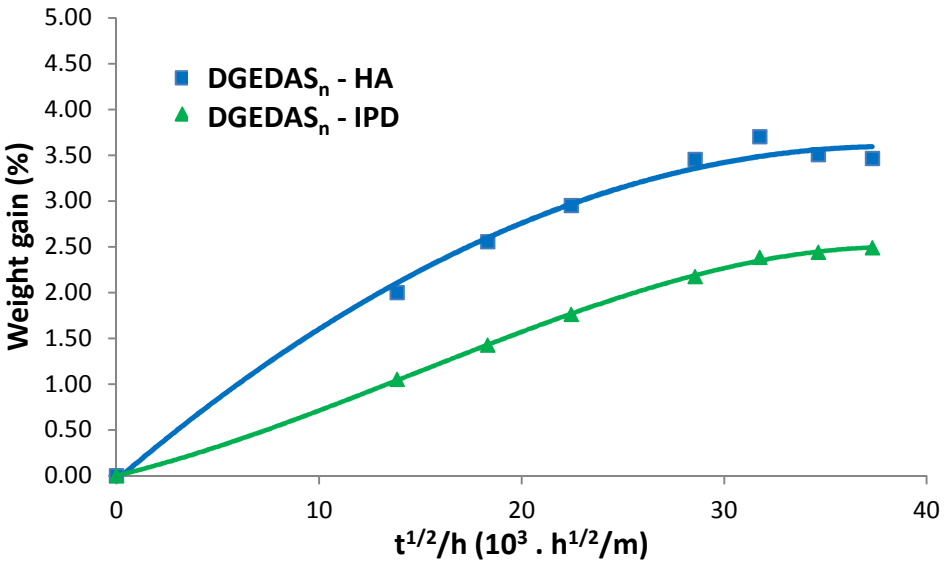

Figure 11. Water sorption kinetics for $DGEDAS_n$ – HA and $DGEDAS_n$ – IPD networks (Samples stored at RT, RH = 50%)

The water sorption kinetics of these two different networks confirm the lower resistance to water of the $DGEDAS_n$ – HA network compared to $DGEDAS_n$ – IPD one. The use of HA as a curing agent enhance the affinity of water for the network.
Whatever the curing agent used the amount of water absorbed by the networks remains very high (more than 2 % weight gain for $DGEDAS_n$ – IPD and more than 3 % for $DGEDAS_n$ – HA) for a gravimetric study under such moderate moisture conditions.

b) Evolution of T_g with ageing

Such affinity of the $DGEDAS_n$-based networks with water may induce plasticization of the networks. Therefore, the evolution of T_g with ageing of $DGEDAS_n$ – HA and $DGEDAS_n$ – IPD networks under controlled atmosphere (20 ± 1°C and 50 ± 5 % RH) was followed.

As an example Figure 12 represents the DSC thermogram obtained for $DGEDAS_n$ – HA network. As represented, two different runs were performed: one between -60°C and 250°C and the other, after a quick cooling, between 25°C and 150°C. The first DSC run shows the T_g of the network (around 30°C) and a light endothermic phenomenon around 110°C that may represents the evaporation of water already absorbed by the network. The second run shows the T_g of the network after evaporation of water (around 61°C). As a remark, this DSC thermogram is obtained for $DGEDAS_n$ – HA network prepared the same day ($t = 0 + \varepsilon$) and already presents a plasticization effect with a decrease of T_g from 61°C to 30°C. This observation underlined the very high affinity of $DGEDAS_n$ – HA network with water.

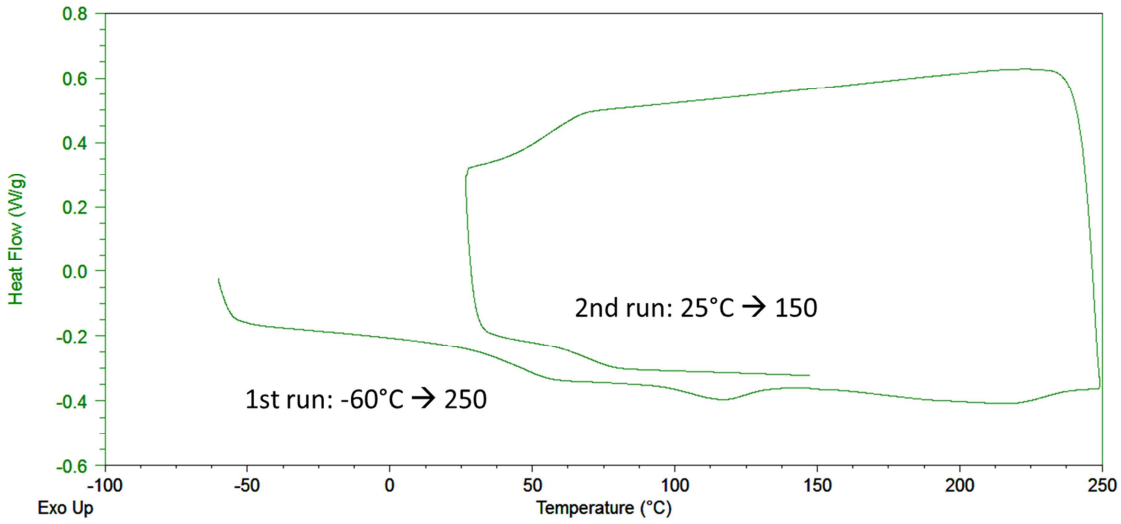

Figure 12. DSC plot for DGEDAS$_n$ – HA network (t = 0)

For comparison, Figure 13 represents the DSC plot of DGEDAS$_n$ – IPD (at t = 0). It appears that no evolution of T_g is observed between the first and the second run. Besides, no endothermic phenomenon is observed during the first run. Unlike, DGEDAS$_n$ – HA no water was absorbed at t = 0 + ε for DGEDAS$_n$ – IPD network.

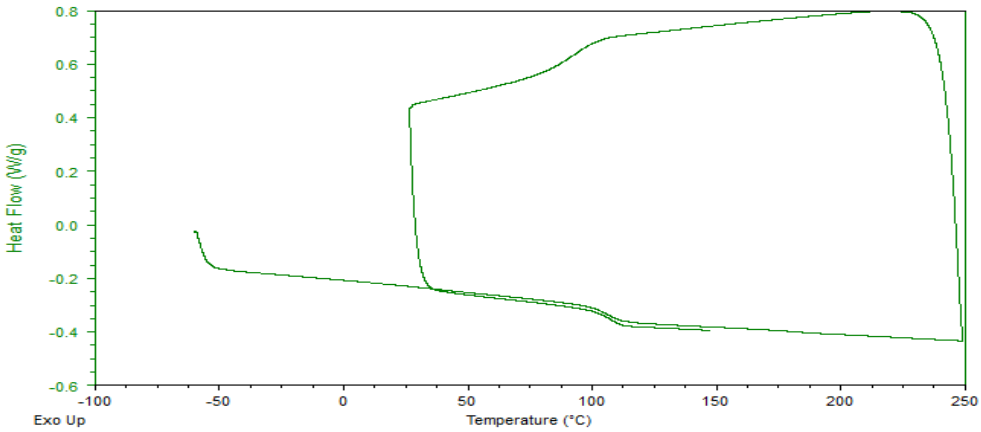

Figure 13. DSC plot of DGEDAS$_n$ – IPD network (t = 0)

Same DSC analyses were performed every week of the ageing of DGEDAS$_n$ – IPD and DGEDAS$_n$ – HA networks at 20 ± 1°C and 50 ± 5 % RH. Figure 14 and Figure 15 represent the evolution of the first DSC run plot with the time of ageing for DGEDAS$_n$ – HA and DGEDAS$_n$ – IPD respectively. Besides, T_g measured in the first runs and in the second runs for all the DSC analyses performed are summarized in Table 6.

It appears that at every step of the DGEDAS$_n$ – HA network's ageing an endothermic phenomenon is observed around 110°C. Even if some of the DSC analyses do not allow a

correct determination of T_g, a decrease of T_g is observed for $DGEDAS_n$ – HA network till 10°C approximately. This plasticization effect seems to be reversible till 3.4 % weight gain by water. Indeed, from this point the T_g in the second runs decreased from 60°C to 50 – 55°C. This may be explained by either irreversible hydrolysis (damage) of the network or by insufficient water evaporation during the first run because of the high amount of water absorbed.

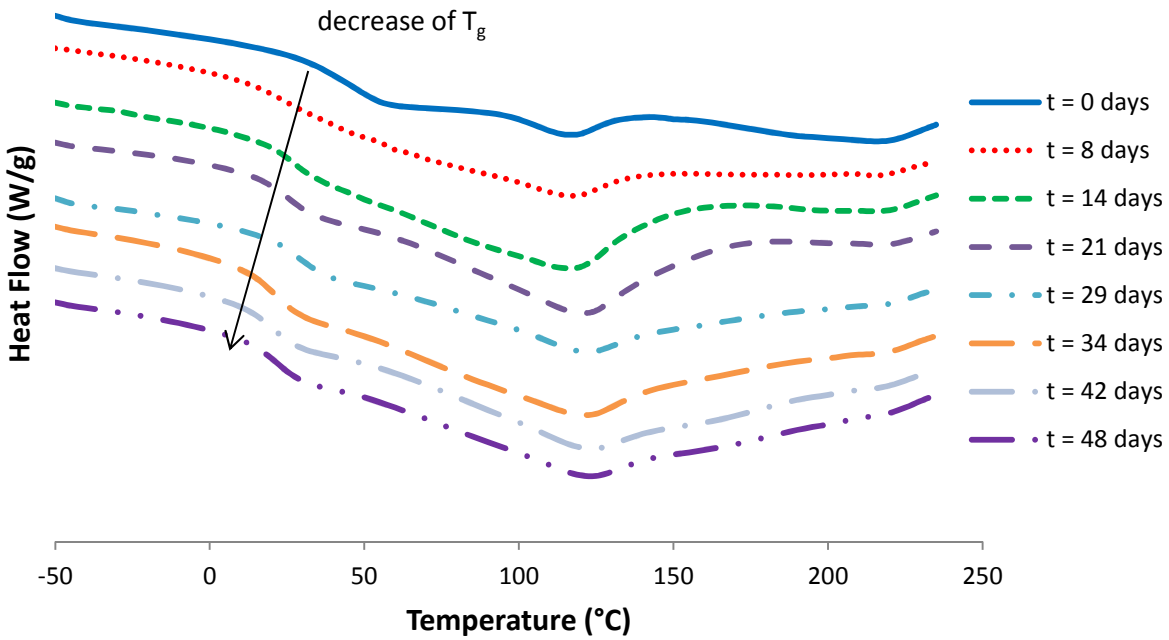

Figure 14. Evolution of T_g with the time of ageing for $DGEDAS_n$ – HA – First DSC run

Concerning the T_g evolution of $DGEDAS_n$ – IPD network, a plasticization of the network is also observed with a decrease of T_g from 101°C to 40 – 60°C. For high amount of water absorbed, T_g became difficult to measure in the first run and two transitions seem to be observed. Unlike $DGEDAS_n$ – HA, no endothermic peak is clearly identified near 100-110°C, this should be explained by a higher T_g value as compared with the one obtained for $DGEDAS_n$ – HA. Glass transition can overlap the endothermic phenomenon of water evaporation which can also explain why T_g is difficult to measure. Finally, the plasticization is reversible as the T_g measured in the second runs were around 100°C; which correspond to the T_g of the $DGEDAS_n$ – IPD in its "dry state". It means that no hydrolysis reactions occurred during the hygrothermal aging.

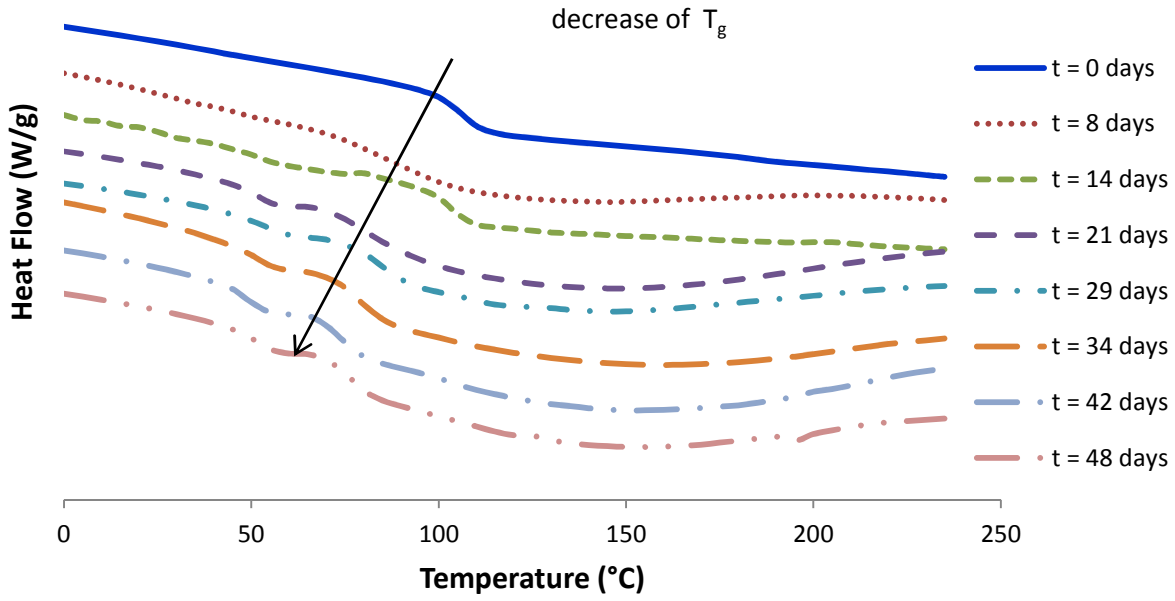

Figure 15. Evolution of T_g with the time of ageing for $DGEDAS_n$ – IPD – First DSC run

Days	$DGEDAS_n$ - HA			$DGEDAS_n$ - IPD		
	% weight gain	T_g (DSC 1st run)	T_g (DSC 2nd run)	% weight gain	T_g (DSC 1st run)	T_g (DSC 2nd run)
0	0.00	28	61	0.00	99	101
8	2.00	10	50	1.05	78	100
14	2.55	17	63	1.43	98	102
21	2.95	13	60	1.76	41/71	101
29	-	18	55	-	43/71	101
34	3.45	12	52	2.17	42/71	100
42	3.70	11	50	2.38	44/68	101
48	3.50	13	51	2.44	40/62	102

Table 6. Evolution of T_g measured by DSC for $DGEDAS_n$ – HA and $DGEDAS_n$ - IPD

The main conclusion is that networks obtained with $DGEDAS_n$ epoxy prepolymers and either HA or IPD as a curing agents are not resistant to water even under atmospheric moisture conditions and have to be stored under inert atmosphere to prevent plasticization of the networks. This phenomenon is important with a significant drop in the glass transition temperature values.

c) Evolution of the surface: observation by SEM

Finally to understand the important fragmentation of the $DGEDAS_n$ – HA networks in water, SEM observation of the $DGEDAS_n$ – HA sample surface before and after immersion in water for 10 min (beginning of fragmentation) were performed.

Figure 16 represents the SEM images of two fracture surfaces: one stored under inert atmosphere and the other immersed in water for 10 min. In both cases, images of the edge and the core of the samples were obtained.

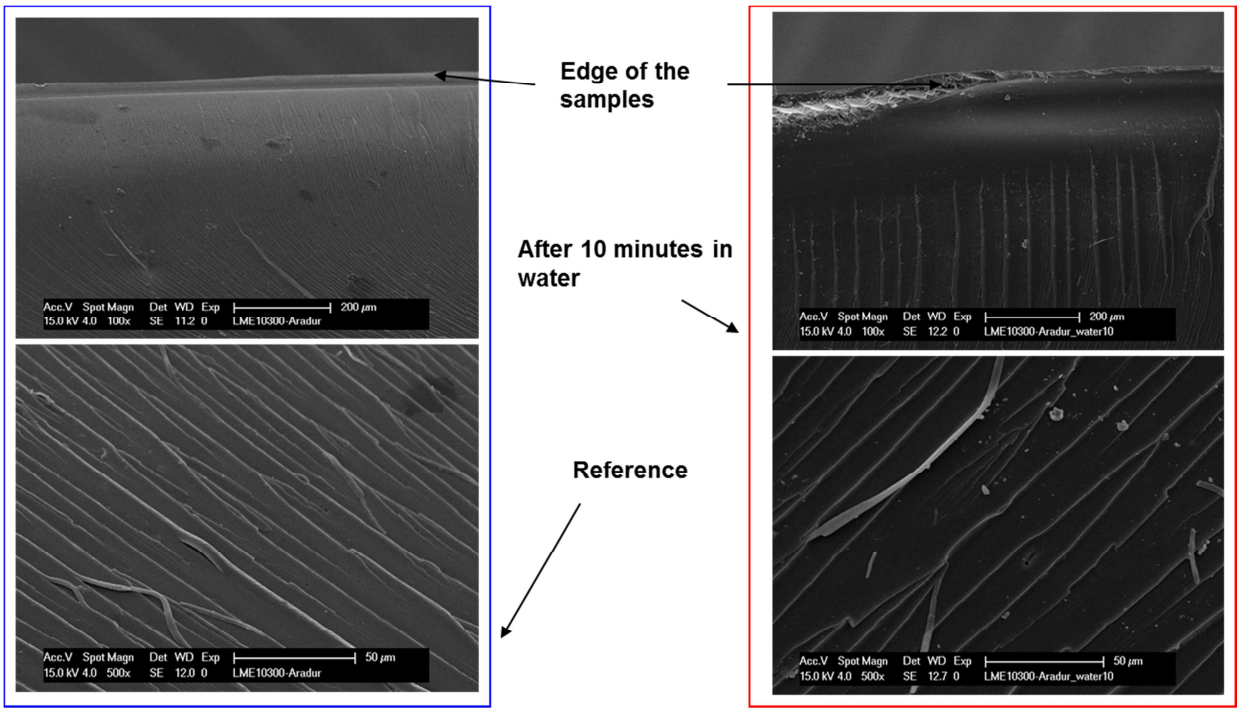

Figure 16. SEM images of the fracture surface of $DGEDAS_n$ – HA networks. Before and after immersion in water for 10 minutes

If no specific differences are observed in the middle of the fracture surface (fracture surface characteristic of a brittle material), the edge seems to present the first water "erosion" effect. Therefore, enlargements of this area were performed and are represented in Figure 17. Initiation of edge degradation is observed after 10 min of water immersion. Enlargement of the zone shows that two different areas may be observed: one that presents a mirror aspect and the other one that presents some "cavities". Heterogeneous diffusion of water in the epoxy network may be at the origin of these two areas.

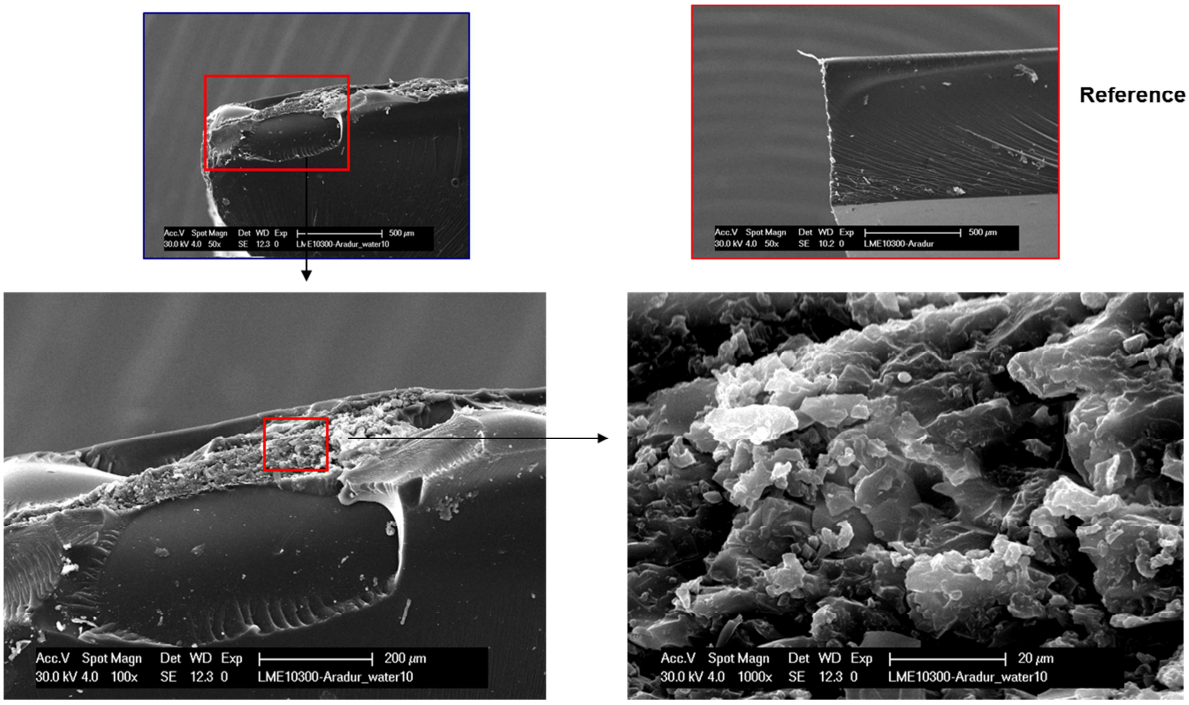

Figure 17. SEM images: focus on the edge of the fracture areas for DGEDAS$_n$ – HA networks before and after ageing in water

Same observations were obtained by Morgan et al. [5] but for tetraglycidyl-4,4'-diaminodiphenylmethane (TGDDM) epoxy prepolymer and 4,4'-diamino-diphenylsulfone (DDS) networks (see Figure 7 and Figure 8 for TGDDM and DDS structures) immersed in water at higher temperature. Scanning Electron micrographs of the cavity obtained by Morgan are represented in Figure 18. According to Morgan, the cavity regions that may contain high water content would be favourable sites for craze initiation and subsequent propagation. The dilatational changes produced in the epoxy by the crazing process enhance the accessibility of moisture to sorption sites within the epoxy to a greater extent than crack propagation alone.

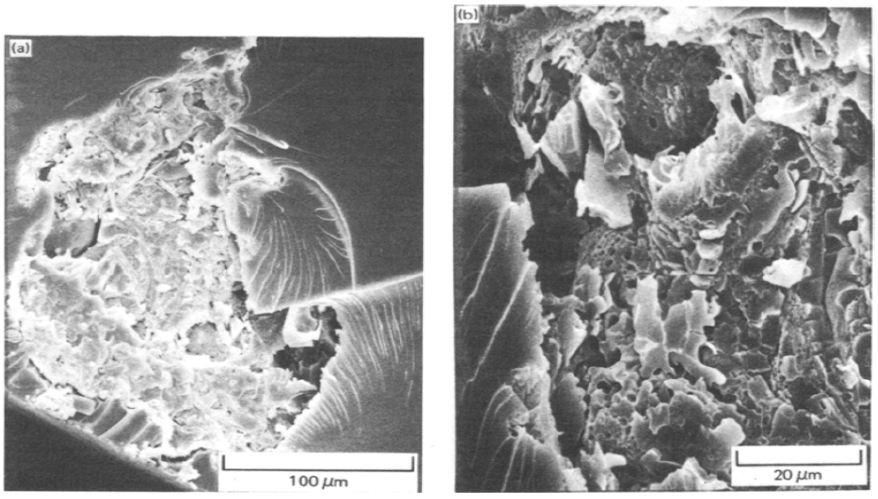

Figure 18. Scanning electron micrographs of fracture surfaces of wet epoxy network according to Morgan [5] (~ 4 wt% water absorbed)

Finally, the higher affinity of $DGEDAS_n$ – based network chemical structure with water enhance the water absorption and therefore the quick degradation observed in our case under low temperature (RT).

3. Conclusion on water absorption of isosorbide-based networks

To replace bisphenol A by an isosorbide-based segment has strong consequences on the water resistance of the networks synthesized from this bio-based prepolymer, with sometimes deterioration of the networks. The reasons for this unexpected behaviour are not clear and more experiments are needed to conclude. Yet, it appears that networks obtained with $DGEDAS_0$ exhibit lightly better water resistance that the ones obtained with $DGEDAS_n$; water affinity of the network being increased by the presence of numerous oligomers with –OH groups.

The following hypotheses can be done to explain the very low water resistance of DGEDAS-based network by comparing the simple cases of DGEBA – IPD and $DGEDAS_0$ – IPD having 1 wt % and 26 wt % water sorption respectively:

-Aliphatic ether cycle (*i.e.* isosorbide) increases the polarity of the material, contrary to aromatic units present in DGEBA structure. Moreover, the conformation of the isosorbide segments between crosslinking points is very particular and may favour water interactions with closed hydrophilic groups (such as –OH groups) and strong hydrogen bonding, that enhance water affinity of the structure.

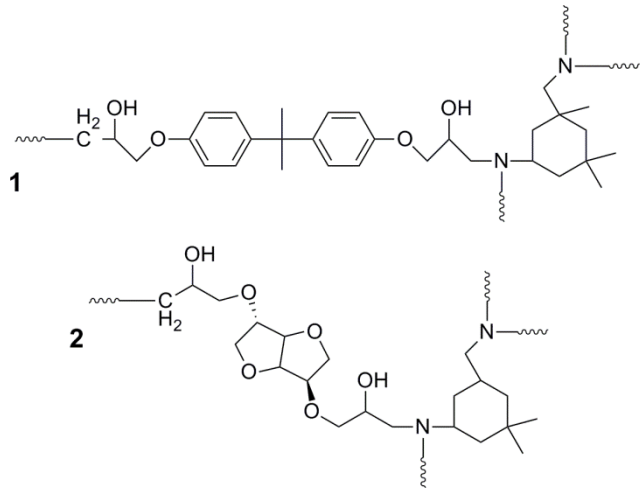

Figure 19. Structure between crosslinking points for 1: DGEBA – IPD and 2: $DGEDAS_0$ - IPD

-Finally, the free volume aspect was not discussed in our study. Yet, high free volume structure can increase water affinity and propagation in the networks.

V. Influence of the epoxy prepolymer structure on water absorption of the networks

Other bio-based epoxy prepolymers were studied in order to obtain bio-based epoxy networks with good water resistance.

1. SPGE-based networks

SPGE are commercially available with different grades. The reference Denacol 622 is a water insoluble Sorbitol Polyglycidyl Ether. The networks based on this prepolymer were studied in the Chapters III and IV. Water resistance of the SPGE-IPD epoxy networks were studied. It appears that contrary to isosorbide-based epoxy networks sorbitol-based ones do not degrades in water. Therefore, gravimetric studies were performed on the SPGE-IPD immersed in distilled water at room temperature. As it was underlined in the third Chapter, the SPGE-based systems exhibit particular behaviour with an increase of T_g with the stoichiometric ratio r. The influence of r on water resistance a SPGE – IPD network at a stoichiometric ratio r > 1 was studied (r = 1.25). Water sorption kinetics of the two SPGE – IPD networks are represented in Figure 20 with the water sorption kinetics of DGEBA – HA network as a reference.

SPGE – IPD (r = 1) has equivalent water resistance as DGEBA – HA with M_∞ around 5 wt % at RT. We observed also that SPGE – IPD networks with r > 1 has a lower water resistance than SPGE – IPD at r = 1, with M_∞ around 20 %. Usually with an excess of amine, the water absorbed is increased but in our case there is also an increase of T_g, which means that a more dense network (see Chapter III) was obtained. This underlined the particularity of SPGE-based systems out of stoichiometry (r > 1). SPGE – IPD networks obtained with an excess of amine include more hydrophilic groups, probably due to Cl-induced side reactions.

Remark: Bio-based networks obtained using another SPGE reference, Denacol 614B, were studied in terms of water resistance. Indeed, this epoxy prepolymer is as $DGEDAS_0$ and $DGEDAS_n$ almost entirely soluble in water. Water resistance of the network (immersed in distilled water at room temperature) obtained with this epoxy prepolymer is presented in Annex D. Very high water absorption was observed (up to 25 wt % water sorption).

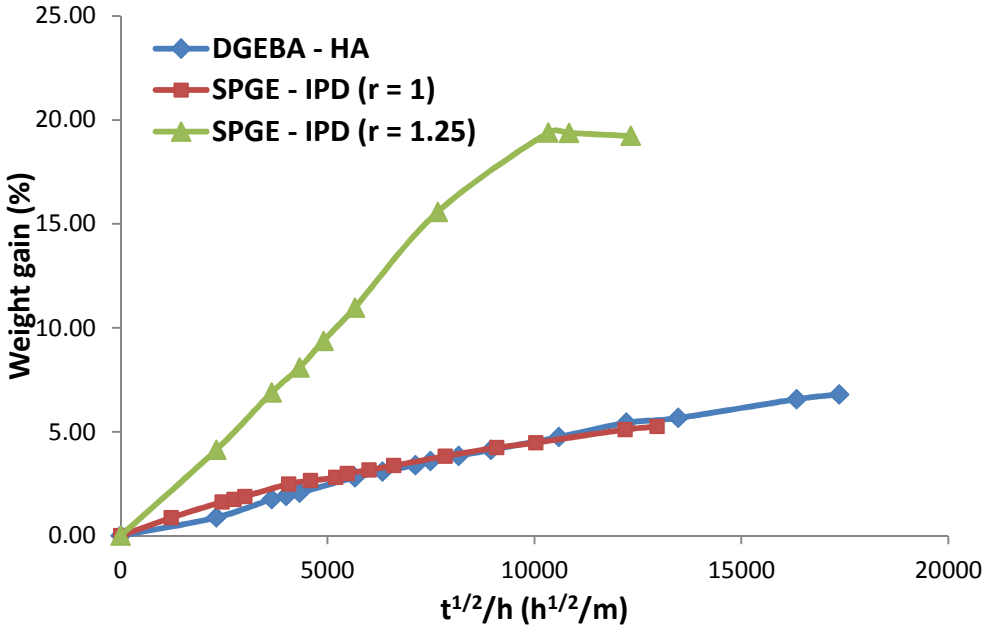

Figure 20. Water sorption kinetics for SPGE - based networks, with DGEBA - HA as a reference (Samples immersed in distilled water)

2. DGECAR-based networks

Cardanol-based epoxy prepolymer, DGECAR, was also studied in combination with IPD or NC540 in the previous chapters. Because of its phenolic structure good water resistance were expected. Therefore, in our study the water resistance of DGECAR-based networks was also characterized. Water sorption kinetics of DGECAR – IPD and DGECAR – NC540 networks are represented in Figure 21, with DGEBA – HA sorption kinetic as a reference.

It appears that DGECAR either combined with a classical curing agent IPD or with bio-based curing agent NC540 exhibit better water resistance than the DGEBA – HA network with a maximum water gain around 1 wt %.

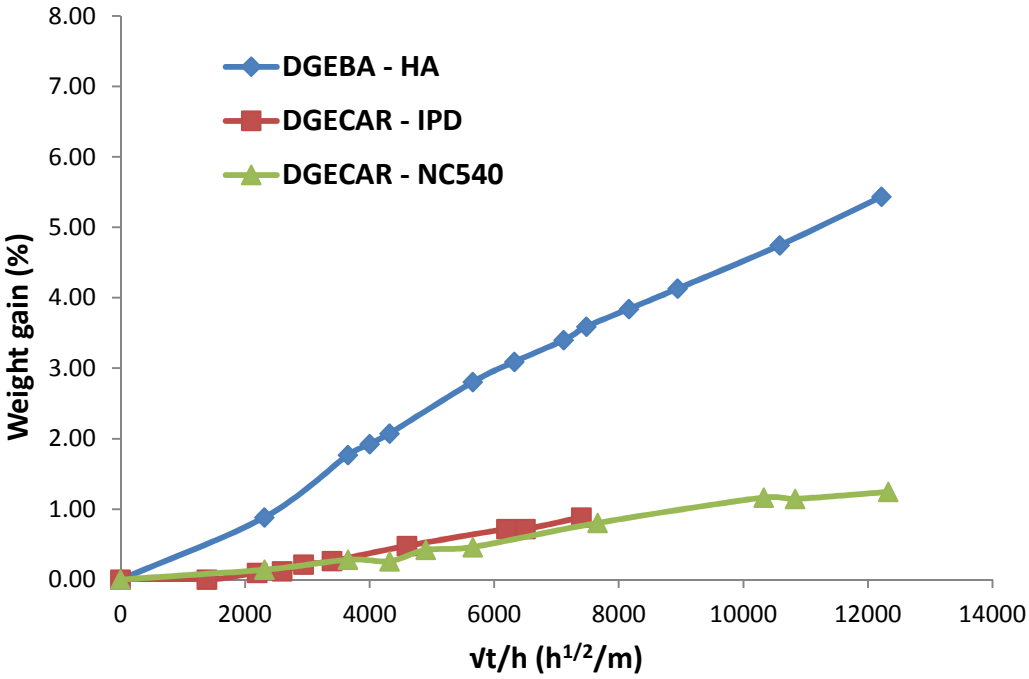

Figure 21. Water sorption kinetics for DGECAR-based networks with DGEBA – HA as a reference (Samples immersed in distilled water)

Conclusions

In this Chapter we focus on the water absorption of the different bio-based networks previously studied. Indeed, water resistance of epoxy networks is an important factor as such networks are known to absorb water that could impact the network properties (plasticization, degradation…).

First, in order to focus on the influence of crosslinking agent on water affinity with the network, different DGEDAS-based networks were studied combined with conventional diamines but also tertiary amines and HA curing agent. It appears that these networks exhibit very poor water resistance whatever the curing agent used. Indeed, with some curing agents (aliphatic and cycloaliphatic) fragmentation was observed. The use of tertiary amine and HA curing agent with its particular mechanism of dual polymerization even lower the water resistance of the networks. It has been also shown in this chapter that the –OH groups present in the structure of the various oligomers of $DGEDAS_n$ increase the affinity of the networks with water. Besides, another important factor should be the free-volume contribution. The free volume of these networks has not been measured, yet it should be important as even with a high amount of water absorbed no swelling is visually observed. The “free-volume” contribution combined with the high hydrophilicity of the DGEDAS structure could increase water affinity of the networks. Nevertheless, investigations remain to be done to fully understand and also to decrease the high water affinity of these networks with water.

Finally, even combined with more hydrophobic curing agents, the DGEDAS-based networks absorb an important amount of water.

Different bio-based epoxy prepolymers were also tested such as SPGE and DGECAR, to focus on the influence of the epoxy prepolymer structure on the water resistance. The networks obtained from SPGE exhibit good water resistance. Finally, DGECAR-based networks are the more hydrophobic networks because of its phenolic structure.

References

[1] Bellenger V, Verdu J, Morel E. Structure-properties relationships for densely cross-linked epoxide-amine systems based on epoxide or amine mixtures. *Journal of Materials Science*. 1989;**24**:63-8.

[2] Adamson MJ. Thermal expansion and swelling of cured epoxy resin used in graphite/epoxy composite materials. *Journal of Materials Science*. 1980;**15**:1736-45.

[3] Gupta VB, Drzal LT, Rich MJ. The physical basis of moisture transport in a cured epoxy resin system. *Journal of Applied Polymer Science*. 1985;**30**:4467-93.

[4] Apicella A, Tessieri R, de Cataldis C. Sorption modes of water in glassy epoxies. *Journal of Membrane Science*. 1984;**18**:211-25.

[5] Morgan RJ, O'Neal JE, Fanter DL. The effect of moisture on the physical and mechanical integrity of epoxies. *Journal of Materials Science*. 1980;**15**:751-64.

[6] Carfagna C, Apicella A. Physical degradation by water clustering in epoxy resins. *Journal of Applied Polymer Science*. 1983;**28**:2881-5.

[7] Danieley ND, Long ER. Effects of curing on the glass transition temperature and moisture absorption of a neat epoxy resin. *Journal of Polymer Science: Polymer Chemistry Edition*. 1981;**19**:2443-9.

[8] Carfagna C, Apicella A, Nicolais L. The effect of the prepolymer composition of amino-hardened epoxy resins on the water sorption behavior and plasticization. *Journal of Applied Polymer Science*. 1982;**27**:105-12.

[9] Soles CL, Yee AF. A discussion of the molecular mechanisms of moisture transport in epoxy resins. *Journal of Polymer Science Part B: Polymer Physics*. 2000;**38**:792-802.

[10] Soles CL, Chang FT, Bolan BA, Hristov HA, Gidley DW, Yee AF. Contributions of the nanovoid structure to the moisture absorption properties of epoxy resins. *Journal of Polymer Science Part B: Polymer Physics*. 1998;**36**:3035-48.

[11] Maxwell ID, Pethrick RA. Dielectric studies of water in epoxy resins. *Journal of Applied Polymer Science*. 1983;**28**:2363-79.

[12] Mensitieri G, Lavorgna M, Musto P, Ragosta G. Water transport in densely crosslinked networks: A comparison between epoxy systems having different interactive characters. *Polymer*. 2006;**47**:8326-36.

[13] Zhou J, Lucas JP. Hygrothermal effects of epoxy resin. Part I: the nature of water in epoxy. *Polymer*. 1999;**40**:5505-12.

[14] Moy P, Karasz FE. Epoxy-water interactions. *Polymer Engineering & Science*. 1980;**20**:315-9.

[15] Banks L, Ellis B. The glass transition temperature of an epoxy resin and the effect of absorbed water. *Polymer Bulletin*. 1979;**1**:377-82.

[16] Morel E, Bellenger V, Verdu J. Structure-water absorption relationships for amine-cured epoxy resins. *Polymer*. 1985;**26**:1719-24.

[17] Kelley FN, Bueche F. Viscosity and glass temperature relations for polymer-diluent systems. *Journal of Polymer Science*. 1961;**50**:549-56.

[18] Tcharkhtchi A. Water absorption characteristics of diglycidylether of butane diol: 3,5-diethyl-2,4-diaminotoluene networks. Kidlington, UK: Elsevier 2000.

[19] Simha R, Boyer RF. On a general relation involving the glass temperature and coefficients of expansion of polymers. *J Chem Phys*. 1962;**37**:1003.

[20] Xiao GZ, Shanahan MER. Water absorption and desorption in an epoxy resin with degradation. *Journal of Polymer Science Part B: Polymer Physics*. 1997;**35**:2659-70.

[21] Zinck P, Gérard JF. Polyepoxide–water interactions: Influence of the chemical structure of the network. *Polymer Degradation and Stability*. 2008;**93**:1231-7.
[22] Li L, Yu Y, Wu Q, Zhan G, Li S. Effect of chemical structure on the water sorption of amine-cured epoxy resins. *Corrosion Science*. 2009;**51**:3000-6.
[23] Rozenberg B. Kinetics, thermodynamics and mechanism of reactions of epoxy oligomers with amines Epoxy Resins and Composites II. In: Dušek K, ed.: Springer Berlin / Heidelberg 1986:113-65.

General conclusion

Throughout this thesis we have studied and characterized novel bio-based epoxy networks. Indeed, as discussed in the first chapter of this manuscript the development of biopolymers and in particular epoxy thermosetting polymers has recently attracted remarkable popularity. Nature offers a huge variety of renewable precursors for the synthesis of attractive precursors that differ in their structure. We study throughout this manuscript the structure-properties relationships of some interesting bio-based precursors.

Among them, isosorbide appears as an interesting bio-based diol candidate. Derived from starch, with a short and cyclic structure, isosorbide is produced in a high purity level by Roquette Frères. In the context of this work, Huntsman and Roquette epoxidized the isosorbide through two different synthetic routes. The second chapter was dedicated to the study of these two bio-based epoxy prepolymers derived from isosorbide ($DGEDAS_0$ and $DGEDAS_n$). Characterization of these two prepolymers was performed. Reactivity and network properties when combined with a conventional amine curing agent (Isophorone Diamine, IPD) were also studied. It appeared that DGEDAS-based epoxy systems lead to interesting bio-based networks yet with lower values of T_g than conventional epoxy – amine system.

Other bio-based epoxy prepolymers were already commercially available such as sorbitol and cardanol-based epoxy prepolymers. These epoxy precursors differ by their structure: cycloaliphatic for the isosorbide diglycidyl ether (DGEDAS), polyfunctional and aliphatic for the sorbitol polyglycidyl ether (SPGE) and with phenolic moieties for the cardanol-based epoxy prepolymer (DGECAR). The third chapter was a study of the influence of epoxy prepolymer structure on the network properties using the three different bio-based epoxy prepolymers: $DGEDAS_0$, SPGE and DGECAR. As expected and due to the presence of long aliphatic chain within its structure, DGECAR-based networks exhibit low T_g. Similar glass transition values were obtained at stoichiometric ratio for $DGEDAS_0$ and SPGE based networks. Yet, this study underlines an unusual behaviour of SPGE – IPD systems through an increase of T_g with the stoichiometric ratio. Higher amount of amine leads to more densely crosslinked networks with higher T_g. High chlorine content of SPGE epoxy prepolymer (around 19 wt%) should be at the origin of this observation, through side reactions / interactions when amine are in excess that increase the crosslinking points.

This study on epoxy prepolymers was completed in the fourth chapter by the formulation of bio-based epoxy systems using various curing agents. Either conventional curing agent (derived from petroleum resources) or bio-based ones were studied to focus also on the influence of the curing agent structure on the systems reactivities and solid-state properties. Besides, the specially formulated curing agent HA was also studied. Using this curing agent, that promote both classical epoxy-amine addition and homopolymerization, the structure of the networks are dependent upon the curing temperature.

Finally, in the last part of the manuscript, Chapter V, we presented the first investigations on the water absorption of the bio-based networks derived from isosorbide, sorbitol and cardanol. The isosorbide-based networks, which appeared promising in terms of reactivity and thermo-mechanical properties as compared to DGEBA–based networks, revealed a very dramatic water resistance, not yet clearly understood, which appears as the main drawback of these materials.

This work clearly underlined the fact that the well-known DGEBA cannot be easily replaced by any other bio-based prepolymers. The replacement by a given type of bio-based prepolymer essentially depends on the applications targeted. In most cases, the whole reactive system must be re-formulated to fit the reactivity and solid-state properties required.

Further investigations

Complementary studies can be performed on the four bio-based epoxy prepolymers studied, $DGEDAS_0$, $DGEDAS_n$, SPGE and DGECAR. Indeed, the high water affinity of the isosorbide-based networks can be a huge problem for many applications; yet the dry networks present interesting properties that can be useful for the replacement of conventional epoxy systems in other applications in which the materials will not be exposed to moisture conditions. Otherwise, combination of isosorbide-based epoxy prepolymers with others reactive products more hydrophobic could be a good compromise as far as it does not impact drastically the “bio-based added value” of isosorbide-based epoxy prepolymers.

Prospects should be done also on the understanding of the particular behavior of SPGE based prepolymers and the influence of this high chlorine content. What chemical reactions can be involved between chlorinated compound and amines that influence on the network structure and therefore the network properties? Further investigations on the effect of such

high chlorine content on the reactivity of the system and the network properties should be done.

Other bio-based epoxy precursors can be also considered. Indeed, Diphenolic Acid (DPA) derived from levunic acid, and other bio-based precursors, presented in Chapter I, that exhibit interesting phenolic structure such as tannin-derived polyols (*e.g.* catechin) can also be attractive candidates for the replacement of Bisphenol-A.

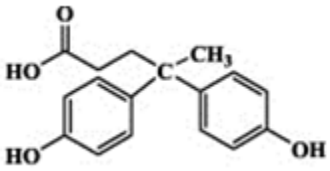

Figure 1. Structure of Diphenol Acid (DPA)

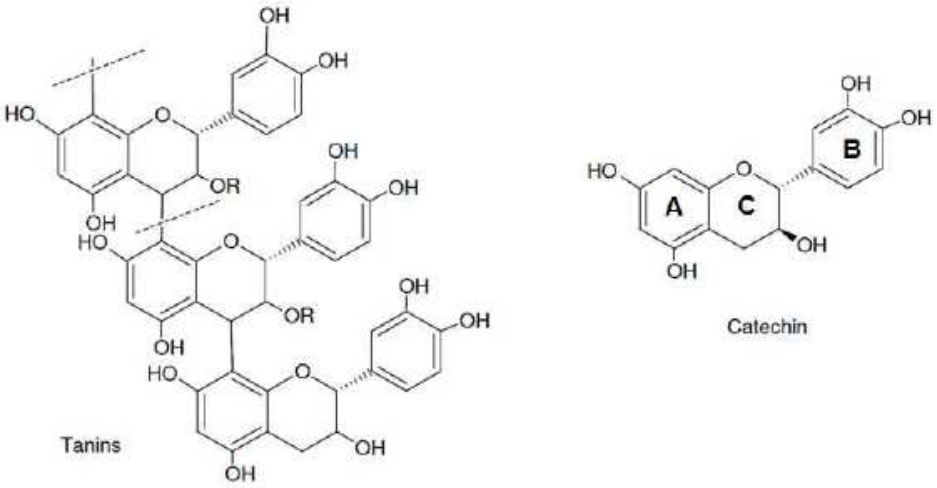

Figure 2. Structure of tanins and catechin

Finally, as underlined in our first chapter fewer investigations have concerned the replacement of current amino-curing agents (or anhydride curing agents) by bio-based ones but should be of interest to obtain fully bio-based epoxy systems.

Concerning the NAFI project, important study remains to be done on the matrix-linen fibres interfaces for the different systems characterized. Nevertheless, one partially bio-based epoxy system was tested with success by Rossignol: DGEBA (80 wt %) + $DGEDAS_n$ (20 wt %) with HA as curing agent. Nevertheless, its bio-based content is low and further formulations can be done to raise this bio-based content knowing the properties of the different epoxy prepolymers and systems studied.

Annexes

Annex A: Additional theoretical background: Theory on molecular modelling

The high speed digital computer has changed the way to visualize organic chemistry. The ability to predict the outcome, in a quantitative sense, of a chemical reaction and to visualize organic molecules in three dimensions is more accessible. This computational approach to chemistry is being used extensively in drug design, protein mutagenesis, biomimetics, catalysis, polymer properties prediction …

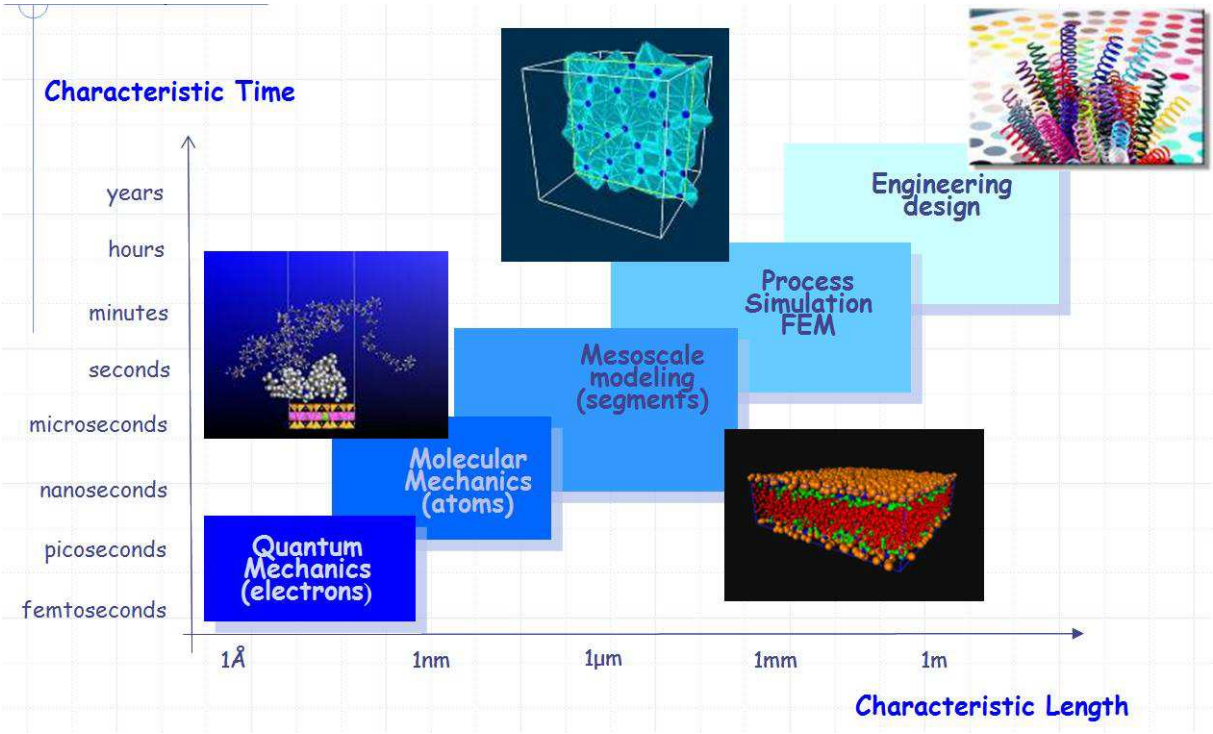

In our study, we have used both group contribution method and molecular dynamics. The following part of the Annexes gives theoretical background concerning the Molecular Modelling.

I. Classical simulations theory

This method considers the molecule or macro-molecule as a classic mechanical system. Simulation time depends mainly on the computer power.

Atomistic simulation is an empiric method based on the hypothesis that atomic nuclei of chemical group of the same nature should have the same energy potential (similar electronic environments) whether it is found in a molecule or another.

Therefore in atomistic simulation, each atom is described in terms of charge, valence, Van der Waals radius… All these parameters will describe the behaviour of the atom during the simulation. They are determined using *ab initio* calculations or by successive confrontations between simulations results and experimental values.

Atomistic simulation fundamental principle consists to apply classic quantum mechanics to describe a system dynamic using the ***Newton's equation of motion***:

$$-\frac{\partial V}{\partial q_i} = \mathrm{m}_i \frac{\partial^2 q_i}{\partial t^2}$$

The potential V is an empirical fit to the potential energy surface, commonly called a forcefield.

II. Forcefields

A crucial part of any simulation is the choice of forcefield. The forcefield describes approximately the potential energy surface on which the atomic nuclei move. Forcefields are usually tuned for particular groups of systems, so the choice of forcefield will depend on the type of structure that is being investigated.

Forcefields commonly used employ a combination of *internal coordinates* and *terms* (bond distances, bond angles, torsions, etc.), to describe that part of the potential energy due to interactions between bonded atoms, and *non-bonded terms* to describe the Van der Waals, electrostatic, etc. interactions between atoms. The functional forms range from simple quadratic forms to Morse functions, Fourier expansions, Lennard-Jones potentials, etc.

The potential energy of a system can be expressed as a sum of valence (or bond), crossterm, and non-bond interactions:

$$V_{total} = V_{valence} + V_{crossterm} + V_{non\text{-}bond}$$

Valence interactions

The energy of valence interactions is generally accounted for the diagonal terms :

-bond stretching (bond)

-valence angle bending (angle)

-dihedral angle torsion (torsion)

-inversion, also called out-of-plane interactions (oop) terms, which are part of nearly all forcefields for covalent systems

$$V_{valence} = V_{bond} + V_{angle} + V_{torsion} + V_{oop}$$

Valence cross-terms

Modern (second-generation) forcefields generally achieve higher accuracy by including *cross-terms* to account for such factors as bond or angle distortions caused by nearby atoms. These terms are required to accurately reproduce experimental vibrational frequencies and therefore, the dynamic properties of molecules. In some cases, research has also shown them to be important in accounting for structural deformations. Cross terms can include the following: stretch-stretch, stretch-bend-stretch, bend-bend, torsion-stretch, torsion-bend-bend, bend-torsion-bend, and stretch-torsion-stretch.

Non-bond interactions

The energy of interactions between non-bonded atoms is accounted for by two terms: Van der Waals interaction terms and electrostatic energy term (Coulomb):

$$V_{non\text{-}bond} = V_{Van\ der\ Waals} + V_{electrostatic}$$

For our simulations, we used the commercial forcefield provided by Accelrys, COMPASS (Condensed Phase Optimized Molecular Potentials of Atomic Simulation Studies). COMPASS represents a technology break-through in forcefield methods. It is the first ab initio forcefield that enables accurate and simultaneous prediction of gas-phase properties (structural, conformational, vibrational, etc…) and condensed-phase properties (equation of state, cohesive energies, etc…) for a broad range of molecules and polymers.

III. Molecular dynamics

Once an energy expression and, if necessary, an optimized structure have been defined for the system of interest, a dynamics simulation can be run[1]. Example of optimized structure is given in Figure 1.

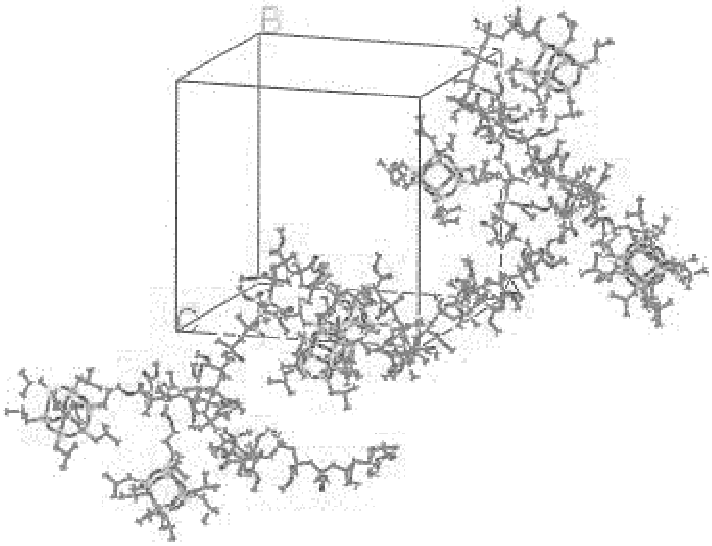

Figure 1. example of Amorphous Cell construction results (DGEBA – IPD)

The bases of this simulation are the classical equations of motion which are modified, when appropriate, to deal with the effects of temperature and pressure on the system. The main product of a dynamic run is a trajectory file that records the atomic configuration, atomic velocities and other information at a sequence of time steps which can be analysed subsequently.

Integrating Newton's equation of motion allows us to explore the constant-energy surface of a system. However, most natural phenomena occur under specific conditions where the system is exposed to external pressure and/or exchanges heat with the environment. Under these conditions, the total energy of the system is no longer conserved and extended forms of molecular dynamics are required.

Several methods are available for controlling temperature and pressure. Depending on which state variables (the energy E, enthalpy H, number of particles N, pressure P, stress S,

[1] Construction of molecular structure and optimization of this structure (by energy minimization) performed using Accelrys modules are not detailed in this section

temperature T, and volume V) are kept fixed, different statistical ensembles can be generated. A variety of structural, energetic, and dynamic properties can then be calculated from the averages or the fluctuations of these quantities over the ensemble generated. Both isothermal (where heat is exchanged with a temperature bath to maintain a constant thermodynamic temperature) and adiabatic (where no heat exchange occurs) ensembles are available:

Constant temperature, constant pressure (NPT)

Constant energy, constant volume (NVE) also referred to as *microcanonical ensemble*

Constant pressure, constant enthalpy (NPH)

Constant pressure, constant volume (NVT) also referred to as *canonical ensemble*

Annex B: Additional results for Chapter II

This Annex gives complements on the molar mass distribution analysis of $DGEDAS_n$ and more precisely the determination of a calibration curve more suitable for $DGEDAS_n$ oligomers mass attribution. Besides, purification of $DGEDAS_n$ epoxy prepolymers by solubilisation in different solvent has been studied. Finally, additional NMR analyses (H-H COSY NMR) have been performed on $DGEDAS_n$ and $DGEDAS_0$ epoxy prepolymers.

I. Complements on $DGEDAS_n$ mass distribution

1. Use of calibration curve for SEC chromatography

Size Exclusion Chromatography (SEC) was performed in THF as elution solvent to determine the molar masses of the different epoxy prepolymers studied in our project (See Chapter II).

For instance, Figure 2 represents the SEC chromatogram of $DGEDAS_n$ epoxy prepolymer. This epoxy prepolymer presents a large mass distribution and the aspect of the chromatogram seem to be the same as the one obtained for solid DGEBA epoxy prepolymers. In order to improve mass attribution, a new calibration is needed (rather than the classical calibration based on polystyrene standards).

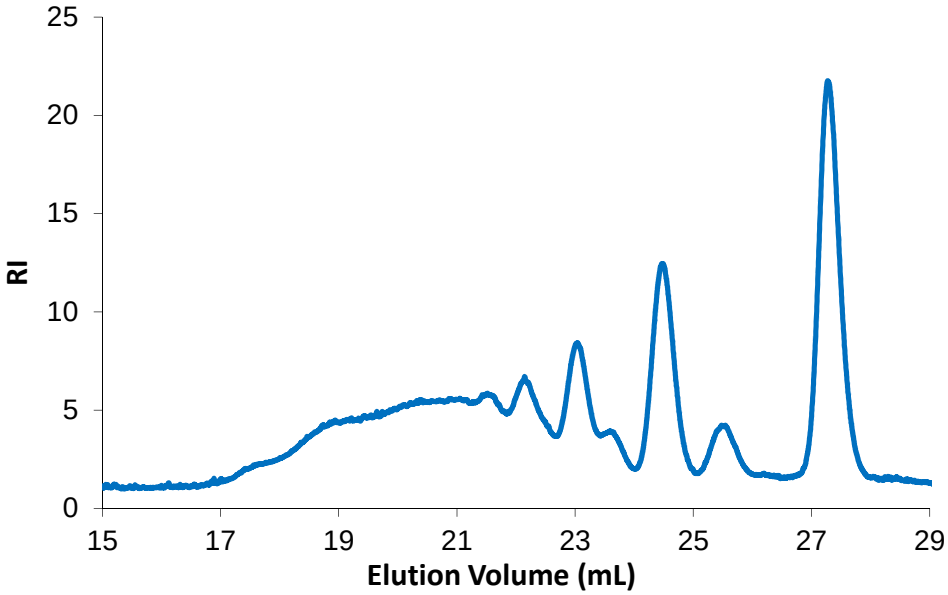

Figure 2. SEC chromatogram of $DGEDAS_n$ epoxy prepolymer

A new calibration curve was then obtained using a DGEBA solid epoxy prepolymer with an epoxy equivalent of 475 – 550 g/ee (commercial reference: DER 671). This commercial DGEBA epoxy prepolymer presents an elution curve similar to the one obtained for $DGEDAS_n$, and attribution of its elution peaks is possible. SEC chromatogram of DER 671 represented in Figure 4.

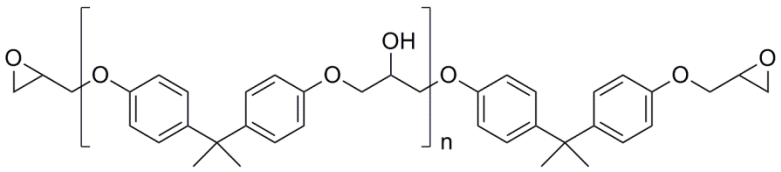

Figure 3.Chemical structure of DER 671 epoxy prepolymer

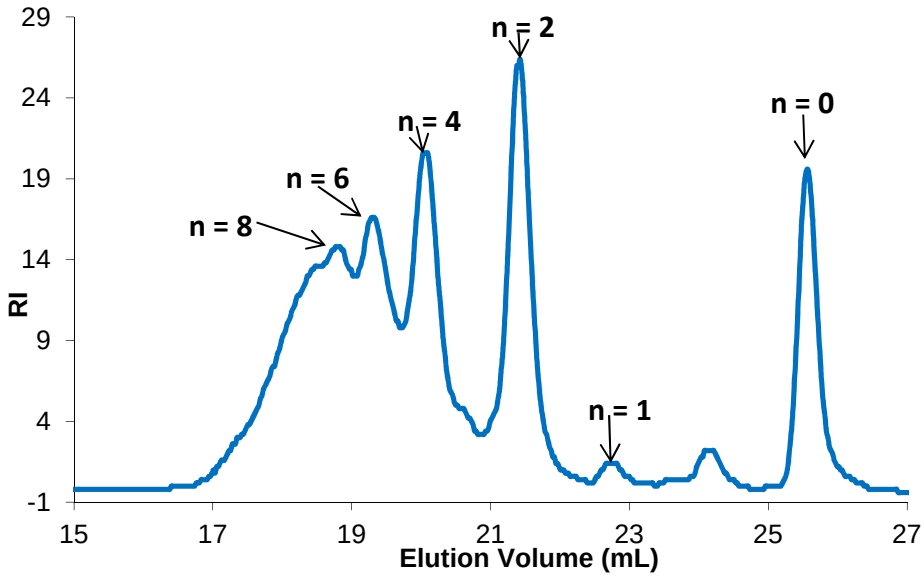

Figure 4. SEC of chromatogram of DER 671

Using this SEC chromatogram and the molar mass peaks attribution, the following SEC calibration curve was obtained. This calibration curve was useful to obtain approximation on molar mass attribution of the different epoxy prepolymers studied in our project.

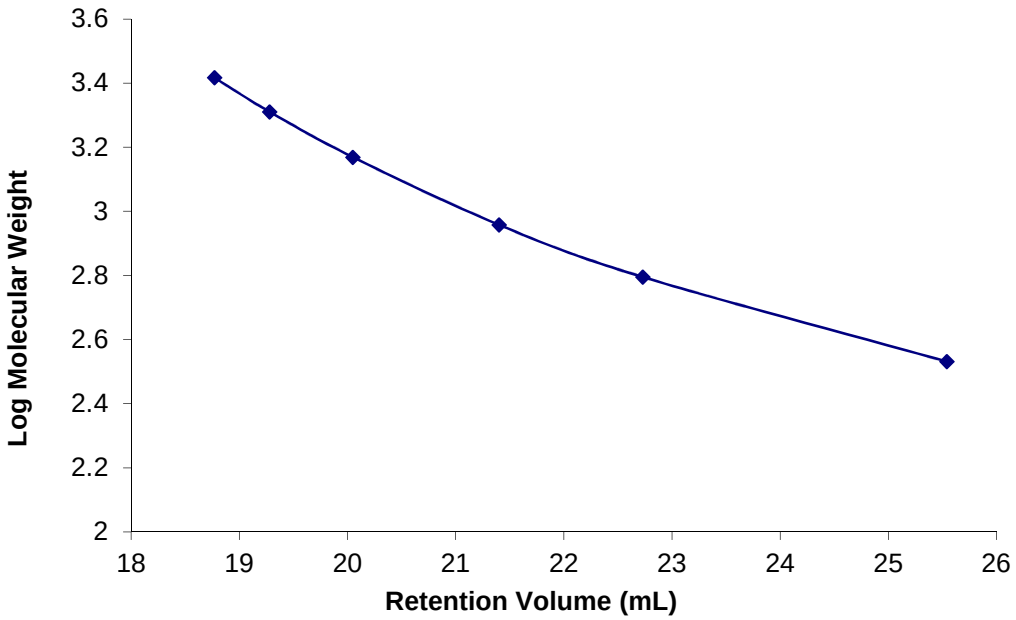

Figure 5. SEC calibration curve obtained from DER 671

2. Separation of DGEDAS$_n$ oligomers by selective solubility

The various mass spectroscopy analyses performed on DGEDAS$_n$ epoxy prepolymer have underlined the presence of numerous oligomers. In the beginning of the project, the only available isosorbide-based epoxy prepolymer was DGEDAS$_n$. In order to reduce the mass distribution of DGEDAS$_n$ and obtain a "pure" epoxy prepolymer (composed of the n = 0 monomer) selective solubility tests were performed on DGEDAS$_n$.

Various solvents were tested. For each solvent tested, 1g of DGEDAS$_n$ epoxy prepolymer was mix under quick agitation with 5 ml of solvent. The solution was filtered and the solvent was evaporated to obtain the soluble compound. These soluble extracts were then tested by SEC analyses to determine which part of DGEDAS$_n$ was solubilized in the solvent tested. The solubility results with various solvents are represented in Table 1.

Superposition of the different SEC analyses is represented in Figure 6.

Solvent	Solubility
Water	Total
THF	Total
Methanol	Partially
Ethanol	Partially
Cyclohexane	Partially
Isopropanol	Partially
Ethyl Acetate	Partially

Table 1. Solubility of $DGEDAS_n$ in various solvents

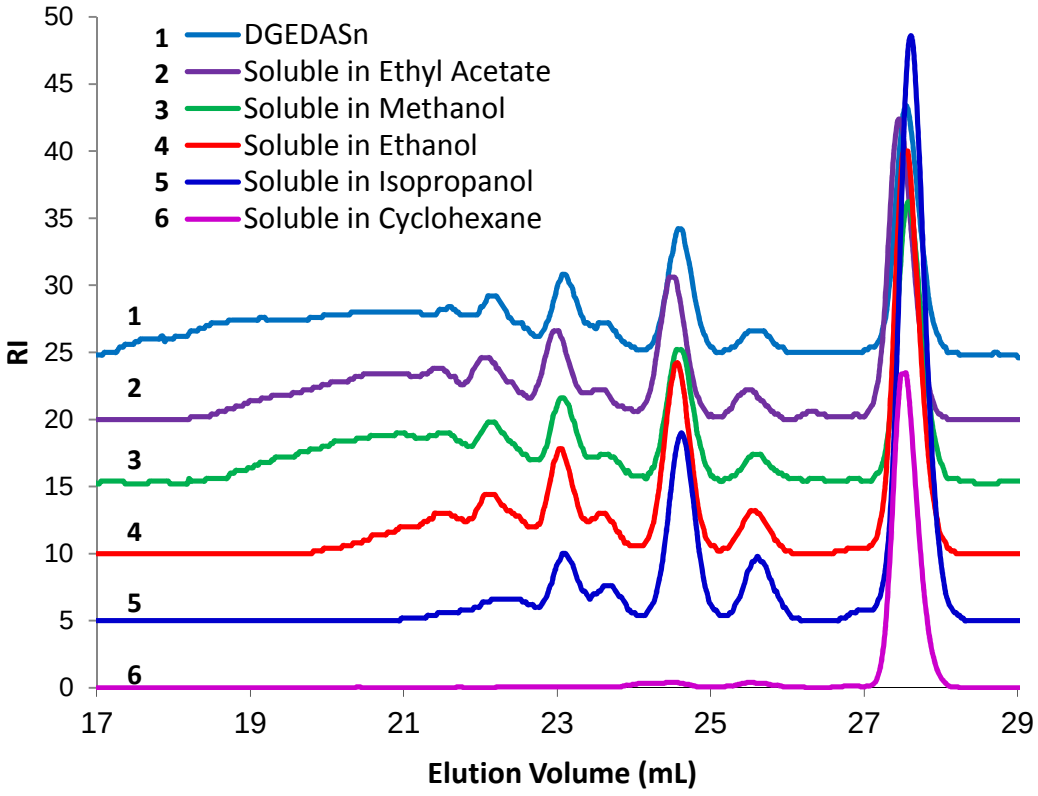

Figure 6. SEC chromatograms superposition of the different extracts

It is difficult to obtain a selective solubility for most of the solvent tested except for cyclohexane. Indeed, only one compound of $DGEDAS_n$ is soluble in cyclohexane as underlined by SEC analysis. As it corresponds to the lowest molar mass compound present in $DGEDAS_n$, this compound should be the pure diglycidyl ether of isosorbide. To confirm this, further NMR analyses were performed on this compound.

Isopropanol is also an interesting solvent as it allows the elimination of $DGEDAS_n$ oligomers of higher molar mass weights.

3. NMR analyses of the oligomeric compound soluble in cyclohexane

The compound solubilized in cyclohexane has been studied by proton NMR (Figure 7). It appears that its NMR spectrum exhibits better resolution that the one obtained for $DGEDAS_n$. Complementary ^{13}C NMR (Figure 8) and DEPT 135 NMR analyses (Figure 9) have been performed on this sample.

Attributions of the different NMR peak are represented in the Figures. All these NMR analyses confirmed that the product solubilized by cyclohexane is only $DGEDAS_0$.

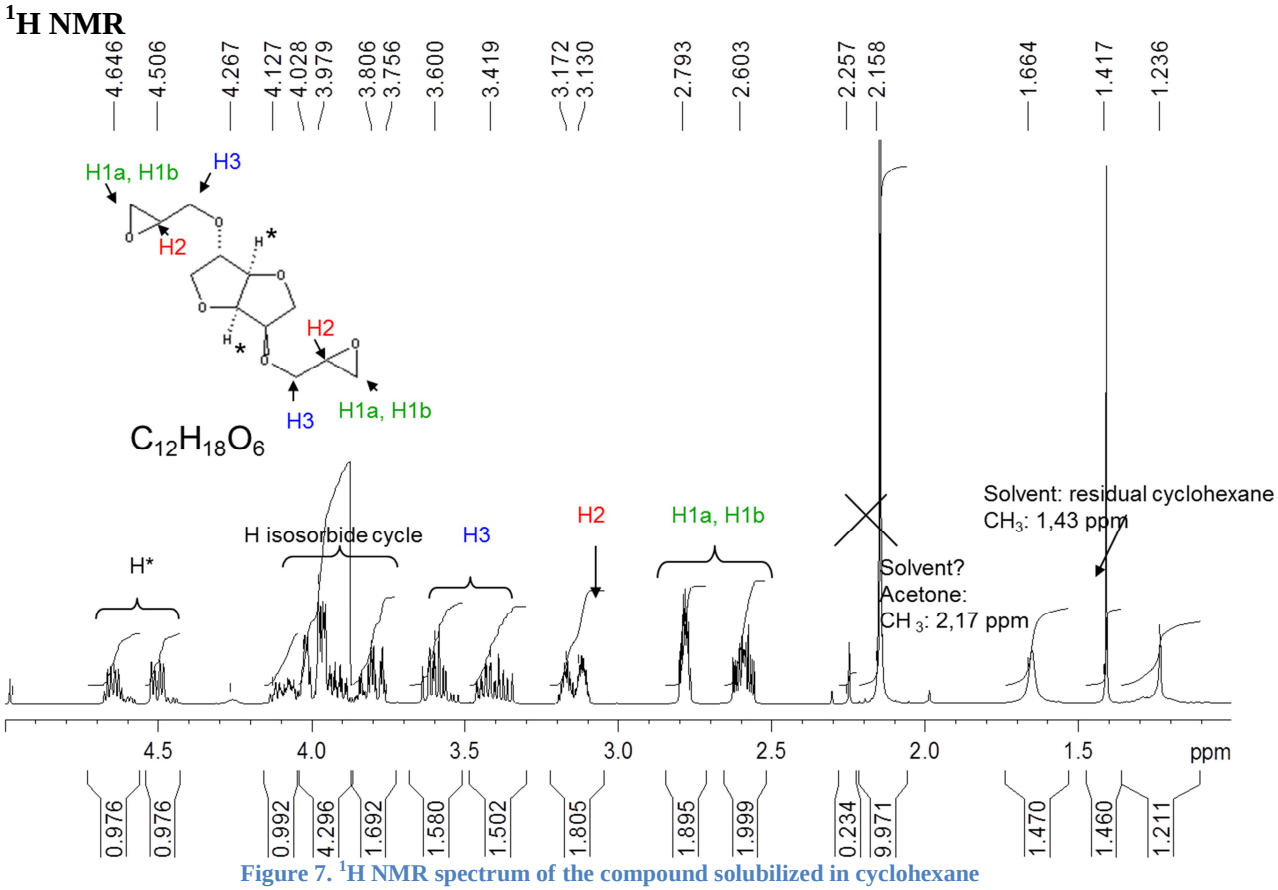

Figure 7. ^{1}H NMR spectrum of the compound solubilized in cyclohexane

^{13}C NMR

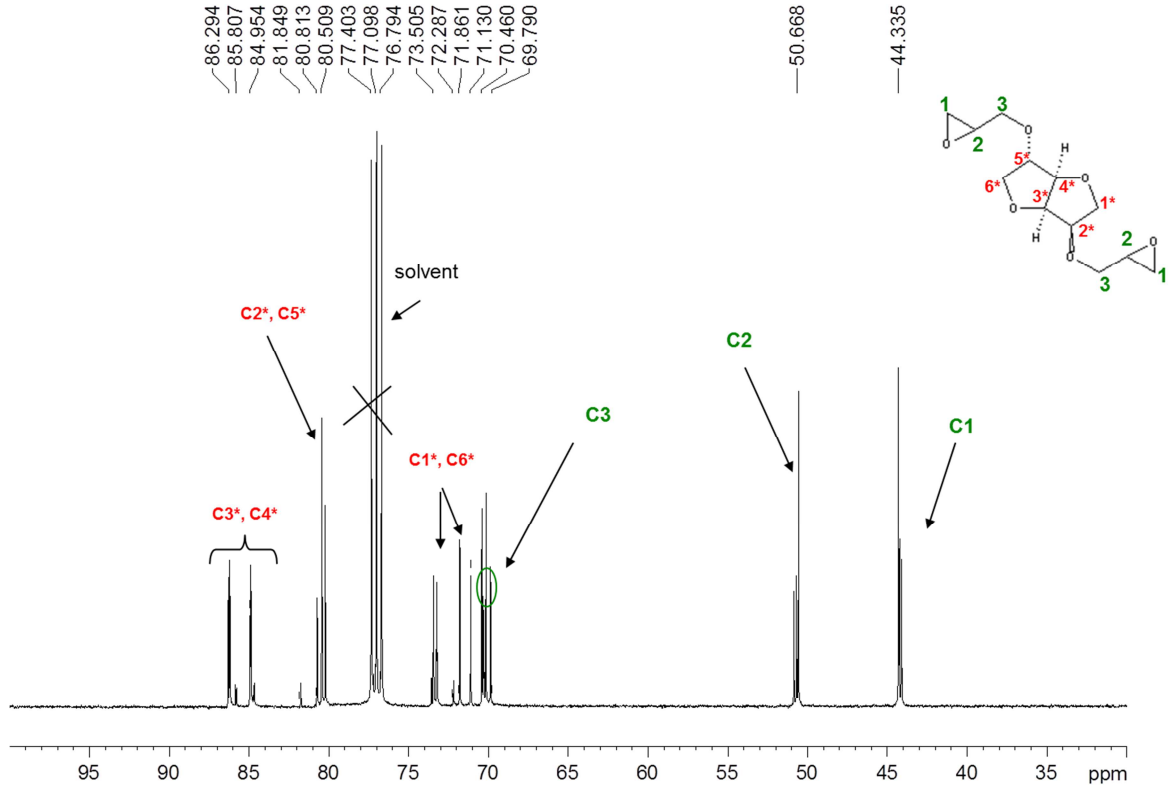

Figure 8. 13C NMR spectrum of the compound solubilized in cyclohexane

DEPT 135 NMR

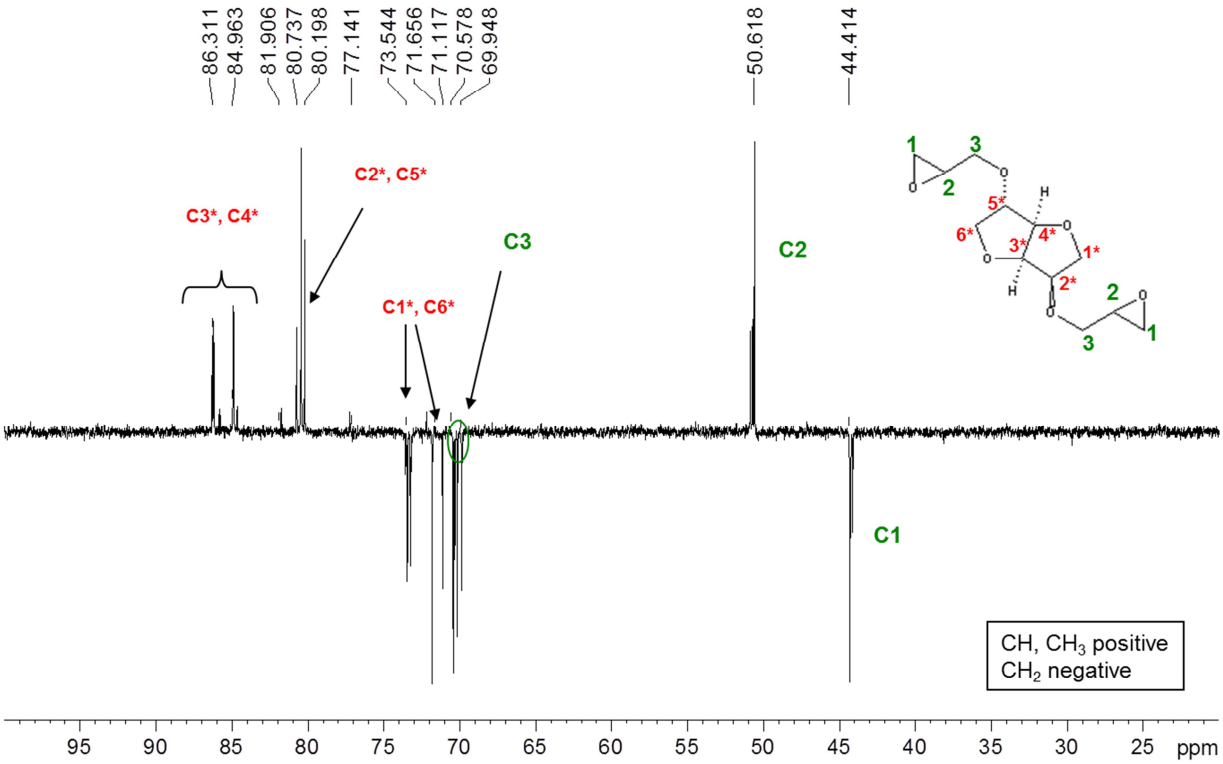

Figure 9. DEPT 135 NMR spectrum of the compound solubilized in cyclohexane

Selective solubilisation of $DGEDAS_n$ in cyclohexane allows us to obtain the pure diglycidyl ether of isosorbide $DGEDAS_0$ from $DGEDAS_n$. Yet, different epoxidation route was performed on isosorbide to have access to the pure diglycidyl ether of isosorbide. This synthetic route is more restrictive than the one used to obtained $DGEDAS_n$ but it has been shown (see Chapter II) that the product synthesized is only composed of $DGEDAS_0$.

II. Complement on NMR characterization for $DGEDAS_0$, $DGEDAS_n$

This part of the Annex presents complementary NMR analyses performed on $DGEDAS_0$ and $DGEDAS_n$ for a better attribution of the chemical shifts especially the ones between 3.2 and 4 ppm.

Peaks corresponding to the epoxy protons (signals between 2.5 and 3.1 ppm) and the protons common to the two isosorbide cycles (signals between 4.4 and 4.6ppm) are isolated and thus easily assigned. In comparison, assignments of the other protons, on the isosorbide cycles and in H3 position, are difficult because of the conformation of the cycle and thus the non-equivalence of these protons.

In order to reconsider the H3 protons attribution, complementary H-H COSY was done on the $DGEDAS_0$ monomer and is represented in Figure 10.

It appears that the H2 protons are coupled with the other epoxy protons (H1a and H1b) and that coupling with the H3 protons appears at different positions. This observation confirms that the conformation of the isosorbide cycles leads to non-equivalence of these protons. It is not possible, to assign separately the remaining protons of the isosorbide cycle and the protons in H3 positions. H3 protons signal is divided and overlaps with isosorbide protons between 3.3 and 4.1 ppm.

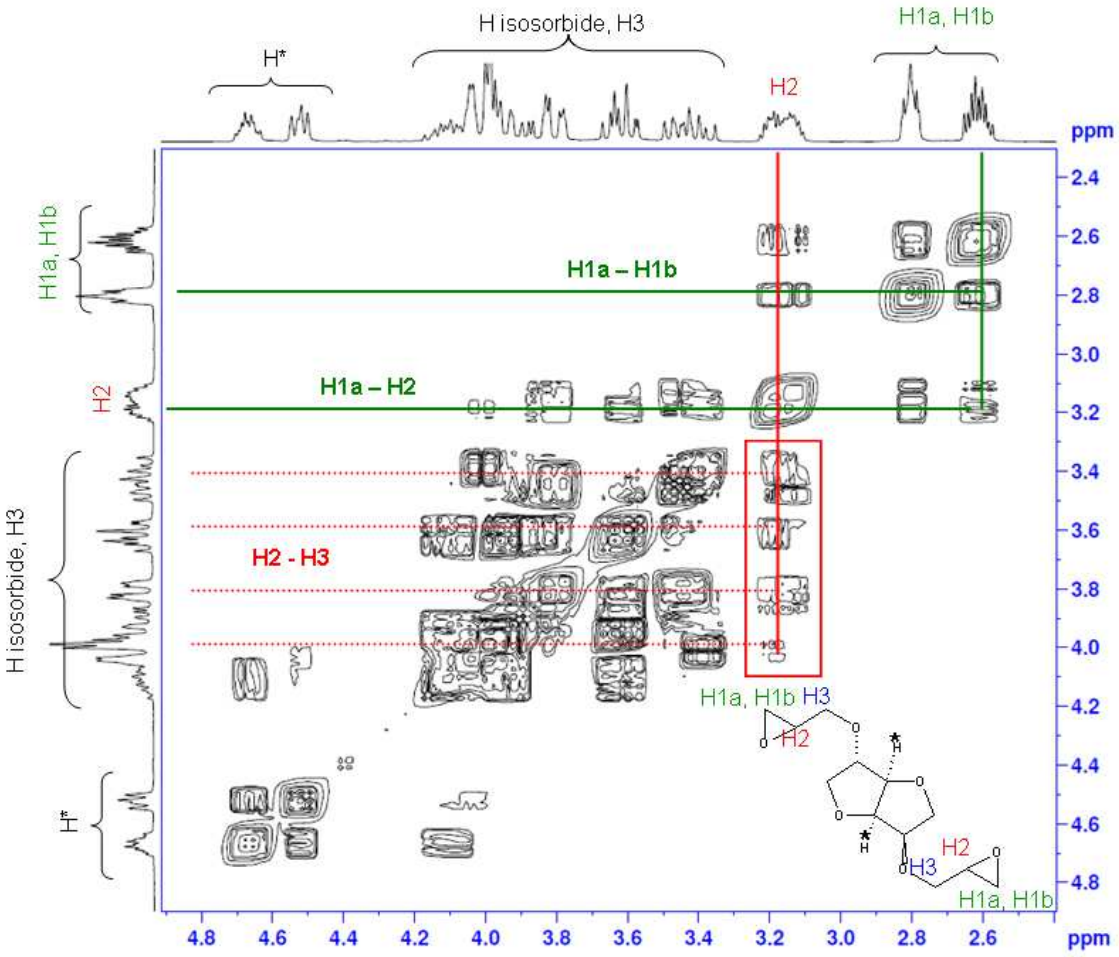

Figure 10. H-H COSY of $DGEDAS_0$

Concerning the ^1H NMR results of $DGEDAS_n$ prepolymer, same conclusion as $DGEDAS_0$ can be done concerning H3 protons, as shown by H-H COSY (Figure 11). Besides due to the broad molar mass distribution of the oligomers, protons are moreover difficult to assign.

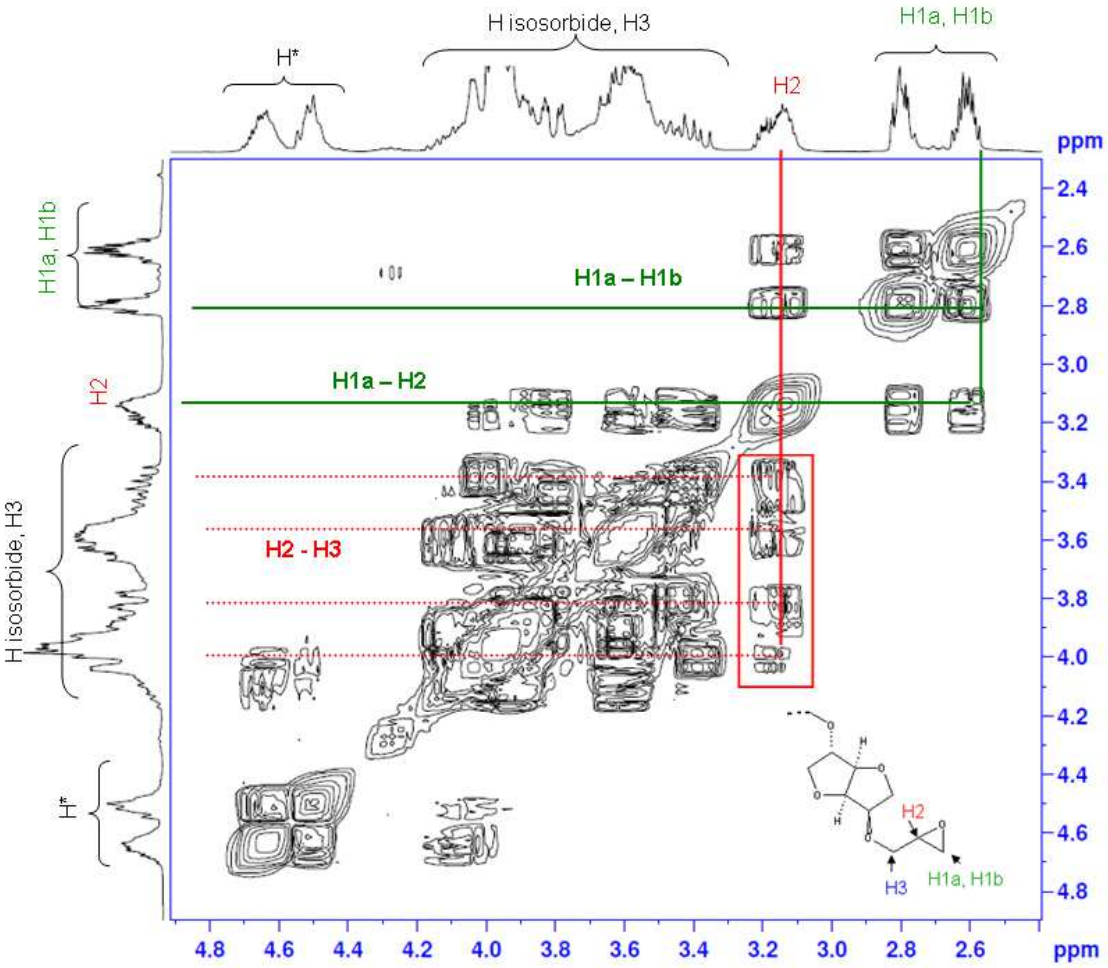

Figure 11. H-H COSY of DGEDAS$_n$

III. Dilatometric measurements of DGEDAS$_0$ – IPD and DGEBA – IPD networks

1. Measurements

The coefficient of linear thermal expansion β was measured at a heating rate of 3°C/min on a Mettler TA (Q400) thermal mechanical analyser. Since β is very small and assuming the sample is isotropic, the coefficient of volume expansion α is given by: $\alpha = 3\beta$.

2. Results

Thermo-mechanical analyses were performed on the bio-based network $DGEDAS_0$ – IPD and the network of reference DGEBA – IPD. TMA curves are represented in Figure 12. Besides, the resulting coefficients of linear thermal expansion (β) determined from the slopes of the dimension change curves are summarized in Table 2.

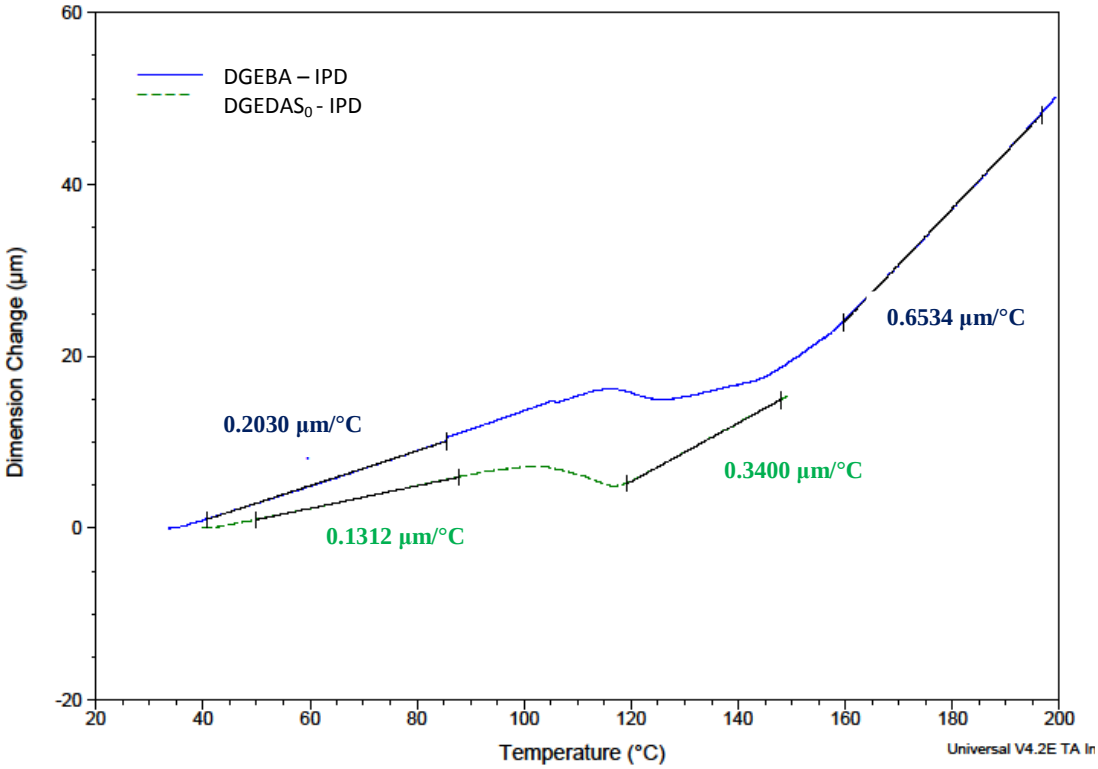

Figure 12. TMA analyses of DGEBA – IPD and $DGEDAS_0$ – IPD networks

Networks	β_1 ($10^{-6}.K^{-1}$) before T_g	β_2 ($10^{-6}.K^{-1}$) after T_g
DGEBA – IPD	60	195
$DGEDAS_0$ – IPD	65	170

Table 2. Thermal expansion coefficient for DGEBA – IPD and $DGEDAS_0$ – IPD networks before and after T_g

It appears that the coefficients of linear thermal expansion of the two networks in the glassy state are slightly lower for DGEBA – IPD network ($60.10^{-6}.K^{-1}$) than DGEDAS0 – IPD network ($65.10^{-6}.K^{-1}$). The coefficients of linear thermal expansion differ in the rubber state. Indeed, DGEBA – IPD exhibit higher value than $DGEDAS_0$ – IPD.

Annex C: Additional results for Chapter III

In Chapter III, the influence of the epoxy prepolymer structure on the reactivity of the systems and the network properties have been studied. Comparison was done between the isosorbide diglycidyl ether $DGEDAS_0$, and two commercial bio-based epoxy prepolymers: the sorbitol polyglycidyl ether (SPGE) and the diglycidyl ether of cardanol (DGECAR). The SPGE prepolymer chosen for the study was the commercial reference Denacol 622. Nevertheless, other commercial grades of SPGE are available and differ in the EEW, the viscosity and the chlorine content. This annex presents additional analyses performed on SPGE – IPD systems and the characterizations of the other grades of Sorbitol Polyglycidyl Ether commercially available.

I. Additional results on SPGE (Denacol 622)- IPD

a) Variation of gel time with r for SPGE – IPD system

Variation of gel time at a temperature, 80°C, with the stoichiometric ratio $r = n_{ah}/n_e$ was performed for SPGE – IPD system. The gel time data are summarized in Table 3. It appears that the augmentation of amine proportion (r > 1) doesn't have an important impact on gel time. Gel times are higher for r = 2 than r = 1, yet the difference is weak and could be the result of the high temperature used for the experiment.

$r = n_{ah}/n_e$	tgel (min)	$\tan\delta_{gel}$	Δ
1	4.73	0.50	0.29
1.5	5.01	0.87	0.45
2	5.90	0.84	0.44

Table 3. Gel time data for SPGE – IPD system at 80°C at various stoichiometry

II. Other commercial references for Sorbitol Polyglycidyl Ether (SPGE)

As presented in the first Chapter, various commercial references are available for Sorbitol Polyglycidyl ether (Table 4). Among these different grades, we focused on the Nagase Chemtex reference: Denacol 622, as this epoxy prepolymer presents the advantage of being insoluble in water (according to TDS). This epoxy prepolymer, called SPGE in our project, was studied in combination IPD and its reactivity, curing behaviour and T_g of the resulting networks were studied using DSC, gel time determination, TMA…

Reference	Producer	EEW (g/eq)	Viscosity (cps, 25°C)	Solubility in water (%)	Chlorine content (%)
EJ 190	JSI Co.	184	4380	N.A.	N.A.
Denacol 611	Nagase chemtex	163	10820	48	13.5
Denacol 612	Nagase chemtex	167	11590	42	13.7
Denacol 614	Nagase chemtex	164	17780	78	11.2
Denacol 614B	Nagase chemtex	171	4450	94	10.1
Denacol 622	Nagase chemtex	191	11440	insoluble	19.1

Table 4. Commercial references of Sorbitol Polyglycidyl ether

In this part of the Annexes, the characterization of the other grades of sorbitol polyglycidyl ether is described: Mass distribution, TGA analyses, determination of T_{g0} of the Denacol 611, 612, 614, 614B, 622. Finally, Denacol 614B – IPD system will be compared with Denacol 622 – IPD system (already presented in Chapter III) in terms of reactivity and glass transition temperatures of the resulting networks.

1. Characterization of the different SPGE grades

a) SEC characterization

The mass distribution of the different grades of sorbitol polyglycidyl ether commercialized by Nagase Chemtex was studied by SEC using THF as elution solvent. The SEC chromatograms of these different grades are represented in Figure 13. It appears that the different epoxy prepolymers studied exhibit almost the same mass distribution; exception

made of Denacol 622 (SPGE, in Chapter III) with a more important part of higher molar mass oligomers. Denacol 622 is among the more viscous SPGE-epoxy prepolymer (viscosity more than 11000 cps at 25°C) and exhibits higher EEW. On the contrary, Denacol 614B is composed of the lower molar mass oligomers as underlined in its SEC chromatography and by its low viscosity (around 4400 cps at 25°C).

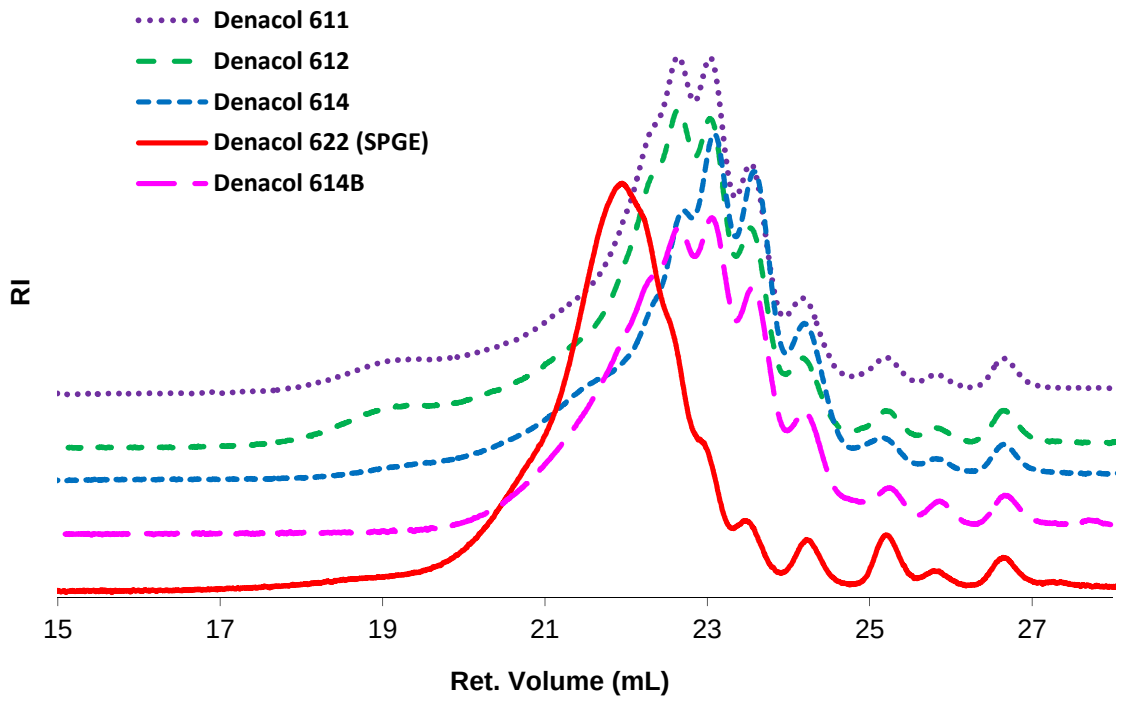

Figure 13. SEC chromatograms of Denacol epoxy prepolymers

b) Determination of T_{g0}

Determination of T_{g0} was performed for the different sorbitol polyglycidyl ether grades by DSC analyses. The DSC thermograms of the different epoxy prepolymers are represented in Figure 14 and values of T_{g0} summarized in Table 5.

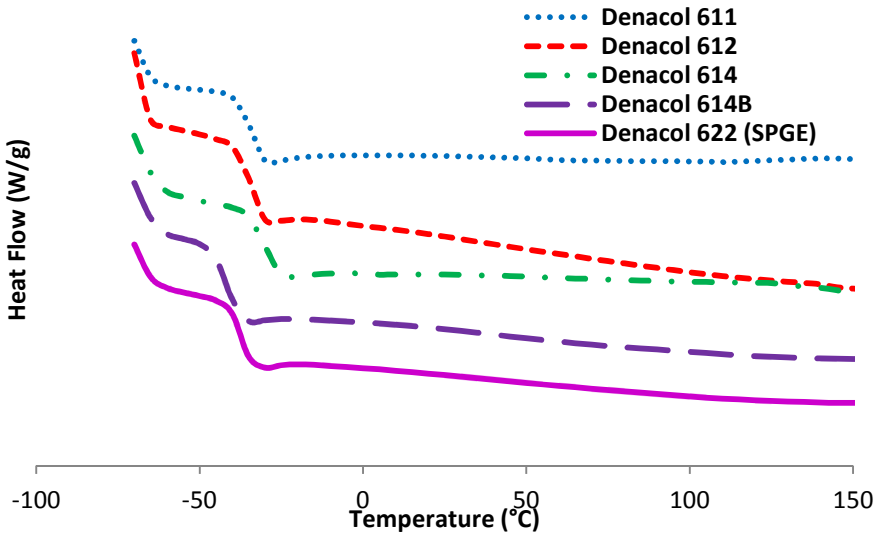

Figure 14. Determination of T_{g0} for sorbitol polyglycidyl ether different grades

Epoxy prepolymer	T_{g0} (°C)
Denacol 611	-38
Denacol 612	-38
Denacol 614	-34
Denacol 614B	-45
Denacol 622 (SPGE)	-40

Table 5. T_{g0} of the different grades of sorbitol polyglycidyl ether

It appears that the different epoxy prepolymers exhibit equivalent T_{g0} around -40°C, except for Denacol 614 that has the higher T_{g0} and Denacol 614B that has the lower T_{g0} around -34°C and -45°C respectively. Indeed, Denacol 614 exhibits the higher viscosity and Denacol 614B the lower one.

c) Thermogravimetric analyses

The mass loss (under inert atmosphere) as a function of temperature for the different sorbitol polyglycidyl ether grades and their derivatives are represented in Figure 15 (a) and (b). The initial degradation temperature ($T_{5\%}$) and the temperature at a maximum rate of degradation (T_{max}) of the different grades are shown in Table 6. The main observation is the slightly higher T_{max} of degradation of Denacol 622 as compared to the others which underlined the presence of less volatile oligomers in Denacol 622 epoxy prepolymer (higher molar mass compounds).

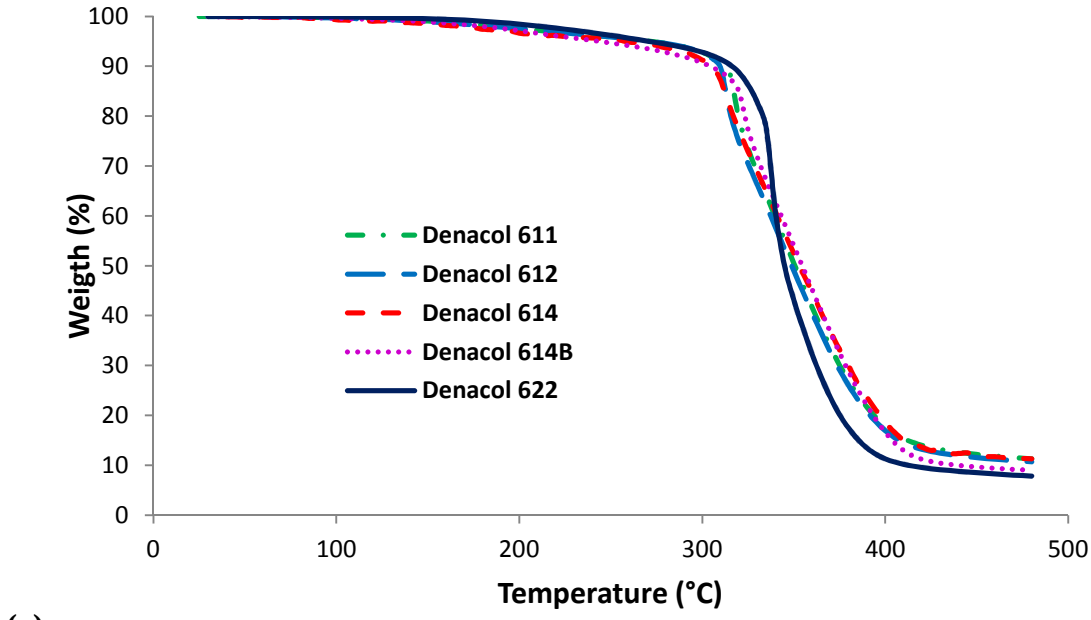

(a)

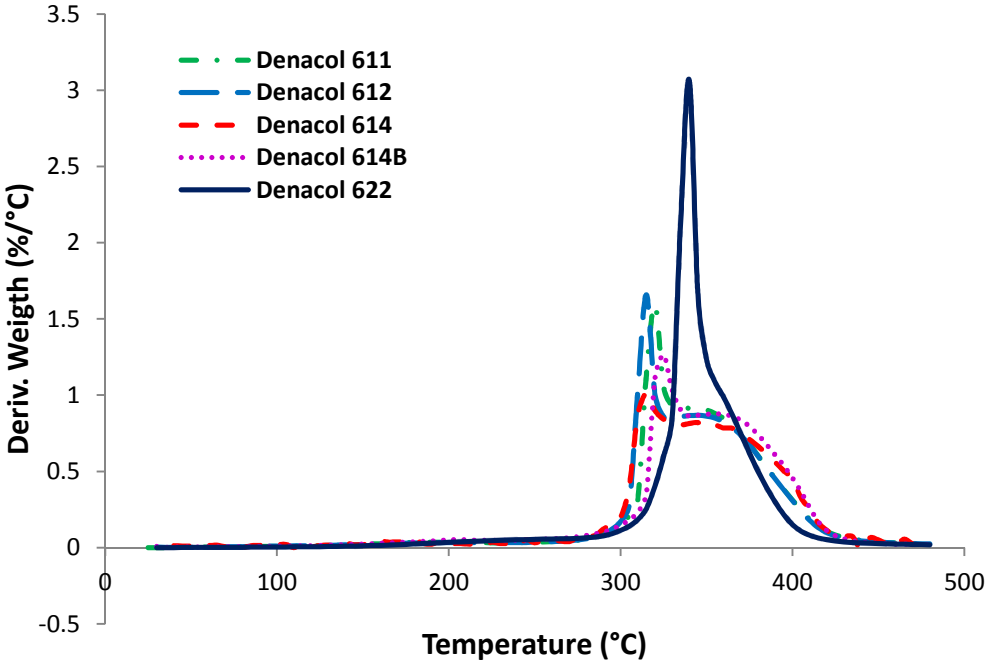

(b)

Figure 15. (a) TGA and (b) DTGA curves of Denacol epoxy prepolymer

Epoxy prepolymer	$T_{(5\%)}$ (°C)	$T_{maximum\ rate}$ (°C)
Denacol 611	270	320
Denacol 612	275	310
Denacol 614	255	315
Denacol 614B	250	322
Denacol 622	270	340

Table 6. Thermal analysis data for the different epoxy prepolymer

2. Study of Denacol 614B – IPD system

The epoxy prepolymer Denacol 622 was the sorbitol polyglycidyl ether with the higher molar mass oligomers, the higher EEW, an acceptable viscosity, not too important as it is with Denacol 614 (around 17000 cps at 25°C). Besides, it has the advantage to be insoluble in water as compared with the others. Therefore, Denacol 622 was chosen for our comparison between the different bio-based epoxy prepolymers (Chapter III). Nevertheless, as compared with Denacol 622, the other sorbitol-based epoxy Denacol 614B is almost totally soluble in water and has the advantage to present lower chlorine content (10.1 %). Therefore, is should of interest to compared the reactivity of Denacol 622 and Denacol 614B – based systems combined with IPD, and the glass transition temperature obtained for the resulting networks.

a) DSC calorimetry study

The DSC thermograms of Denacol 614B – IPD and Denacol 622 – IPD systems at a stoichiometric ratio r = 1 are summarized in Figure 16. The values of T_{g0}, ΔH and T_{peak} of these systems are summarized in Table 7.

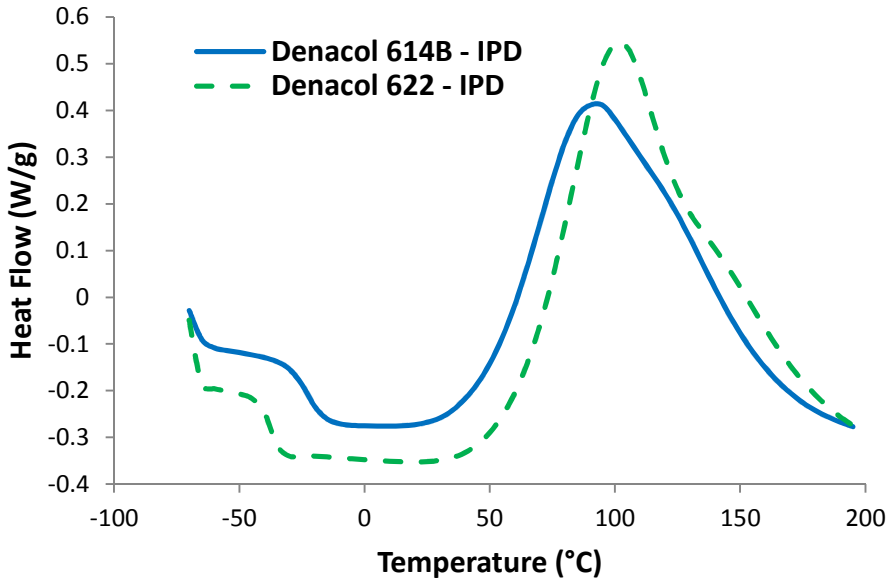

Figure 16. DSC thermograms for Denacol 614B – IPD and Denacol 622 (SPGE) – IPD system

System	T_{g0} (°C)	ΔH (kJ/g)	ΔH (kJ/ee)	T_{peak} (°C)
Denacol 614B – IPD	-30	305	65	93
Denacol 622 (SPGE) – IPD	-41	338	79	101

Table 7. DSC results for Denacol 614B – IPD and Denacol 622 (SPGE) – iPD systems

It appears that T_{g0} of Denacol 622 – IPD is lower than the one obtained for Denacol 614B – IPD system. Denacol 614B – IPD is more reactive than Denacol 622 – IPD with a lower value of T_{peak}, 93°C and 101°C respectively.

Concerning the exothermy of the systems, it appears that Denacol 614B – IPD exhibits lower ΔH as compared with Denacol 622 – IPD.

b) Determination of glass transition temperatures

Values of glass transition temperatures were obtained by DSC analyses. Not much difference is observed for the glass transition temperatures of Denacol 614B – IPD and Denacol 622 – IPD networks; the two networks exhibit equivalent T_g around 100°C.

Nevertheless, to focus on the influence of the chlorine content on the network properties the evolution of T_g with r for Denacol 614B – IPD, could be of interest for further investigations.

Annex D: Additional results for Chapter IV

This part of the annexes is dedicated to the additional results related to the chapter IV. First, complementary result on $DGEDAS_n$ – D230 system is given with the study of the influence of stoichiometry on glass transition temperatures for this system.

I. $DGEDAS_n$ – D230 system

1. Influence of stoichiometry on glass transition temperatures

As it was done for IPD curing agent, the influence of stoichiometry on glass transition was studied using D230 as curing agent for $DGEDAS_n$ epoxy prepolymer. Different $DGEDAS_n$ – D230 networks were prepared at various stoichiometry $r = n_{ah}/n_e$ to verify that this system presents only addition mechanism when combined also with another curing agent than IPD. The T_g of the networks were determined at each ratio r by DSC. The evolution of T_g with r is plotted in Figure 17. As for $DGEDAS_n$ – IPD, the maximum T_g attainable is for r = 1. This confirms that for $DGEDAS_n$- D230 epoxy-amine system no side reactions occur.

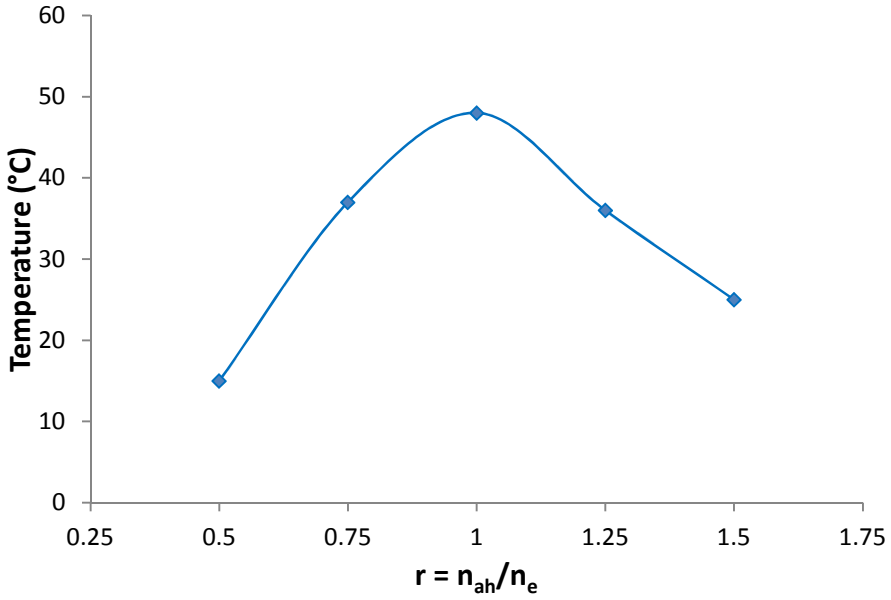

Figure 17. Glass transition temperature versus r for $DGEDAS_n$ – D230 networks

Using an aliphatic curing agent such as D230, a maximum T_g is always obtained for a stoichiometric ratio r = 1, which confirms that DGEDAS based prepolymers are not at the origin of side reactions; the only parameter that could promote such side reactions should be the curing agent.

Annex E: Additional results for Chapter V

Annex E gives additional results for the chapter V dedicated to the study of water absorption of the different systems. First, trial to reduce the hydrophilicity of $DGEDAS_n$ is presented with the reduction of –OH groups initially present in $DGEDAS_n$ oligomers structure. Then, various formulations based on DGEBA – HA (epoxy-amine system used in Rossignol application) containing different amount of $DGEDAS_n$ will be characterized. Finally, study on sorbitol based epoxy network (Denacol 614B – IPD) affinity with water will be discussed in this annex.

I. Influence of the polarity of immersion solvent

To study the influence of the polarity of the immersion solvent, $DGEDAS_n$ – HA networks were immersed in various solvents that exhibit different polarity. The Table 8 presents the different solvent tested and their respective polarity according to Hansen solubility parameters [1].

Solvent	Polarity
Water	16.0
Methanol	12.3
Ethanol	8.8
THF	8.2

Table 8. Solvent polarity

As previously described, networks break up totally in water. Concerning methanol, fragments are observed after 3 h of immersion. Nevertheless, the fragmentation is less rapid than in water and the sample's core remains. No significant change is observed after one week. Using ethanol as immersion solvent brings very few fragmentation. No significant change is also observed after a week. Finally, no fragmentation is observed in THF.

For every solvent tested, the solution of immersion was collected, filtered and the solvent was evaporated at 70°C. Solubilized compound in methanol represents almost 1 % of the initial sample weight and less than 0.1 % of the network was solubilized in ethanol.

Solubilized products were analysed by SEC. Nevertheless, products resulting from the solubilisation in water, and methanol were not soluble in THF. Collected compound using ethanol as solvent was however soluble in THF and was analysed by SEC. The SEC chromatograms of this compound and the one of $DGEDAS_n$ are shown in Figure 18.

First, it appears that a single product is predominantly solubilized in ethanol as SEC chromatogram presents a major peak at an elution volume of 23.3 mL. This product can correspond to one oligomer of $DGEDAS_n$ at an elution volume of 23.6 mL. The molar mass of these two compounds were calculated using a high molar DGEBA calibration curve[2] and were found equal to 503 g/mol and 466 g/mol respectively. The oligomer of 466 g/mol can be the $DGEDAS_n$ oligomer at n = 1 (2A + 3B)[3]. The product solubilized in ethanol had 37 g/mol more than 2A + 3B $DGEDAS_n$ oligomer. No further information on this product structure was obtained.

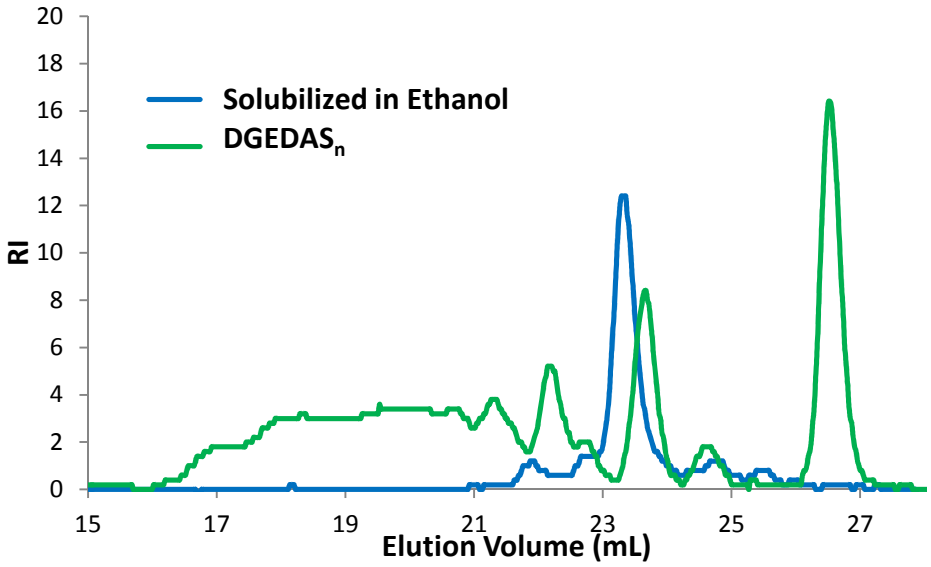

Figure 18. Superposition of SEC chromatograms of the solubilized compound in Ethanol and the epoxy prepolymer $DGEDAS_n$

[2] See Calibration curve in Annexe B
[3] See Chapter II

II. Reduction of the hydrophilicity of DGEDAS$_n$

It has been underlined in the chapter IV, that the –OH groups present in the DGEDAS$_n$ oligomers structure, as shown in Figure 19, increased the affinity of water of the DGEDAS$_n$-based networks.

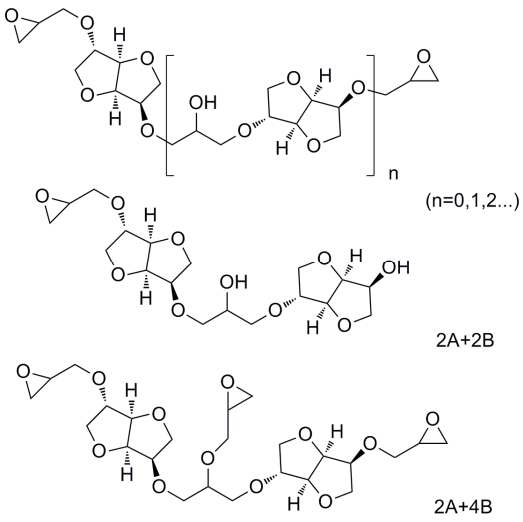

Figure 19. Structure of oligomers in DGEDAS$_n$ (see Chapter II)

Therefore in order to improve water resistance of the DGEDASn-based networks trial was done to block the –OH groups by reaction of p-totyl isocyanate (pTI) with DGEDAS$_n$ in stoichiometric ratio as represented in Figure 20. As a remark, a hydroxyl number I_{OH} = 105 mg/gKOH was determined by titrimetry for DGEDAS$_n$.

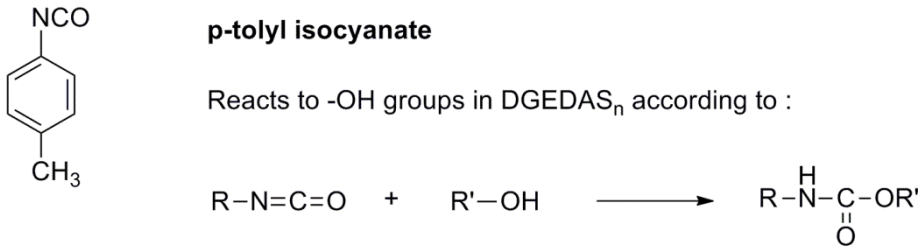

Figure 20. Structure of PTI (p-tolyl isocyanate) and reaction with –OH groups

The pTI was mixed vigorously with the epoxy prepolymer DGEDAS$_n$ at 60°C. The addition of pTI to DGEDAS$_n$ was followed by FT-IR a drop of reactive mixture was put between two KBr pellets and heated at 60°C. Figure 21 represents the evolution of pTI addition on DGEDAS$_n$ followed by FT-IR. It appears that the –OH groups decreased (3400 cm^{-1}) with the N=C=O groups (2270 cm^{-1}). After 30 min, the N=C=O absorption band

disappeared. Besides, the FT-IR analysis shows that the epoxy groups were not affected by the addition of pTI.

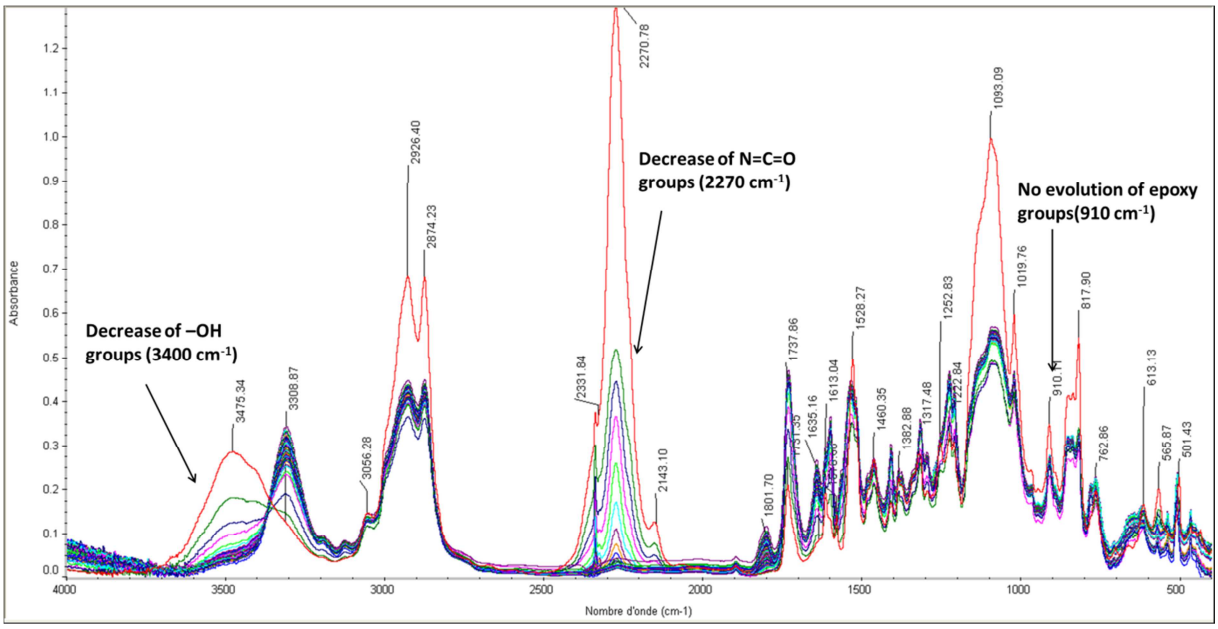

Figure 21. Evolution of pTI addition on $DGEDAS_n$ followed by FT-IR

We manage to block the –OH groups of $DGEDAS_n$ oligomers, nevertheless, the viscosity of the resulting product was too high to correctly use it, and therefore no crosslink with amine curing agents were performed.

III. Incorporation of $DGEDAS_n$ in DGEBA – HA formulations – Influence on the water affinity of the networks

For the NAFI project application (ski boards) it was interesting to incorporate bio-based epoxy prepolymer $DGEDAS_n$ in their formulation. Nevertheless, it has been underline that $DGEDAS_n$ has an important affinity with water. Therefore, investigations were performed to determine the correct amount of $DGEDAS_n$ that could be incorporated in the formulation without an important loss of properties.

1. DSC calorimetry study

Various formulations were studied comprising from 20 wt % to 80 wt % of $DGEDAS_n$, and were compared with fully DGEBA – HA and $DGEDAS_n$ – HA systems. This systems were prepared in order to keep the epoxy/amine ratio equal to r = 0.27 (specific stoichiometric ratio of DGEBA – HA system as explained in Chapter IV). The DSC thermograms of the different systems studied are superposed in Figure 22, and their curing characteristics are summarized in Table 9.

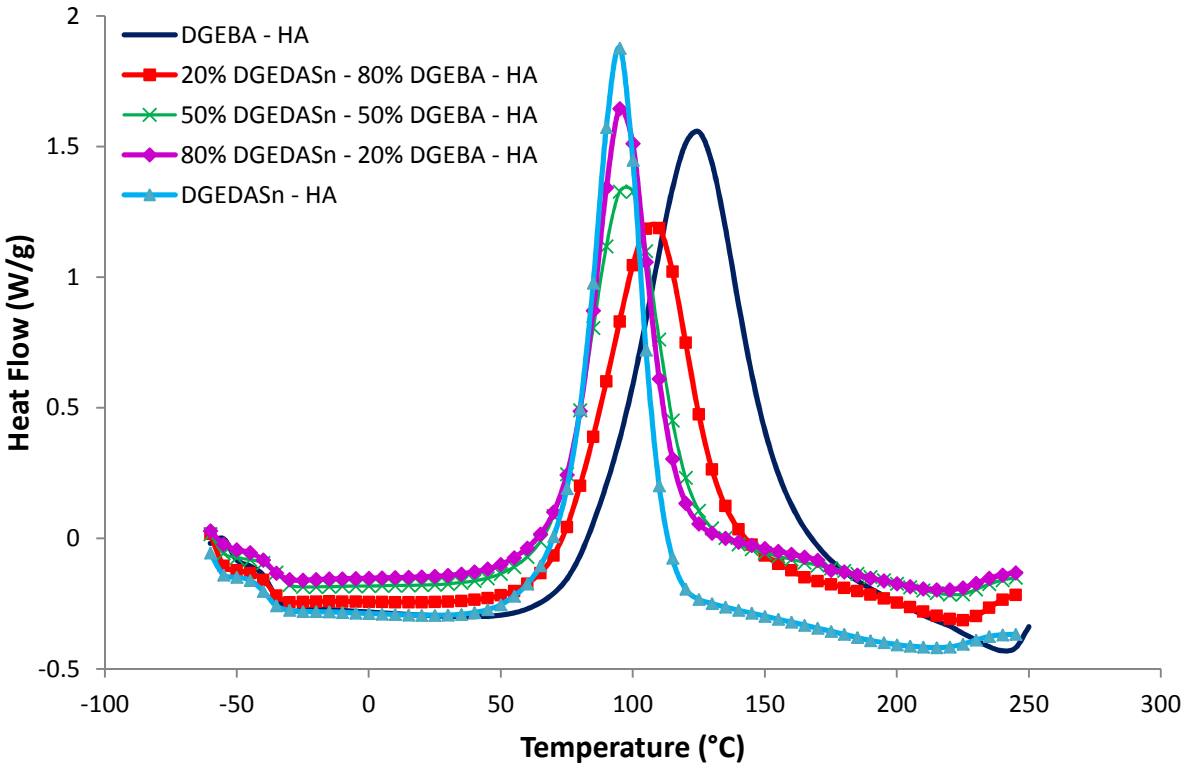

Figure 22. DSC calorimetry study of DGEBA – HA formulations with different amount of $DGEDAS_n$

% $DGEDAS_n$	T_{g0} (°C)	$\Delta H_{reaction}$ (J/g)	T_{peak} (°C)
0	-40	430	125
20	-40	372	108
50	-38	323	98
80	-42	297	96
100	-30	307	98

Table 9. DSC curing data of DGEBA – HA formulations with different amounts of $DGEDAS_n$

It appears that the increasing amount of $DGEDAS_n$ incorporated to the system shifted the maximum peak temperature to lower values (down to 98°C from 50 % of $DGEDAS_n$ added to the formulation). Besides, the reactions became less exothermic with the increasing incorporation of $DGEDAS_n$.

2. Determination of T_g

The glass transition temperatures of the different systems were determined using DSC analyses and are summarized in Table 10. Their evolution with the amount of $DGEDAS_n$ is represented in Figure 23. It appears that T_g decreased up to ~60°C from 50 wt % of $DGEDAS_n$ incorporated. The addition of 20 % of $DGEDAS_n$ in the system allows keeping a T_g acceptable for ski board application.

% $DGEDAS_n$	T_g (°C)
0	90
20	81
50	60
80	64
100	60

Table 10. Evolution of glass transition temperatures with $DGEDAS_n$ %

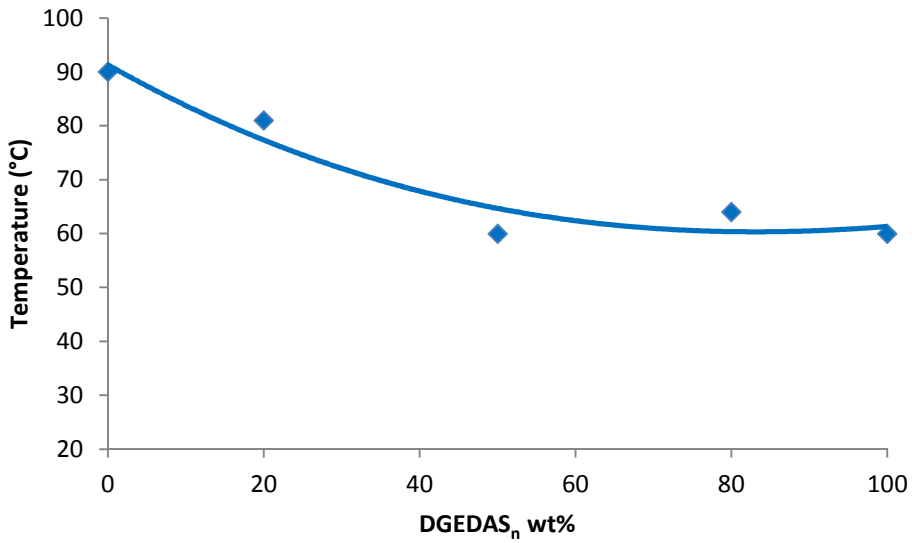

Figure 23. Evolution of T_g with the amount of $DGEDAS_n$ in the DGEBA – HA system

3. Water affinity of the networks

For first information on water affinity of DGEBA – HA systems with different amounts of $DGEDAS_n$, normalized samples were aged in distilled water at room temperature and their weight gain absorption after 5 days of immersion are summarized below (Table 11). Besides, the evolution of water absorption after 5 days with the amount of $DGEDAS_n$ incorporated to the system is represented in Figure 24.

% $DGEDAS_n$	Weight gain (%)
0	0.94
10	1.65
20	2.96
30	6.47
40	11.98
50	15.01
80	Fragmentation
100	Fragmentation

Table 11. Water absorption after 5 days of immersion in distilled water at RT for DGEBA – HA networks with different amount of $DGEDAS_n$

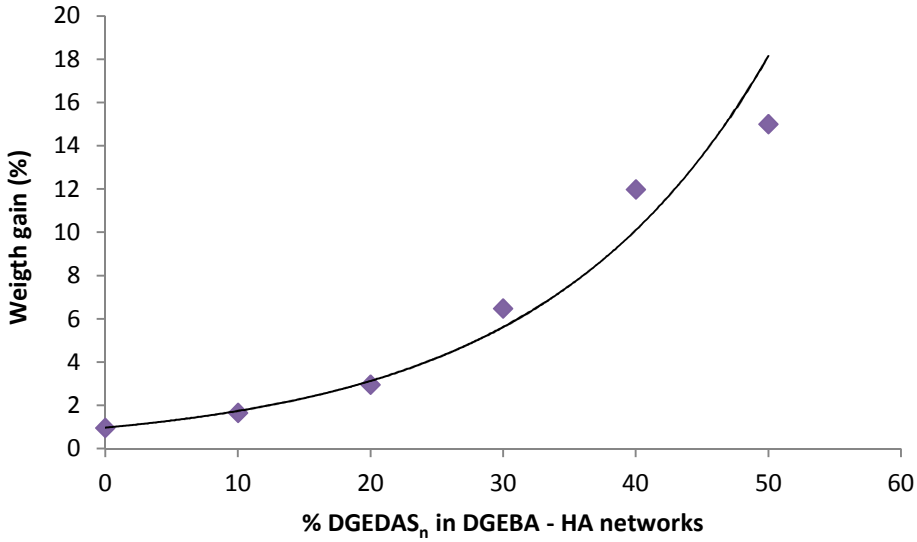

Figure 24. Evolution of water absorption of DGEBA – HA networks containing DGEDASn in function of the amount of DGEDASn in the formulations

It appears that degradation occurs for networks containing more than 50 % of $DGEDAS_n$ epoxy prepolymer. Besides, the evolution of water absorption with the amount of $DGEDAS_n$ seems to be parabolic rather than linear.

Water absorption kinetics were performed for some DGEBA – $DGEDAS_n$ networks (20 wt% of $DGEDAS_n$ and 50 wt % of $DGEDAS_n$) immersed in distilled water at room temperature and they were compared to DGEBA – HA as a reference. Both partially bio-based epoxy systems exhibit higher water absorption than the reference DGEBA – HA. If the water sorption curve of DGEBA – $DGEDAS_n$ (20 %) – HA seems to be Fickian it is not the case for the water sorption of DGEBA – $DGEDAS_n$ (50 %) – HA. Some irreversible hydrolysis of the network has occurred.

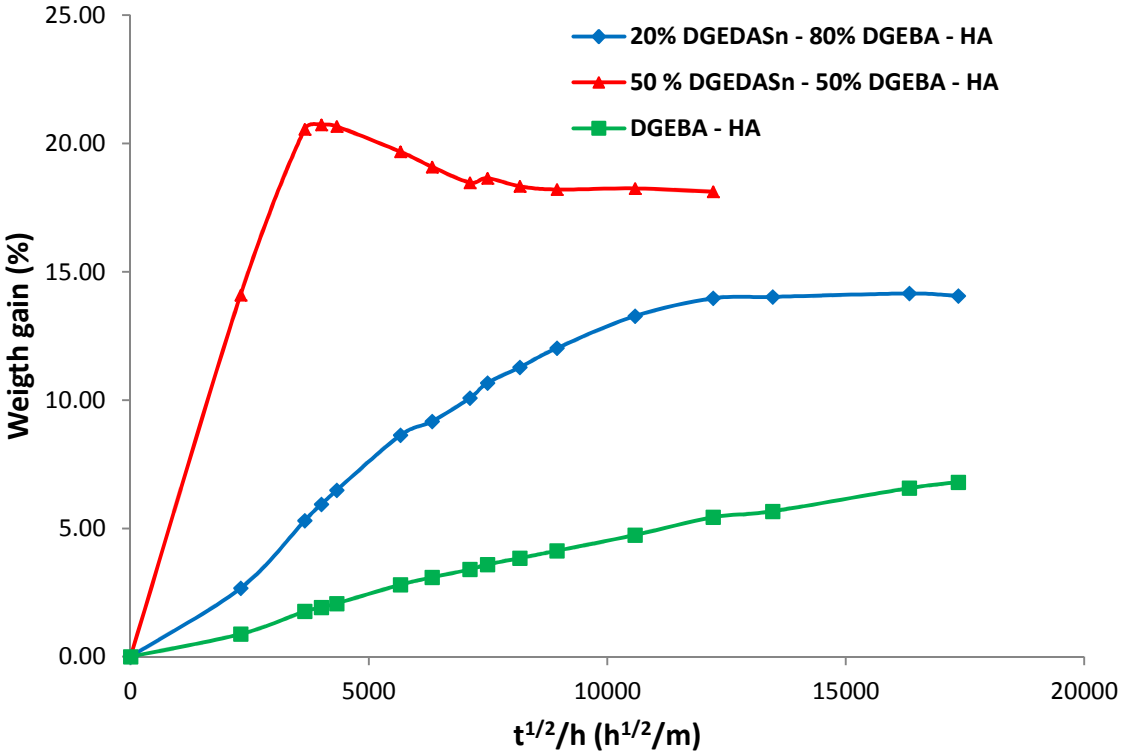

Figure 25. Water soption kinetics for DGEBA – HA with different amount of $DGEDAS_n$ (Samples immersed in distilled water)

Therefore, it appears that the DGEBA – HA system comprising 20 wt % of $DGEDAS_n$ could be a good compromise to keep interesting network properties and avoid water degradation.

IV. Comparison of the water absorption of Denacol 614B – IPD and Denacol 622 (SPGE) – IPD networks

Finally, investigation was also performed on the water sorption kinetic on the other sorbitol polyglycidyl ether reference (Denacol 614B), that is an epoxy prepolymer soluble in water, with a lower Cl content than the Denacol 622 used in our study. Water sorption kinetics (Figure 26) performed on the networks immersed in distilled water at room temperature show that the Denacol 614B – IPD is more sensitive to water than Denacol 622 – IPD network. This could be explaining by more hydrophilic groups (such as –OH) as Denacol 622 and Denacol 614B differs by their epoxy equivalent. Besides, as underlined in Table 4, Denacol 614B contains less Cl content that could act as hydrophobic groups and are more important in Denacol 622 reference. Influence of the Cl content on the network structure and the resulting water affinity is again underlined.

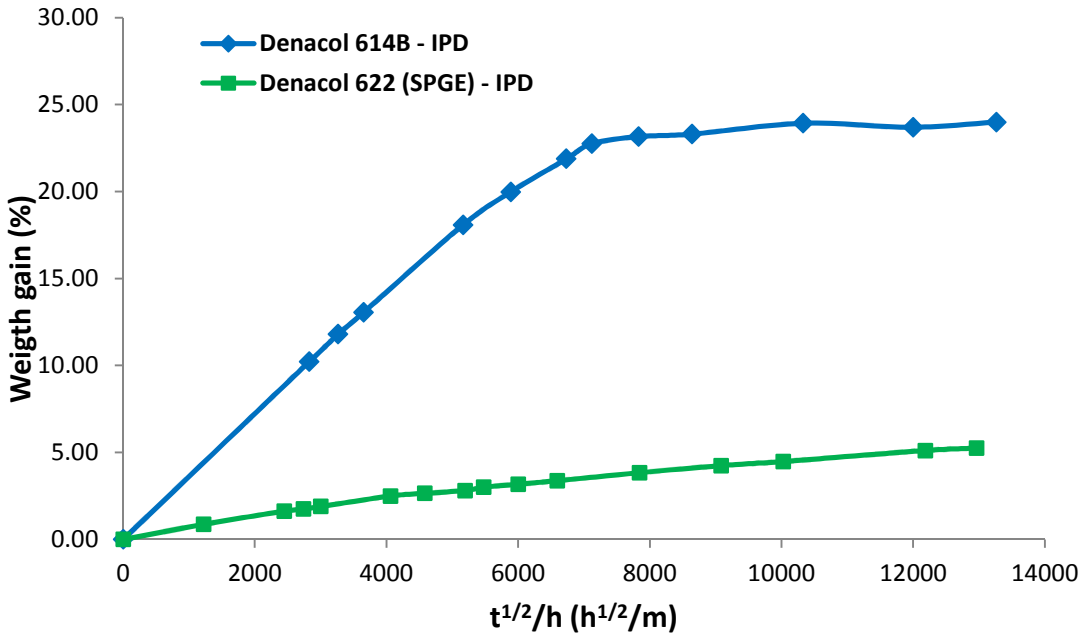

Figure 26. Water sorption kinetics for Denacol 614B – IPD and Denacol 622 (SPGE) – IPD (Samples immersed in distilled water)

Extended abstract in French – Résumé étendu

I. Introduction

Récemment, les polymères obtenus à partir de ressources renouvelables font l'objet de nombreuses investigations [1-3]. Le remplacement des matériaux plastiques actuels par des matériaux bio-sourcés est intéressant à la fois du fait de la diminution des ressources pétrolières mais aussi à cause de la toxicité de certains précurseurs communément utilisés. En effet, parmi les matériaux thermodurcissables [4], et plus précisément les réseaux époxy, le monomère le plus utilisé est le Diglycidyl Ether de Bisphénol A [5], dérivé de ressources pétrolières et dont la toxicité du précurseur, Bisphénol A, a été démontrée.

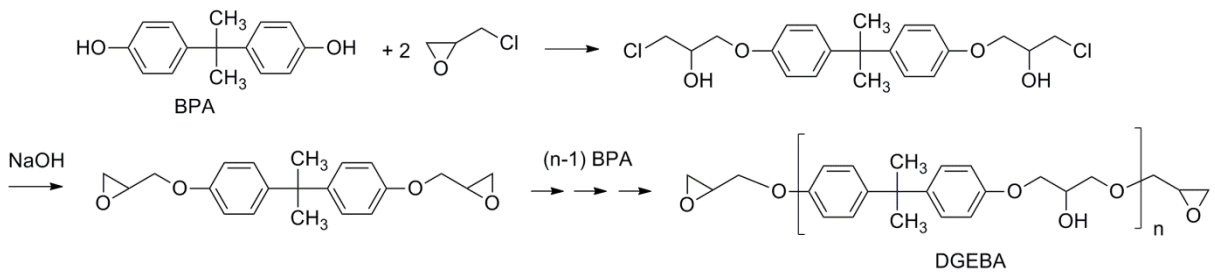

Figure 1. Synthèse du DGEBA principal prépolymère époxy à partir du Bisphénol A

Dans le cadre du remplacement des réseaux époxy obtenus à partir de DGEBA par des réseaux bio-sourcés, les premières ressources testées ont été les huiles végétales [6-8].

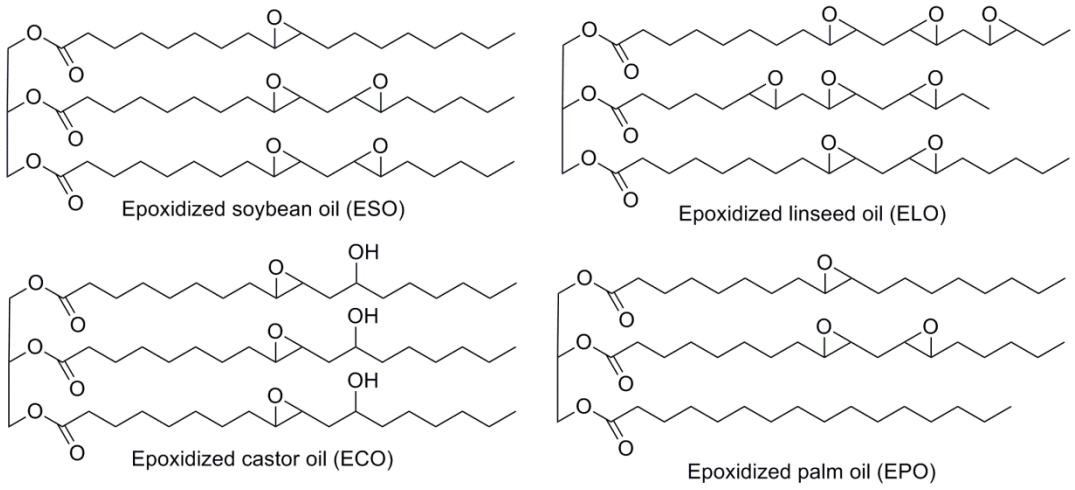

Figure 2. Structure des principales huiles végétales époxidées étudiées en remplacement de DGEBA

Abondantes et intéressantes aussi en termes de coût, les huiles végétales peuvent être époxydées (Figure 2) et ont été utilisées pour le développement de matériaux époxy. Néanmoins, les propriétés thermomécaniques des réseaux ainsi obtenus (T_g, modules…) sont faibles du fait de la structure de ces triglycérides (longues chaines aliphatiques). Ces matériaux peuvent difficilement concurrencer ceux obtenus à partir de DGEBA et être utilisés pour des applications de hautes-performances comme dans les composites.

Récemment, d'autres précurseurs bio-sourcés ont été testés pour la synthèse de monomères époxy tels que le cardanol dérivé de noix de cajou (Figure 3) dont la structure aromatique avec une longue chaine aliphatique peut s'avérer intéressante [9].

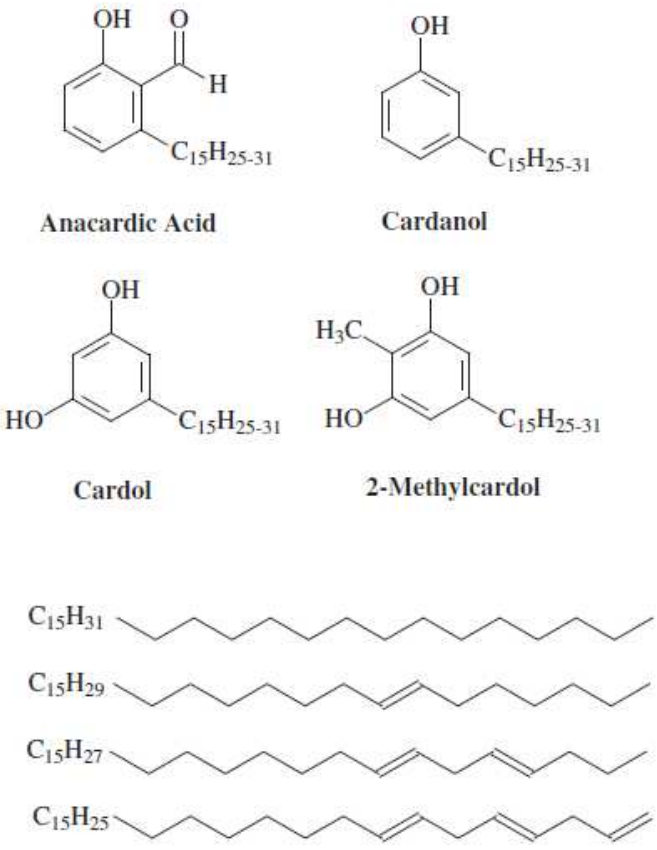

Figure 3. Structure du cardanol

De même, des précurseurs dérivés des polysaccharides tels que le sorbitol [10] et l'isosorbide [11, 12] (Figure 4) ont aussi étés testés. L'isosorbide présente une structure courte et cyclique qui laisse envisager des propriétés intéressantes [13].

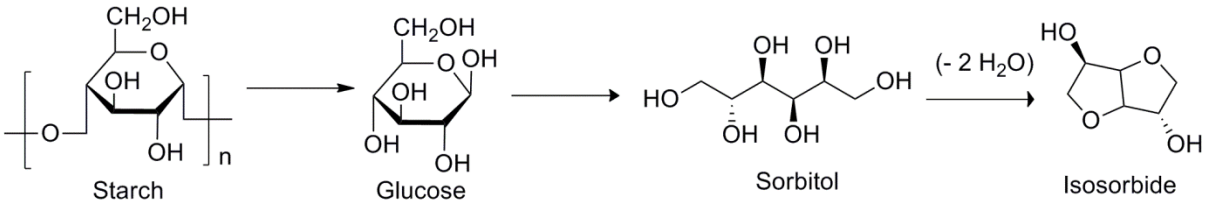

Figure 4. Glucose, sorbitol et isosorbide dérivés de l'amidon

Nous nous sommes intéressés dans notre étude, au remplacement du prépolymère époxy DGEBA par des prépolymères époxy obtenus à partir de l'**isosorbide** (selon deux voies de synthèse) et des prépolymères époxy bio-sourcés commerciaux dérivés du **sorbitol** et du **cardanol**.

II. Prépolymères époxy bio-sourcés

1. Différents prépolymères époxy étudiés

a) Prépolymères époxy dérivés de l'isosorbide

L'isosorbide est produit par la société Roquette, néanmoins son dérivé époxydé n'est pour le moment pas disponible commercialement. La synthèse du diglycidyl éther d'isosorbide a été réalisée selon deux voies de synthèses distinctes représentées ci-dessous [14]. Une voie classique, industriellement utilisé pour la production de la majorité des dérivés époxidés, faisant intervenir l'épichlorhydrine (Figure 5) permet d'obtenir l'isosorbide époxydé $DGEDAS_n$ avec un équivalent époxy de 184g/eq. La deuxième synthèse, via la formation d'un dérivé allylique (Figure 6), est plus contraignante mais permet d'obtenir le pur diglycidyl éther d'isosorbide $DGEDAS_0$ (sans les différents oligomères potentiellement obtenus lors d'une époxydation classique comme c'est le cas pour $DGEDAS_n$). $DGEDAS_0$ est obtenu avec un équivalent époxy de 143 g/eq.

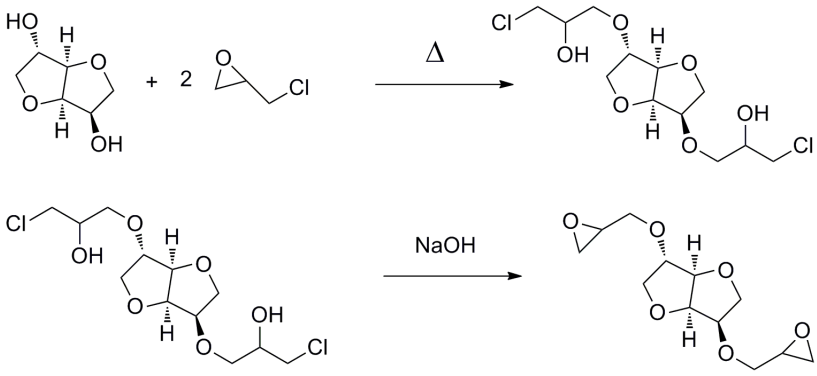

Figure 5. Synthèse de l'isosorbide diglycidyl ether – voie classique avec épichlorhydrine

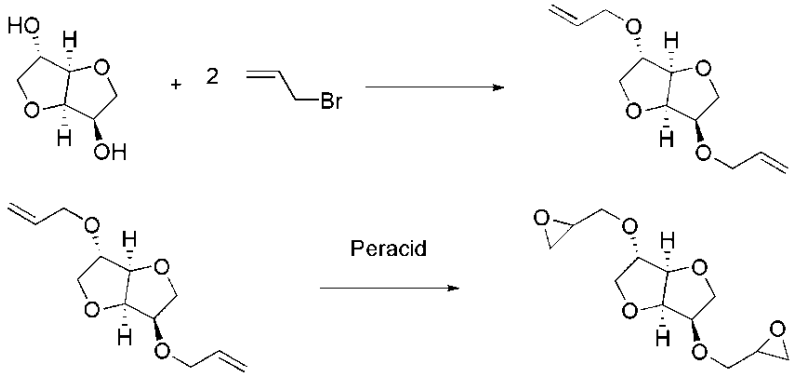

Figure 6. Synthèse de l'isosorbide diglycidyl ether – intermédiaire allylique

b) Prépolymères époxy bio-sourcés commerciaux

Le sorbitol époxydé (SPGE) ainsi que le cardanol époxydé (DGECAR) sont des produits industriels dont la structure simplifiée est représentée ci-dessous avec des équivalents époxy respectifs de 191 g/eq et de 490 g/eq.

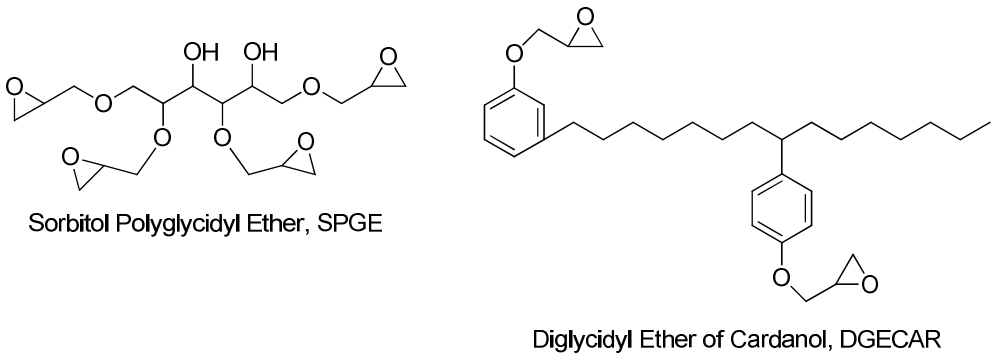

Figure 7. Structures simplifiées du sorbitol polyglycidyl éther SPGE et du diglycidyl éther of cardanol DGECAR

2. Caractérisations des différents prépolymères époxy bio-sourcés

Les différents prépolymères époxy utilisés ont été caractérisés (GPC, ESI-TOF, RMN ^{1}H et ^{13}C, FT-IR, ATG…). Parmi les différentes analyses menées sur ces prépolymères époxy, l'étude de la distribution de masses par chromatographie d'exclusion stérique (GPC) et spectroscopie de masse Electro-Spray (ESI-TOF) est développée ci-dessous.

a) GPC

La distribution de masses des deux prépolymères dérivés de l'isosorbide a été étudiée par GPC (Figure 8) et comparée à celle du prépolymère DGEBA. Le prépolymère $DGEDAS_n$ présente une large distribution de masse mettant en évidence la présence de nombreux oligomères. A contrario, le chromatogramme de $DGEDAS_0$ met en évidence un unique composé, le diglycidyl éther d'isosorbide pur.

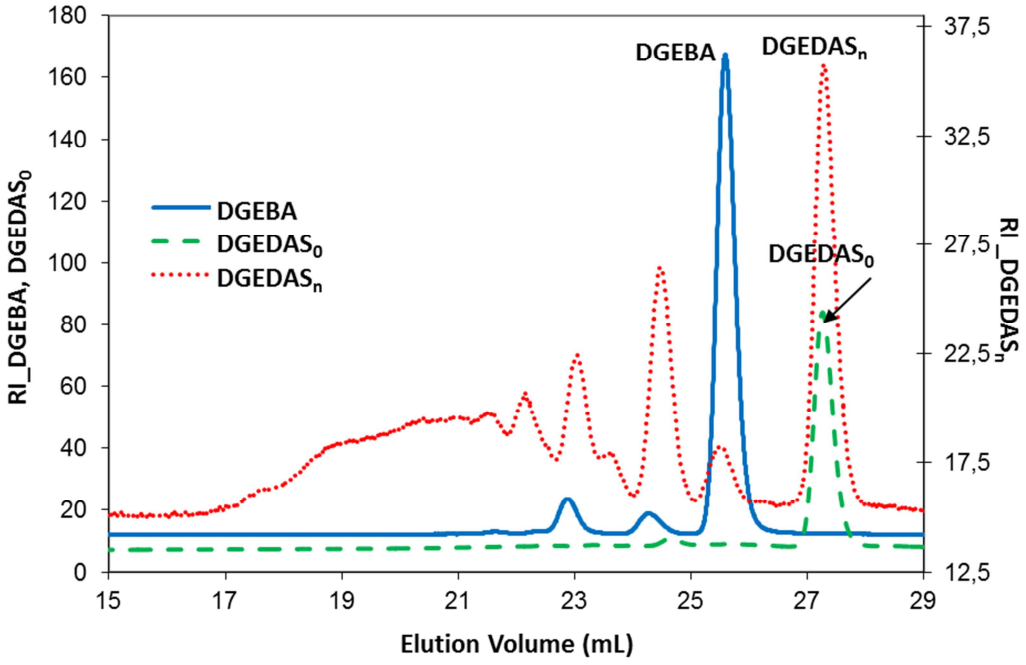

Figure 8. Chromatogrammes GPC des deux isosorbides époxydés $DGEDAS_n$ et DGEDAS0

Les chromatogrammes GPC des deux prépolymères commerciaux SPGE and DGECAR sont représentés en Figure 9 et mettent aussi en évidence la présence de nombreux oligomères pour SPGE et DGECAR.

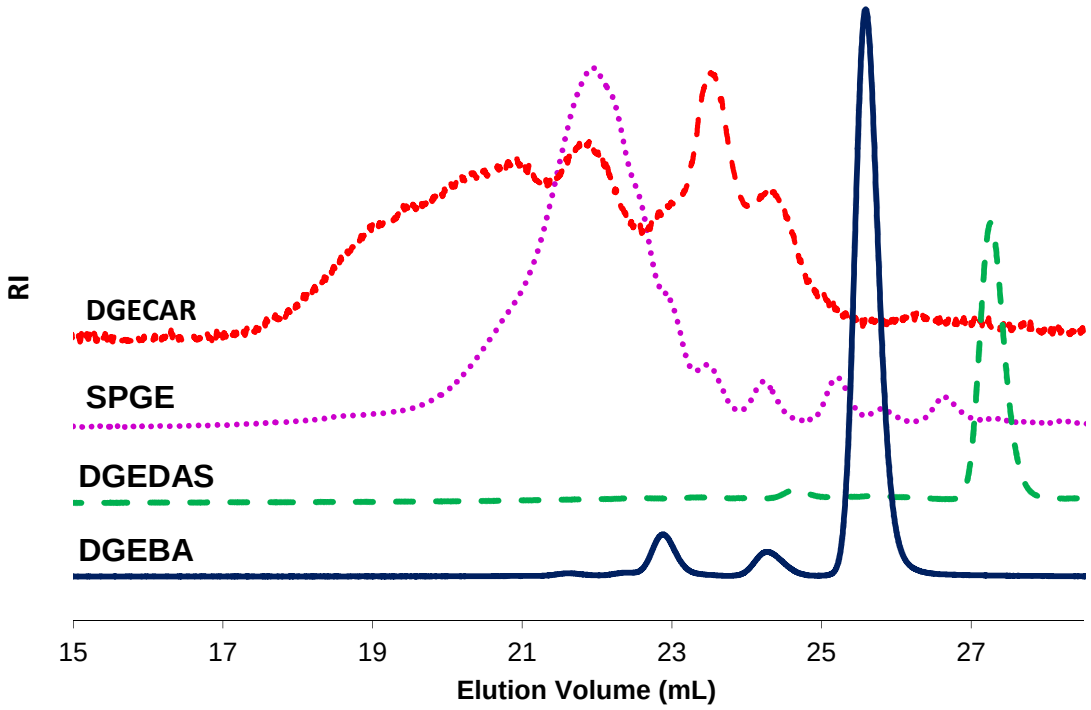

Figure 9. Chromatogrammes GPC de SPGE, DGECAR, $DGEDAS_0$ et DGEBA

b) Analyses Electro-Spray

La spectroscopie de masse de $DGEDAS_0$ met en évidence un seul composé tandis que celle de DGECAR souligne la présence de nombreux oligomères. Les analyses Electro-Spray apportant le plus d'information sont celles de $DGEDAS_n$ et SPGE et sont discutées ci-dessous :

$DGEDAS_n$:

La présence de nombreux oligomères dans la composition de $DGEDAS_n$ a été mis en évidence par GPC. Cette observation a été confirmée par spectroscopie de masse (Electro-Spray, Figure 10). Les composés sont cationisés sous la forme $[M+Na]^+$. La formule brute correspondant aux principaux pics a été confirmée par une mesure de masse exacte. Les valeurs de masses obtenues peuvent être reliées à des structures probables d'oligomères (Figure 11). Les attributions sont données dans le Tableau 1.

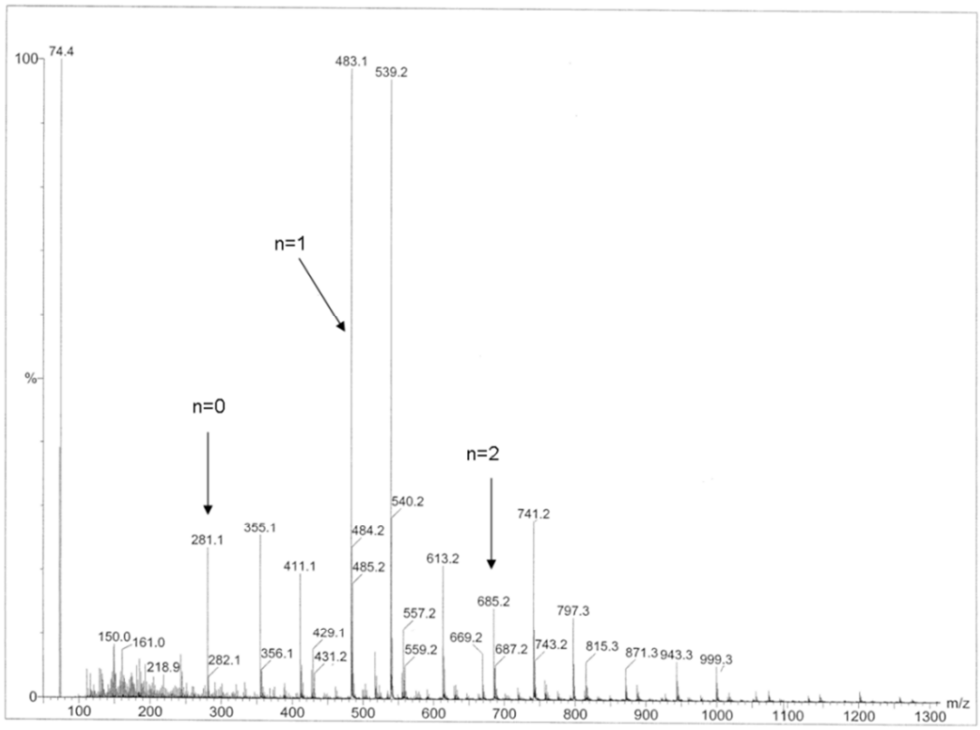

Figure 10. Spectre Electro-Spray de $DGEDAS_n$

Masses Molaires (g/mol)	Formules	Structures
258	$C_{12}H_{18}O_6$	A+2B (n = 0)
404	$C_{18}H_{28}O_{10}$	2A+2B
460	$C_{21}H_{32}O_{11}$	2A+3B (n = 1)
516	$C_{24}H_{36}O_{12}$	2A+4B
662	$C_{30}H_{46}O_{16}$	3A+4B (n = 2)
718	$C_{33}H_{50}O_{17}$	3A+5B
774	$C_{36}H_{54}O_{18}$	3A+6B

Tableau 1. Principaux oligomères de $DGEDAS_n$ révélés par spectroscopie de masse (Electro-Spray)

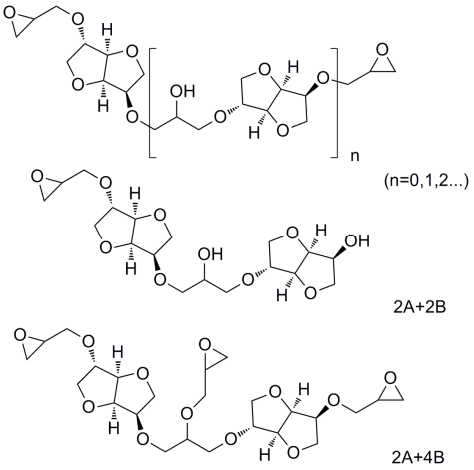

Figure 11. Structures des principaux oligomers de $DGEDAS_n$ mises en évidence par ESI-Tof

SPGE :

Une observation intéressante peut être faite à partir de l'analyse d'Electro-Spray de SPGE (Figure 12), à savoir la présence de nombreux oligomères chlorés. Une analyse élémentaire complémentaire a confirmé ce taux important de chlore dans SPGE soit 19.5 % massique. Ceci peut s'expliquer par la méthode de synthèse (via l'épichlorhydrine) et la faible réactivité des –OH secondaires présents dans la structure du sorbitol qui rendent l'étape de déchlorination plus difficile ; le chlore reste dans la structure du prépolymère époxy (Scheme 1). Ce taux de chlore important doit avoir une influence sur les propriétés du prépolymère SPGE (réactivité et structure du réseau époxy obtenu).

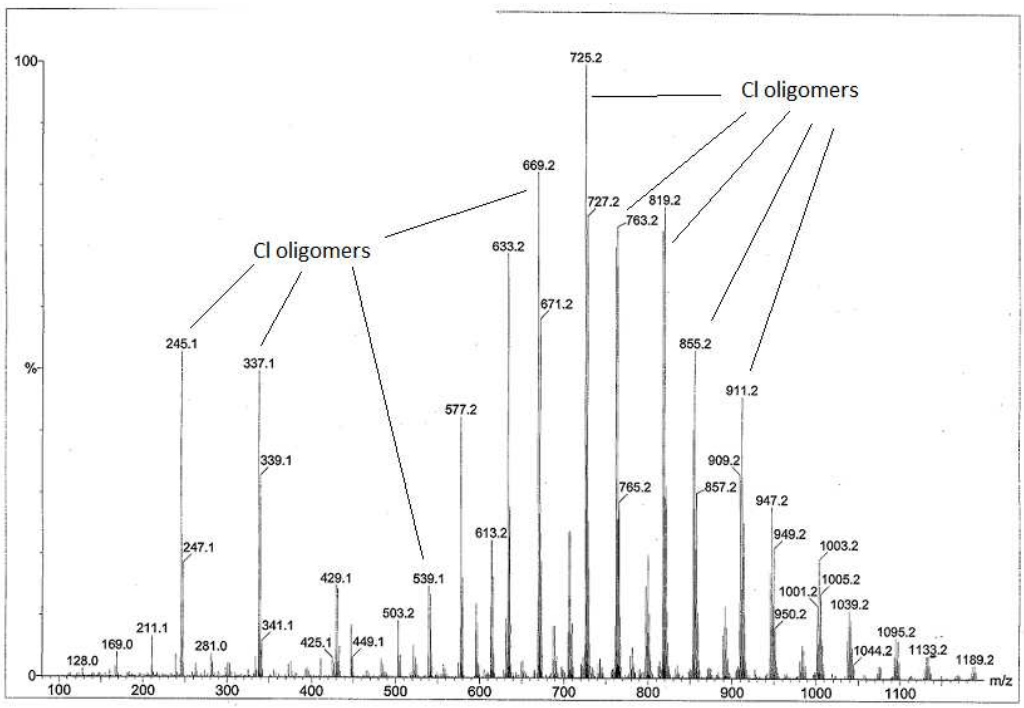

Figure 12. Spectre ESI-TOF de SPGE

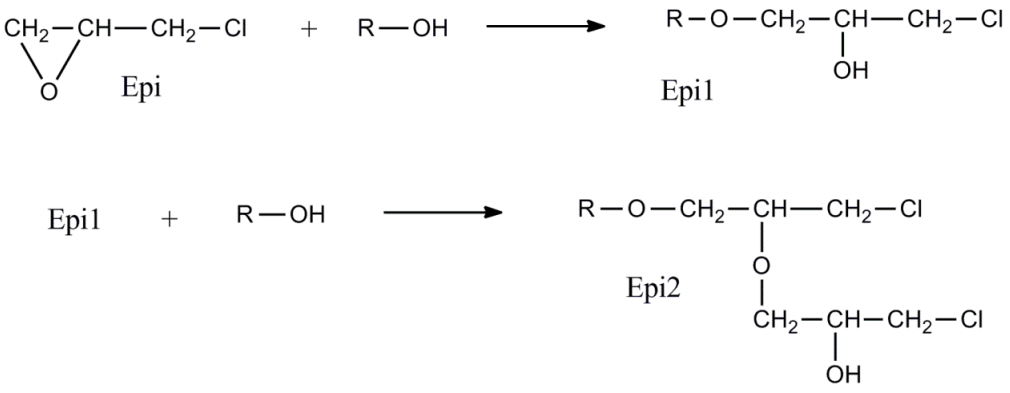

Scheme 1. Formation de chlorhydrines

III. Etude des différents systèmes époxy-amines bio-sourcés

Différents systèmes époxy-amines ont été étudiés à partir de ces prépolymères époxy bio-sourcés. Dans cette partie du résumé étendu sont abordées l'étude de la réactivité de ces différents systèmes par DSC, l'étude des transitions vitreuses obtenues pour les différents réseaux par DSC ainsi que celle de leurs propriétés thermomécaniques (T_α, modules…) par DMA.

1. Influence de la structure du prépolymère époxy

Pour s'intéresser à l'influence de la structure du prépolymère époxy, un durcisseur classique a été utilisé : l'isophorone diamine IPD (Figure 13). Les différents systèmes ont été formulés pour avoir un rapport stœchiométrique $r = n_{ah}/n_e = 1$. Les réseaux étudiés ont été obtenus après une réticulation en étuve 1 h à 80°C suivi de 2 h à 180°C.

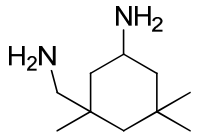

Isophorone Diamine, IPD

Figure 13. Structure du durcisseur isophorone diamine IPD

a) Etude de la réactivité des systèmes

Les thermogrammes DSC des différents systèmes réactifs obtenus avec IPD comme durcisseur sont représentés Figure 14. Les résultats de ces analyses sont résumés dans le Tableau 2. Il apparait que les T_{g0} sont de l'ordre de -40°C, exception faite du système $DGEDAS_0$ – IPD avec une T_{g0} à -60°C du fait de la masse molaire plus faible du prépolymère $DGEDAS_0$. Les enthalpies de réactions pour DGEBA – IPD, $DGEDAS_0$ – IPD et $DGEDAS_n$ – IPD sont autour de 90 kJ/eq de l'ordre de systèmes époxy-amine classiques. Dans le cas de SPGE – IPD et DGECAR – IPD les enthalpies de réactions obtenues sont plus faibles. La température maximale de réaction T_{peak} la plus faible est obtenue pour le système SPGE – IPD.

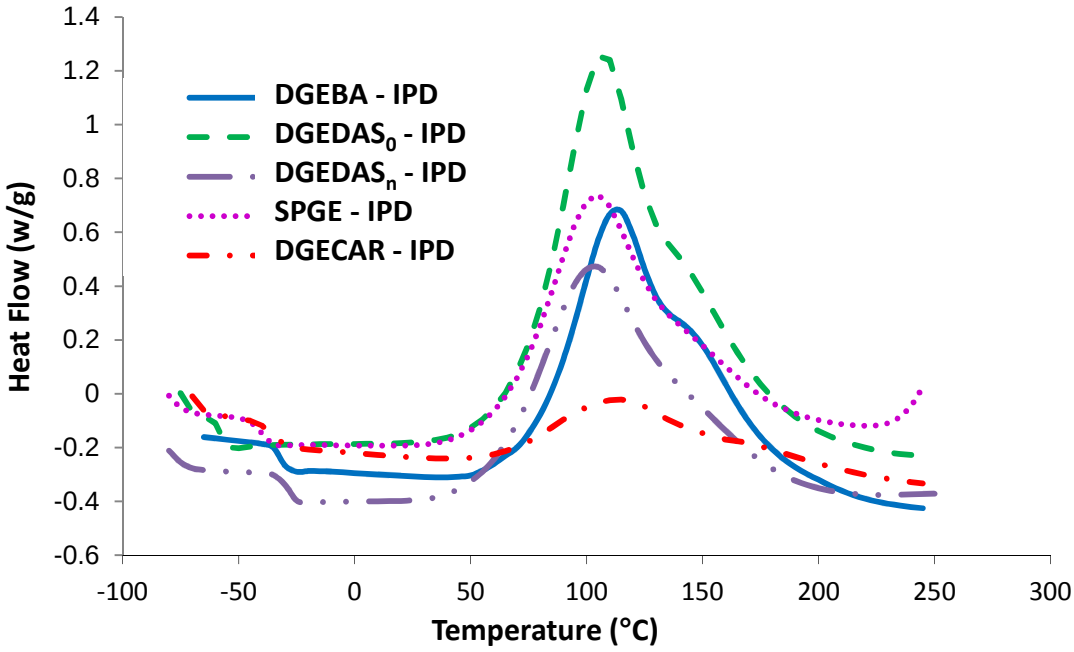

Figure 14. Thermogrammes DSC en montée en température (10°C/min) des différents systèmes

Systèmes	T_{g0} (°C)	ΔH (J/g)	ΔH (kJ/ee)	T_{peak} (°C)
DGEBA – IPD	-35	415	92	114
$DGEDAS_n$ – IPD	-36	404	91	104
$DGEDAS_0$ – IPD	-60	547	89	108
SPGE – IPD	-41	338	79	101
DGECAR – IPD	-41	127	68	116

Tableau 2. Résultats d'analyse DSC pour les différents systèmes époxy-amines étudiés

b) Influence de la stœchiométrie sur les valeurs de T_g

Il a été prouvé que la valeur maximale de T_g est obtenue pour le rapport stœchiométrique r = 1 dans l'hypothèse où l'unique mécanisme intervenant est celui d'addition époxy-amine classique [15]. Nous nous sommes donc intéressés à l'évolution de la T_g avec le rapport r. Les T_g des différents réseaux ont été mesurées par DSC et leur évolution est représentée en Figure 15.

La première observation est que pour r = 1, la plus haute T_g est obtenue pour le réseau non bio-sourcé DGEBA – IPD. Pour les systèmes DGEBA – IPD, $DGEDAS_0$ – IPD et $DGEDAS_n$ – IPD on se trouve dans le cas d'un mécanisme d'addition époxy amine

uniquement où le maximum de T_g est obtenu pour un rapport stœchiométrique r = 1. On observe une évolution inattendue de T_g avec r pour les réseaux SPGE – IPD. Nous en avons déduit que le taux important de Cl dans le prépolymère SPGE devait avoir une influence sur la formation du réseau en impliquant de fortes intéractions ioniques.

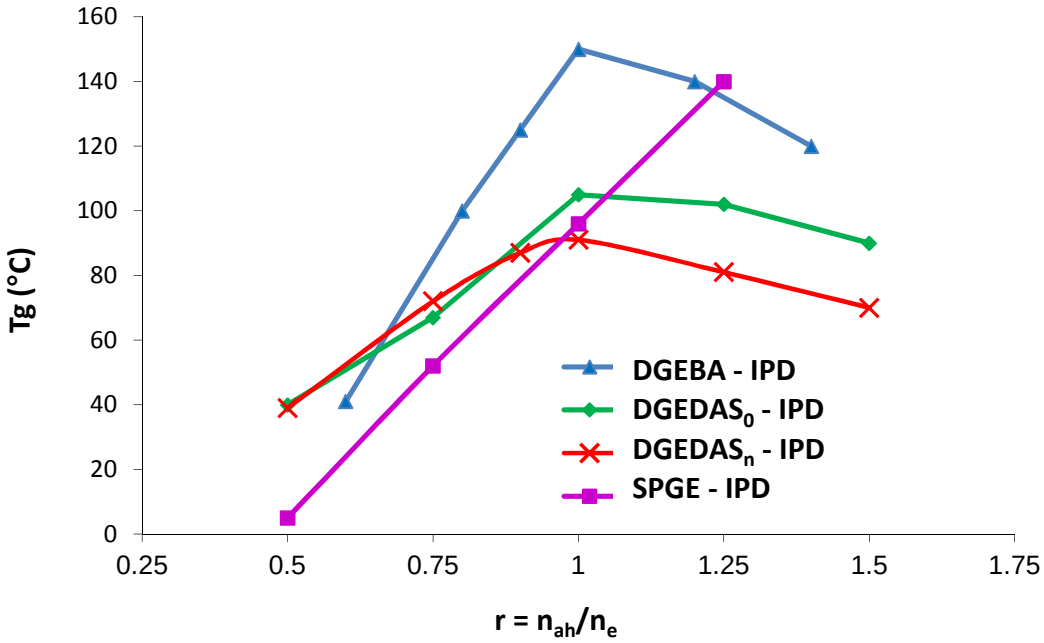

Figure 15. Evolution de la T_g avec le rapport r

c) Propriétés thermo-mécaniques des réseaux

Pour r=1

Les propriétés mécaniques dynamiques ont été mesurées en torsion sur des échantillons conservés en dessiccateur après leur réticulation en étuve. Les évolutions du modules de conservation G' et du facteur de perte tanδ en fonction de la température pour les différents réseaux sont représentées en Figure 16 et Figure 17. La relaxation α, ayant lieu aux plus hautes températures, est associée à la transition vitreuse, tandis que la seconde relaxation β plus faible en amplitude a lieu aux plus faibles températures et est attribuée aux mouvements locaux de groupes moléculaires, plus particulièrement les groupes hydroxyl éther dans le cas des réseaux époxy-amine. Selon la théorie de l'élasticité caoutchoutique, il est possible de déterminer la masse molaire moyenne entre nœuds M_c selon la relation :

$$G' = dRT/M_c$$

où d est la densité du réseau, R la constante des gaz parfaits et G' le module de conservation à T_g + 30°C.

Les valeurs de T_β, T_α, G' et M_c sont reportées dans le Tableau 3. Pas de différence majeure n'est observée concernant T_β pour les réseaux DGEBA – IPD, $DGEDAS_0$ - IPD, $DGEDAS_n$ – IPD et SPGE – IPD, entre -40°C et -50°C. La transition sous-vitreuse β n'est pas observée pour DGECAR – IPD ce qui peut s'expliquer par une faible intensité de la transition du fait qu'il y ait globalement moins de groupements hydroxy-éther en raison de la valeur élevée de l'équivalent époxy du prépolymère DGECAR. Les valeurs de T_α sont en adéquation avec les valeurs de T_g mesurées précédemment par DSC. La plus faible valeur de module est obtenue pour le réseau DGECAR – IPD ce qui s'explique par la présence de chaine aliphatiques flexibles dans la structure du prépolymère DGECAR. La valeur de masse entre nœuds la plus haute est obtenue pour DGECAR – IPD (970 g/mol) tandis que le réseau avec la plus faible masse molaire entre nœuds est celui dérivé du sorbitol.

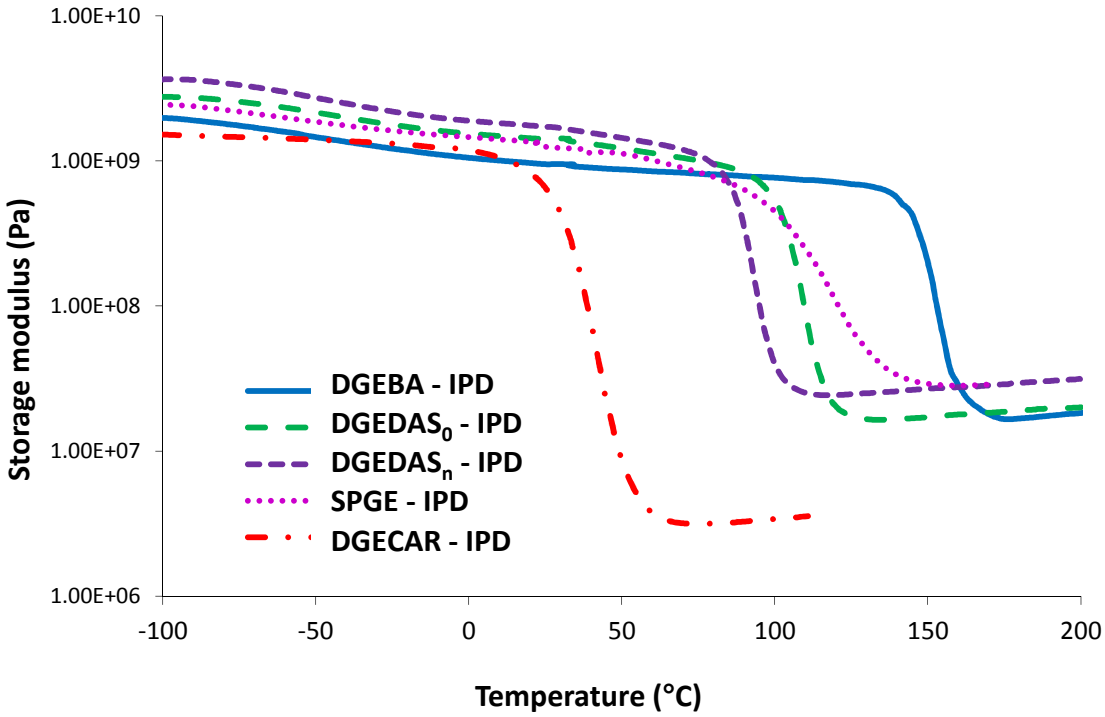

Figure 16. Evolution du module de conservation G' pour les différents systèmes époxy-amine à r = 1

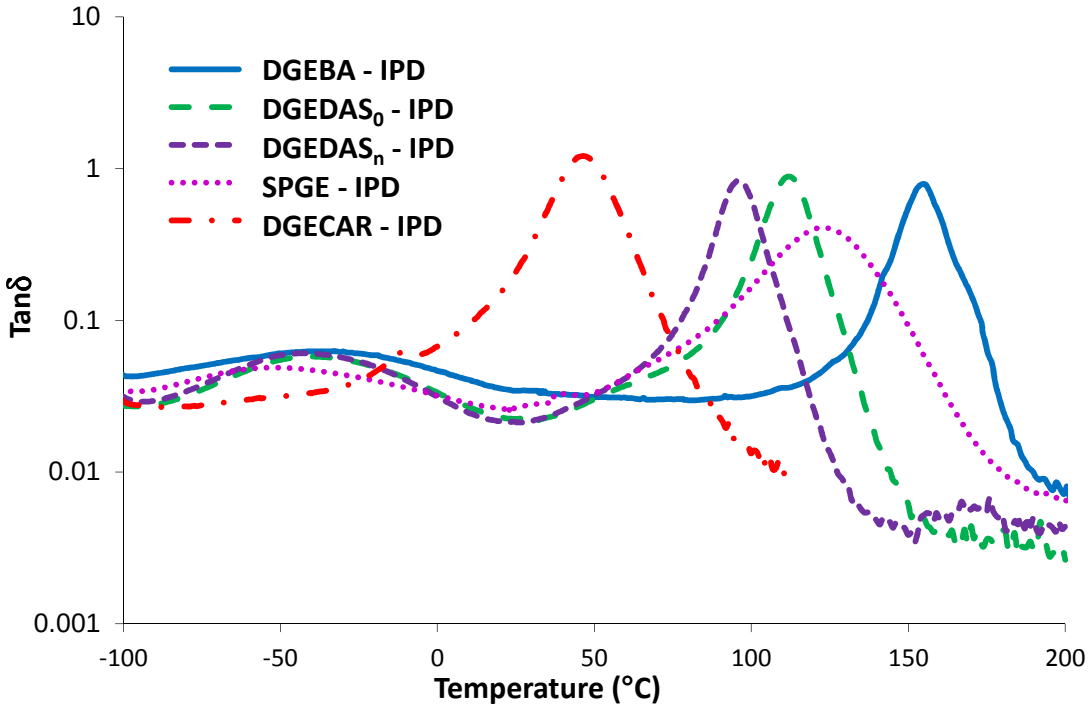

Figure 17. Evolution du facteur de perte tanδ pour les différents systèmes époxy-amines à r = 1

Systems	T_β (°C)	T_α (°C)	G'_R (MPa) (at Tg+30°C)	d (g/cm^3)	M_c (g/mol)
DGEBA – IPD	-46	155	17.1	1.13	250
$DGEDAS_n$ – IPD	-42	96	24.7	1.24	170
$DGEDAS_0$ – IPD	-40	112	16.6	1.25	260
SPGE – IPD	-52	120	29.3	1.24	150
DGECAR – IPD	-	50	3.2	1.06	970

Tableau 3. Analyses dynamiques mécaniques des différents réseaux (r = 1)

Evolution des propriétés thermomécaniques avec r

Les propriétés thermomécaniques ont été mesurées pour les réseaux SPGE – IPD à différentes stœchiométries. La principale observation est l'augmentation de T_α avec r, soit l'augmentation de la T_g, ce qui confirme les précédents résultats obtenus par DSC.

2. Influence de la structure du durcisseur

Plusieurs durcisseurs classiques commerciaux ainsi que des durcisseurs plus spécifiques dérivés de ressources renouvelables tels que l'acide tannique (TA) et un durcisseur amine obtenu à partir du cardanol (NC540) ont été utilisés. Ces différents durcisseurs sont décrit dans le Tableau 4.

Non	Structure	Masse molaire (g/mol)	Fonctionalité
IPD, isophorone diamine	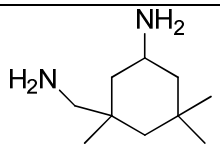	170	4
Jeffamine D230, polyetheramine	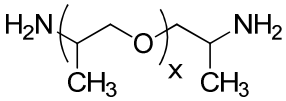	230	4
MXDA, m-xylylene diamine	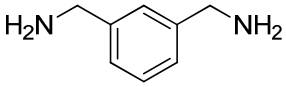	136	4
MCDEA, 4,4'-methylene bis (3-chloro-2,6-diethylaniline)	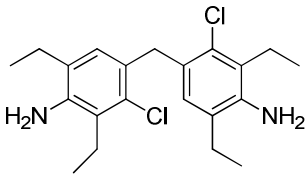	379	4
DETDA, diethyl toluene diamine	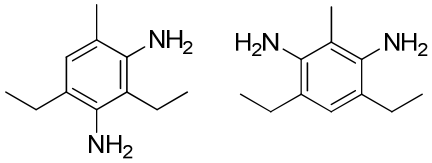 75 - 81 % 18 - 20 %	178	4
NC-540, phenalkamine	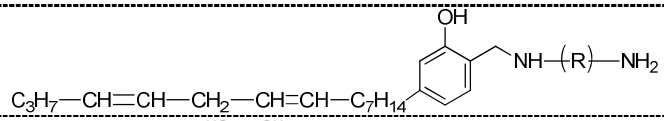	Active Hydrogen equivalent (AHEW) = 81	
TA, tannic acid	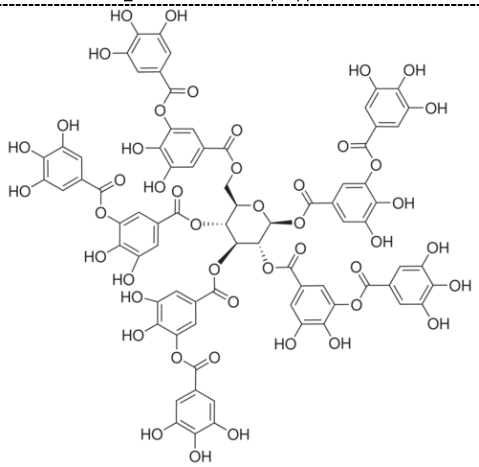	Hydroxyl value I_{OH} = 68,05 g/eOH	

Tableau 4. Structure des différents durcisseurs amines utilisés

a) Etude de la réactivité des systèmes

L'étude de la réactivité des différents systèmes a été réalisée par le biais d'analyses DSC pour des rapports stœchiométriques $r = n_{ah}/n_e = 1$ dans le cas des durcisseurs amines, et $r = n_{OH}/n_e = 1$ dans le cas de l'acide tannique. Il est à noter que pour notre étude, l'acide tannique a été préalablement dissous dans du propane diol (PDO). L'indice hydroxyl du PDO a été aussi pris en compte lors du calcul des proportions Prépolymère époxy / Durcisseur.

Les principaux résultats de ces analyses DSC sont repris dans le Tableau 5.

Système	T_{g0} (°C)	ΔH (J/g)	ΔH (kJ/ee)	T_{peak} (°C)
DGEBA – IPD	-35	415	92	114
$DGEDAS_n$ – IPD	-36	404	91	104
$DGEDAS_n$ – D230	-48	347	86	120
$DGEDAS_n$ - MXDA	-38	438	96	104
$DGEDAS_n$ – MCDEA	-19	NA	NA	>250
$DGEDAS_n$ – DETDA	-30	NA	NA	190
$DGEDAS_0$ – IPD	-60	547	89	108
$DGEDAS_0$ – D230	-70	443	100	124
$DGEDAS_0$ – MXDA	-56	600	102	102
SPGE - IPD	-41	338	79	101
SPGE - MXDA	-47	477	108	104
SPGE – NC540	-43	294	81	99
SPGE – TA/PDO	-42	NA	NA	208
DGECAR – IPD	-41	127	68	116
DGECAR – NC540	-44	122	71	110

Tableau 5. Résultats d'analyse DSC pour les différents systèmes époxy-amines étudiés

On retrouve la réactivité connue des différents durcisseurs amines classiques pour les prépolymères bio-sourcé, comme classée ci-dessous en fonction de leur structure chimique:

aliphatique > cyclo-aliphatique > aromatique.

Il apparait aussi que l'acide tannique nécessite une température de réticulation importante.

b) Détermination des températures de transitions vitreuses

Les différents systèmes étudiés ont été réticulé et les températures de transitions vitreuses des réseaux ainsi obtenus ont été mesurés et sont répertoriés dans le tableau ci-dessous. Il apparait que quel que soit le durcisseur utilisé les valeurs de T_g obtenues sont toujours plus faibles pour les réseaux obtenus à partir de prépolymère époxy bio-sourcés que pour les réseaux dérivés de la DGEBA. De même, les faibles valeurs de T_g obtenues pour les réseaux dérivés du cardanol époxydé excluent l'utilisation de ce dernier pour des applications composites.

Système	Cycle de réticulation	T_g (°C)
DGEBA – IPD	1h à 80°C + 2h à 180°C	150
$DGEDAS_n$ – IPD	1h à 80°C + 2h à 180°C	91
$DGEDAS_n$ – D230	2h à 80°C + 2h à 180°C	48
$DGEDAS_n$ – MXDA	1h à 80°C + 2h at 160°C	74
$DGEDAS_n$ – MCDEA	10h à 170°C	120
$DGEDAS_n$ – DETDA	2h à 180°C	112
$DGEDAS_0$ – IPD	1h à 80°C + 2h à 180°C	102
$DGEDAS_0$ – D230	2h à 80°C + 2h à 180°C	52
$DGEDAS_0$ – MXDA	1h à 80°C + 2h à 160°C	79
SPGE – IPD	1h à 80°C + 2h à 180°C	100
SPGE – MXDA	1h à 80°C + 2h à 160°C	67
SPGE – NC540	1h à 80°C + 2h à 180°C	76
SPGE – TA/PDO	2h à 180°C	41
DGECAR – IPD	1h à 80°C + 2h à 180°C	22
DGECAR – NC540	1h à 80°C + 2h à 180°C	33

Tableau 6. Températures de transitions vitreuses des différents réseaux

c) Propriétés thermomécaniques des réseaux

Les Figure 18 et Figure 19 représentent respectivement l'évolution du module de conservation et du facteur de perte en fonction de la température obtenus par analyse DMA pour certains réseaux intéressant. Les résultats de ces analyses sont répertoriés en Tableau 7. Ceci confirme la faible valeur de T_α obtenue pour le réseau DGECAR – NC540. De plus une

certaine hétérogénéité du réseau SPGE – NC540 est mis en évidence par la transition α très élargie (ΔT important).

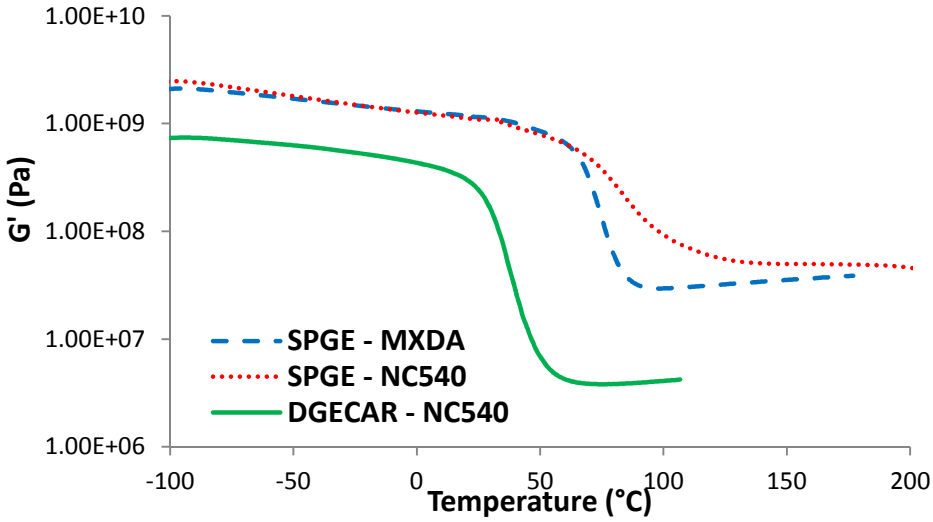

Figure 18. Evolution de G' en fonction de la température pour SPGE – MXDA, SPGE – NC540, DGECAR – NC540

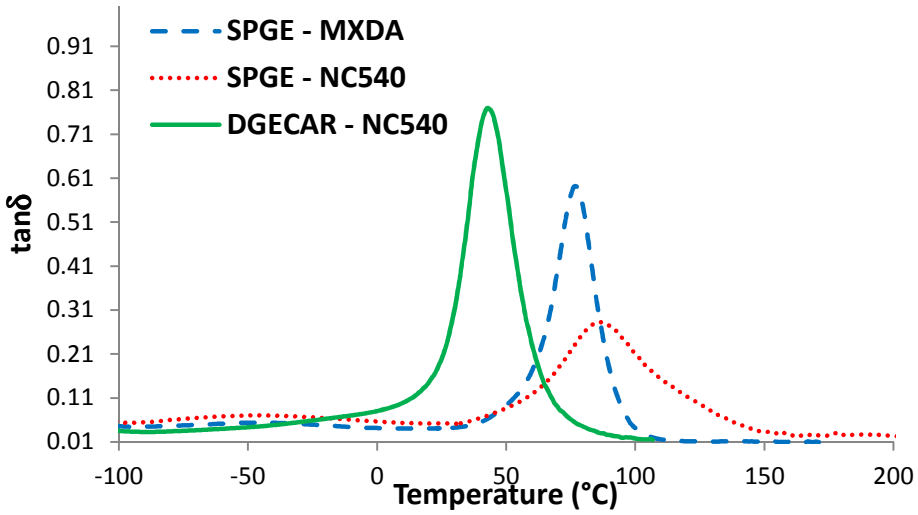

Figure 19. Evolution de tanδ avec la température pour SPGE – MXDA, SPGE – NC540, DGECAR – NC540

Réseau	T_β (°C)	T_α (°C)	tanδ max	ΔT (°C)	G' (MPa) (at T_α+30°C)	d (g/cm^3)	M_c (g/mol)
SPGE – MXDA	-44	77	0.59	20	30.1	1.31	137
SPGE – NC540	-45	85	0.28	48	63.5	1.25	63
DGECAR – NC540	NA	43	0.77	23	3.8	1.07	810

Tableau 7. Résultats d'analyses dynamiques mécaniques de SPGE – MXDA, SPGE – NC540 et DGECAR – NC540

3. Durcisseur amine particulier – polymérisation duale

Un durcisseur particulier a aussi été utilisé dans le cadre de notre projet. Ce durcisseur a été spécialement formulé par Huntsman pour l'application Rossignol. La particularité de ce durcisseur est qu'il se compose de deux amines (monofonctionnelle et trifonctionnelle) ainsi que la présence d'amines tertiaires (Tableau 8). Ces amines tertiaires catalysent la réaction d'homopolymérisation des groupes époxy et conduisent ainsi à une polymérisation duale (addition époxy-amine et homopolymérisation).

Non	%	Structure	Masse Molaire (g/mol)	fonctionnalité
HA1: N(3-dimethylaminopropyl)-1,3-propylenediamine	30	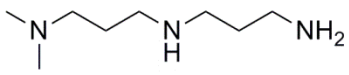	M_{a1} = 159	f_{a1} = 3
HA2: 3-[[3-(dimethylamino)propyl]-amino]propiononitrile	70	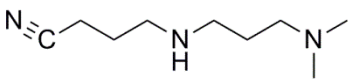	M_{a2} = 155	f_{a2} = 1

Tableau 8. Description du durcisseur HA

L'influence de l'homopolymérisation catalysée par les amines tertiaires a été mise en évidence par une analyse des propriétés thermomécaniques. Ainsi comme représenté sur les figures ci-dessous et souligné dans le Tableau 9, on observe que les réseaux obtenus avec le durcisseur HA ont une T_α plus faible pour une température de réticulation importante (150°C) qu'à plus faible température de réticulation (80°C). On peut faire la même observation sur les réseaux obtenus à partir de $DGEDAS_0$ – HA avec une T_g (mesurée par DSC) plus faible pour les réseaux obtenus à plus haute température de réticulation (Tableau 10).

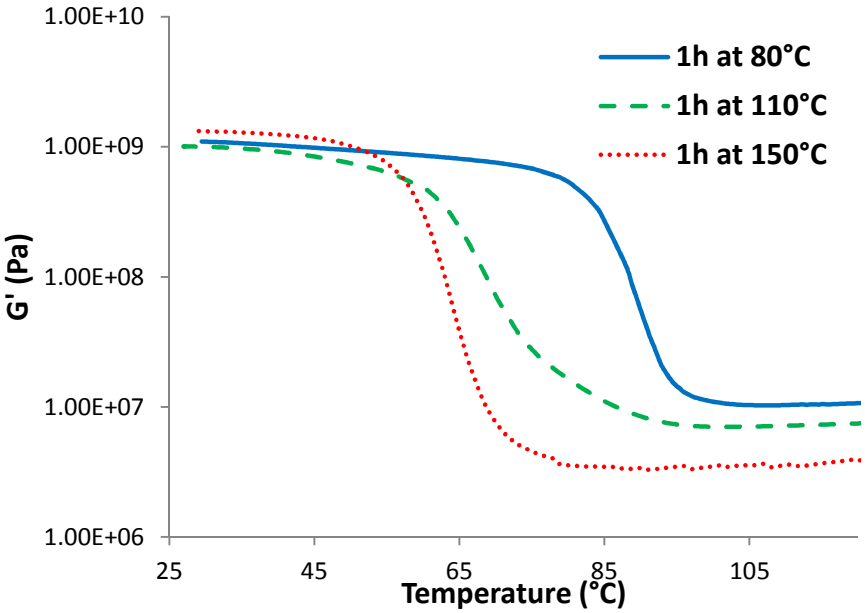

Figure 20. Evolution du module de conservation pour les réseaux DGEBA – HA réticulés à différentes températures.

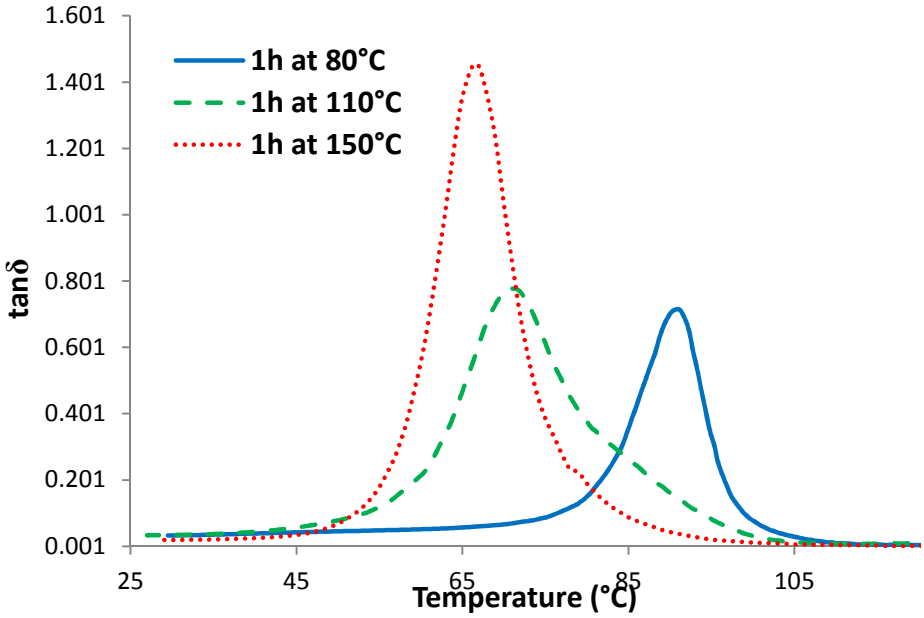

Figure 21. Evolution du facteur de perte tan δ pour les réseaux DGEBA – HA réticulés à différentes températures

Cycle de réticulation	T_α (°C)	tanδ max	ΔTα (°C)	G' (MPa) (at T_α +30°C)	d (g/cm^3)	ν (10^{-3} mol/cm^3)	M_c (g/mol)
1 h à 80°C	90	0.70	10	10.7	1.17	3.3	357
1 h à 110°C	70	0.77	16	7.1	1.17	2.3	511
1 h à 150°C	67	1.45	10	3.3	1.16	1.1	1081

Tableau 9. Propriétés thermomécaniques des réseaux DGEBA – HA en fonction de la température de réticulation

Cycle de réticulation	T_g (°C)
2 h à 80°C	68
2 h à 140°C	55

Tableau 10. Evolution de la T_g (mesurée par DSC) pour le système $DGEDAS_0$ – HA en fonction de la température de réticulation

4. Tenue à l'eau des réseaux

Le dernier point abordé a été la tenue à l'eau des différents réseaux obtenus à partir d'isosorbide, de sorbitol et de cardanol époxydé. En effet, les matériaux époxy sont connus pour être sensibles au vieillissement humide, celui-ci pouvant avoir d'importantes conséquences sur les propriétés des matériaux : plastification, dégradation… Il était alors intéressant de s'intéresser à la tenue à l'eau de ces nouveaux matériaux.

a) Réseaux à base d'isosorbide époxydé

La tenue à l'eau des réseaux époxy obtenus à partir d'isosorbide et différents durcisseur (rapport stœchiométriques $r = n_{ah}/n_e = 1$) a été étudiée. Après 5 jours d'immersion dans de l'eau distillée à température ambiante le % d'eau absorbé par les différents échantillons est reporté dans le tableau suivant.

Réseau	T_g (°C) initiale	% d'eau absorbée (5 jours)	Observations
DGEBA – IPD	150	1	Systèmes référence
DGEBA – HA	90	0.9	
$DGEDAS_0$ – IPD	102	26	
$DGEDAS_0$ – D230	52	29	
$DGEDAS_0$ – MXDA	79	ND	Quelques fragments après 5h d'immersion
$DGEDAS_n$ – IPD	91	ND	Léger gonflement, fragmentation aprés1h
$DGEDAS_n$ – D230	48	ND	Gonflement moyen, fragmentation après 30 min
$DGEDAS_n$ – MCDEA	120	8.4	
$DGEDAS_n$ – DETDA	112	29	
$DGEDAS_n$ – HA	61	ND	Fragmentation après 15 min

Tableau 11. Tenue à l'eau des réseaux à base d'isosorbide

Il apparait que les réseaux époxy à base d'isosorbide sont très hydrophiles et absorbent jusqu'à 30 % massique d'eau. L'absorption d'eau est réduite en utilisant un durcisseur aromatique tel que MCDEA, mais reste importante (8.4 %) comparée à l'absorption mineure des réseaux de référence (< 1 %). On observe même dans certains cas une dégradation des réseaux avec la fragmentation de ceux-ci.

La très mauvaise tenue à l'eau des réseaux à base d'isosorbide apparait alors comme le principal inconvénient de ces matériaux.

Afin de suivre la cinétique d'absorption de l'eau de ces réseaux, des conditions de vieillissement plus « douces » ont été choisies. Le comportement des réseaux DGEDAS$_n$ – HA et DGEDAS$_n$ –IPD en chambre climatique (25°C, 50 % Humidité) a ainsi été suivi. Il apparait que l'utilisation du durcisseur IPD diminue légèrement l'absorption d'eau par rapport au durcisseur HA. Néanmoins, la quantité d'eau absorbée dans de telles conditions reste très importante (environ 3.5 % après un mois de stockage) et entraine une plastification importante des réseaux. Ces matériaux restent très sensibles à l'humidité atmosphérique.

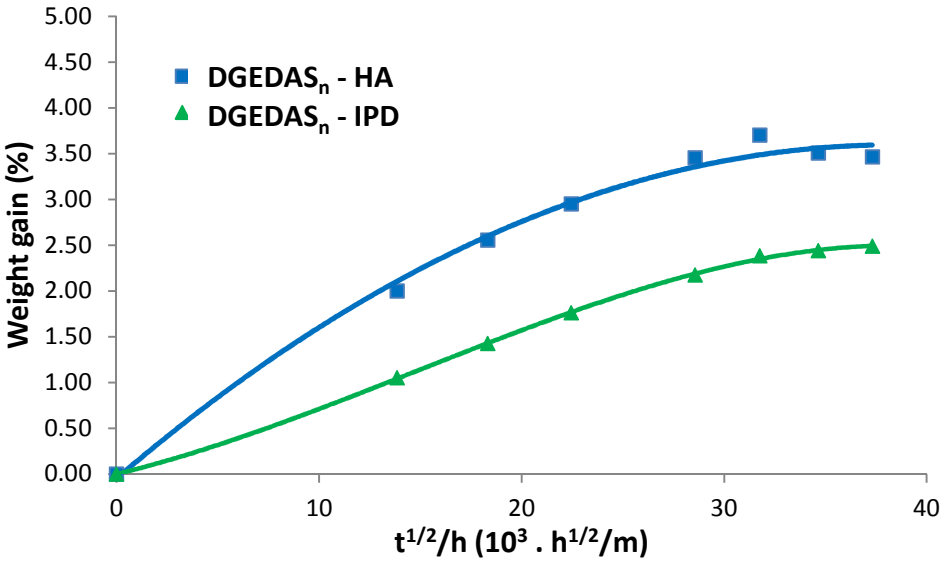

Figure 22. Cinétique d'absorption d'eau en atmosphère humide pour DGEDAS$_n$ – HA et DGEDAS$_n$ – IPD (T$_{amb}$, Hum. 50 %)

b) Réseaux à base de sorbitol époxydé et de cardanol

A l'opposé, les réseaux obtenus à partir de sorbitol époxydé présentent une tenue à l'eau intéressante voire équivalente à celle du réseau DGEBA – HA.

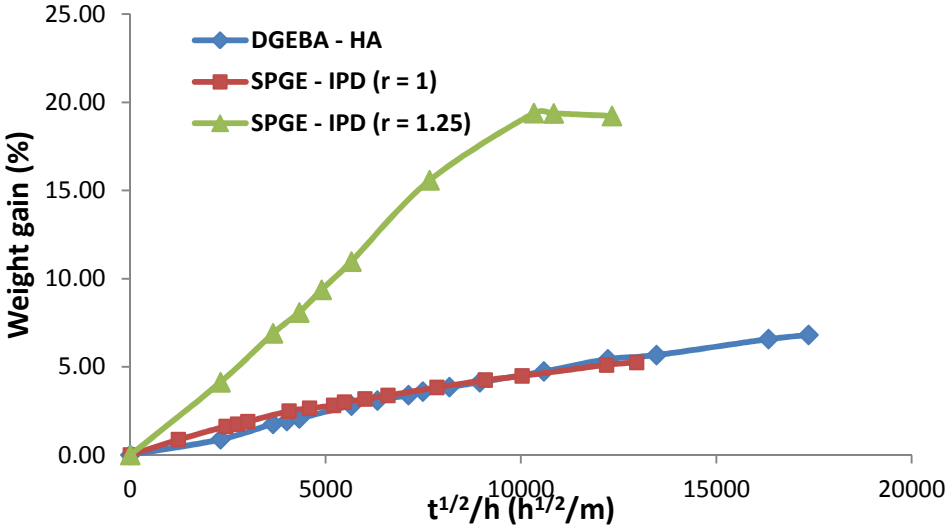

Figure 23. Cinétique d'absorption d'eau pour SPGE – IPD (r = 1 et r = 1.25). Echantillons en immersions dans de l'eau distillée à T_{amb}.

Les réseaux obtenus à partir de cardanol présentent une excellente tenue à l'eau ce qui peux s'expliquer par la structure phénolique du prépolymère époxy dérivé du cardanol. Néanmoins ces réseaux ont de très faibles T_g.

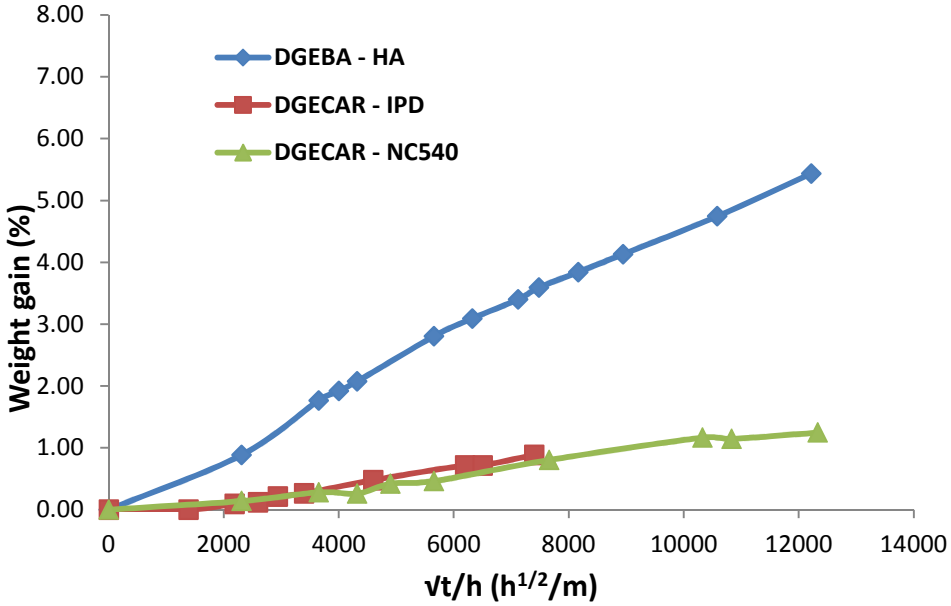

Figure 24. Cinétique d'absorption d'eau pour DGECAR – IPD et DGECAR – NC540 Echantillons en immersions dans de l'eau distillée à T_{amb}.

Conclusions

Deux types d'isosorbide époxydé ont été synthétisés, un isosorbide époxydé oligomère et un comprenant uniquement le diglycidyl éther d'isosorbide pur. Ces deux prépolymères époxy ont été polymérisés en utilisant un durcisseur amine classique (IPD) et comparés aux deux principaux prépolymères époxy disponibles sur le marché, dérivés du sorbitol et du cardanol. Le comportement particulier du sorbitol époxydé est à noter avec une augmentation de la T_g avec le rapport stœchiométrique. Cette augmentation de la T_g a été attribuée au fort pourcentage de Cl résiduels. De plus, les réseaux dérivés du cardanol sont à écarter du fait de leur faible T_g. L'influence de la structure du durcisseur a aussi été étudiée en utilisant différent durcisseurs à la fois classiques (mais présentant différentes structures) ainsi que bio-sourcés tels que l'acide tannique et le cardanol amine. L'évolution des réactivités des différents systèmes avec les durcisseurs associés est classique et fonction du durcisseur. Il apparait aussi que quel que soit le durcisseur, de plus faibles T_g sont obtenues pour les réseaux bio-sourcés. Enfin, la tenue à l'eau des réseaux dérivés de sorbitol, isosorbide et cardanol a été étudiée et met en évidence la très forte hydrophilie des réseaux à base d'isosorbide représentant ainsi le principal inconvénient de ces matériaux. En contrepartie, bien qu'ayant une faible T_g les réseaux à base de cardanol présentent une excellente tenue à l'eau. Un important travail de formulation reste à faire pour obtenir les propriétés nécessaires à une application composite.

Références

[1] Gandini A. Epoxy Polymers : New materials and innovations: Pascault JPP, Williams RJJ, Eds. Wiley-VCH 2010.

[2] Gandini A. Polymers from Renewable Resources: A Challenge for the Future of Macromolecular Materials. *Macromolecules*. 2008;**41**:9491-504.

[3] Kaplan DL. Biopolymers from Renewable Ressources. Berlin: Springer-Verlag 1998.

[4] Pascault JP, Sautereau H, Verdu J, Williams RJJ. Thermosetting Polymers: Taylor & Francis Books, Inc. 2002.

[5] Shen L, Haufe J, Patel MK. Product overview and market projection of emerging biobased plastics. *PROBIP 2009*.

[6] Jin F-L, Park S-J. Thermomechanical behavior of epoxy resins modified with epoxidized vegetable oils. *Polymer International*. 2008;**57**:577-83.

[7] Park S-J, Jin F-L, Lee J-R. Effect of Biodegradable Epoxidized Castor Oil on Physicochemical and Mechanical Properties of Epoxy Resins. *Macromolecular Chemistry and Physics*. 2004;**205**:2048-54.

[8] Park SJ, Jin FL, Lee JR. Synthesis and Thermal Properties of Epoxidized Vegetable Oil. *Macromolecular Rapid Communications*. 2004;**25**:724-7.
[9] Patel MB, Patel RG, Patel VS. Effects of reactive diluent diepoxidized cardanol and epoxy fortifier on curing kinetics of epoxy resin. *Journal of Thermal Analysis and Calorimetry*. 1989;**35**:47-57.
[10] Acierno D, Russo P, Savarese R. Mechanical and dynamic-mechanical properties of biodegradable epoxy resins. *Proceedings of the Polymer Processing Society*. Salerno, Italy. 2008.
[11] East A JM, Zhang Y, Catalini LH,. Ethers of bisanhydrohexitols. US Patent US 2008/0021209A1 2008.
[12] Feng X, East AJ, Hammond WB, Zhang Y, Jaffe M. Overview of advances in sugar-based polymers. *Polymers for Advanced Technologies*. 2011;**22**:139-50.
[13] Fenouillot F, Rousseau A, Colomines G, Saint-Loup R, Pascault JP. Polymers from renewable 1,4:3,6-dianhydrohexitols (isosorbide, isomannide and isoidide): A review. *Progress in Polymer Science*. 2010;**35**:578-622.
[14] Chrysanthos M, Galy J, Pascault JP. Preparation and properties of bio-based epoxy networks derived from isosorbide diglycidyl ether. *Polymer*. 2011;**52**:3611-20.
[15] Galy J, Sabra A, Pascault JP. Characterization of epoxy thermosetting systems by differential scanning calorimetry. *Polymer Engineering & Science*. 1986;**26**:1514-23.

FOLIO ADMINISTRATIF

THESE SOUTENUE DEVANT L'INSTITUT NATIONAL DES SCIENCES APPLIQUEES DE LYON

NOM : CHRYSANTHOS DATE de SOUTENANCE : 21 Juin 2012

Prénoms : Marie

TITRE :

Novel bio-based epoxy networks derived from renewable resources: Structure-property relationships

NATURE : Doctorat Numéro d'ordre : 2012ISAL0051

Ecole doctorale : Matériaux de Lyon

Spécialité : Matériaux Polymères et Composites

RESUME:
Récemment, les polymères obtenus à partir de ressources renouvelables ont connus un véritable engouement pour le remplacement de matériaux obtenus à partir de ressources pétrolières. L'objectif de notre étude a été de développer de nouveaux systèmes bio-sourcés réactifs, plus précisément des systèmes époxy, pour des applications dans le domaine des matériaux composites.
Le monomère le plus souvent utilisé pour formuler des réseaux époxy est le diglycidyl éther de bisphenol A, DGEBA, obtenu à partir du bisphenol A et de l'épichlorhydrine. L'intérêt pour le remplacement du bisphénol A par un précurseur bio-sourcé est accentué par la toxicité de ce dernier.
Dans cette étude, nous avons étudié différents systèmes obtenus à partir de prépolymères époxy bio-sourcés et les avons comparés à un système classique à base de DGEBA en utilisant l'isophorone diamine (IPD) comme agent durcisseur.
Parmi les différents prépolymères époxy bio-sourcés étudiés, certains ont été obtenus à partir de dérivés polysaccharides tels que le sorbitol et l'isosorbide. Le sorbitol polyglycidyl éther est disponible commercialement, tandis que le diglycidyl éther d'isosorbide a été synthétisé soit par une voie classique faisant intervenir l'épichlorhydrine soit par l'intermédiaire du diallyle isosorbide. Un autre prépolymère époxy dérivé du cardanol a été étudié et est aussi un produit commercial.
Les structures chimiques de ces prépolymères époxy bio-sourcés ont été analysées. Les phénomènes de gélification et de réticulation des systèmes obtenus à partir de ces prépolymères et de l'IPD ont été étudiés. L'influence de la structure du prépolymère bio-sourcé et de l'agent de réticulation (classique ou dérivé de ressources renouvelables) sur les propriétés des réseaux ainsi que l'absorption d'eau par ces réseaux ont également été discutés.

MOTS-CLES: Réseaux époxy; bisphenol A; isosorbide; sorbitol; cardanol; relation structure propriétés; réactivité; propriétés des réseaux; absorption d'eau

Laboratoire (s) de recherche : Institut des Matériaux Polymères/ Laboratoire des Matériaux Macromoléculaires UMR 5223 INSA de Lyon

Directeur de thèse: Jocelyne GALY

Président de jury :

Composition du jury:

E. BOURGEAT-LAMI	Directrice de recherche CNRS (CPE Lyon)	
B. BOUTEVIN	Professeur (ENSCM)	Rapporteur
J. CHRISTOUD	Responsable service Matériaux (Rossignol)	
J. GALY	Directrice de recherche CNRS (INSA de Lyon)	
P. GOTTIS	Docteur (Huntsman)	
M. LAVORGNA	CNR Researcher (ICBM - Naples, Italy)	Rapporteur
J.P. PASCAULT	Professeur (INSA de Lyon)	
P. SABRE	Renewable Chemistry Management (Roquette Frères)	